ACTA PROTOZOOLOGICA

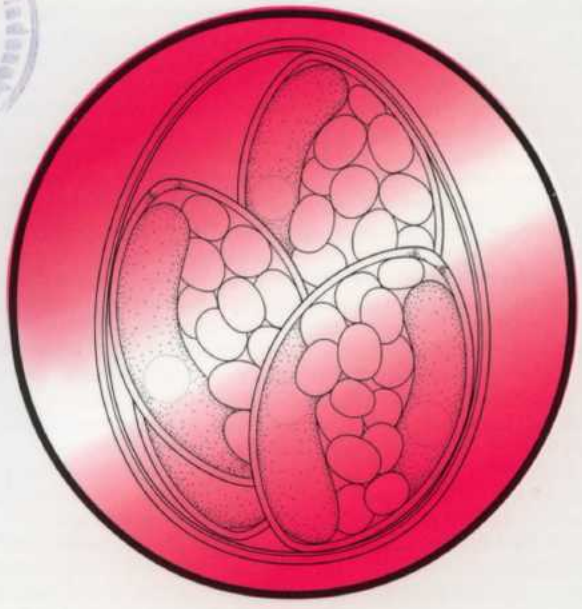

NENCKI INSTITUTE OF EXPERIMENTAL BIOLOGY
WARSAW, POLAND

2006

VOLUME 45 NUMBER 3
ISSN 0065-1583

Polish Academy of Sciences
Nencki Institute of Experimental Biology
and
Polish Society of Cell Biology

ACTA PROTOZOOLOGICA
International Journal on Protistology

ACTA PROTOZOOLOGICA appears quarterly.

The price (including Air Mail postage) of subscription to *Acta Protozoologica* at 2006 is: 200.- € by institutions and 120.- € by individual subscribers. Limited numbers of back volumes at reduced rate are available. Terms of payment: check, money order or payment to be made to the Nencki Institute of Experimental Biology account: 91 1060 0076 0000 4010 5000 1074 at BPH PBK S.A. Warszawa, Poland. For the matters regarding *Acta Protozoologica*, contact Editor, Nencki Institute of Experimental Biology, ul. Pasteura 3, 02-093 Warszawa, Poland; Fax: (4822) 822 53 42; E-mail: j.sikora@nencki.gov.pl For more information see Web page **http://www.nencki.gov.pl/ap.htm**

Front cover: Jirků M. and Modrý D. (2005) *Eimeria fragilis* and *E. wambaensis*, two new species of *Eimeria* Schneider (Apicomplexa: Eimeriidae) from African anurans. *Acta Protozool.* **44:** 167-173

This publication is supported by the Ministry of Science and Higher Education

Desktop processing: Justyna Osmulska, Information Technology Unit of the Nencki Institute
Printed at the MARBIS, ul. Poniatowskiego 1
05-070 Sulejówek, Poland

ACTA
PROTOZOOLOGICA

ANNOUNCEMENT

The Jagiellonian University, - New Publisher of *Acta Protozoologica*

The Nencki Institute of Experimental Biology of the Polish Academy of Sciences, the publisher of the journal *Acta Protozoologica* since 1963, informs all readers and authors that it will cease publishing the journal as of January 1, 2007. As the present Publisher, the Institute declares that all benefits and rights to the journal after January 1, 2007 shall be owned Jagiellonian University, Kraków, Poland.

I am convinced the cooperation of the Polish Society of Cell Biology in financial support of the journal *Acta Protozoologica* will be as generous as over the previous decade.

The present Publisher extends its sincere thanks to all Members of Editorial Board, editors and collaborating scientists around the world who over the years have dedicated their valuable time and expertise to reviewing papers submitted for publication in *Acta Protozoologica*.

Jerzy Duszyński
Director

New Editorial of *Acta Protozoologica*:

Krzysztof Wiąckowski, Ph. D. - Editor-in-Chief;
Janusz Fyda, Ph. D. - Editor

Address:

Department of Hydrobiology
Institute of Environmental Sciences
Jagiellonian University
Gronostajowa 7
30-387 Kraków, Poland
Phone: +48 12 664-51-80
Fax: +48 12 664-69-12
E-mail: wiacko@eko.uj.edu.pl

Acta Protozool. (2006) 45: 215 - 224

ACTA
PROTOZOOLOGICA

Contribution by the Methanogenic Endosymbionts of Anaerobic Ciliates to Methane Production in Dutch Freshwater Sediments

Angela H.A.M. van HOEK*, Theo A. van ALEN, Godfried D. VOGELS and Johannes H.P. HACKSTEIN

Department of Evolutionary Microbiology, Faculty of Science, Radboud University Nijmegen, Nijmegen, The Netherlands

Summary. Biogenic methane contributes substantially to the atmospheric methane concentration and thus to global warming. This trace gas is predominantly produced by strictly anaerobic methanogenic archaea, which thrive in the most divergent ecological niches, e. g. paddy fields, sediments, landfills, and the digestive tract of various animals. Methanogenic archaea also live as endosymbionts in the cytoplasm of anaerobic protozoa. In marine sediments these endosymbionts can contribute up to 90% to the overall rate of methanogenesis, whereas their role of in freshwater sediments is largely unknown. Here we describe the results of a one year's survey of the methanogenesis by endosymbiotic methanogens in four different Dutch freshwater sediments. The abundance of anaerobic protozoa, in particular ciliates, the methane production rates by the ecosystem and by the protists, and a number of abiotic parameters were measured. A novel method (heat-shock for 5 min) for estimating the contribution by endosymbiotic methanogens was established. Our results reveal large fluctuations of ciliate abundance throughout the year, but on average, only minor contributions by methanogenic endosymbionts to the total methanogenesis in these environments.

Key words: anaerobic ciliates, endosymbionts, freshwater sediments, methanogenesis, single cell PCR, SSU rRNA.

INTRODUCTION

Methanogenic archaea account for an annual global production of some 400 million metric tons of methane (Ferry 1997). This has a profound impact on the global change, because the atmospheric methane, which originates from these biological sources, can contribute for about 20% to global warming (Lindau *et al*. 1993). Since atmospheric methane concentrations have increased steadily by about 1-2% per year through the last decades, (Ferry 1997), detailed information about the biological - but also the unconventional, i.e. plant-dependent - sources of methane production is required for an assessment of the possibilities for a global management of greenhouse gasses (Chynoweth 1996, Waßmann and Rennenberg 1996, Hansen *et al*. 2000, Frankenberg *et al*. 2005, Keppler *et al*. 2006).

Methane formation by methanogenic archaea occurs in nearly all anaerobic environments such as, for example, marine- and freshwater sediments, marshes, wetlands, and tundra's (Williams and Crawford 1984,

Address for correspondence: Johannes H. P. Hackstein, Department of Evolutionary Microbiology, Faculty of Science, Radboud University Nijmegen, Toernooiveld 1, NL-6525ED Nijmegen, The Netherlands; Fax: +31-24-3553450; E-mail: j.hackstein@science.ru.nl

*Present address: RIKILT Institute of Food Safety, Bornsesteeg 45, NL-6708PD, Wageningen, The Netherlands.

Zinder 1993). Also, the gastro-intestinal tracts of arthropods and herbivorous vertebrates represent significant sources for atmospheric methane (Crutzen *et al.* 1986, Fraser *et al.* 1986, Hackstein and Stumm 1994, Hackstein *et al.* 1996, Moss *et al.* 2000). Notably, certain methanogenic archaea thrive as intracellular symbionts in the cytoplasm of anaerobic protozoa such as amoebae, flagellates and ciliates (Vogels *et al*. 1980; van Bruggen *et al.* 1983; Fenchel and Finlay 1995; van Hoek *et al.* 2000; Hackstein *et al.* 2002, 2006). The basis for these endosymbiotic, mutualistic associations between protozoa and methanogenic archaea is provided by the host's hydrogenosomes, organelles that generate hydrogen, carbon dioxide, acetate, and ATP (Müller 1993, Fenchel and Finlay 1995, Hackstein *et al*. 2001, Martin *et al*. 2001, Embley *et al*. 2003, Yarlett and Hackstein 2005). These hydrogenosomes provide the nutritional basis for the persistence of hundreds to thousands of methanogenic endosymbionts, which colonise a single host cell (Wagener *et al.*1990, Fenchel and Finlay 1992, Finlay and Fenchel 1992, Esteban *et al.* 1993, van Hoek *et al.* 2000, Hackstein *et al*. 2002).

In marine sediments, the methanogenic endosymbionts of anaerobic protozoa can contribute substantially to biogenic methane production (Fenchel 1993). Also, rumen protozoa with their episymbionts can play an important role in the methanogenesis in the gastrointestinal tract of large herbivorous animals: elimination of these protozoa from the ruminal ecosystem can result in a decrease of methane production by some 9-45% (Newbold *et al.* 1995, Tokura *et al.* 1999). Lastly, the methanogenic endosymbionts of anaerobic ciliates in cockroaches are believed to be the major source of methane in the hindgut of these insects (Gijzen *et al.* 1991, Gijzen and Barughare 1992).

In certain freshwater sediments and rice field soils anaerobic protozoa (with methanogenic endosymbionts) can be rather abundant (Finlay and Fenchel 1991; Khalil and Shearer 1993; Finlay *et al.* 1998, 1999; Schwarz and Frenzel 2005). However, only a few studies have attempted unravelling the contribution of their endosymbionts to the production of methane in these environments so far, although anoxic freshwater environments are believed to account for more than 20% to the total methane flux to the atmosphere globally. Also, seasonal changes in methane production and the abundance of ciliates did not find the necessary attention in the past. Therefore, we have monitored the abundance of anaerobic ciliates, methane production by ciliates and free-living archaea and several biotic and abiotic parameters in four Dutch freshwater sediments over a period of one year. We established a novel technique (heat-shocking) for assaying the contributions of anaerobic ciliates to the methane emissions in strictly anaerobic microcosms. With the aid of this technique, we were able to demonstrate that the contribution of the endosymbionts of anaerobic ciliates to methanogenesis in these ecosystems differs locally by at least one order of magnitude, and is subject to substantial annual fluctuations. However, on average, the contribution of anaerobic ciliates is marginal with respect to the total emissions of methane in Dutch freshwater ecosystems.

MATERIALS AND METHODS

Freshwater sediments

The samples were collected from October 1994 to September 1995 in one-month-intervals at four different locations in the vicinity of Nijmegen, The Netherlands (51°45'North 5°55'East (QRA-locator: JO21XS)), i.e. in a ditch of a minerotrophic peat-land ("de Bruuk"), a sludge backing pond of a wastewater treatment ("Dekkerswald"), an oligotrophic pond ("Plasmolen") and a low-land brook ("Tielebeek"). Sampling in 1l bottles was performed under strictly anaerobic conditions as described by Lomans *et al.* (1997). The *in situ* temperature of the sediment was measured prior to sampling. At larger intervals the alkalinity, the conductivity, the pH, and the velocity of the streaming water at the different sampling sites was measured with the aid of a YSI model 33 SCT meter.

Ciliate count

The number of the anaerobic ciliates was determined under a dissecting microscope at 50× magnification after diluting 100 µl sediment slurry with an equal amount of filter-sterilised (0.2 µm) sediment (pore)-water. The average ciliate number was determined by five independent counts using a Sedgewich rafter (Graticules LTD, Tonbridge, Kent, UK). The anaerobic ciliates were determined to the genus level with the aid of Hausmann (1985) and Patterson and Hedley (1992), which are useful for a rapid determination *in vivo*. Light- and epifluorescence microscopy of selected (living) specimen at 400× magnification was used to confirm the identity of the anaerobic ciliates and the presence endosymbiotic methanogenic archaea by their characteristic autofluorescence *in vivo* (Doddema and Vogels 1978).

Molecular identification

Single ciliates were isolated from the sample with the aid of a micropipette made from a drawn out Pasteur pipette, washed three times with sterile, anaerobic electromigration buffer (van Hoek *et al.* 1999), transferred to a Eppendorf tube and centrifuged. After addition of 50 µl of a 5% Chelex-100 suspension (Walsh *et al.* 1991) the samples were frozen and stored at -20°C. DNA extraction was performed by adding proteinase K (10 mg/ml), incubation for 3-4 h at 56°C, and subsequent heating at 95°C for 10 min. After centrifuga-

tion, the supernatant was used for PCR with primers directed against the 16S and 18S rRNA genes of the endosymbionts and the ciliate, respectively, as described earlier (van Hoek *et al.* 1998, 2000).

Phylogenetic analysis

Small ribosomal DNA sequences from the anaerobic ciliates and their methanogenic endosymbionts were aligned using the PileUp program of the Wisconsin package, version 8.1 (Wisconsin package Version 8.1, Genetics Computer Group (GCG), Madison, Wisconsin). EDNADIST (Rice *et al.* 1995) was used to calculate the sequence similarity and evolutionary distances using the Jukes and Cantor (1969) nucleotide substitution model. Phylogenetic trees were constructed using the neighbour-joining method (Saitou and Nei 1987). The 18S rRNA gene sequences of the following ciliates were used for the construction of the phylogenetic trees: *Brachonella* sp. from "de Bruuk" (AJ009665), *Brachonella* sp. from "Plasmolen" (AJ009664), *Caenomorpha*-like sp. 1 from "Dekkerswald" (AJ009658), *Caenomorpha* sp. 2 from "Dekkerswald" (AJ009660), *Caenomorpha*-like sp. 4 from "Dekkerswald" (AJ009661), *Caenomorpha*-like sp. 8 from "Dekkerswald" (AJ009662), *Caenomorpha* sp. 10 from "Dekkerswald" (AJ009659), *Caenomorpha* sp. from "Plasmolen" (AJ009663), *Caenomorpha uniserialis* (U97108), *Metopus contortus* (Z29516), *Metopus palaeformis* (M86385), *Plagiopyla nasuta* (Z29442), *Plagiopyla frontata* (Z29440), *Trimyema compressum* (Z29438), *Blepharisma americanum* (M97909). The 16S rRNA gene sequences of the corresponding methanogenic endosymbionts have the following accession numbers: *Caenomorpha*-like sp. 1 from "Dekkerswald" (AJ132648), *Caenomorpha*-like sp. 4 from "Dekkerswald" (AJ132649), *Caenomorpha*-like sp. 8 from "Dekkerswald" (AJ132650), *Caenomorpha* sp. 10 from "Dekkerswald" (AJ132651), *Caenomorpha* sp. 2 from "Dekkerswald" (AJ132652), *Caenomorpha* sp from "Plasmolen" (AJ132653), *Brachonella* sp from "de Bruuk" (AJ132655), *Brachonella* sp. from "Plasmolen" (AJ132654), *Metopus contortus* (Z13957), *Metopus palaeformis* (M86386), *Plagiopyla frontata* (Z29439), *Plagiopyla nasuta* (Z29437), *Trimyema compressum* (M96976), *Methanococcus voltae* (M59290)

Sediment incubations and methane measurements

After settling for at least 1 h the sediment samples were adjusted to a sediment/water ratio of 1:1 (v/v) by either removing water or sediment in an anaerobic glove box. The sediment samples were thoroughly mixed and aliquots of 20 ml were dispensed in 60 ml crimp top serum bottles. The bottles were sealed with black butyl rubber stoppers and flushed with oxygen-free nitrogen gas. Ethane was added as an internal standard for methane concentration measurements. The sediment slurries were incubated in the dark without shaking at 15°C for 24-48 h. At regular time intervals gas samples were taken from the headspace after shaking of the bottles. The gas sample was analysed on a Pye Unicam gas chromatograph equipped with a flame ionisation detector and a Porapak Q (80/100 mesh) column for the presence of methane. The methane production rate was determined from the linear increase of CH_4 in time using linear regression analysis. The measurements were not extended beyond 48 h in order to avoid excystation of ciliates from resting stages and to guarantee a survival of all ciliates present in the sample over the whole incubation period.

The dry weight of the sediment was determined after the incubation period by drying to a constant weight at 80°C. To determine the organic weight of the sediments, the dried sediment was reduced to ashes by heating to 550°C for 4 h.

Measuring the contribution to methane production by anaerobic ciliates

To estimate the contribution of anaerobic protozoa to the methane production several separation/removal methods, such as filtration over a 100 µm nylon gaze, the ice-elution method of Uhlig (Uhlig 1964), electromigration (Wagener *et al*. 1986, van Hoek *et al*. 1999), and micropipetting were tested for feasibility and reproducibility. Since all these methods were very time consuming and, in addition, led to irreproducible results, a novel method, a heat treatment of the sediment was developed. A heat-shock of 45°C for 5 min was applied to the incubation flasks in a waterbath. This treatment effectively killed all anaerobic ciliates present in the sediment.

For the determination of the contribution of the methanogenic endosymbionts, well mixed 20 ml of sediment slurries were adjusted to a sediment/water ratio of 1:1 (v/v) and dispensed into 60 ml bottles in an anaerobic glove box. Half of the bottles prepared this way were heat-shocked for 5 min at 45°C to allow determination of the methane production by free-living methanogens, the other half was not heat-shocked for a measurement of the methane production by the undisturbed sediment. The contribution of the endosymbionts was calculated from the difference between both measurements.

RESULTS

Abiotic parameters of the sampling sites

The four different sampling places near Nijmegen, The Netherlands, [51°45'N 5°55'E (QRA-locator: JO21XS)], are substantially different, but characteristic for many freshwater sediments in the Netherlands (Table 1). "de Bruuk" is a ditch in a minerotrophic peatland, "Dekkerswald" a sludge backing pond of a wastewater treatment, "Plasmolen"an oligotrophic pond in a deciduous forest, and "Tielebeek"a low-land brook. Three of the sampling places contained more or less complex communities of anaerobic ciliates; one site ("Tielebeek"), however, did not contain any anaerobic ciliates throughout the year. The yearly temperature course in the sediments followed largely the average ambient and ground temperatures as documented by the National Centre for Meteorology, the KNMI in de Bilt, The Netherlands (Fig. 1).

Seasonal variations in the abundance of anaerobic (ciliated) protozoa

The four different freshwater sediments were screened once a month for the presence of anaerobic protists as

Table 1. Features of the four Dutch freshwater sediments.

	de Bruuk	Dekkerswald	Plasmolen	Tielebeek
Characteristics	ditch of a minerotrophic peatland	sludge backing pond of a wastewater treatment	oligotrophic pond	low-land brook
Depth (m)	1.0-1.5	0.25-0.5	0.5-0.75	0.25-0.5
Alkalinity (mM)	0.4	0	0	0.01
Conductivity (µS)	430	425	380	170
pH	6.3	6.5	6.4	5.9
Velocity (m/s)	0	0	0	0.02
Organic matter[1]	15 ± 4.2	28.5 ± 6.4	58.8 ± 5.7	11.3 ± 3.3
Sediment colour	Black	green/brown	red/brown	green

[1]The organic matter was calculated as the year's average of the percentage organic weight of the dry weight of the sediment samples.

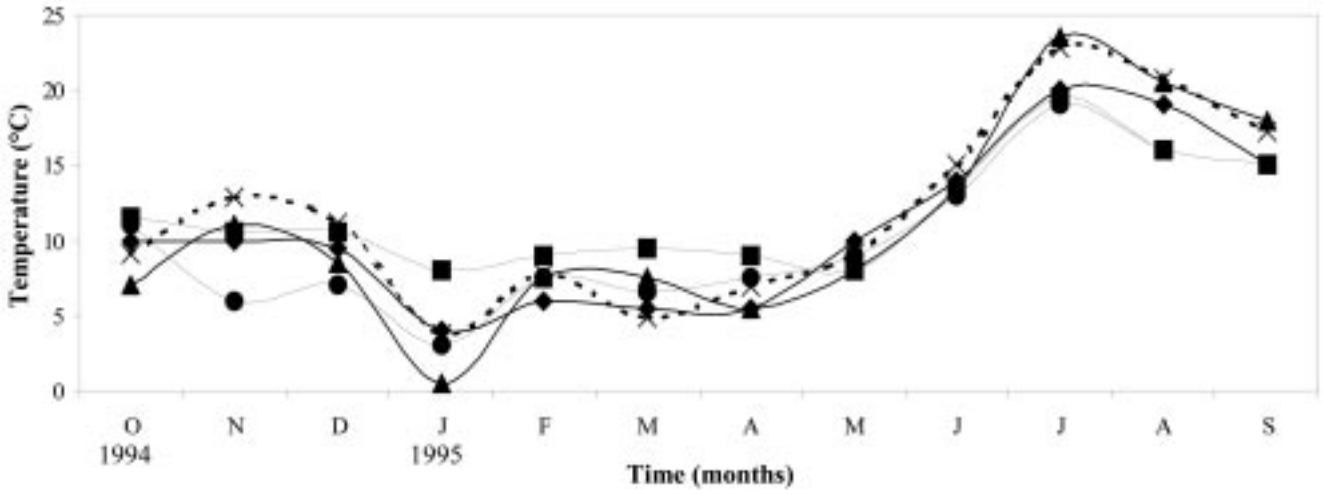

Fig. 1. *In situ* sediment temperature and average day temperature (according to the KNMI, The Netherlands) during the sampling days, from October 1994 until September 1995. "de Bruuk" sediment - filled circle, "Dekkerswald" sediment - filled triangle, "Plasmolen" sediment - filled diamond, "Tielebeek" sediment - filled square, and KNMI data - ×.

described in Materials and Methods by direct observation *in vivo*. Ciliates were the most abundant anaerobic protists in 3 out of the 4 sediments. Only a few anaerobic flagellates and amoebae were observed. Anaerobic ciliates were completely absent in the "Tielebeek" sediments over the whole one-year's survey. At the other three sampling places, the number of anaerobic ciliates exhibited a substantial variation over the year with remarkable differences between the different locations (Fig. 2). For example, the number of anaerobic ciliates exceeded 100/ml in the "de Bruuk" sediment only in the first two months of our survey (October, November), but declined to less than 50 ciliates per ml sediment for the rest of the year (Fig. 2A). The number of ciliates in "Plasmolen" sediment revealed no clear trends - during some months ciliate numbers were as low as 25 ciliates/ml sediment, whereas in other months up to 90 ciliates/ml sediment were counted (Fig. 2C). On the other hand, the number of ciliates in the "Dekkerswald" sediment exhibited a distinct peak in March with more

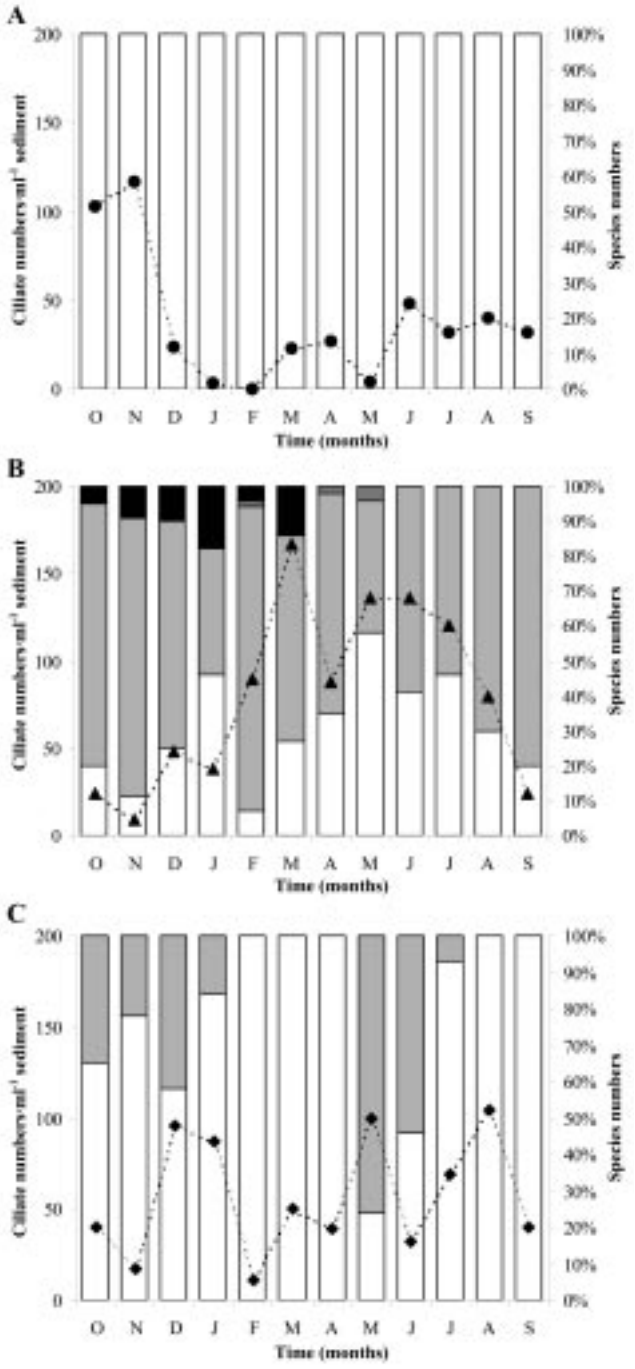

Figs 2A-C. The total number of anaerobic ciliates and the distribution of the species in the four different sediments; **A** - "de Bruuk" sediment; **B** - "Dekkerswald" sediment; **C** - "Plasmolen" sediment. At regular time intervals gas samples were taken from the headspace after shaking. The "Tielebeek" sediment did not contain any anaerobic ciliates throughout the screening. The circles, the triangles, and the diamonds indicate the total number of anaerobic ciliates in the three different sediments, respectively. Open bars indicate the percentage of *Brachonella* spp. of the total number of anaerobic ciliates; light-grey bars *Caenomorpha* spp.; dark-grey bars *Metopus* spp.; black bars *Plagiopyla* spp.

than 150 ciliates/ml, which remained at a rather high level of more than 100 ciliates /ml in the following months, with a short dip in April followed by a constant decline of ciliate numbers (Fig. 2B).

Methane production in freshwater sediments

The methane concentration in the headspace was measured in regular time intervals up to 48 h, when the ciliates were still alive. Figure 3 shows that the methane production rates in the four sampling places were different. All exhibited pronounced seasonal variations. "Dekkerswald" sediment had the highest methane production rate of all sites, up to a maximum of 17 µmol CH_4/g organic weight/h. The maximal rates of the other three sediments were 5-10 times lower; they did not exceed some 2-3 µmol CH_4/g organic weight/h. Also the seasonal pattern was different for the "Dekkerswald" sediment: the methane production rate showed an unimodal distribution from November until September of the next year with a peak in May while the other three sediments exhibited a bimodal distribution of methane production with a minimum production in May (Figs 3A, C, D).

Contribution to methane production by anaerobic ciliates

Figure 3 clearly shows that in all three ciliate containing sediments the peaks of methane production did not coincide with the maxima of the ciliate abundance. Accordingly, the removal of the ciliates in the microcosms by heat-shocking had no significant effect on the methane production in the ciliate-free slurries. Only in samples with ciliate counts above 70-80 ciliates/ml the methane production was slightly, but significantly, lowered after the removal of the ciliates (grey bars in Fig. 3). This was the case only the months February, March, and April in the "Dekkerswald" samples (Fig. 3B), and the month July in the "Plasmolen" samples. Unexpectedly, the heat-shock treatment of "Dekkerswald" samples in the months May, June, and July led to a slightly increased methane production (Fig. 3B). In all other months, the removal of ciliates by the heat-shock treatment did not cause significant changes in the methane production, confirming a minor role of the methanogenic endosymbionts in methane formation. Notably, the validity of the heat-shock technique for the removal of the ciliates was confirmed by the absence of any significant changes in methane production by the samples in 11 out of the 12 months studied from the "Tielebeek" location where ciliates were absent through-

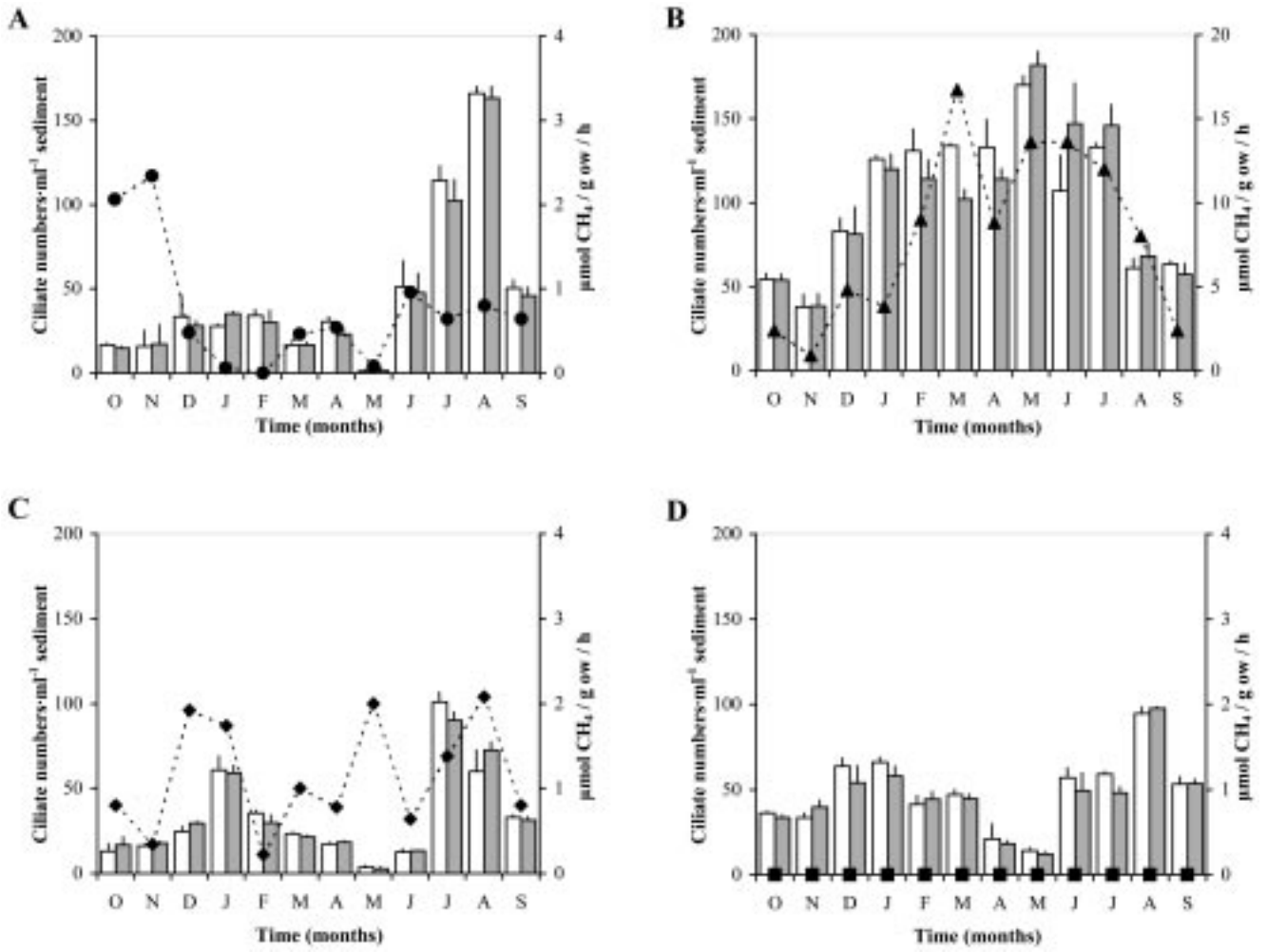

Figs 3A-D. Methane production rates of the various sediment samples; **A** - "de Bruuk" sediment; **B** - "Dekkerswald" sediment; **C** - "Plasmolen" sediment; **D** - "Tielebeek" sediment. The open bars represent untreated sediment slurries and the grey bars represent heat-shocked sediment samples (5 min 45°C). All scales are similar with the exception of the methane production of "Dekkerswald", which had to be enlarged because of the height of the production rates. The standard deviations are indicated by bars; they are based on three independent measurements. "g ow" indicates organic weight in gram. The total number of anaerobic ciliates in the four sediments is also indicated (circles, triangles, diamonds, and squares, respectively, see Fig. 2).

out the year (Fig. 3D). In 8 of such samples, heat-shock treatment caused an insignificant decrease of the methane production, whereas in 3 samples a slight, but insignificant increase could be observed.

Diversity of the anaerobic ciliates

Sediments lacking anaerobic ciliates completely, (and significant numbers of anaerobic flagellates as well), can produce up to 2 µmol CH_4/g organic weight/h (Fig. 3D, "Tielebeek"). These methane emissions, on average, are higher than those from "Plasmolen" samples that can host up to some 90 ciliates/ml, and only slightly lower than those from "de Bruuk", where up to 150 ciliates/ml were observed. The "Dekkerswald" sediments on the other hand, have methane production rates, which are up to four times higher. In the latter sediment, the highest numbers of ciliates and the highest ciliate diversity were observed (Figs 2, 3). To rule out whether these differences correlate with ciliate diversity or not, single cell PCR was used to discriminate between identical and different ciliate species in the various sampling places and to get a preliminary overview about complexity of

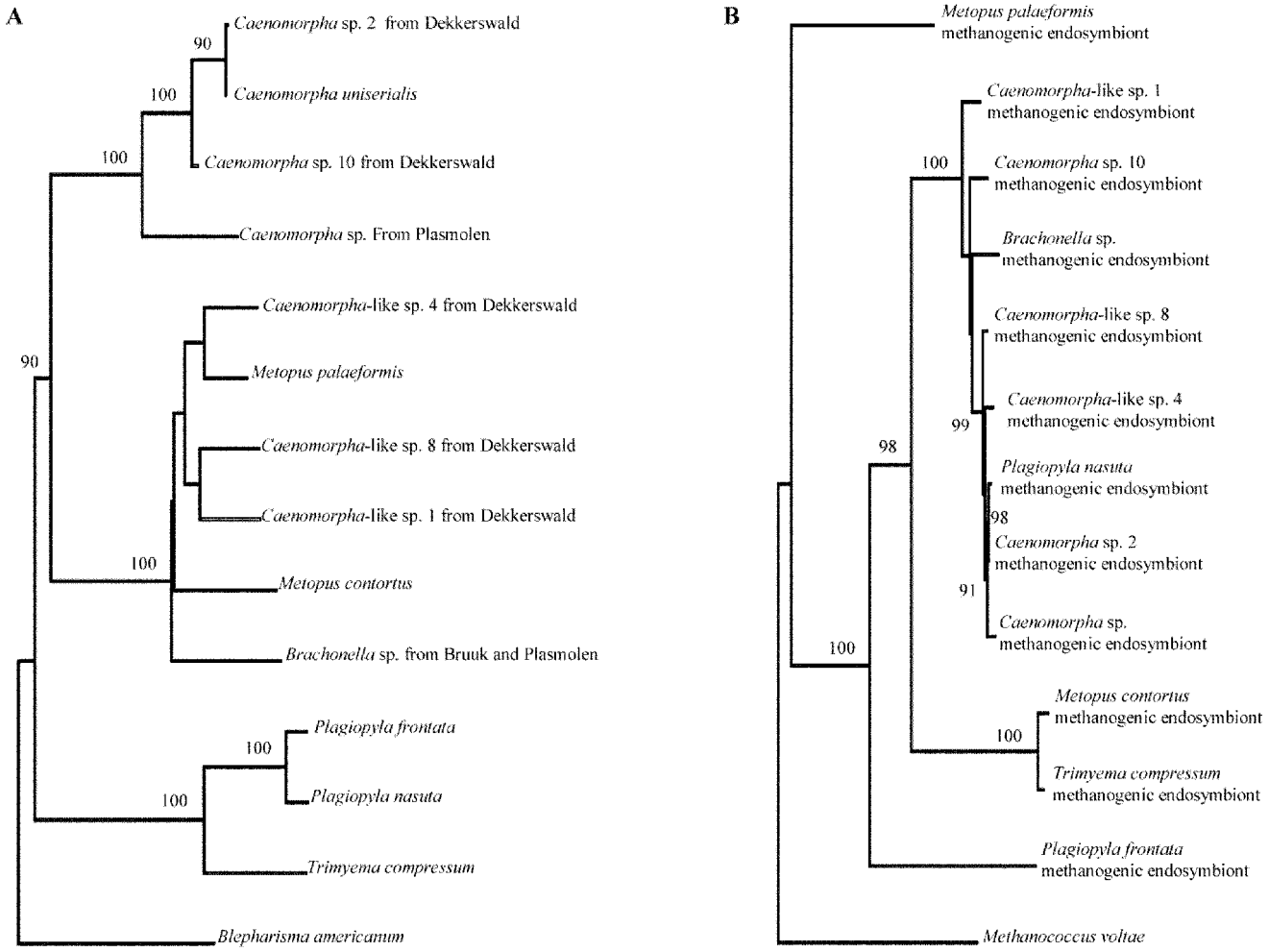

Figs 4A, B. A - phylogenetic relationship of free-living anaerobic ciliates; **B** - and their methanogenic endosymbionts, based on the SSU rRNA gene. The alignments were reduced to approximately 460 (18S) and 770 (16S) positions in order to remove hypervariable regions and gaps. The trees were constructed by the neighbour-joining method. The distance data were bootstrap resampled 100 times (Felsenstein 1985). Only bootstrap values above 90% are displayed. For accession numbers of the sequences used see Materials and Methods.

the ciliate population. The isolation of DNA from single cells allows the retrieval of SSU rDNA sequences from both the ciliate and the endosymbiont, which permits an unequivocal identification of identical species (van Hoek *et al.* 2000). Therefore, the 18S rDNA of individual ciliates and the 16S rDNA of their methanogenic endosymbionts were amplified by PCR: and subjected to DNA sequence analysis. Phylogenetic analysis revealed that a distinct ciliate 18S rDNA always correlated with a specific 16S rDNA from the methanogenic endosymbiont, regardless of the sampling place. On this basis, it was possible to identify even closely related ciliates unequivocally. Figure 4 shows, that ciliates with nearly identical "ribotypes" could be discriminated by their different methanogenic endosymbionts. On this basis, in the "Dekkerswald" sediment the most diverse population of anaerobic ciliates could be identified - exceeding the expectations based on the *in vivo* identification by far (Figs 2, 4).

Especially, it revealed the existence of ciliates, which look very similar to *Caenomorpha uniserialis,* but are phylogenetically rather unrelated, i.e. the various *Caenomorpha*-likes. On the other hand, the combination of ciliate and endosymbiont SSU rRNA data also

demonstrated unequivocally that only the *Brachonella* sp. found in both "de Bruuk"- and "Plasmolen" sediments were identical (i.e. *Brachonella* sp., Fig. 4). All other anaerobic ciliates studied here were unique for their particular sampling places.

DISCUSSION

Analysis of four different sampling sites near Nijmegen, The Netherlands, at monthly intervals over a period of one year, clearly showed that a correlation between the methane emissions and the number of anaerobic ciliates in the particular sample did not exist. Ciliate counts of about 100 ciliates/ml can correlate with methane emission rates of less than 1 µmol CH_4/g organic weight/h, but also with emission rates of up to 15 µmol CH_4/g organic weight/h. Even sediments lacking anaerobic ciliates completely, (and significant numbers of anaerobic flagellates or amoebae with endosymbiotic methanogens as well; i.e. "Tielebeek") can produce up to 2 µmol CH_4/g organic weight/h (Fig. 3). Thus, given a comparable abundance of anaerobic ciliates in a sample, the methane emissions of these samples can vary by a factor of ten or more if normalised for organic matter in the sediments. Organic matter appeared to be the most convenient basis for comparisons between different freshwater sediments; Table 1 displays the average correlations between dry-weight and organic weight for the various sample places. Consequently, neither indirect effects by grazing nor the direct contributions to methane formation by the methanogenic endosymbionts of the anaerobic ciliates can be responsible for the observed differences in methane production in these Dutch freshwater sediments. Rather, free-living methanogens must account for the vast majority of the methane emissions in these ecosystems. Our data also reveal that even in the presence of high numbers of anaerobic ciliates in the sediments (i.e. more than 90 ciliates/ml) the endosymbionts can contribute for maximally 10% to the methane emissions of a freshwater sediment. The four Dutch freshwater sediments on average produce approximately 60 nmol methane per hour per ml of sediment. Given that a single freshwater ciliate should not produce more than 1-5 pmol methane/h, then 100 to 180 ciliates/ml, which represents the maximum abundance in the sediments studied here, could account for not more than 180-900 pmol methane/h - about 2% of the total methane production. This figure is well in the range of the 1-3 µmol methane/g organic weight/h that could be attributed to the ciliates in this study using the heat-shock technique (Fig. 3B). These 1-3 µmol correspond to 5-18% of the total methane production in these samples, but this contribution is limited to a few months of the year and to samples with the highest ciliate numbers. It is obvious that the calculations based on measurements of isolated ciliates *in vitro* (Fenchel and Finlay 1992, Schwarz and Frenzel 2005) lead to a slight underestimation of the contribution to methane production *in situ* by isolated ciliates. The composition of the ciliate community and the overall level of methane production in particular sediment seem to have a certain influence on the contribution by ciliates. Furthermore, it seems likely that grazing effects on the microbiota and differences in ciliate physiology are of greater importance than the mere number of methanogenic endosymbionts. In order to account for a contribution of 50% to the methane production in the sediments studied here, the number of ciliates in the samples must be one to two orders of magnitude higher than observed in this study. Such numbers are unlikely to be found in any Dutch freshwater sediment, but such numbers of ciliates can be reached in certain tropical environments.

The composition of the ciliate community seems to exert some influence on the methane emission. Our (preliminary) molecular analysis revealed that a meaningful assessment will require a detailed community analysis allowing identifying all changes of ciliate abundance quantitatively. Unfortunately, such a technique was not available when the survey was conducted. The increasing 18S rDNA databases of ciliates and the available molecular techniques for accessing the composition of the protozoal community in freshwater sediments will make such an analysis feasible in near future.

We have shown here, that the contribution of anaerobic ciliates to the methane production in Dutch freshwater sediments - in general - is marginal throughout the year (Fig. 3) - in clear contrast to the situation in marine sediments (Fenchel 1993), where the contribution of anaerobic ciliates to the methane production is significant. These observations principally confirm earlier speculations about a minor impact of freshwater ciliates on methane emissions (Finlay and Fenchel 1991; Khalil and Shearer 1993; Finlay *et al.* 1998, 1999) which were based on measurements of isolated ciliates under highly artificial conditions. However, the lack of suitable methods to measure the methane production of freshwater sediments after the removal of ciliates did not allow testing the validity of the extrapolations so far. Here, we

have established that heat-shocking for 5 min at 45°C allows a quantitative and efficient killing of the anaerobic ciliates in the sample without interfering significantly with the methane production by the free-living methanogens in the sample. This method requires only a short temperature pulse and avoids the difficult interpretation of results obtained after the treatment of freshwater sediments with high doses of antibiotics. All ciliates in the sample burst and become completely disintegrated within 5 min. Endosymbiotic methanogens from *Caenomorpha/Caenomorpha*-like ciliates might survive outside their hosts for some 48 h, but it is very unlikely that significant numbers of the endosymbionts of the other ciliates can survive in pore water of such a low osmotic pressure. Microscopical observations suggest that the methanogens burst easily after release from their ciliate hosts due to osmotic shock both in freshwater sediments and cockroach guts (unpublished).

Studies on several *Nyctotherus* strains from the hindgut of cockroaches have revealed substantial differences in the number of methanogenic endosymbionts between ciliates from different lines of cockroaches (van Hoek *et al.* 2000). A similar situation can be anticipated for the various anaerobic ciliates from the freshwater sediments on the basis of differences of the intensity of the autofluorescence of the ciliates (not shown). However, because of the sensitivity of the anaerobic ciliates for manipulations, and a rapid fading of the autofluorescence of the endosymbionts it is rather difficult to count the endosymbionts of the various species with the necessary accuracy. Interestingly, a simple correlation between the number of methanogenic endosymbionts and the methane production rates of the various ribotypes of cockroach-dwelling ciliates does not exist (van Hoek *et al.* 2000). Rumen ciliates produce approximately a hundred times more methane (83-250 pmol/h) - potentially due to the high numbers of methanogens, which can attach to the surface of the rumen ciliates (Kisidayova *et al.* 2000, Ushida and Jouany 1996). Nevertheless, it is possible to make some rough estimation about the methane production by the endosymbionts. Assuming that a single methanogenic bacterium can produce about 1 fmol CH_4/h (Fenchel and Finlay 1992), then a single ciliate with some 1000-5000 endosymbiotic methanogens would be able to produce 1-5 pmol methane per hour. Comparable values have been measured after incubation of anaerobic freshwater ciliates *in vitro* (Fenchel and Finlay 1992) and for *Nyctotherus ovalis* isolated from the cockroach hindgut (2.6-7.1 pmol CH_4/ciliate/h; van Hoek *et al.* 2000), but measurements *in situ*, which can take into account the real diversity of ciliates in the samples and the availability of nutrients and methanogenic substrates will allow to obtain more detailed results in the future.

Acknowledgements. This work was supported by a grant from the Netherlands Organisation for the Advancement of Pure Research (NWO) to A. H. A. M. van Hoek. The assistance of Xandra H. Dikhoff is gratefully acknowledged. We would like to thank Profs. W. Foissner and J. Newbold for critically reading of the manuscript.

REFERENCES

Chynoweth D. P. (1996) Environmental impact of biomethanogenesis. *Environ. Monit. Assessm.* **42:** 3-18

Crutzen P. J., Aselmann I., Seiler W. (1986) Methane production by domestic animals, wild ruminants, other herbivorous fauna and humans. *Tellus* **38B:** 271-284

Doddema H. J., Vogels G. D. (1978) Improved identification of methanogenic bacteria by fluorescence microscopy. *Appl. Environ. Microbiol.* **36:** 752-754

Embley T. M., van der Giezen M., Horner D. S., Dyal P. L., Foster P. (2003) Mitochondria and hydrogenosomes are two forms of the same fundamental organelle. *Phil. Trans. R. Soc. London, Ser. B* **358:** 191-201

Esteban G., Guhl B. E., Clarke K. J., Embley T. M., Finlay B. J. (1993) *Cyclidium porcatum* n. sp.: a free-living anaerobic scuticociliate containing a stable complex of hydrogenosomes, eubacteria and archaeobacteria. *Eur. J. Protist.* **29:** 262-270

Felsenstein J. (1985) Confidence limits on phylogenies: an approach using the bootstrap. *Evolution* **39:** 783-791

Fenchel T. (1993) Methanogenesis in marine shallow water sediments: the quantitative role of anaerobic protozoa with endosymbiotic methanogenic bacteria. *Ophelia* **37.** 67-82

Fenchel T., Finlay B. J. (1992) Production of methane and hydrogen by anaerobic ciliates containing symbiotic methanogens. *Arch. Microbiol.* **157:** 475-480

Fenchel T., Finlay B. J. (1995) Ecology and Evolution in Anoxic Worlds. Oxford University Press, Oxford, New York, Tokyo

Ferry J.G. (1997) Methane: small molecule, big impact. *Science* **278:** 1413-1414

Finlay B. J., Fenchel T. (1991) An anaerobic protozoon, with symbiotic methanogens living in municipal landfill material. *FEMS Microbiol. Ecol.* **85:** 169-180

Finlay B. J., Fenchel T. (1992) An anaerobic ciliate as a natural chemostat for the growth of endosymbiotic methanogens. *Eur. J. Protist.* **28:** 127-137

Finlay B. J., Esteban G. F., Fenchel T. (1998) Protozoan diversity: converging estimates of the global number of free-living ciliate species. *Protist* **149:** 29-37

Finlay B. J., Esteban G. F., Olmo J. L., Tyler P. A. (1999) Global distribution of free-living microbial species. *Ecography* **22:** 138-144

Frankenberg C., Meirink J. F., van Weele M., Platt U., Wagner T. (2005) Assessing methane emissions from global space-born observations. *Science* **308:** 1010-1014

Fraser P. J., Rasmussen R. A., Creffield J. W., French J. R., Khalil M. A. K. (1986) Termites and global methane - another assessment. *J. Atmosph. Chem.* **4:** 295-310

Gijzen H. J., Barughare M. (1992) Contribution of anaerobic protozoa and methanogens to hindgut metabolic activities of the American cockroach, *Periplaneta americana*. *Appl. Environ. Microbiol.* **58:** 2565-2570

Gijzen H. J., Broers C. A. M., Barughare M., Stumm C.K. (1991) Methanogenic bacteria as endosymbionts of the ciliate *Nyctotherus ovalis* in the cockroach hindgut. *Appl. Environ. Microbiol.* **57:** 1630-1634

Hackstein J. H. P., Stumm C. K. (1994) Methane production in terrestrial arthropods. *Proc. Nat. Acad. Sci. USA* **91:** 5441-5445

Hackstein J. H. P., Langer P., Rosenberg J. (1996) Genetic and evolutionary constraints for the symbiosis between animals and methanogenic bacteria. *Environ. Monit. Assess.* **42:** 39-56

Hackstein J. H. P., Akhmanova A., Voncken F., van Hoek A., van Alen T., Boxma B., Moon-van der Staay S. Y., van der Staay G., Leunissen J., Huynen M., Rosenberg J., Veenhuis M. (2001) Hydrogenosomes: convergent adaptations of mitochondria to anaerobic environments. *Zoology* **104:** 290-302

Hackstein J. H. P., van Hoek A. H. A. M., Leunissen J. A. M., Huynen M. (2002) Anaerobic ciliates and their methanogenic endosymbionts. In: Symbiosis: Mechanisms and Model Systems (Ed. J. Seckbach), Kluwer Academic Publishers, Dordrecht, The Netherlands 451-464

Hackstein J. H. P., van Alen T. A , Rosenberg J. (2006) Methane production by terrestrial arthropods. In: Intestinal Microorganisms of Termites and Other Invertebrates. Soil Biology, Manual for Soil Analysis, (Eds. H. König, A.Varma). Springer Verlag, Heidelberg, Germany **6:** 155-180

Hansen J., Sato M., Ruedy R., Lacis A., Oinas V. (2000) Global-warming in the twenty-first century: an alternative scenario. *Proc. Nat. Acad. Sci. USA* **97:** 9875-9880

Hausmann K. (1985) Protozoologie. Thieme Verlag Stuttgart, New York

Jukes T. H., Cantor C. R (1969) Evolution of protein molecules. In: Mammalian Protein Metabolism (Ed. H. N. Munro), Academic Press, New York, 21-132

Keppler F., Hamilton J. T. G., Brass, M., Rockmann T. (2006) Methane emissions from terrestrial plants under aerobic conditions. *Nature* **439:** 187-191

Khalil M. A. K., Shearer M. J. (1993) Sources of methane: an overview. In: Atmospheric Methane: Sources, Sinks, and Role in Global Change (Ed. M. A. K. Khalil), Springer Verlag, Heidelberg, Berlin, Germany180-198

Kisidayova S., Varadyova Z., Zelenak I., Siroka P. (2000) Methanogenesis in rumen ciliate cultures of *Entodinium caudatum* and *Epidinium ecaudatum* after long-term cultivation in a chemically defined medium. *Folia Microbiol.* **45:** 269-274

Lindau C. W., Patrick Jr. W. H, DeLaune R. D. (1993) Factors affecting methane production in flooded rice soils. In: Agricultural Ecosystem Effects on Trace Gases and Global Climate Change (Eds. D. E. Rolston, L. A. Harper), American Society of Agronomy special publication no. 55, Madison, USA, 157-165

Lomans B. P., Smolders A. J. P., Intven L. M., Pol A., Op den Camp H. J. M., van der Drift C. (1997) Formation of dimethyl sulfide and methanethiol in anoxic freshwater sediments. *Appl. Environ. Microbiol.* **63:** 4741-4747

Martin W., Hoffmeister M., Rotte C., Henze K. (2001) An overview of endosymbiotic models for the origins of eukaryotes, their ATP-producing organelles (mitochondria and hydrogenosomes), and their heterotrophic lifestyle. *Biol. Chem.* **382:** 1521-1539

Moss A. R., Jouany J. P., Newbold J. (2000) Methane production by ruminants: its contribution to global warming. *Anns Zootech.* **49:** 231-254

Müller M (1993) The hydrogenosome. *J. Gen. Microb.* **139:** 2879-2889

Newbold C. J., Lassalas B., Jouany J. P. (1995) The importance of methanogens associated with ciliate protozoa in ruminal methane production *in vitro*. *Lett. Appl. Microbiol.* **21:** 230-234

Patterson D. J., Hedley S. (1992) Free-Living Freshwater Protozoa; A Color Guide. Wolfe Publishing Ltd, England

Rice P., Lopez R., Doelz R., Leunissen J (1995) EGCG 8.0. *EMBnet.news*: **2:** 5-7

Saitou N., Nei M. (1987) The neighbor-joining method: a new method for reconstructing phylogenetic trees. *Mol. Biol. Evol.* **4:** 406-425

Schwarz M. V. J., Frenzel P. (2005) Methanogenic symbionts of anaerobic ciliates and their contribution to methanogenesis in an anoxic rice field soil. *FEMS Microbiol. Ecol.* **52:** 93-99

Tokura M., Chagan I., Ushida K., Kojima Y. (1999) Phylogenetic study of methanogens associated with rumen ciliates. *Curr. Microbiol.* **39:** 123-128

Uhlig G. (1964) Eine einfache Methode zur Extraktion der vagilen, mesopsammelen Mikrofauna. *Helgoländer wiss. Meeresunters.* 11**:** 178-185

Ushida K., Jouany J. P. (1996) Methane production associated with rumen ciliated protozoa and its effect on protozoan activity. *Lett. Appl. Microbiol.* **23:** 129-132

Van Bruggen J .J. A., Stumm C. K., Vogels G. D. (1983) Symbiosis of methanogenic bacteria and sapropelic protozoa. *Arch. Microbiol.* **136:** 89-95

Van Hoek A. H. A. M., van Alen T. A., Sprakel V. S. I., Hackstein J. H. P., Vogels G. D. (1998) Evolution of anaerobic ciliates from the gastrointestinal tract: phylogenetic analysis of the ribosomal repeat from *Nyctotherus ovalis* and its relatives. *Mol. Biol. Evol.* **15:** 1195-1206

Van Hoek A. H. A. M., Sprakel V. S. I., van Alen T. A., Theuvenet A. P. R., Vogels G. D., Hackstein J. H. P. (1999) Voltage-dependent reversal of anodic galvanotaxis in *Nyctotherus ovalis*. *J. Euk. Microbiol.* **46:** 427-433

Van Hoek A. H. A. M., van Alen T. A., Sprakel V. S. I., Leunissen J. A. M., Brigge T., Vogels G. D., Hackstein J. H. P. (2000) Multiple acquisition of methanogenic archaeal symbionts by anaerobic ciliates. *Mol. Biol. Evol.* **17:** 251-258

Vogels G. D., Hoppe W. F., Stumm C. K. (1980) Association of methanogenic bacteria with rumen ciliates. *Appl. Environ. Microbiol.* **40:** 608-612

Wagener S., Stumm C. K., Vogels G. D. (1986) Electromigration, a tool for studies on anaerobic ciliates. *FEMS Microbiol. Ecol.* **38:** 197-203

Wagener S., Schulz S., Hanselmann K. (1990) Abundance and distribution of anaerobic protozoa and their contribution to methane production in Lake Cadagno (Switzerland). *FEMS Microbiol. Ecol* **74:** 39-48

Walsh P. S., Metzger D. A., Higuchi R. (1991) Chelex-100 as a medium for simple extraction of DNA for PCR-based typing from forensic material. *BioTechniques*, **10:** 506-513

Waßmann R., Rennenberg H. (1996) Die Methanemission aus Reisfeldern. *Biologie unserer Zeit*. **26:** 272-281

Williams R. T. Crawford R. L. (1984) Methane production in Minnesota peatlands. *Appl. Environ. Microbiol.* **47:** 1266-1271

Yarlett N., Hackstein J. H. P. (2005) Hydrogenosomes: One organelle, multiple origins. *Bioscience* **55/8:** 657-668

Zinder S. H. (1993) Physiological ecology of methanogens. In: Methanogenesis (Ed. J. G. Ferry). Chapman and Hall, New York, London, 128-206

Received on 8th December, 2005; revised version on 14th April, 2006; accepted on 27th April, 2006

Acta Protozool. (2006) 45: 225 - 230

ACTA
PROTOZOOLOGICA

Preliminary Study on the Effect of Exposure to Low Temperature on the Viability of Both Mixed and Monocultures of Rumen Protozoa

Gabriel de la FUENTE[1], Manuel PÉREZ-QUINTANA[3], José Alvaro CEBRIÁN[2] and Manuel FONDEVILA[1]

[1] Departamento de Producción Animal y Ciencia de los Alimentos and [2] Departamento de Bioquímica y Biología Molecular y Celular, Universidad de Zaragoza, Zaragoza, Spain; [3] Departamento de Química y Biología, Universidad de Matanzas, Matanzas, Cuba

Summary. The effect of low temperatures on the viability of rumen protozoa was studied. In Trial 1, samples of mixed rumen contents were diluted and cultured at 38, 15 and 5°C for 2, 4 and 6 h, respectively. Viability of *Isotrichidae* was not affected by either the length of incubation or the temperature ($P < 0.10$). Incubation at low temperatures negatively affected the viability of *Entodinium*, *Diplodiniinae* and *Ophryoscolex*. Differences between 15 and 5ºC were not significant except for *Entodinium* spp. ($P = 0.07$). The reduction of viability increased with time, this effect being noticeable ($P < 0.10$) for *Entodinium* (after 4 and 6 h), *Diplodiniinae* (at 6 h) and *Ophryoscolex* (at 2 and 6 h). Preservation of mixed rumen protozoa for at least 4 h at 15 or 5°C did not markedly affect viability, suggesting that cultures can be recovered after short-term refrigeration. In Trial 2, monocultures of *Entodinium caudatum* and *Diploplastron* (*Metadinium*) *affine* were cultured at 5°C for 4, 8 and 24 h with or without milk powder/egg yolk solution as a membrane protector. For both species, viability was not affected after 4 h at 5°C, but decreased from 8 h onwards ($P < 0.01$). The use of a membrane protector improved viability of *D. affine* at all time periods ($P < 0.05$), but only at 24 h for *E. caudatum* ($P = 0.07$), showing that the use of membrane protector may be positive at medium or long exposure to low temperatures, depending on the species.

Key words: *Diploplastron* (*Metadinium*) *affine*, *Entodinium caudatum*, low temperatures, rumen protozoa, viability.

Abbreviations used: c.v. - coefficient of variation; s.e. - standard error.

INTRODUCTION

Survival of rumen protozoa is markedly reduced when they are subjected to low temperatures, making difficult their storage under refrigeration and later recovery. Most rumen ciliate species do not grow below 35°C (Williams and Coleman 1992). Although the cryopreservation of rumen protozoa has been studied (Kisidayova 1996, 1997; Nsabimana *et al*. 2003; de la Fuente *et al*. 2004, 2006), the possibility of maintaining samples of different protozoal species at refrigeration temperatures (below 15°C) for a moderate period of time has not been investigated.

Low temperatures can affect the viability of rumen protozoa either through loss of membrane integrity or lowered metabolic activity. De la Fuente *et al*. (2004) studied the viability of rumen protozoa by the double stain-fluorescence method of Harrison and Vickers (1990). This is based on the ability of carboxyfluorescein

Address for correspondence: Manuel Fondevila, Departamento de Producción Animal y Ciencia de los Alimentos, Universidad de Zaragoza, Miguel Servet 177, 50013 Zaragoza, Spain; Fax: 34-976 761590; E-mail: mfonde@unizar.es

diacetate to pass across the cell membrane and be converted to carboxyfluorescein by membrane esterases, thus staining the cytoplasm green. At the same time, propidium iodide can pass through the cell membrane only if it is damaged, thus staining nucleic acids in red. Therefore, results of low temperature incubation can be evaluated with respect to both membrane damage and inefficient enzymatic activity.

This experiment studies the effect of maintaining rumen protozoa at low temperatures for a short period of time. Effects of including a membrane protector in the medium on viability, either in mixed rumen samples or in established monocultures of two significant rumen species, was also investigated.

MATERIALS AND METHODS

Trial 1: **Viability of mixed rumen protozoa at refrigeration temperatures**

Rumen contents of a type A fauna (Eadie 1967) were obtained on four different sampling days from a donor rumen cannulated sheep. The animal was fed a 50:50 alfalfa hay: barley straw mixed diet enriched with a vitamin-mineral mixture. Samples were filtered through three layers of gauze and diluted 1:10 in a culture tube with protozoal culture medium M (Dehority 1998) under a stream of CO_2. Four tubes with 10 ml of mixed rumen protozoa at a 10^{-2} dilution were obtained by diluting 1.0 ml samples from the 1:10 dilution into separate culture tubes each containing 9.0 ml of the same medium. Dilution tubes were previously warmed up to 38°C and fed with 0.1 ml of a suspension of 1.5 % ground corn and 1.0 % alfalfa meal gassed with CO_2 for 20 min. One of the tubes was immediately processed to get an initial reference value (INIT) for protozoal concentration and viability, and the other three tubes were incubated at 38, 15 or 5°C. The temperature for refrigerated tubes was reduced to 15°C at 3ºC min^{-1} (for both 15 and 5°C treatments), and from 15 to 5°C at 6ºC min^{-1} for 5°C tubes, and maintained at those temperatures by incubation in a water bath. After 2, 4 and 6 h of inoculation, contents of the tubes were mixed by gentle agitation. Tubes were opened under a CO_2 stream, and 1 ml was sampled for viability studies, resulting four samples for each experimental treatment.

Trial 2: **Viability of pure protozoa cultures at 5°C**

Tubes with monocultures of *Entodinium caudatum* and *Diploplastron* (*Metadinium*) *affine* maintained in our laboratory were used as representative species of the rumen protozoa. Both cultures were previously obtained from strained sheep rumen fluid, by picking up one or two cells and transferring them to tubes with medium M for their anaerobic culture. Establishment and maintenance of cultures were performed as specified by de la Fuente *et al.* (2004).

A 10 ml volume per tube of each culture (38°C) was used in each of three experimental days. Tubes were initially sampled (1 ml) for viability measurement as in Trial 1 (0 h), and then two 4 ml aliquots were used to inoculate two tubes which contained 4 ml of medium M, either alone or with a 0.2 dilution of 11 % milk powder and 5.5 % egg yolk in distilled and de-ionized water as membrane protector. These tubes were previously fed with 0.05 ml of the substrate suspension under CO_2. Tubes were refrigerated at 5°C as in Trial 1 and kept for 4, 8 and 24 h. At each sampling time, 2 ml were removed from each tube and processed as above for determination of viability, resulting in three samples for each experimental treatment. To validate culture recovery, 2 ml of medium M were added to the remaining 2 ml of culture (after 24 h incubation) and a 1.0 ml aliquot was sampled and diluted 1:1 in 18.5 % formaldehyde for cell counts. The remaining 3 ml was incubated for 96 h at 38°C. Tubes were fed anaerobically once daily with 0.05 ml of substrate suspension.

Analyses

The double-stain fluorescence method was performed as described by de la Fuente *et al*. (2004) for viability studies. The 1 ml samples were centrifuged (500 × g, 3 min), 700 µl of the supernatant were discarded and 250 µl from the residue were used. Protozoa cells were fixed in 5 µl of 1.7 mM formaldehyde, and 5 µl of propidium iodide (Sigma; 7.3 µM in distilled water) and 5 µl of carboxyfluorescein diacetate (Sigma; 10 µM in distilled water) were added and the mixture incubated at 37°C for 15 min avoiding light exposure. Two 15 µl subsamples were counted in a fluorescence microscope at 100× magnification with fluorescein and rodamine standard filters. Red-dyed cells were considered as non viable, whereas those only in green were considered as viable. Protozoal concentration was determined by counting in an optical microscope at 100× magnification after staining with brilliant green and diluting in 1 ml 30 % glycerol (Dehority 1984).

Results from both trials for each type of protozoa were statistically analyzed by ANOVA using the Statistix 8.0 statistical package (Analytical Software 2003), considering the experimental day as a block. Non-orthogonal contrasts were planned to compare treatment means. Nine contrasts were established in Trial 1 to study the effect of the incubation along time within protozoal types (INIT *vs.* 2, 4 or 6 h at 38°C), the effect of temperature (INIT *vs*. 15 or 5°C; 15 *vs*. 5°C) at all time intervals and the effect of temperature along time (38 *vs.* 15 and 5°C for 2, 4 or 6 h). The five contrasts planned for each species in Trial 2 were established to study the effect of incubation time (0 h *vs*. 4, 8 or 24 h) and the use of membrane protector, either at all incubation periods (with *vs*. without protector for 4, 8 and 24 h) or only at long-term incubation (with *vs*. without at 24 h).

RESULTS

Trial 1: **Viability of mixed rumen protozoa at refrigeration temperatures**

Protozoal species present in the rumen inocula were *Entodinium* spp. (*E. caudatum, E. dubardi, E. exiguum, E. nanellum, E. vorax), Ophryoscolex caudatus, Diploplastron* (*Metadinium*) *affine, Polyplastron multivesiculatum, Enoploplastron triloricatum, Isotricha prostoma and Dasytricha*

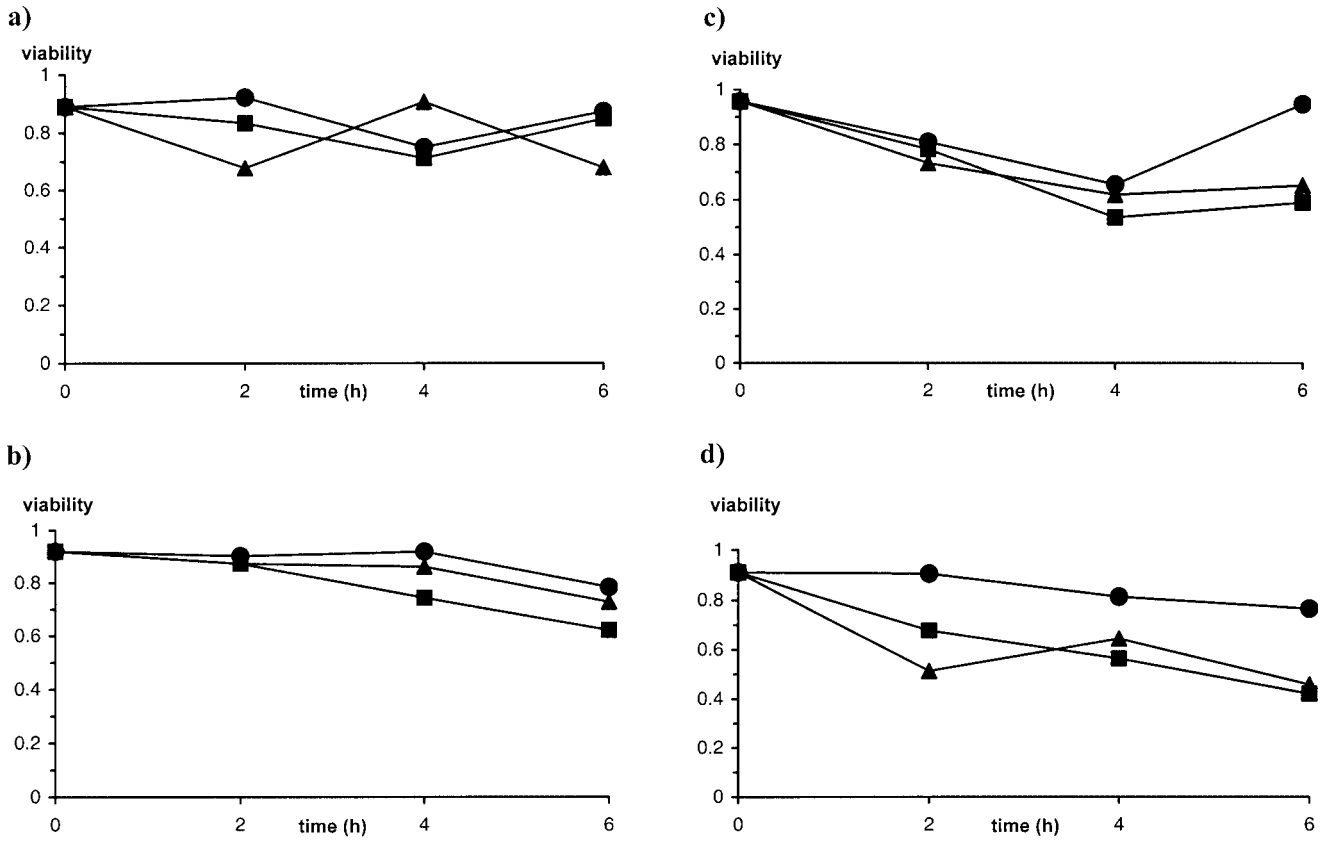

Fig. 1. Viability (proportion of non damaged cells) of *Isotrichidae* (**a**; s.e. = 0.1028), *Entodinium* (**b**; s.e. = 0.0476), *Diplodiniinae* (**c**; s.e. = 0.1145) and *Ophryoscolex* (**d**; s.e. = 0.1162) from mixed rumen samples depending on the temperature (38°C, circles; 15°C, squares; 5°C, triangles) and time of incubation, in Trial 1 (n = 4).

Table 1. Summary (probability, P, and s.e. of the contrast) of the non-orthogonal contrasts established in Trial 1 to study the effects of time (INIT *vs.* 2, 4 or 6 h at 38°C), temperature (INIT *vs.* 15 or 5°C; 15 *vs*. 5°C) and temperature *vs*. time (38 *vs*. 15 and 5°C for 2, 4 and 6 h) on viability of mixed rumen protozoa.

	Isotrichidae		Entodinium		Diplodiniinae		Ophryoscolex	
	P	s.e.	P	s.e.	P	s.e.	P	s.e.
Time								
INIT *vs.* 2 h (38°C)	NS	0.145	NS	0.067	NS	0.162	NS	0.184
vs. 4 h (38°C)	NS	0.163	NS	0.067	0.08	0.162	NS	0.164
vs. 6 h (38°C)	NS	0.145	0.05	0.067	NS	0.162	NS	0.184
Temperature								
INIT *vs.* 15°C	NS	0.356	0.004	0.165	0.03	0.397	0.02	0.403
vs. 5°C	NS	0.364	0.09	0.167	0.04	0.397	0.01	0.403
15 *vs.* 5°C	NS	0.262	0.07	0.120	NS	0.281	NS	0.285
Temp. *vs.* time								
38 *vs.* 15.5°C (2 h)	NS	0.252	NS	0.117	NS	0.281	0.08	0.329
38 *vs.* 15.5°C (4 h)	NS	0.300	0.06	0.117	NS	0.281	NS	0.285
38 *vs.* 15.5°C (6 h)	NS	0.252	0.08	0.120	0.03	0.281	0.07	0.329

NS: non-significant differences (p > 0.10); n = 4 for each experimental treatment.

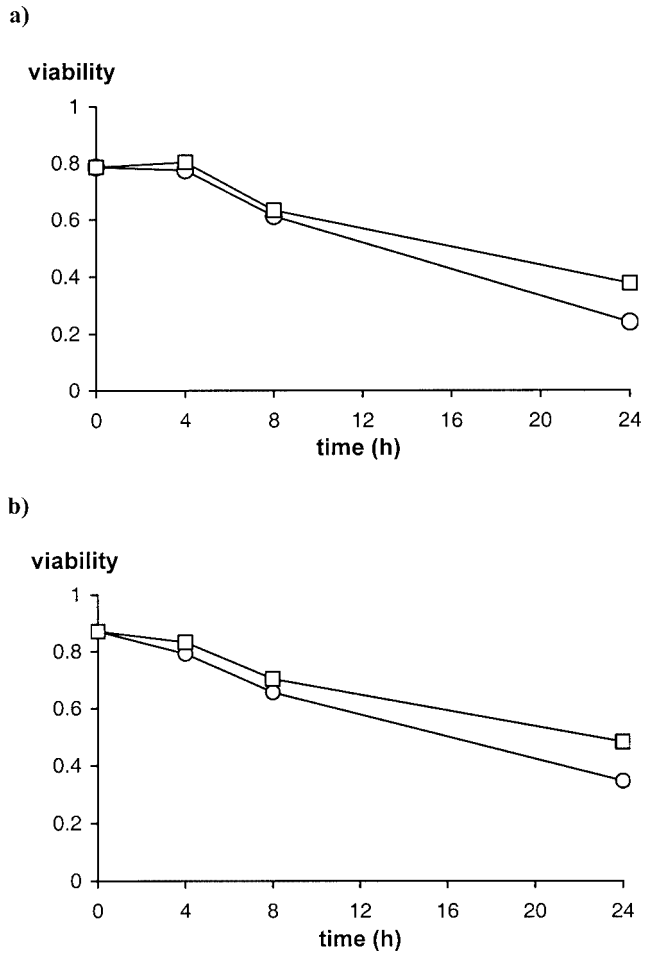

Fig. 2. Viability (proportion of non damaged cells) in monocultures of *Entodinium caudatum* (**a**; s.e. = 0.0476) and *Diploplastron affine* (**b**; s.e. = 0.0326) after 4, 8 or 24 h incubation at 5°C, with (squares) or without (circles) the membrane protector, in Trial 2 (n = 3).

ruminantium. For practical purposes, results of protozoal viability are presented grouped into Family *Isotrichidae*, genus *Entodinium*, Subfamily *Diplodiniinae* and genus *Ophryoscolex*. Protozoal concentration (cells ml^{-1}; n = 4) at the starting of the trial (INIT) were *Isotrichidae*, 223 ± 73.5; *Entodinium*, 5468 ± 693.1; *Diplodiniinae*, 397 ± 74.9; *Ophryoscolex*, 293 ± 151.4. It is worth noting the high variability observed in the initial concentration of cells within the different groups. Average cell viability for INIT ranged from 0.89 to 0.96, with coefficients of variation (c.v.) between 0.08 and 0.13.

The viability (proportion of cells without membrane damage) of cells for each type of protozoa in the mixed samples, as affected by temperature and time of incubation and the significance of the planned contrasts to compare treatments, are shown in Fig. 1 and Table 1, respectively. None of the established contrasts for studying the effects on viability of either the duration of incubation or the temperature during the control period of protozoa from the Family *Isotrichidae* were significant. Incubation of mixed rumen protozoa at 38°C up to 6 h did not affect viability of *Ophryoscolex*, whereas a reduction in this parameter after 6 h was observed in *Entodinium* (0.920 and 0.783 at 0 and 6 h; P = 0.05) as well as a slight (P < 0.10) decrease in the Subfamily *Diplodiniinae* at 4 h incubation (0.957 *vs.* 0.654). The negative effect of incubation at low temperatures on viability compared to the control was observed for *Entodinium*, *Diplodiniinae* and *Ophryoscolex* protozoa, without differences between 15 and 5ºC. However, there was a trend for lower viability of *Entodinium* at 15 than at 5°C (0.746 *vs.* 0.821, respectively), mainly because of differences between both refrigeration temperatures at 6 h.

The reduction of protozoal viability caused by low temperatures increased with time, this effect being noticeable (P < 0.10; Table 1) for *Entodinium* (after 4 and 6 h), *Diplodiniinae* (at 6 h) and *Ophryoscolex* (at 2 and 6 h).

Trial 2: **Viability of pure protozoal cultures at 5°C**

Viability of the cultures at 38°C at the starting of the trial (0 h) was 0.786 ± 0.0324 for *E. caudatum* and 0.872 ± 0.0386 for *D. affine* (n = 3). The average viability of the monocultures of *E. caudatum* and *D. affine* depending on the time of exposure to 5°C and with or without the use of membrane protector is shown in Figure 2 and a summary of the results of the planned contrasts is presented in Table 2. Incubation of *E. caudatum* at 5°C did not affect viability compared with the control (0 h) in the first 4 h of incubation (0.785 and 0.789, respectively), but this effect was significant after 8 and 24 h (0.623 and 0.308). The use of a membrane protector did not improve viability of this species, but a trend for a higher viability was observed after 24 h (0.376 *vs.* 0.242; P = 0.07). In the same way, viability was also significantly reduced for *D. affine* after its incubation at 5°C for 8 and 24 h, though not at 4 h, compared with the control (0.872, 0.812, 0.679 and 0.415 at 0, 4, 8 and 24 h). For this species, the positive effect of the membrane protector was clearly manifested throughout the incubation period, reaching a 0.13 units higher viability after 24 h (0.483 *vs.* 0.347; P = 0.01).

Table 2. Summary (probability, P, and s.e. of the contrast) of the non-orthogonal contrasts established in Trial 2 to study the effect of incubation of monocultures at 5° along time (control *vs.* 4, 8 or 24 h) and the effect of the membrane protector, overall (with *vs.* without) or at long term incubation (with *vs*. without at 24 h).

	E. caudatum		*D. affine*	
	P	s.e.	P	s.e.
Incubation at 5°C				
0 h *vs.* 4 h	NS	0.117	NS	0.080
vs. 8 h	0.02	0.117	0.001	0.080
vs. 24 h	0.001	0.117	0.001	0.080
Membrane protector				
with *vs.* without (all times)	NS	0.117	0.02	0.080
with *vs.* without (24 h)	0.07	0.067	0.01	0.046

NS - non-significant differences ($p > 0.10$); n = 3 for each experimental treatment.

Concentration of *E. caudatum* after 24 h at 5°C was 3223 ± 2308 and 2764 ± 1192 cells per ml with or without membrane protector, respectively. Refrigerated cultures were then maintained at 38°C for 96 h, and these resulted in culture recoveries below 0.20 of the cells counted after 24 h refrigeration. For *D. affine*, the average cell concentration was 582 ± 157.8 and 917 ± 261.6 cells ml^{-1} after 24 h of incubation at 5°C with or without membrane protector, but after 96 h incubation at 38°C cultures were only recovered from tubes from one day of the refrigeration trial (cell concentration 2.97 and 0.54 times the number of cells after 24 h at 5°C, respectively). For both species, it seems that recovery was not improved by the use of the protector.

DISCUSSION

Considering the low concentration of some protozoal species in the rumen (Williams and Coleman 1992, Dehority 2003) mainly in the small sample volume used for viability measurements (15 µl), and because rapid counting is needed in fluorescence microscopy and species identification requires considerable time, we grouped them into genera or families to reach sufficient numbers for more meaningful analyses. This decision may have the drawback of not considering the existing differences in tolerance to low temperatures among species within a genus or subfamily. Except for the *Entodinium* spp., the other types studied in Trial 1 were in low numbers, and results therefore must be considered with caution.

The main goal of this work was to assess the possibility of preserving protozoa for short periods of time at low temperatures (over 0°C) for an easier handling and processing of cells for culture studies. As expected from previous results (de la Fuente *et al*. 2004, 2006), rumen protozoa were affected by incubation at refrigeration temperatures (15 and 5°C). A lower concentration and an adequate medium composition after diluting in protozoa specific culture medium would allow for an increasing resistance to cold stress. Even though, viability was considerably reduced after a short time at either 15 or 5°C for *Entodinium, Diplodiniinae* and *Ophryoscolex*. Despite considerable variation in the response, viability of *Entodinium* was reduced in 0.15 after their culture at 38°C for 6 h compared with the initial numbers (Table 1). A similar response can also be inferred in *Diplodiniinae,* indicating that the response to temperature may be partly confounded by the resistance of some organisms to these *in vitro* culture conditions. However, the fact that results from incubation at 15 and 5°C were in general lower than those at 38°C for the longer incubation times reduces the potential impact of this bias.

Viability proportions after 4 and 6 h incubation at 15°C and 5°C were of a lesser magnitude than those observed in the same periods at 38°C, the response depending on the studied type of protozoa. Values were as low as 0.68 for *Isotrichidae,* 0.62 for *Entodinium*, 0.53 for *Diplodiniinae* and 0.42 for *Ophryoscolex*. Therefore, although in most of the cases the low temperatures affected protozoal viability from 4 h onwards, the effects were of a lower magnitude than those initially

expected considering previous reports (Williams and Coleman 1992). From these results, the preservation of rumen protozoa for at least 4 h at 15 or 5°C without a marked drop of viability could be expected. Even though samples were not cultured at 38°C for a period after being exposed to 5 and 15°C in these incubation trials, the magnitude of the observed viabilities after 4 and even 6 h suggest that the cultures can be successfully recovered after refrigeration and subsequently maintained at 38°C.

In a more specific approach to the effect of low temperature on rumen protozoa for a longer period of refrigeration, *E. caudatum* and *D. affine*, chosen as representative species of a type-A rumen population, were studied in Trial 2. The lack of a negative effect of incubation at 5°C for 4 h suggests that these organisms can be stored for short periods of time at refrigeration temperatures. However, incubation for a longer time (more than 8 h) negatively affected viability of both cultures. In the case of *D. affine*, this depression was more noticeable when membrane protector was not added indicating that some extent of membrane damage primarily occurs with longer refrigeration times. However, this effect was not as clear for *E. caudatum*, suggesting that the response is species dependent. Although this would support the practice of adding membrane protector for preserving some species of rumen protozoa at refrigeration temperatures, results for culture recovery did not show a clear benefit in such practice. In this regard, incubation of both *E. caudatum* and *D. affine* at low temperatures for 24 h does not seem to ensure the culture recovery in a further incubation at 38ºC. It may be speculated that some extent of long term cell damage not detected by the double stain technique would affect cell viability in terms of its metabolic activity, since recovery was even lower than expected from results of incubation at 5°C for 24 h. In all cases, viability at 24 h was considerably lower.

Therefore, refrigeration temperatures affect viability of rumen protozoa, although the effect at incubation times shorter than 4 h is not significant. However, there is no data available on recovery after this incubation time. The variability of this response to refrigeration and the difficulty in culturing some protozoa types *in vitro* limit the possibilities for their manipulation. The use of membrane protectors may be positive for medium to long term refrigeration, the extent of the response depending on the species, but the low viability of cells reduces its potential benefit.

Acknowledgements. This work has been financed by the Project AGL 2004-02910 (CICYT, España). Dr. Manuel Pérez Quintana was supported by a MAE fellowship. Thanks are given to Prof. B. A. Dehority for his critical review of the manuscript.

REFERENCES

Analytical Software (2003) Statistix 8 for Windows. Analytical Software, Tallahasee, FL, USA

Dehority B. A. (1984). Evaluation of subsampling and fixation rumen procedures used for counting rumen protozoa. *Appl. Environ. Microbiol.* **48:** 182-185

Dehority B. A. (1998) Generation times of *Epidinium caudatum* and *Entodinium caudatum* determined *in vitro* by transferring at various time intervals. *J. Anim. Sci.* **76:** 1189-1196

Dehority B. A. (2003) Rumen Microbiology. Nottingham University Press, Nottingham, UK

Eadie J. M. (1967) Studies on the ecology of certain rumen ciliate protozoa. *J. Gen. Microbiol.* **49:** 175-194

de la Fuente G., Cebrián J. A., Fondevila M. (2004) A cryopreservation procedure for the rumen protozoon *Entodinium caudatum*: estimation of its viability by fluorescence microscopy. *Lett. Appl. Microbiol.* **38:** 164-168

de la Fuente G., Cebrián J. A., Fondevila M. (2006) Effect of the cryopreservation conditions on the viability of the rumen ciliate *Diploplastron* (*Metadinium*) *affine*. *Lett. Appl. Microbiol.* **42:** 573-577

Harrison R. A. P., Vickers S. E. (1990) Use of fluorescent probes to assess membrane integrity in mammalian spermatozoa. *J. Reprod. Fertil.* **88:** 343-352

Kisidayova S. (1996) The cryopreservation of some large ciliate entodiniomorphid protozoa taken from the rumen. *Lett. Appl. Microbiol.* **23:** 389-392

Kisidayova S. (1997) Parameters associated with optimum two-step freezing of rumen ciliate *Entodinium caudatum*. *J. Microbiol. Meth.* **30:** 119-124

Nsabimana E., Kisidayova S., Macheboeuf D., Newbold C. J., Jouany J. P. (2003) Two-step freezing procedure for cryopreservation of rumen ciliates, an effective tool for creation of a frozen rumen protozoa bank. *Appl. Environ. Microbiol.* **69:** 3826-3832

Williams A. G., Coleman G. S. (1992) The Rumen Protozoa. Brock-Springer Series in Contemporary Bioscience, Springer-Verlag, New York

Received on 6th March, 2006; revised version on 10th May, 2006; accepted on 29th May, 2006

Acta Protozool. (2006) 45: 231 - 240

ACTA
PROTOZOOLOGICA

Biological Activities of Essential Oil Obtained from *Cymbopogon citratus* on *Crithidia deanei*

Raíssa Bocchi PEDROSO[1], Tânia UEDA-NAKAMURA[2], Benedito Prado DIAS FILHO[2], Diógenes Aparício Garcia CORTEZ[3], Lúcia Elaine Ranieri CORTEZ[4], José Andrés MORGADO-DÍAZ[5] and Celso Vataru NAKAMURA[2]

[1]Programa de Pós-Graduação em Microbiologia da Universidade Estadual de Londrina; [2]Departamento de Análises Clínicas, Laboratório de Microbiologia Aplicada aos Produtos Naturais e Sintéticos; [3]Departamento de Farmácia e Farmacologia, Universidade Estadual de Maringá, PR; [4]Centro de Ensino Superior de Maringá - CESUMAR; [5]Divisão de Biologia Celular, Instituto Nacional do Câncer, Rio de Janeiro, RJ, Brazil

Summary. We report the effect of the essential oil extracted from *Cymbopogon citratus* on endosymbiont-harbouring and endosymbiont-free strains of the insect trypanosomatid *Crithidia deanei* grown at 28°C in a chemically defined medium. A dose-dependent antiprotozoan effect of the essential oil of *C. citratus* could be observed on both strains of *C. deanei*. The IC_{50} values (50% inhibitory concentration) for symbiont-bearing and symbiont-free strains were 120 and 60 µg/ml, respectively. The viability assay showed that the symbiont-free strain is more sensitive to the presence of the essential oil, because lysed cells were observed after 2 h of exposure at higher concentrations. In addition, alterations in the ultrastructure and in the detection of cell-surface carbohydrate residues in both strains of *C. deanei* after treatment with the essential oil were also evaluated. Both strains showed ultrastructural alterations in the cellular and flagellar pocket membranes, as revealed by transmission electron microscopy. In the lectin assay, the essential oil influenced the expression of carbohydrates in symbiont-free *C. deanei*, as evidenced by a reduction of sialic acid residues on the cell surface.

Key words: antiprotozoan activity, *Crithidia deanei*, *Cymbopogon citratus*, medicinal plants.

INTRODUCTION

The family Trypanosomatidae harbours protozoans that are agents of important illnesses in humans and animals (such as the agents of leishmaniasis and Chagas´ disease), and in plants (*Phytomonas*). This family also includes some lower trypanosomatids such as *Crithidia*, *Blastocrithidia*, and *Herpetomonas*, monoxenous protozoans usually found in insect hosts and not considered capable of causing parasitic diseases in vertebrates (Wallace 1966). *Crithidia deanei*, which has a choanomastigote form, normally contains intracellular symbiotic bacteria, and, like other trypanosomatids, is easily cultured under axenic conditions. These insect trypanosomatids contain homologues of virulence factors of the pathogenic ones (d´Avila-Levy *et al.* 2003),

Address for correspondence: Celso Vataru Nakamura, Universidade Estadual de Maringá; Departamento de Análises Clínicas, Laboratório de Microbiologia Aplicada aos Produtos Naturais e Sintéticos, Bloco I-90 Sala 123 CCS, Avenida Colombo, 5790; BR-87020-900, Maringá, PR, Brazil. Fax: +55 44 3261-4860; E-mail: cvnakamura@uem.br

and therefore have been used as laboratory models for biochemical and molecular studies (McGhee and Cosgrove 1980, Santos *et al.* 2004).

In trypanosomatids, the possibility of elimination of the endosymbiont by antibiotic treatment has increased interest in the study of endosymbiont-harbouring species (De Souza and Motta 1999). The available data indicate that the presence of the endosymbiont induces morphological changes, interferes with several aspects of metabolism (Freymüller and Camargo 1981; De Souza and Motta 1999; d´Avila-Levy *et al.* 2001, 2003), and modulates the surface properties of the protozoan, such as the exposure of carbohydrate residues (Esteves *et al.* 1982, Oda *et al.* 1984, Faria-e-Silva *et al.* 1994) and the expression of glycoproteins (Dias Filho *et al.* 2005).

The human diseases caused by *Trypanosoma cruzi* and *Leishmania* are responsible for mortality in tropical and subtropical countries. In addition, there are recent reports of the presence of trypanosomatids other than *Trypanosoma* and *Leishmania* in certain opportunistic cutaneous infections in immunocompromised individuals (Dedet *et al.* 1995, Boisseau-Garsaud *et al.* 2000) and also in individuals with no history of immunodepression (Boisseau-Garsaud *et al.* 2000). Drugs such as benznidazole (used in the acute and intermediate phases of Chagas' disease) and the polyene amphotericin B (used for leishmaniasis) have limited action, and the side effects are drastic (Goad *et al.* 1984, Castro *et al.* 2003). Because of this, more attention should be given to extracts and biologically active compounds isolated from plants commonly used in herbal medicine (Essawi and Srour 2000). The practice of herbalism has become mainstream throughout the world. This is due in part to the recognition of the value of traditional medical systems, and the identification of medicinal plants from indigenous pharmacopeias (Elvin-Lewis 2001). Medicinal plants occur worldwide, but they are most abundant in tropical countries (Calixto 2000).

Essential oils are aromatic oily liquids obtained from plant material. They can be obtained by expression, fermentation or extraction, but steam distillation is the most commonly used method (Burt 2005). Some essential oils have antibacterial (Wannissorn *et al.* 2005), antifungal (Nakamura *et al.* 2004), antiviral (Bishop 1995), antitoxigenic (Juglal *et al.* 2002), and antiprotozoal (Holetz *et al.* 2003, Ueda-Nakamura *et al.* 2006) properties.

Cymbopogon citratus is a plant used in traditional folk medicine in Brazil for the treatment of nervous and gastrointestinal disturbances, and in various other countries to treat fevers (Melo *et al.* 2001). The volatile oil obtained from fresh leaves of this plant is widely used by the perfume and cosmetics industries. It has also been used in chemical synthesis, because of its high citral content (Rauber *et al.* 2005).

Here we report the effect of the essential oil extracted from *C. citratus* on the growth, viability, cell-surface carbohydrate residues, and ultrastructure of endosymbiont-harbouring and endosymbiont-free strains of *C. deanei* cultured in a defined medium at 28°C.

MATERIALS AND METHODS

Plant material. *Cymbopogon citratus* was collected in Maringá, Paraná, Brazil, and identified. A voucher No. HUM 520 is deposited at the Maringá State University Herbarium. Fresh leaves from the plant were cut into pieces and steam-distilled by Clevenger´s apparatus. The essential oil was then stored at -20°C until needed.

Microorganisms. Cultures of symbiont-bearing *Crithidia deanei* (ATCC 30255) were maintained by weekly transfers into a chemically defined medium (Mundin *et al.* 1974), added in 5 ml volumes to screw-capped tubes. The symbiont-free strain of *C. deanei* was maintained in the same defined medium, supplemented with 0.03 g/l of nicotinamide (Sigma Chemical Company, St. Louis, MO, U.S.A.) (Mundin and Roitman 1977). Cells were grown at 28°C for 48 h and stored at 4°C.

Antiprotozoan activity of *Cymbopogon citratus* essential oil. For this experiment, symbiont-bearing and symbiont-free strains of *C. deanei* were incubated in the defined medium supplemented with 0.03 g/l of nicotinamide containing different concentrations of the essential oil, initially diluted in 2% Tween 80. Cells were grown in 13×100 mm tubes containing 1 ml of the medium, and the starting inoculum consisted of cells in logarithmic growth phase (2×10^6 cells/ml). After 24, 48, 72, and 96 h at 28°C, cell growth was estimated by counting in a haemocytometer (Improved Double Neubauer). All the experiments were performed in triplicate. The results were expressed as log number (cells/ml) and as the percentage of growth inhibition at 48 h. Amphotericin B (FUNGIZON®, Bristol-Myers Squibb, São Paulo, Brazil) and benznidazole (N-benzyl-2-nitro-1-imidazolacetamide, Roche Pharmaceuticals, Rio de Janeiro, Brazil) were prepared in the same defined medium and used as reference drugs.

Viability assay. In order to evaluate the viability of the protozoa treated with essential oil, each solution was added to microcentrifuge tubes containing 2×10^7 cells in the logarithmic growth phase, and incubated at 28°C. After addition of the essential oil, 25 µl of the protozoan suspension was removed after 2, 4, 6, 8, 12, and 24 h and was mixed in an equal volume of 0.4% trypan blue, and the cell viability was quantified by light microscopy. All preparations were made in duplicate. The percentage of viability was determined by counting at least 200 cells (Berry *et al.* 1991).

Agglutination with lectins. The agglutination tests were made in 96-well plaques using a microtitrator. Equal volumes (25 µl) of the

cell suspension (2×10^8 cell/ml), treated with the IC_{50} concentration (50% inhibitory concentration) of the essential oil and each lectin were mixed and then left at room temperature (25°C) for 1 h. The agglutination of the cells was always scored visually with a hand lens after the settled cells had been gently resuspended, and also by observations using an inverted microscope (Zeiss Axiovert 25). The agglutination inhibition assays were carried out at room temperature in the presence of specific monosaccharides. All lectins were purchased from Sigma Chemical Co. (St. Louis, MO).

Ultrastructure analysis. Both symbiont-bearing and symbiont-free cells of *C. deanei* were treated with the IC_{50} and IC_{90} amounts (90% inhibitory concentration) of the *C. citratus* essential oil or amphotericin B in the defined medium supplemented with 0.03 g/l of nicotinamide at 28°C for 48 h. Cells were collected by centrifugation, washed in PBS, and fixed with 2.5% glutaraldehyde in 0.1 M sodium cacodylate buffer, pH 7.2, at 4°C. The cells were then rinsed with 0.1 M sodium cacodylate buffer and postfixed for 30 min at room temperature in 1% osmium tetroxide plus 0.8% potassium ferrocyanide and 5.0 mM $CaCl_2$, dehydrated in acetone, incubated in an acetone-epon mixture (2:1, 1:1, 1:2), and embedded in Epon resin. Ultrathin sections obtained with a Reichert Ultracut E ultramicrotome were stained with uranyl acetate and lead citrate, and observed with a Zeiss CEM-900 electron microscope.

RESULTS

Antiprotozoan activity of the essential oil

A dose-dependent antiprotozoan effect of the essential oil from *C. citratus* on *C. deanei* is evident in Fig. 1. The inhibitory effect of the essential oil was apparent in the cells treated with the highest concentrations of the oil. The endosymbiont-free *C. deanei* (Fig. 1B) appeared to be more sensitive to the essential oil at concentrations over 100 µg/ml, compared to the endosymbiont-harbouring strain, in which the cell growth was inhibited at concentrations over 200 µg/ml (Fig. 1A). In Fig. 2, the inhibitory effect of the essential oil, benznidazole, and amphotericin B on both strains in the logarithmic phase (48 h) can be seen. The IC_{50} and IC_{90} concentrations for the symbiont-bearing strain treated with the essential oil were 120 and 157 µg/ml, respectively (Fig. 2A). For the symbiont-free strain, the IC_{50} and IC_{90} were 60 and 92 µg/ml (Fig. 2B). Amphotericin B showed an inhibitory effect at concentrations lower than 5 µg/ml. In cells of *C. deanei* containing the endosymbiont, the IC_{50} and IC_{90} concentrations were 3.4 and 4.7 µg/ml; and in the endosymbiont-free strain, 3.6 and 5 µg/ml, respectively. For benznidazole-treated cells, much higher concentrations of the drug were necessary to reach the IC_{50}: for the symbiont-bearing strain, 841.7 µg/ml, and for the symbiont-free strain, 700 µg/ml were necessary. Tween 80 and dimethyl sulfoxide, the dilution agents, and petrolatum oil, used as an indifferent oil, had no effect on protozoan growth (data not shown).

Cell viability

The viability of treated and control cells were assessed by a trypan blue dye exclusion test. The percentages of non-viable cells obtained by exposing the protozoan cells to different concentrations of the essential oil and the drugs are shown in Fig. 3. The endosymbiont-harbouring strain of *C. deanei* had its viability reduced at high concentrations (500 and 250 µg/ml) after 8 h of exposure to the essential oil, with only 5 and 9 % of viable cells, respectively (Fig. 3A). At concentrations lower than 100 µg/ml, viability was more than 71.5% at 24 h. The endosymbiont-free *C. deanei* appeared to be more sensitive, because after 2 h of exposure at 500 µg/ml of the essential oil, all the cells were lysed, and after 8 h at 250 µg/ml, all the cells were non-viable (Fig. 3B). Concentrations below 100 µg/ml showed a protozoan viability over 79%, after 24 h of incubation. Benznidazole did not interfere with the viability of either strain, even at concentrations as high as 1000 µg/ml. For amphotericin B, the endosymbiont-free strain was more sensitive than the symbiont-harbouring cells (data not shown).

Agglutination test with lectins

The lectin agglutination of cells from both strains of *C. deanei*, treated or not with the essential oil, is shown in Table 1. The lectins are classified according to their sugar specificities, and the results were expressed as the minimum concentration of lectins required to agglutinate the cells. The binding reaction was more specific with cells which were agglutinated at the lowest lectin concentration. For symbiont-bearing cells of *C. deanei* treated with the essential oil, only *Dolichos biflorus* and *Glicine max*, D-GalNAc binding lectins, altered the minimum concentration required to agglutinate the cells, to 125 and 15.6 µg/ml, respectively. For the symbiont-free strain, alterations in cells treated with the essential oil were observed for many lectins, as a decrease in the binding specificity of *Limulus polyphemus*, a sialic acid-binding lectin, and an increase in the binding specificity of *Arachys hypogaeae*, a D-Gal-binding lectin. *Artocarpus integrifolia* and *G. max*, D-GalNac-binding lectins, and *Lens culinaris*, a lectin that has binding sites complementary to D-mannose-like residues, also had their sugar-binding specificity increased in the presence

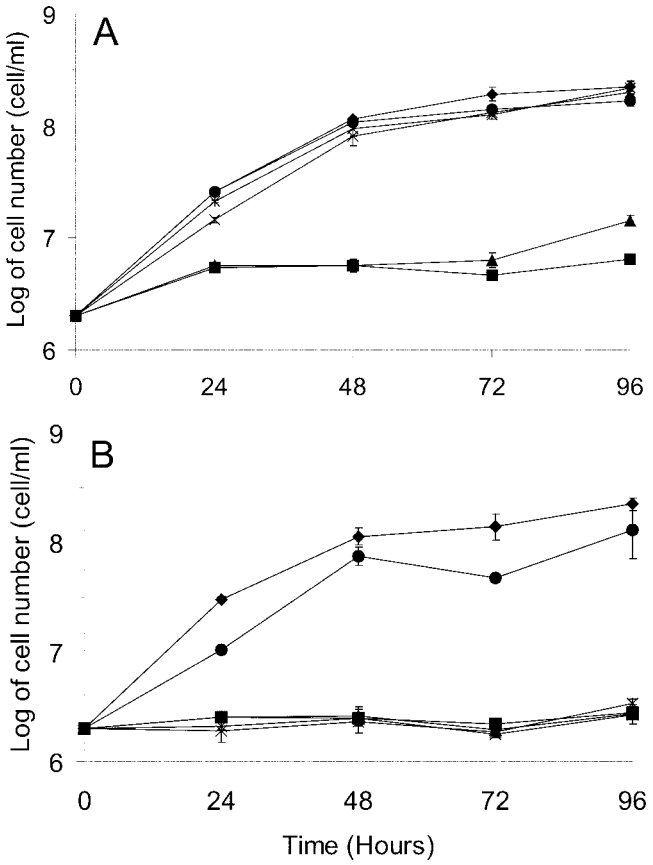

Fig. 1. Growth curves of strains of *Crithidia deanei* treated with the essential oil from *Cymbopogon citratus*: (A) endosymbiont-harbouring; (B) endosymbiont-free. Control cells - filled diamond; 50 µg/ml - filled circle; 100 µg/ml - open circle; 150 µg/ml - open square; 200 µg/ml - filled triangle; 250 µg/ml - filled square.

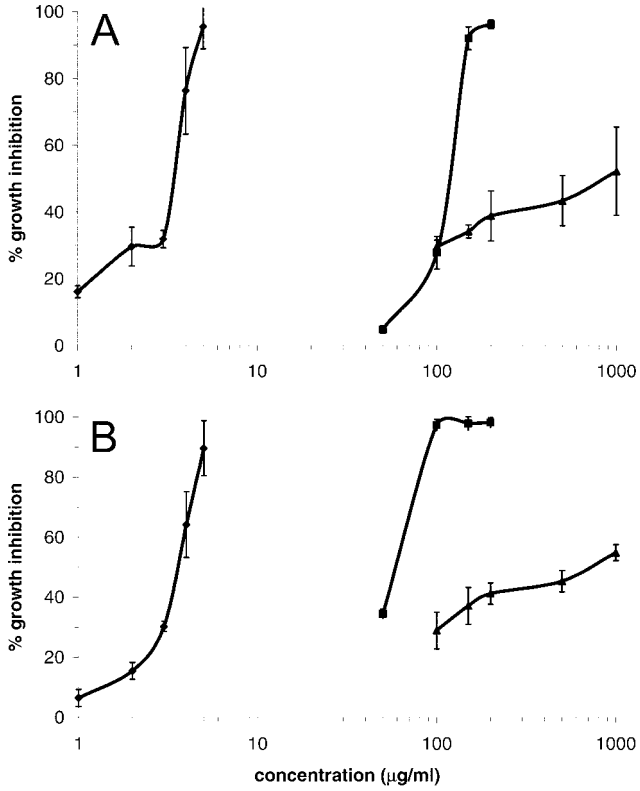

Fig. 2. Effect of the essential oil from *Cymbopogon citratus* (filled square), benznidazole (filled triangle), and amphotericin B (filled diamond) on the growth inhibition of strains of *Crithidia deanei* in defined medium at 28°C after 48 h. (A) endosymbiont-harbouring; (B) endosymbiont-free.

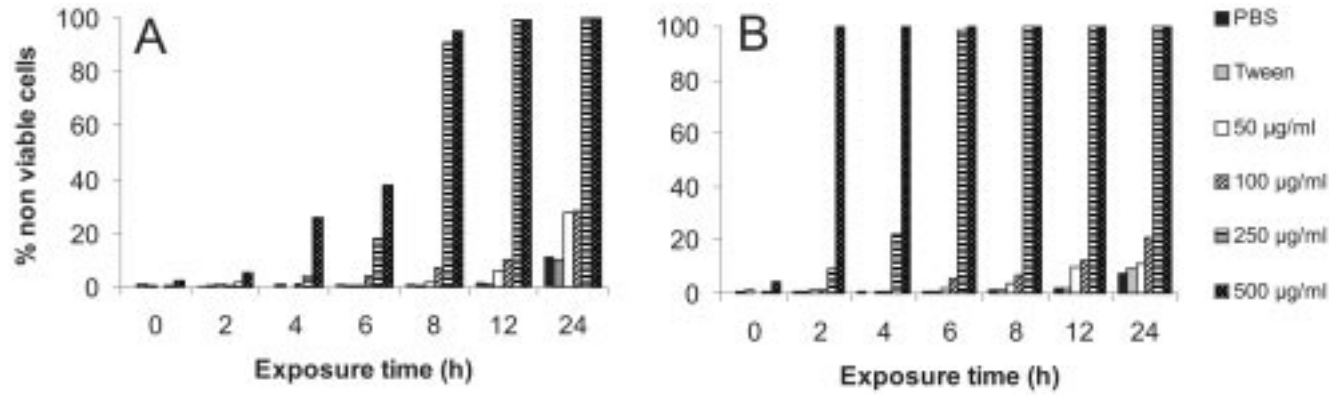

Fig. 3. Effect of the essential oil from *Cymbopogon citratus* on the viability of strains of *Crithidia deanei*: (A) endosymbiont-harbouring; (B) endosymbiont-free.

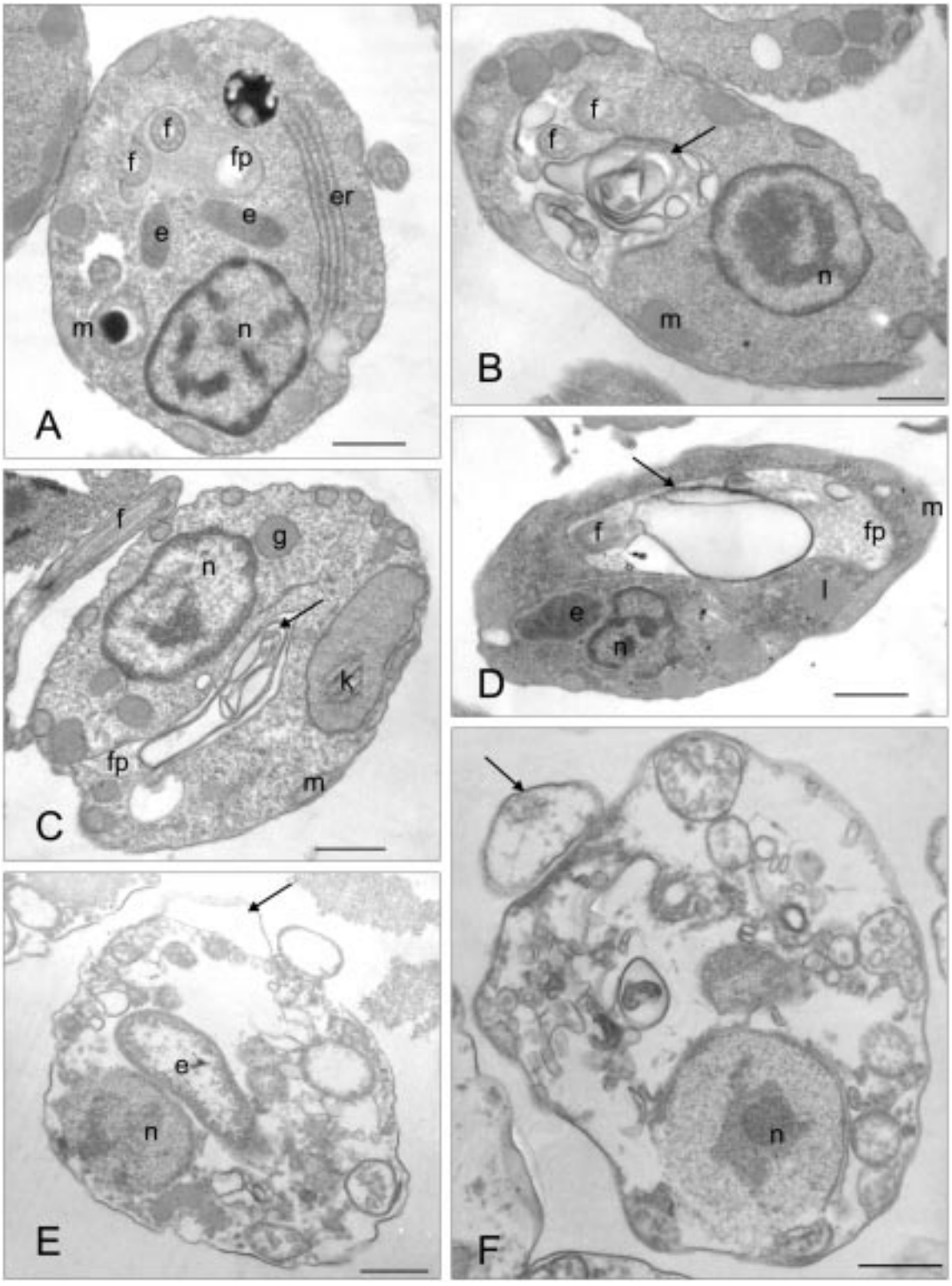

Figs 4A-F. Ultrastructural morphology of the endosymbiont-harbouring strain of *Crithidia deanei* cultured at 28°C for 48 h in the absence (**A**) or in the presence of the following compounds: the IC_{50} concentrations of essential oil from *Cymbopogon citratus* (**B** and **C**) or amphotericin B (**D**); and the IC_{90} concentrations of the essential oil from *Cymbopogon citratus* (**E**) or amphotericin B (**F**). e - endosymbiont; f - flagellum; fp - flagellar pocket; g - glycosome; k - kinetoplast; l - lipid inclusion; m - mitochondria, n - nucleus. Arrows indicate the presence of membraneous material in the flagellar pocket of treated cells at the IC_{50} concentration, and membranes detaching from the cell at the IC_{90} concentration. Scale bars: 1 µm.

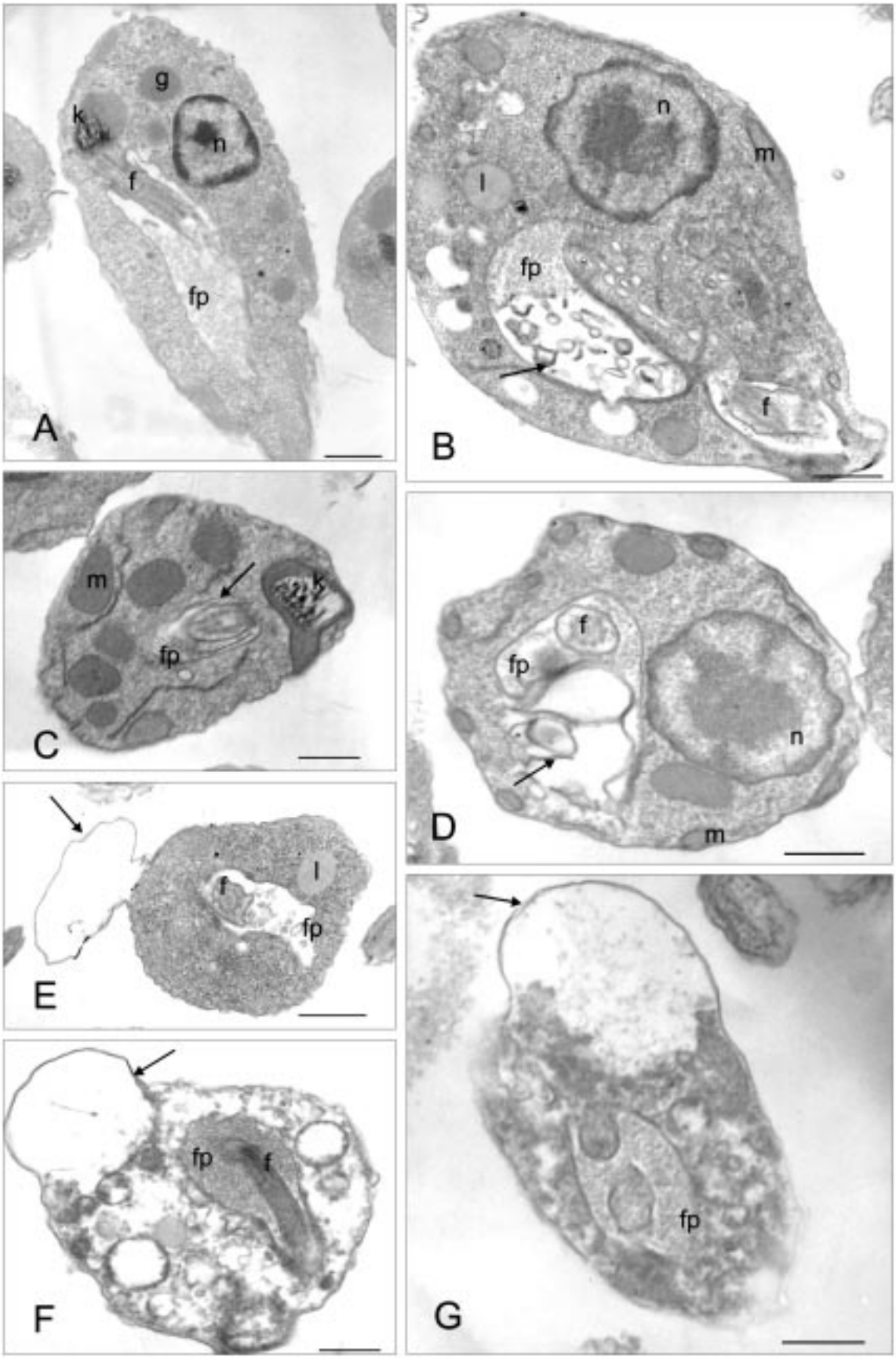
g
k
n
f
fp
A
n
m
l
fp
f
B
m
k
fp
C
f
fp
n
m
D
l
f
fp
E
fp
f
F
fp
G

Table 1. Minimum lectin concentration (µg/ml) required to agglutinate strains of *Crithidia deanei* in the presence of the essential oil of *Cymbopogon citratus.*

	Symbiont-harbouring		Symbiont-free	
	Control cells	Cells treated with essential oil	Control cells	Cells treated with essential oil
D-GlcNAc-binding lectins				
Phytolaca americana	>500	>500	<7.8	15.6
Triticum vulgares	>500	>500	125	62.5
D-GalNAc-binding lectins				
Dolichos biflorus	>500	125	<7.8	62.5
Wisteria floribunda	>500	>500	15.6	15.6
Phaseolus vulgaris	>500	>500	15.6	<7.8
Glicine max	62.5	15.6	31.2	<7.8
Artocarpus integrifolia	<7.8	<7.8	250	15.6
D-Gal-binding lectins				
Arachys hypogaeae	>500	>500	125	<7.8
D-Man-binding lectins				
Canavalia ensiformis	>500	>500	<7.8	>500
Lens culinaris	>500	250	62.5	15.6
L-fucose-binding lectins				
Ulex europeus	>500	>500	62.5	31.2
Sialic acid-binding lectins				
Limulus polyphemus	>500	>500	<7.8	31.2

of the essential oil. On the other hand, *D. biflorus* and *Canavalia ensiformis* (a D-mannose-like binding lectin) had their sugar-binding specificity decreased. Agglutination was inhibited by the respective specific monosaccharides (D-GalNAc, D-Gal, and a-D-methyl mannoside) at 0.1 M.

Ultrastructural analysis

In order to determine the ultrastructural changes in symbiont-harbouring and symbiont-free strains of *C. deanei* treated with the IC_{50} and IC_{90} of the essential oil of *C. citratus* and amphotericin B, an analysis was done by means of transmission electron microscopy. For the symbiont-harbouring strain treated with the essential oil at the IC_{50} level, alterations in the flagellar pocket membrane were observed, with invaginations of this membrane and the presence of membraneous material, and an enlargement of the flagellar pocket (Figs 4B, C). When this strain was treated with the essential oil at the IC_{90} level, extensive vacuolisation and portions of the membrane detaching from the cell body (blebs) appeared (Fig. 4E). The control cells had a proeminent nucleus with symbionts located close to it and near the flagellar pocket, and the endoplasmic reticulum was also well characterised (Fig. 4A). For the symbiont-free *C. deanei*, the essential oil also affected the membrane of the flagellar pocket (Figs 5B, C). Cells treated with the IC_{50} concentration showed small membrane fragments and enlargement of the flagellar pocket, with membraneous material present inside it. For cells treated with IC_{90}, cytoplasmic alterations, extensive vacuolisation, and the presence of blebs were evident (Figs 5F, G). Control cells had the nucleus located at the anterior end of the protozoa, and glycosomes were situated close to it. The kinetoplast could be observed inside the mitochondria and close to the flagellum (Fig. 5A). When symbiont-harbouring and symbiont-free strains of *C. deanei* were treated with amphotericin B, similar alterations were observed (Figs 4D, F; 5D, E,G). Blebs detaching from the cytoplasmic membrane at the IC_{50}

Figs 5A-G. Ultrastructural morphology of the endosymbiont-free strain of *Crithidia deanei* cultured at 28°C for 48 h in the absence (**A**) or in the presence of the following compounds: the IC_{50} concentrations of essential oil from *Cymbopogon citratus* (**B** and **C**) or amphotericin B (**D** and **E**); and the IC_{90} concentrations of the essential oil from *Cymbopogon citratus* (F) or amphotericin B (**G**). e - endosymbiont; f - flagellum; fp - flagellar pocket; g - glycosome; k - kinetoplast; l - lipid inclusion; m - mitochondria; n - nucleus. Arrows indicate the presence of membraneous material in the flagellar pocket of treated cells, and the presence of blebs. Scale bar: 1 µm.

could only be seen in the symbiont-free strain treated with amphotericin B (Fig. 5E).

DISCUSSION

A dose-dependent antiprotozoan effect of the essential oil extracted from *C. citratus* on *C. deanei* could be observed, with differences in the growth inhibition of both the endosymbiont-harbouring and symbiont-free strains. The concentration of the essential oil necessary to inhibit the endosymbiont-harbouring strain of *C. deanei* was higher than that necessary to inhibit the endosymbiont-free cells. Some investigators have reported that the presence of the endosymbiont interferes with the protozoan metabolism and induces morphological and biochemical changes (Freymüller and Camargo 1981, De Souza and Motta 1999). *Cymbopogon citratus* is an herb known worldwide as lemongrass, and the tea made from its leaves is popularly used in Brazil as an antispasmodic, analgaesic, anti-inflammatory, antipyretic, diuretic, and sedative (Carlini *et al.* 1986). Published reports indicate that the essential oil obtained from fresh leaves of this plant has antibacterial and antifungal properties (Onawunmim 1989, Lima *et al*. 1993, El-Kamil *et al.* 1998). Recently, Luize *et al*. (2005) reported that a crude hydroalcoholic extract of *C. citratus* is active against promastigote and amastigote forms of *L. amazonensis* and *T. cruzi*, with inhibition rates over 90% at 100 µg/ml.

Because *C. deanei* is a member of the family Trypanosomatidae, the drugs benznidazole and amphotericin B were used to compare the effect of essential oil on the protozoans. Benznidazole is a drug used in the chemotherapy of the acute and intermediate phases of Chagas' disease, which is caused by *T. cruzi*. It acts through a different mechanism, which involves covalent modification of macromolecules by nitroreductive intermediates (Castro *et al.* 2003). Holetz *et al.* (2003) demonstrated that *Herpetomonas samuelpessoai* has a natural resistance to benznidazole (IC_{50} higher than 3,840 µM). For *C. deanei* with and without endosymbionts, the IC_{50} concentrations were 841.7 and 700 µg/ml, respectively, indicating a possible resistance to this drug. Amphotericin B is a valuable drug used in the treatment of leishmaniasis. It interacts with sterols of protozoan membranes, and preferentially with ergosterol (Goad *et al.* 1984). When *C. deanei* was treated with amphotericin B, concentrations lower than 5 µg/ml were sufficient to inhibit cell growth, indicating that this drug is efficacious against the protozoan.

At the ultrastructural level, both strains of *C. deanei* treated with the essential oil of *C. citratus* and amphotericin B showed alterations in the membrane of the flagellar pocket. These changes included invagination and the presence of membraneous material, and certain modifications in the cytoplasmic membrane, such as the presence of blebs. Alterations in trypanosomatid membranes have been reported for other compounds. Braga *et al.* (2004) reported alterations in the cytoplasmic membrane and an enlargement of the flagellar pocket of *T. cruzi* treated with squalene synthase inhibitors. Other alterations were observed by Rodrigues *et al.* (2005), who analyzed promastigote forms of *L. amazonensis* treated with BPQ-OH, a specific inhibitor of squalene synthase, which induced ruptures of the plasma membrane with disconnection from the subpellicular microtubules, the formation of elaborate structures, and intense membrane shedding. Other studies have reported analogous alterations in *Trypanosoma brucei* treated with proanthocyanidins from *Kola acuminata* (Kubata *et al.* 2005). Santos *et al.* (2006) reported alterations of the cellular membrane in *Phytomonas serpens* treated with antipain and leupeptin (cystein peptidase inhibitors), including fragmentation of the flagellar pocket.

Due to these ultrastructure alterations, the expression of membrane carbohydrate residues was determined using the lectin agglutination assay. All parasites have carbohydrates on their surfaces, as part of their cytoskeletons or in their internal structures, and because of this, lectins can be directly used in agglutination assays. Lectins have been defined as carbohydrate-binding proteins other than enzymes or antibodies (Jacobson and Doyle 1996). A study of cell-surface carbohydrates using lectins has been done on different members of the family Trypanosomatidae, such as *Trypanosoma, Leishmania, Herpetomonas*, *Phytomonas*, and *Crithidia* (De Souza 1989). Esteves *et al.* (1982) studied the cell-surface carbohydrates in endosymbiont-bearing and endosymbiont-free strains of *C. deanei.* They observed that the symbiont-free strain agglutinated with a wider variety of lectins than did the other strain, and that the concentration of lectins required to agglutinate the cells was lower than for the symbiont-harbouring *C. deanei*.

This pattern could also be observed in the present study. For symbiont-harbouring *C. deanei*, the essential oil increased the binding specificity of surface D-GalNAc

residues observed with the *G. max* and *D. biflorus* lectins. For the symbiont-free strain treated with the oil, there was a depletion of the binding specificity for the sialic acid residues, observed with *L. polyphemus*, and an increase of its binding specificity for D-Gal and D-GalNac sugar residues. Sialic acids are a family of nine carbon sugars that are found at the non-reducing end of glycoconjugates, and are linked to galactose and N-acetyl-D-galactosamine (Shauer and Kamerling 1997). This result indicates that the essential oil may have removed the sialic acid residues and exposed other sugar residues, or that the essential oil may be interfering with the expression of these sialic acid glycoconjugates at the cell surface. Also for the symbiont-free treated cells, there was a diminution in the recognition of mannose residues, confirmed by the *C. ensiformis* lectin.

In conclusion, this study of the effect of the essential oil from *C. citratus* on the trypanosomatid *C. deanei* with and without endosymbionts demonstrated the importance of these protozoans as a biological model in the evaluation of the cellular alterations and the influence of the symbiont's presence in trypanosomatids treated with herbal and commercial drugs. These results can contribute to understanding the drug's mechanism of action, opening new prospects of finding more effective, less toxic, and relatively inexpensive drugs of vegetable origin, in the treatment of diseases caused by trypanosomatids.

Acknowledgments. This study was supported by grants from the Conselho Nacional de Desenvolvimento Científico e Tecnológico (CNPq), Coordenação de Aperfeiçoamento de Pessoal de Nível Superior (CAPES), Financiadora de Estudos e Projetos - FINEP, PRONEX/ Fundação Araucária, and Programa de Pós-graduação em Microbiologia da Universidade Estadual de Londrina.

REFERENCES

Berry M. N., Edwards A. M., Barritt G. J. (1991) Isolated hepatocytes. Preparation, Properties and Applications. Elsevier, Amsterdam, New York, Oxford

Bishop C. D. (1995) Antiviral activity of the essential oil of *Melaleuca alternifolia* (Maiden Betche Cheek (tea tree) against tabacco mosaic virus. *J. Essent. Oil Res.* **7:** 641-644

Boisseau-Garsaud A. M., Cales-Quist D., Desbois N., Jouannelle A., Pratlong F., Dedet J. P. (2000) A new case of cutaneous infection by presumed monoxenous trypanosomatid in the island of Martinique (French West Indies). *Trans. Roy. Soc. Trop. Med. Hyg.* **94:** 51-52

Braga M. V., Urbina J. A., De Souza W. (2004) Effects of squalene synthase inhibitors on the growth and ultrastructure of *Trypanosoma cruzi*. *Int. J. Antimicrob. Agents.* **24:** 72-78

Burt S. (2005) Essential oils: their antibacterial properties and potential applications in foods - a review. *Int. J. Food Microbiol.* **94:** 223-253

Calixto J. B. (2000) Efficacy, safety, quality control, marketing and regulatory guidelines for herbal medicines (phytotherapeutic agents). *Braz. J. Med. Biol. Res.* **33:** 179-189

Carlini E. A., Contar J. D. P., Silva-Filho A. R., Silveira-Filho M. L., Frochtengarten O. F. A., Bueno J. (1986) Pharmacology of lemongrass (*Cymbopogon citratus* Stapf). I. Effects of teas prepared from the leaves on laboratory animals. *J. Ethnopharmacol.* **17:** 37-64

Castro C. R., Mecca M. M., Fanelli S. L., Ferreyra E. C., Diaz E. G., Castro J. A. (2003) Benznidazole-induced ultrastructural and biochemical alterations in rat esophagus. *Toxicology* **191:** 189-198

d´Avila-Levy C. M., Melo A. C. N., Vermelho A. B. and Branquinha M. H. (2001) Differential expression of proteolytic enzymes in endosymbiont-harboring *Crithidia* species. *FEMS Microbiol. Lett.* **202:** 73-77

d´Avila-Levy C. M., Souza R. F., Gomes R. C., Vermelho A. B.and Branquinha M. H. (2003) A metalloproteinase extracellularly released by *Crithidia deanei*. *Can. J. Microbiol.* **49:** 625-632

Dedet J. P., Roche B., Pratlong F., Cales-Quist D., Jouannelle J., Benichou J. C., Huere M. (1995) Diffuse cutaneous infection caused by a presumed monoxenous trypanosomatid in a patient infected with HIV. *Trans. Roy. Soc. Trop. Med. Hyg.* **89:** 644-646

De Souza W. (1989) Components of the cell surface of trypanosomatids. *Prog. Protistol.* **3:** 87-184

De Souza W., Motta M. C. M. (1999) Endosymbiosis in protozoan of the Trypanosomatidae family. *FEMS Microbiol. Lett.* **173:** 1-8

Dias Filho B. P.,Ueda-Nakamura T., Lopes C. H., Tsuneto L. T., Abreu Filho B., Nakamura C. V. (2005) Cell surface glycoproteins in *Crithidia deanei*: influence of the endosymbiont. *Acta Protozool.* **44:** 13-17

El-Kamil H. H., Ahmed A. H., Mohammed A. S., Yahia A. A. M., El-Tayeb I. H., Ali A. A. (1998) Antibacterial properties of essential oils from Nigella sativa seeds, *Cymbopogon citratus* leaves and *Pulicaria undulata* aerial parts. *Fitoterapia.* **69:** 77-78

Elvin-Lewis M. (2001) Should we be concerned about herbal remedies. *J. Ethnopharmacol.* **75:** 141-167

Essawi T., Srour M. (2000) Screening of some Palestinian medicinal plants for antibacterial activity. *J. Ethnopharmacol.* **70:** 343-349

Esteves M. J. G., Andrade A. F. B., Angluster J., De Souza W., Mundim M. H., Roitman I., Perreira M. E. A. (1982) Cell surface carbohydrates in *Crithidia deanei*: influence of the endosymbiont. *Eur. J. Cell Biol.* **26:** 244-248

Faria-e-Silva P. M., Fiorini J. E., Soares M. J., Alviano C. S., De Souza W. and Angluster J. (1994) Membrane-asociated polyssacharides composition, nutricional requirements and cell differentiation in *Herpetomonas roitmani*: influence of the endosymbiont. (Kinetoplastida: Trypanosomatidae). *J. Euk. Microbiol.* **41:** 55-59

Freymüller E., Camargo E. P. (1981) Ultrastructure differences between species of trypanosomatids with and without endosymbionts. *J. Protozool.* **28:** 175-182

Goad L. J., Holz G. G., Beach D. H. (1984). Sterols of *Leishmania* species. Implications for biosynthesis. *Mol. Biochem. Parasitol.* **10:** 161-170

Holetz F. B., Ueda-Nakamura T., Dias Filho B. P., Cortez D. A. G., Morgado-Díaz J. A., Nakamura C. V. (2003) Effect of essential oil of *Ocimum gratissimum* on the Trypanosomatid *Herpetomonas samuelpessoai*. *Acta Protozool.* **42:** 269-276

Jacobson R. L., Doyle R. J. (1996) Lectin-parasite interaction. *Parasitol. Today* **12:** 55-61

Juglal S., Govinden R., Odhav B. (2002) Spice oils for the control of co-occurring mycotoxin-producing fungi. *J. Food Prot.* **65:** 683-687

Kubata B. K., Nagamune K., Murakami N., Merkel P., Kabututu Z., Martin S. K., Kalulu T. M., Mustakuk H., Yoshida M., Ohnishi-Kameyama M., Kinoshita T., Duszenko M., Urade Y. (2005) *Kola acuminata* proanthocyanidins: a class of anti-trypanosomal compounds effective against *Trypanosoma brucei*. *Int. J. Parasitol.* **35:** 91-103

Lima E. O., Gompertz O. F., Giesbrecht A. M., Paulo M. Q. (1993) In vitro antifungal activity of essential oils obtained from officinal plants against dermatophytes. *Mycoses* **36:** 333-336

Luize P. S., Tiuman T. S., Morello L. G., Maza P. K., Ueda-Nakamura T., Dias Filho B. P., Cortez D. A. G., Mello J. C. P, Nakamura

C. V. (2005) Effects of medicinal plants extracts of *Leishmania* (L.) *amazonensis* and *Trypanosoma cruzi*. *Braz. J. Pharm. Sci*. **41:** 85-94

McGhee R. B., Cosgrove W. B. (1980) Biology and physiology of the lower Trypanosomatidae. *Microbiol. Rev.* **44:** 140-173

Melo S. F., Soares S. F., Costa R. F., Silva C. R., Oliveira M. B. N., Bezerra R. J. A. C., Caldeira-de-Araújo A., Bernardo-Filho M. (2001) Effect of the *Cymbopogon citratus, Maytenus ilicifolia* and *Baccharis genistelloides* extracts against the stannous chloride oxidative damage in *Escherichia coli*. *Mutat. Res.* **496:** 33-38

Mundin M. H., Roitman I. (1977) Extra nutritional requirements of artificially aposymbiotic *Crithidia deanei. J. Protozool.* **24:** 329-331

Mundin M. H., Roitman I., Herman M. A., Kitajima E. W. (1974) Simple nutrition of *Crithidia deanei*, a reduviid trypanosomatid with a symbiont. *J. Protozool.* **21**: 518-521

Nakamura C. V., Ishida K., Faccin L. C., Dias Filho B. P., Cortez D. A. G., Rozental S., De Souza W., Ueda-Nakamura T. (2004) In vitro activity of essential oil from *Ocimum gratissimum* L. against four *Candida* species. *Res. Microbiol.* **155:** 579-586

Oda L. M., Alviano C. S., Silva-Filho F. C., Angluster J. Roitman I., De Souza W. (1984) Surface anionic groups in symbiont-bearing and symbiont-free strains of *Crithidia deanei*. *J. Protozool.* **31:** 131-134

Onawunmim G. O. (1989) Evaluation of the antimicrobial activity of citral. *Lett. Appl. Microbiol.* **9:** 105-108

Rauber C. S., Guterres S., Schapoval E. E. S. (2005) LC determination of citral in *Cymbopogon citratus* volatile oil. *J. Pharm. Biochem. Analysis* **37:** 597-601

Rodrigues J. C. F., Urbina J. A., Souza W. (2005) Antiproliferative and ultrastructural effects of BPQ-OH, a specific inhibitor of squalene synthase, on *Leishmania amazonensis*. *Expl Parasitol.* **111:** 230-238

Santos D. O., Bourguignon S. C., Castro H. C., Silva J. S., Franco L. S., Hespanhol R., Soares M. J., Corte-Real S. (2004) Infection of Mouse dermal fibroblasts by the monoxenous trypanosomatid protozoa *Crithidia deanei* and *Herpetomonas roitmani*. *J. Euk. Microbiol.* **51:** 570-574

Santos S. L. A., d'Avila-Levy C. M., Dias F. A., Ribeiro R. O., Pereira F. M., Elias C. G. R., Souto-Padro T. S., Lopes A. H. C. S., Alviano C. S., Branquinha M. H., Soares R. M. A. (2006) *Phytomonas serpens*: cysteine peptidase inhibitors interfere with growth, ultrastructure and host adhesion. *Int. J. Parasitol*. **36:** 47-56

Schauer R., Kamerling J. P. (1997) Chemistry, biochemistry and biology of sialic acids In: Glycoproteins II (Eds. J. Montreuil, J. F. G. Vliegenthart, H. Schachter). Elsevier, Amsterdam, 243-402

Ueda-Nakamura T., Mendonça-Filho R. R., Morgado-Díaz J. A., Maza P. K., Dias Filho B. P., Cortez D. A G., Alviano D. S., Rosa M. S. S., Lopes A. H. C. S., Alviano C. S., Nakamura C. V. (2006) Antileishmanial activity of eugenol-rich essential oil from *Ocimum gratissimum*. *Parasitol. Int.* **55:** 99-105

Wallace F. G. (1966) The trypanosomatid parasites of insect and arachnids. *Expl Parasitol.* **18:** 124-193

Wannissorn B., Jarikasen S., Siriwangchai T., Thubthimthed S. (2005) Antibacterial properties of essential oils from Thai medicinal plants. *Fitoterapia* **76:** 233-236

Received on 16th March, 2006; revised version on 10th May, 2006; accepted on 29th May, 2006

Acta Protozool. (2006) 45: 241 - 248

ACTA
PROTOZOOLOGICA

Isolation, Characterization and Phylogenetic Analysis of the Cytochrome B Gene (*Cyb*) from the Hypotrichous Ciliate *Pseudourostyla cristata*

Xing-Yin LIU[1], Kam-Len Daniel LEE[2,3], Yong-Zhen MAO[1], Li-Pei JIN[1]

[1]School of Life Sciences, Sun Yat-Sen (Zhongshan) University, Guangzhou, China; [2]Department of Applied Biology and Chemical Technology, Hong Kong Polytechnic University, Hong Kong, China; [3]State Key Laboratory of Chinese Medicine and Molecular Pharmacology, Shenzhen, China

Summary. To date, no genes have been characterized from mitochondrial DNA of hypotrichous ciliates. Here we present the complete sequence of the gene (*cyb*) encoding cytochrome *b* in the hypotrichous ciliate *Pseudourostyla cristata*. Analysis of nucleotide and deduced amino acids sequences predicts a protein of 393 amino acids encoded by *cyb*. CYB amino acid similarity and phylogenetic tree analyses strongly support a close evolutionary relationship between *Paramecium*, *Tetrahymena* and *Pseudourostyla*. The heat stress-dependent expression pattern of CYB was verified by semi-quantitative real-time reverse transcriptase polymerase chain reaction (RT-PCR) analysis.

Key words: ciliate, cytochrome *b*, heat stress, mitochondrion, *Pseudourostyla cristata*.

INTRODUCTION

Ciliates comprise a large and structurally diverse group of unicellular eukaryotes (protists). Phylogenetic reconstructions, inferred from the small subunit rRNA gene and protein-encoding gene sequences demonstrate that ciliates represent a relatively evolved lineage among the protists (Greenwood *et al*. 1991, Bernhard *et al*. 1995, Bernhard and Schlegel 1998, Budin and Philippe 1998, Tourancheau *et al*. 1998). Unlike other eukaryotes, ciliates possess two types of nuclei: polyploidy macronuclei (for protein synthesis) and diploid micronuclei (for heritability). Additionally, they contain numerous mitochondria. It is known that the protozoan mitochondrial genomes diverged extremely from all other genomes (Gray *et al*. 2004). This reflects an early branching event and a rapid evolution at the primary sequence level and at the levels of genome content and organization. Furthermore, it represents an evolution of genetic codon usage (Gray *et al*. 2004). The ciliates have among the most rapidly evolving mitochondrial genomes as evidenced by the large number of putative proteins for which function cannot be readily assigned (Brunk *et al*. 2003). Oligohymenophorea and Hypotrichea are distant classes within the Ciliophora phylum. Mitochondrial DNA (mtDNA) data from the ciliates is only limited in *Tetrahymena* and *Paramecium* species (in the

Address for correspondence: Li-Pei Jin, School of Life Sciences, Sun Yat-Sen (Zhongshan) University Guangzhou 510275, Guangdong, People's Republic of China; Fax: +86-020-84036215; E-mail: lssjlp@zsu.edu.cn

class Oligohymenophorea) (Pritchard *et al.* 1990a, Burger *et al*. 2000, Brunk *et al*. 2003), and mtDNA investigations on the thousands of Hypotrichea organisms have not been conducted. Mitochondrial genes are attractive markers for inferring phylogenies of closely related species because of their rapid evolutionary rates compared to those of nuclear DNA (Saccone *et al.* 2000). In particular, among the protein coding genes of mtDNA, cytochrome b (*cyb*) can be used for resolving phylogenetic relationships within a genus and among higher orders, covering a divergence time of roughly 70 million years (Myr) (Irwin *et al*. 1991, Johns and Avise 1998, Callejas and Ochando 2000). Until now, in all ciliate groups, the *cyb* gene has been characterized only in *Paramecium* and *Tetrahymena* (Pritchard *et al*. 1990b, Burger *et al*. 2000, Brunk *et al*. 2003).

The hypotrichous ciliate *Pseudourostyla cristata* is a free-living ciliated protozoan that is characterized by a highly differentiated pattern of the vegetative cell. Recently, we unexpectedly isolated a full-length mt *cyb* cDNA from heat stress-induced phase mRNA of the *P*. *cristata.* This study represents the first description of CYB in hypotrichous ciliates, so it has allowed us to initiate a molecular phylogenetic comparison with the CYB sequences available from the other species. CYB is an indispensable component of the cytochrome bc_1 respiratory complex, which is responsible for ubiquinol-cytochrome c reductase activity in the mitochondrion (Esposti *et al*. 1993). It has never been reported as an up-regulated gene when responding to heat stress. Thus, our finding is relevant for elucidating the stress signal response role of the bc_1 complex.

MATERIALS AND METHODS

Cell culture and heat stress

Pseudourostyla cristata was originally isolated from a fresh water pond outside Shanghai, China. The cells were cultured in Pringsheim's solution with wheat grains and the food organism *Chilomonas paramecium* at 25-27°C, as described previously (Jin and Ng 1989). The *C. paramecium* was isolated with three cycles of gentle centrifugation (1000 rpm for 1 min.). For the heat stress treatment, the culture dishes containing approximately 10^4 cells were incubated for 30 min at 42°C.

RNA Isolation and smart cDNA synthesis

Total RNA samples from those cells with two hours post-heat stress were extracted using reagents and protocols described previously (Liu *et al.* 2004). Smart cDNA was synthesized from the 500 ng total RNA samples using the SMART PCR cDNA synthesis Kit (Clontech) with minor modification: Reverse transcription was conducted in a 10 µl reaction volume at 42°C for 1 h with the 3' BD SMART CDS Primer II A (A modified oligo(dT) primer: 5'-AGCAGTGGTATCAACGCAGAGTACT$_{[30]}$VN-3', and ignoring the BD SMART II A oligonucleotide (5'-AGCAGTGGTATCAACGCAGAGTACGCGGG-3') required in manufacture's protocol (Clontech SMART PCR cDNA synthesis Kit User manual PT3041-1). 2.5 µl of this diluted first strand synthesis reaction mixture was added to 98 µl of the Master mix containing 2 µl of the 5' PCR Primer II A (5'-AAGCAGTGGTATCAACGCA GAGT-3'). The mixture was PCR amplified in a PTC-100 thermal cycler (MJ Research, USA) as follow: 95°C, 1 min; 21 × [95°C, 15 s; 65°C, 30 s; 68°C, 6 min]. In order to demonstrate that the template for the LD-PCR product was cDNA and not genomic DNA, a minus-reverse transcriptase control was performed.

Gel electrophoresis, cloning and sequencing

The resulting cDNA products were analyzed in a 1.2% agarose gel. The predominant bands were excised from the gel, and DNA was extracted from the gel slices using the QIAquick Gel Extraction Kit (Qiagen), cloned into the TA cloning vector pMD-T-18 (Takrara) and transformed into *E. coli*, DH5a cells. Plasmid DNA samples were prepared from the confirmed recombinant transformants using the EZNA Plasmid Miniprep Kit I (Omega). Both strands of the DNA inserts were sequenced using the 370 DNA Sequencer (Applied Biosystem). The acquired sequences were analyzed with the DNAStar software.

Determination of open reading frames (ORFs) and characteristics of the cloned cDNA

Using the ORF finder at http://www.ncbi.nlm.nih.gov/gorf/gorf.html, the cloned cDNA sequence was translated with the protozoan mitochondrial genetic code (Aldritt *et al*. 1989). Similarity searches were performed with the Basic Local Alignment Search Tool X (BLASTX). The protein properties were predicted using ProtParam (Appel *et al*. 1994). The transmembrane (TM) domain of the CYB protein was predicted using TMHMM version 2 software (Sonnhammer *et al*. 1998). The 3D structure of the inferred CYB protein was modeled by the 3D-Pssm Program (Version 2.6.0) (Kelley *et al*. 2000).

Semi-quantitative real time reverse transcriptase (RT)-PCR analysis

Total RNA from the non-heat stress and the 0, 1, 2 and 3 h post-heat stress cells were extracted as described above. cDNA was synthesized from 500 ng of total RNA of each sample using the Omniscript-RT Kit (Qiagen) according to the manufacturer's instructions. Real-time fluorescence signals were measured with SYBR Green I (Roche) in the ABT PRISM 7700 (PE Applied Biosystem). The 17s rRNA (GenBank Accession Number: AY940212) was used as the internal control, and the RT-PCR CYB and 17s rRNA primers were designed with Primer Premier 5.0 software.

All RT-PCR reactions and the minus-reverse transcriptase control were performed in triplicate. The ΔC_T value was determined by

subtracting the target C_T of each sample from its respective 17s rRNA C_T value. The $\Delta\Delta C_T$ was calculated as the difference between ΔC_T of each sample and ΔC_T of the non-heat stress sample. Fold expression differences for CYB were determined by $2^{-\Delta\Delta}C_T$ (Livak and Schmittgen 2001). All statistical analyses were performed with SPSS version 12.0 software (SPSS Inc, IL, USA).

Data and phylogenetic analysis

The amino acid sequence data of CYB were obtained from the Entrez Protein program (http://ncbi.nlm.nih.gov/entrez/index.htm). All amino acid sequences were manually optimized and aligned using a computer-assisted procedure, ClustalW, version 1.80 (Thompson *et al*. 1997). The phylogenetic trees were constructed using several members of each major taxon to accurately gauge the CYB global topology rooted with *Rickettsia prowazekii* and *Paracoccus denitrificans*, and the CYB phylogenetic trees were generated with the neighbor-joining (NJ) method implemented in the PHYLIP software package, version 3.6 (Felsenstein 2002). For the NJ analysis, the NEIGHBOR program was used, and the bootstrap proportions were calculated by analyzing 1,000 replications. The distance matrix was computed with PROTDIST; 1,000 bootstrap replications were obtained by the SEQBOOT program.

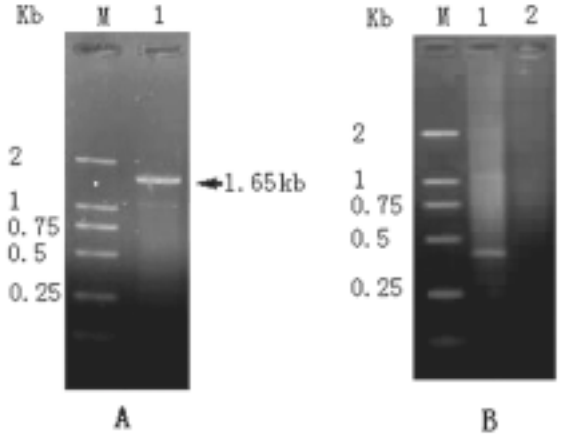

Fig 1. Agarose gel electrophoresis of RT-PCR products. RT-PCR products of RNA from 2 h post-heat stress were analyzed by electrophoresis in a 1.2 % agarose gel. **A -** lane M: Marker (DL 2000, Takrara); lane 1: cDNA was synthesized as described in the material and method. The arrow indicates a strong band at 1.65kb. **B -** lane M: Marker (DL 2000, Takrara); lane 1: cDNA was synthesized as described in Clontech SMART PCR cDNA synthesis Kit User manual; lane 3: A minus-reverse transiptase control.

RESULTS AND DISCUSSION

Isolation and sequence of the cytochrome b gene

Agarose gel electrophoresis of the RT-PCR products illuminates a strong band at approximately 1.65 kb for the two hours post-heat stressed RNA samples (Fig. 1A: Lane 1). 3'BD SMART CDS primer II A primers sequences was found in the 5' and 3' ends. The minus-reverse transcriptase control (Fig. 1B: Lane 2) demonstrated that the RT-PCR template for the product was cDNA and not genomic DNA. The unexpected result was a surprise and was reconfirmed, but when we used the two hour post-heat stress sample for RT-PCR per Clontech's SMART system instructions with 3' BD SMART CDS primer II A. and BD SMART II A oligonucleotide, the above result can not be repeated and a smear of cDNA without the characteristic bright band was found (Fig. 1B: Lane 1). Brunk *et al*. (2003) found that the *Tetrahymena thermophila* mitochondrial genome appears to have two transcriptional units, transcribed from a nearly central bi-directional promoter set. Therefore, we hypothesized that this product may be up-regulated under heat stress, and that it may be a bidirectional transcription. It will be very interesting to investigate whether a similar phenomenon occurs in other ciliates, for example, among *Tetrahymena* and *Paramecium* species. Furthermore, constructing a heat-inducible gene expression system in these simple organisms is recommended.

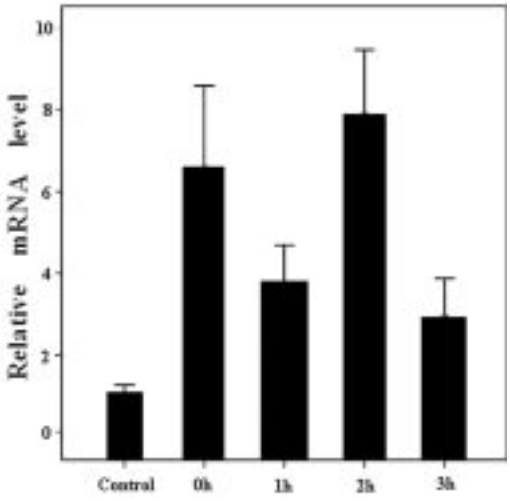

Fig. 2. CYB expression patterns in *Pseudourostyla cristata* under the condition of heat stress. The relative CYB mRNA expression level in the non-heat stress control was regarded as 1.000. Relative to the non-heat stress control, a 6.37-fold increase in the CYB mRNA was found immediately (0 h) post-heat stress treatment. One and two hours post-heat stress treatment, 3.58 and 7.76-fold increases were observed, respectively. Even at three hours post- heat stress treatment, a 2.53-fold increase remained.

After deleting the BD SMART CDS Primer II A sequence, the sequence was 1538 bp long and encompassed a full-length ORF with a protein sequence of 393

Table 1. Codon usage in *Pseudourostyla cristata cyb* gene

aa	Codon	#	%	aa	Codon	#	%	aa	Condon	#	%	aa	Condon	#	%
Phe	TTT	37	88.1	Ser	TCT	3	15.8	Tyr	TAT	29	90.6	Cys	TGT	4	66.7
	TTC	5	11.9		TCC	3	15.8		TAC	3	9.4		TGC	2	33.3
Leu	TTA	38	84.4		TCA	7	36.8	Ter	TAA	*	100	Trp	TGA	14	93.3
	TTG	3	6.7		TCG	6	31.6		TAG	0	0		TGG	1	6.7
	CTT	2	4.4	Pro	CCT	5	38.5	His	CAT	14	87.5	Arg	CGT	3	50
	CTC	1	2.2		CCC	0	0		CAC	2	12.5		CGC	1	16.7
	CTA	1	2.2		CCA	5	38.5	Gln	CAA	6	100		CGA	2	33.3
	CTG	0	0		CCG	3	23.1		CAG	0	0		CGG	0	0
Ile	ATT	28	77.8	Thr	ACT	8	40	Asn	AAT	17	85	Ser	AGT	2	40
	ATC	3	8.3		ACC	0	0		AAC	3	15		AGC	3	50
	ATA	5	13.9		ACA	5	25	Lys	AAA	7	87.5	Arg	AGA	4	100
Met	ATG	11	100		ACG	7	35		AAG	1	12.5		AGG	0	0
Val	GTT	14	60.9	Ala	GCT	5	41.7	Asp	GAT	9	75	Gly	GGT	8	36.4
	GTC	3	13.0		GCC	0	0		GAC	3	25		GGC	0	0
	GTA	6	26.1		GCA	1	8.3	Glu	GAA	16	88.9		GGA	10	45.4
	GTG	0	0		GCG	6	50		GAG	2	11.1		GGG	4	18.2

Percentage (%) indicates the proportion of codons used for each amino acid. Asterisk (*) denote stop codon, excluding ATT as initiation codon.

amino acids (GenBank accession Number: AY940211). AUU is used as the initiation codon, and the first AUG codon is 114 nt downstream. The termination codon is UAA. This codon usage is consistent with that of *Tetrahymena pyriforms* mtDNA (Edqvist *et al*. 2000). Continuity of the ORF and normal-length protein sequence rule out the presence of introns. BLASTx search shows the protein sequences with the highest homologies or similarities were the CYB sequences.

Expression pattern of CYB under heat stress

To determine the CYB mRNA expression levels in the heat stress-induced *P. cristata*, a semi-quantitative real-time RT-PCR analysis was performed (Fig. 2). Relative to the non-heat stress control, a six-fold increase in the CYB mRNA immediately (0 h) post heat-treatment for 30 min was observed. Following one h and two h post-heat stress, the cells exhibited four-and seven-fold differences respectively. Even at three h post-heat stress, a near two half-fold increase was maintained (Fig. 2). We hypothesized that the dynamic expression pattern may adapt to the heat stress response. The high level of cellular CYB expression may reflect a high demand for mitochondrial electron transport and respiratory activities to compensate for the imposed heat stress. However, because the mitochondrial complex was not isolated from the organism, it is impossible to establish an experimental link between respiration and heat stress. Since similar findings in other unicellular organisms have not been reported, we only can speculate CYB protein as the locus of regulation of electron transport in *P. cristata* mitochondria under the conditions of heat stress. Thus the heat stress-induced up-regulation of CYB mRNA may reflect a concurrent increase in CYB protein levels, which could increase respiratory rates and thus ATP synthesis for survival and ciliary movement.

Analysis and Comparison of CYB amino acid sequence

The deduced amino acid sequence is a 47-kDa protein with an isoelectric point of 5.68. The total number of negatively charged residues (Asp + Glu) is 30, and the total number of positively charged residues (Arg + Lys) is 18. The ratio of negative to positive residues is 1.76. The grand average of hydropathicity (GRAVY) is 0.419. The aliphatic index is 100.41. The deduced protein contains ten putative TM domains, and thus the TM profile is similar to that of the *Paramecium aurelia* CYB (Brunk *et al*. 2003). The results of 3D structure prediction is most similar to that of the *Gallus gallus* cytochrome bc1 transmembrane subunit (PSSM E-value of: 1.66e-08, = 95% certainty).

Fig. 3 shows an alignment of CYB sequences from CYB amino acid sequences from *P. cristata, Tetrahymena pyroformis, Paramecium tetraurelia, Plasmo-*

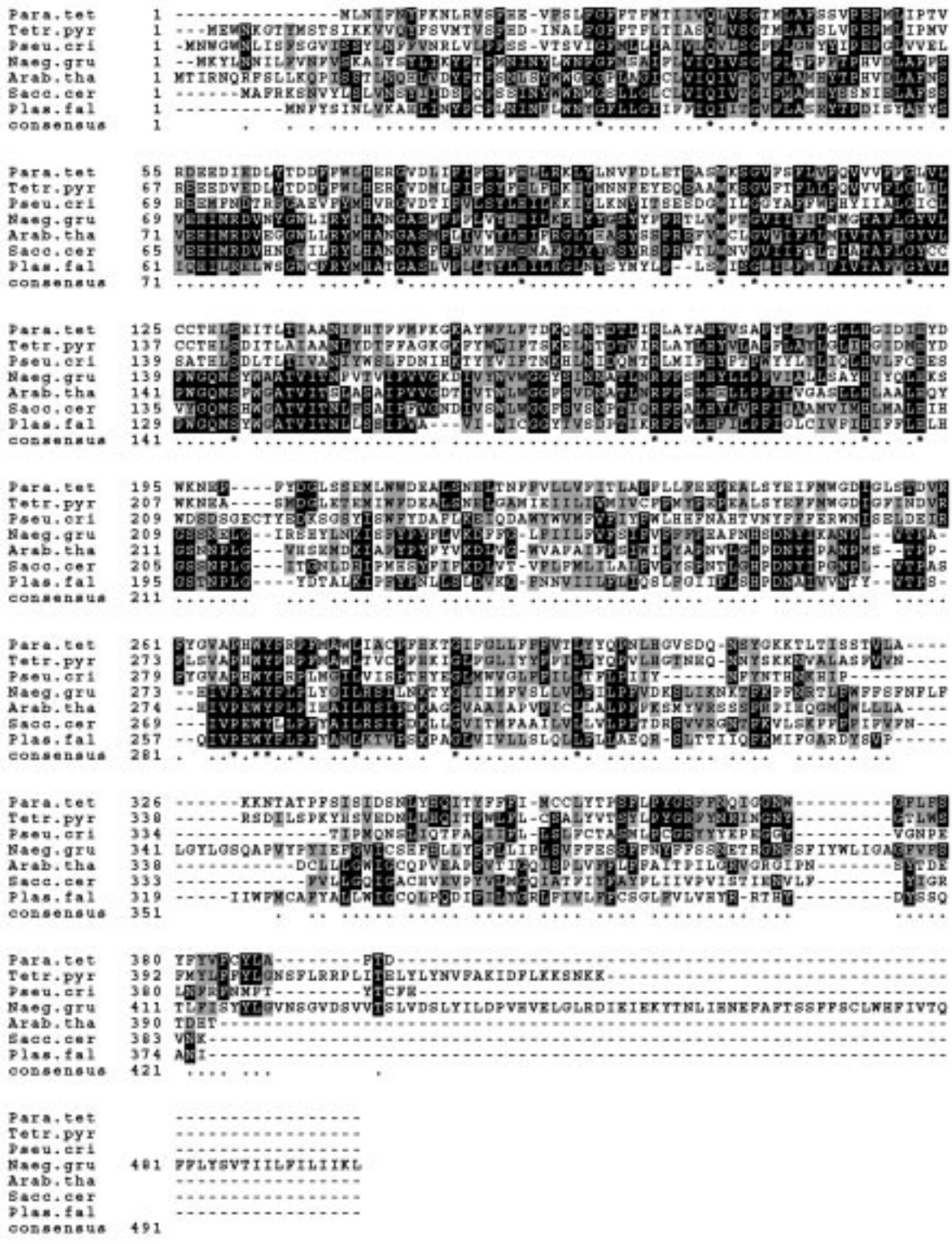

Fig. 3. CYB amino acid sequence alignment from various organisms. CYB amino acid sequences from *Pseudourostyla cristata* (Pseu. cri), *Tetrahymena pyroformis* (Tetr. pyr), *Paramecium tetraurelia* (Para. tet)**,** *Plasmodium falciparum* (Plas. fal), *Naegleria gruberi* (Naeg, gru), *Arabidopsis thaliana* (Arab, tha), and *Saccharomyces cerevisae* (Sacc. cer) were aligned by CLUSTALW. Identical amino acids are darkly shaded and similar amino acids are lightly shaded. Positions with the highest consensus, i.e. identical amino acid sequences, are denoted by asterisks (*****) along the bottom line (consensus line). Other positions with consensus are denoted by dots (**.**). Gaps were introduced to improve alignment and these are marked with dashes (-) along the individual sequences.

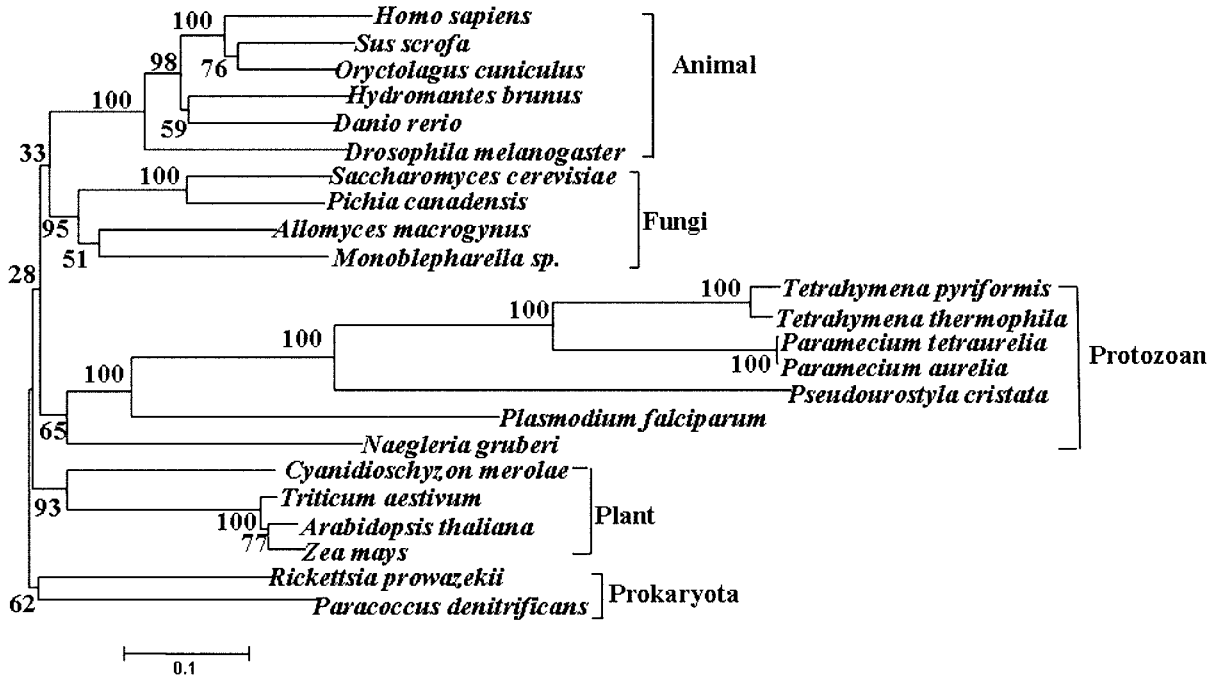

Fig. 4. Neighbor-joining (NJ) phylogenetic tree based on CYB amino acid sequence alignment. Bootstrap support, calculated from 1,000 replicates, is shown at each branch (in %, only values > 50% are listed). The sequences used in this study are available from the GenBank/EMBL databases with the following accession numbers: *Pseudourostyla cristata* (**AY940211**), *Paramecium aurelia* (**NP_059398**), *Paramecium tetraurelia* (**P15585**), *Tetrahymena thermophila* (**NP_149395**), *Tetrahymena pyriformis* (**NP_049598**), *Naegleria gruberi* (**AAG17790**), *Monoblepharella sp.* (**NP_803529**), *Hydromantes brunus* (**YP_097270**), *Danio rerio* (**NP_059343**), *Saccharomyces cerevisiae* (**CAA58861**), *Drosophila melanogaster* (**NP_008288**), *Arabidopsis thaliana* (**NP_178804**), *Plasmodium falciparum* (**AAT00449**), *Oryctolagus cuniculus* (**AAS54913**), *Sus scrofa* (**AAU04561**), *Zea mays* (**CAA25367**), *Rickettsia prowazekii* (**CAA14733**), *Paracoccus denitrificans* (**AAA25572**), *Homo sapiens* (**AAB58955**), *Pichia canadensis* (**BAA06572**), *Allomyces macrogynus* (**AAC49221**), *Triticum aestivum* (**P07747**), *Cyanidioschyzon merolae* (**BAA34655**). *Rickettsia prowazekii* and *Paracoccus denitrificans* are selected as the outgroup species.

dium falciparum, Naegleria gruberi, Arabidopsis thaliana, and *Saccharomyces cerevisae*. CYB from the ciliates *T. pyroformis* and *P. tetraurelia* show higher amino acid similarity (41.5 % and 43.7 % respectively) to *P. cristata* CYB. Notably, CYB from the more distantly related organisms *Sachhromyces cerevisae, Arabidopsis thaliana, Plasmodium falciparum,* and *Naegleria gruberi* show lower level of similarity (31.0%, 27.7%, 30.7% and 26.1% respectively) to *P. cristata* CYB. These results are consistent with the idea that ciliate mt DNA sequence branched from other groups early in evolution and evolved very rapidly (Brunk *et al*. 2003).

The protein alignment also reveals a conserved peptide (VAPHWYFRP) among three ciliate taxa. Four invariant histidine residues (Fig. 4: Asterisks (*) indicated H86, H100, H187 and H 201) proposed as the heme-binding sites in CYB (Edqvist *et al*. 2000) were present in the *P. cristata* CYB sequence.

Codon usage

The overall deduced codon usage for *cyb* gene of *P. cristata* is summarized in Table 1. Like *T. pyrjiformis*, TGA is used preferentially to encode Trp. The *P. cristata cyb* (72% A+T) also exhibits a preference for A or T in the third position of codons (80% A+T), whereas first (excluding Trp and Met) and second position A+T biases are lower (60% and 68%, respectively). First position preferences for A or T in Leu codons contribute to the high A+T content of the gene. Of 40 Leu residues, 33 are specified by TTA, whereas TTG, CTA and CTC, CTT together account for only 7 codons, and CTG is not used at all. Changes in mitochondrial codon frequencies can occur as a result of AT selection pressure. Such

pressure is manifested by an increase in the A+T content of spacer regions or the third positions relative to first. Table 1 shows that 12 of 13 Trp residues are encoded using the TGA codon (a universal stop codon). Only one Trp residues was encoded using the universal TGG codon. As in *P. aurelia* mtDNA, TGA and TGG appear with almost equal frequency, but *T. pyriformis* mt DNA uses TGA almost exclusively (Brunk *et al*. 2003). The variant assignment of TGA among three kinds of ciliates further illustrates the point that codon usage is highly variable and basically uninformative with respect to understanding global phylogenetic relationship (Lang *et al*.1987, Paquin and Lang 1996).

Phylogenetic reconstruction based on CYB sequence comparisons

A CYB phylogeny based on neighbor-joining (NJ) analyses (Fig. 4) shows four major clades: protozoa, plants, fungi and animals with moderate to very high bootstrap support. Animals and fungi are each robustly monophyletic. Regarding CYB evolutionary trends, protozoan CYB was closest to plant CYB. Within the protozoan clade, the apicomplexan species (*Plasmodium falciparum)* and the ciliate species (*Paramecium, Tetrahymena* and *Pseudourostyla)* form a well-supported (100% bootstrap) monophyletic group, in agreement with nuclear rRNA trees, although overall support for the protozoan clade is low (bootstrap value 63%). Within the class Oligohymenophorea of ciliates, *Paramecium* and *Tetrahymena* are sister species, forming a monophyletic grouping with long branches. Since *P. cristata* belongs to the class Hypotrochea, the tree shows Oligohymenophorea and Hypotrochea branching together to form a basal clade with 100% bootstrap support. This is in agreement with morphological data and other protein coding gene tress (Tourancheau *et al*.1998). The long branches indicate that the common ancestor of ciliates must have possessed a highly divergent *cyb* gene; moreover their *cyb* genes are obviously evolving at an accelerated and unequal rate. The extreme divergence in ciliates complicates phylogenetic reconstruction and assessment of relationships. It also highlights the importance of isolating and characterizing other ciliate mitochondrial genes, which should provide additional information into codon usage and insights about the evolution of protozoan.

Acknowledgments. This work was supported by the Natural Science Foundation of China (Project Number 30370210) to LPJ and an Internal Research Fund from The Hong Kong Polytechnic University to KLDL.

REFERENCES

Aldritt S. M., Joseph J. T., Wirth D. F. (1989) identification of cytochrome b in *Plasmodium gallinaceum. Mol. Cell Biol.* **9:** 3614-20

Appel R. D., Bairoch A., Hochstrasser D. F. (1994) A new generation of information retrieval tools for biologists: the example of the ExPASy WWW server. *Trends Biochem. Sci.* **19:** 258-260

Bernhard D., Schlegel M. (1998) Evolution of histoneH4 and H3 genes in different ciliate lineages. *J. Mol. Evol.* **46:** 344-354

Bernhard D., Leipe D. D., Sogin M. L., Schlegel M. (1995) Phylogenetic relationships of the Nassulidia within the phylumciliophora inferred from the complete small subunit rRNA genesequences of *Furgasonia blochmanni, Obertrumia georgania*, and *Pseudomicrothorax dubius*. *J. Euk. Microbiol.* **42:** 126-131

Brunk C. F., Lee, L. C., Tran A. B., Li J. (2003) Complete sequence of the mitochondrial genome of *Tetrahymena thermophila* and comparative methods for identifying highly divergent genes. *Nucl. Acids Res.* **31:** 1673-1682

Budin K., Philippe H. (1998) New insights into the phylogeny of eukaryotes based on ciliate Hsp70 sequences. *Mol. Biol. Evol.* **15:** 943-56

Burger G., Zhu Y., Littlejohn T. G., Greenwood S. J., Schnare M. N., Lang B. F., Gray M.W. (2000) Complete sequence of the mitochondrial genome of *Tetrahymena pyriformis* and comparison with *Paramecium aurelia* mitochondrial DNA. *J. Mol. Biol.* **297:** 365-380

Callejas C., Ochando M. D. (2000) Recent radiation of Iberian barbell fish (Teleostei, Cyprinidae) inferred from cytochrome *b* genes. *J. Hered.* **91:** 283-288

Esposti M., Devries D. S., Crimi M., Ghelli A., Patarnello T., Meyer A. (1993) Mitochondrial cytochrome *b* evolution and structure of the protein. *Biochem. Biophys. Acta* **1143:** 243-271

Edqvist J., Burger G., Gray M. W. (2000) Expression of mitochondrial protein-coding genes in *Tetrahymena pyriformis*. *J. Mol. Biol.* **297:** 381-93

Felsenstein J. (2002) PHYLIP (Phylogeny Inference Package) Version 3.6. Distributed by the author, Washington:Department of Genome Sciences, University of Washington, Seattle

Gray M. W, Lang B. F., Burger G. (2004) Mitochondria of Protists. *Ann. Rev. Genetics* **38:** 477-524

Greenwood S. J., Sogin M. L., Lynn D. H. (1991) Phylogenetic relationships within the class Oligohymenophora, phylum Ciliophora, inferred from the complete small subunit rRNA gene sequences of *Colpidium campylum, Glaucoma chattoni* and *Opisthonecta henneguyi*. *J. Mol. Evol.* **33:** 163-174

Irwin D. M., Kocher T. D., Wilson A. C. (1991) Evolution of the cytochrome b gene of mammals. *J. Mol. Evol.* **32:** 128-144

Jin L. P., Ng S. F. (1989) The somatic function of the germ nucleus in *Pseudourostyla cristata:* asexual reproduction and stomatogenesis. *J. Protozool.* **36:** 315-326

Johns G. C., Avise J. C. (1998) A comparative summary of genetic distances in the vertebrates from the mitochondrial cytochrome b gene. *Mol. Biol. Evol.* **15:** 1481-1490

Kelley L. A., MacCallum R. M., Sternberg M. J. E. (2000) Enhanced genome annotation using structural profiles in the program 3D-PSSM. *J. Mol. Biol.* **299:** 501-522

Lang B. F., Cedergren R., Gray M. W. (1987). The mitochondrial genome of the fission yeast, Schizosaccharomyces pombe. Sequence of the large-subunit ribosomal RNA gene, comparison of potential secondary structure in fungal mitochondrial large-subunit rRNAs and evolutionary considerations. *Eur. J. Biochem.* **3:** 527-537

Livak K. J., Schmittgen T. D. (2001) Analysis of relative gene expression data using real-time quantitative PCR and the $2^{-\Delta\Delta C}$T method. *Methods* **25:** 402-408

Liu X. Y., Mao Y. Z., Chen J. H., Lee K. L-D., Jin L. P.(2004) Total RNA Extraction from Large Ciliates. *Chinese J. Zool.* **39:** 44-47

Paquin B., Lang B. F. (1996) The mitochondrial DNA of *Allomyces macrogynus*: the complete genomic sequence from an ancestral fungus. *J. Mol. Biol.* **5:** 688-701

Pritchard A. E., Seilhamer J. J., Mahalingam R., Sable C. L., Venuti S. E., Cummings D. J. (1990a) Nucleotide sequence of the mitochondrial genome of *Paramecium*. *Nucl. Acids Res.* **18:** 173-180

Pritchard A. E., Sable C. L., Venuti S. E., Cummings D. J. (1990b) Analysis of NADH dehydrogenase proteins, ATPase subunit 9, cytochrome b, and ribosomal protein L14 encoded in the mitochondrial DNA of Paramecium. *Nucl. Acids Res.* **18:** 163-71

Saccone C., Gissi C., Lanave C., Larizza A., Pesole G., Reyes A. (2000) Evolution of the mitochondrial genetic system: an overview. *Gene* **261:** 153-159

Sonnhammer E. L., Heijne G., Krogh A. (1998) A hidden Markov model for predicting transmembrane helices in protein sequences. *Proc. Int. Conf. Intell. Syst. Mol. Biol.* **6:** 175-182

Thompson J. D., Gibson T. J., Plewniak F., Jeanmougin F., Higgins D. G. (1997) The CLUSTAL_X Windows interface: flexible strategies for multiple sequence alignment aided by quality analysis tools. *Nucl. Acids Res.* **24:** 4876-488

Tourancheau A. B., Villalobo E., Tsao N., Torres A., Pearlman R. E. (1998) Protein coding gene trees in ciliates: comparison with rRNA-based phylogenies. *Mol. Phylogenet Evol.* **10:** 299-309

Received on 2nd November, 2005; revised version on 9th May, 2006; accepted on 28th May, 2006

Acta Protozool. (2006) 45: 249 - 254

ACTA
PROTOZOOLOGICA

Karyotype and Genome Size of *Nadelspora canceri* Determined by Pulsed Field Gel Electrophoresis

Harold P. AMOGAN[1], J. Patrick MARTINEZ[2], Lynda M. CIUFFETTI[2], Katharine G. FIELD[1] and Paul W. RENO[1, 3]

[1]Department of Microbiology, Oregon State University, Corvallis, USA; [2]Department of Botany and Plant Pathology, Oregon State University, Corvallis, USA; [3]Coastal Oregon Marine Experiment Station, Newport, USA

Summary. Pulsed field gel electrophoresis was used to characterize the genome of microsporidian *Nadelspora canceri*. *N. canceri* spores isolated from Dungeness crab (*Cancer magister*) and red rock crab (*Cancer productus*) both yielded a karyotype of 10 chromosome-sized DNA bands. Close inspection of the band patterns and band sizes showed a difference in genome size between the two isolates. Spore isolates from Dungeness crab had a genome size of 7.4 Mb while spore isolates from red rock crab had a genome size of 7.3 Mb. Previously characterized microsporidians have a genome size range of 2.9-19.5 Mb and a karyotype ranging from 7-18 chromosome-sized DNA bands. *N. canceri* falls well within the genome size range and karyotype number of known microsporidians. The difference in genome size observed between the two spore isolates indicates intraspecies chromosome-size polymorphism.

Key words: chromosome-size polymorphism, microsporidia, protists.

INTRODUCTION

Phylum Microsporidia consists of eukaryotic protists parasitic to vertebrates and invertebrates. Members of this phylum have 7-18 chromosome-sized DNA bands (Wittner and Weiss 1999). Within-species variations in chromosome number and size have been detected in the phylum (Malone and McIvor 1993, Biderre *et al.* 1998). Variations in chromosome number and size may imply plasticity of the genomes and clonal reproduction of isolates (Venegas *et al.* 1997).

The microsporidian *Nadelspora canceri* is a pathogen of Dungeness (*Cancer magister*) and red rock crabs (*Cancer productus*). Among sampled populations of Dungeness crabs, *N. canceri* has a prevalence of infection ranging from 0.4% (Bodega Bay, CA) to 41.4% (Tillamook Bay, OR) (Childers *et al.* 1996). *N. canceri* has the potential to affect crabs important to commercial and sport fishermen. The geographic distribution, prevalence of infection, and spore ultrastructure of *N. canceri* has been described (Olson *et al.* 1994, Childers *et al.* 1996). However, information describing *N. canceri's* genome is lacking and warrants investigation. Based on small subunit ribosomal DNA (SSU

Address for correspondence: Paul W. Reno, Coastal Oregon Marine Experiment Station, 2030 South Marine Science Drive, Newport, Oregon, 97365, USA; FAX number: 1-541-867-0138; E-mail: paul.reno@hmsc.orst.edu

rDNA) sequence analysis, the parasite was placed in Baker's *Icthyosporidium* group (Baker *et al.* 1995, Amogan 2004). To further characterize the organism, we estimated the karyotype and genome size of *N. canceri* by pulsed field gel electrophoresis (PFGE).

MATERIALS AND METHODS

Collection of infected crabs

A Dungeness crab containing *N. canceri* was donated for this study by Dr. Robert Olson (Coastal Oregon Marine Experiment Station, Oregon State University, Newport, OR). A red rock crab containing *N. canceri* was donated by a recreational fisherman in Yaquina Bay, Newport, OR. Crabs were caught using baited crab pots and rings. Infected crabs were detected by examining for milky white or yellowish crab muscle tissue observed at the carapace-leg junction. Infection was confirmed by microscopic observation of *N. canceri* spores. Spore samples obtained from the Dungeness crab were identified as NC1 and spores obtained from the red rock crab were identified as NC2.

Spore purification

To purify spores from crab muscle tissue, the infected tissue was minced with a razor blade and homogenized using a Dounce homogenizer. The homogenized sample was filtered twice through cheesecloth to remove large fragments of muscle tissue. The filtrate was then centrifuged for 30 min at 1,000 g. A pellet was obtained and resuspended in 5 ml of deionized water. The sample was added to 30 ml of 70% Percoll (Sigma-aldrich, St. Louis, USA) and centrifuged for 1 h at 1,000 g. Crab muscle tissue sedimented to the bottom of the centrifuge tube, and also formed a thin band above the 70% Percoll. Percoll lying between the thin band and pelleted crab muscle tissue was used for subsequent spore purification. Approximately 24-26 ml of Percoll were removed from the centrifuge tube and diluted to 40% Percoll using deionized water. The diluted Percoll was centrifuged for 1 h at 1,000 g. A pellet was obtained and resuspended in 250 ml of deionized water. The 40% Percoll was centrifuged three more times to obtain a total of 1 ml of spores suspended in deionized water. Spore concentration was estimated using a hemacytometer. Sample NC1 had a spore count of 7.51×10^7 spores/ml and sample NC2 had a spore count of 8.64×10^6 spores/ml.

Preparation of plugs and DNA extraction

The spore samples were first centrifuged for 30 min at 10,000 g. The pellets were then resuspended in 500 ml of 0.2 M KCl (pH 12.0) for 30 min at 30°C to induce polaroplast release. Five hundred microliters of melted 1.6% low melting point agarose (IBI, New Haven, USA) were added to the germinated spore sample to give a final concentration of 0.8% agarose. The 0.8% agarose-spore mixture was immediately pipetted into several plug molds (Bio-Rad, Hercules, USA) and allowed to solidify for 10 min at 4°C.

To obtain spore DNA, the prepared agarose plugs were immersed in 2.5 ml of lysis buffer (1% lauryl sarcosine, 100 mM EDTA, 10 mM Tris at pH 7.8, and 1 mg/ml Proteinase K). The plugs were then incubated in a 50°C water bath for 48 h. After 48 h the lysis buffer was replaced with 3 ml of 500 mM EDTA and incubated overnight at 4°C. The 500 mM EDTA was then replaced with 50 mM EDTA and the plugs stored at 4°C until ready to run PFGE. Crab muscle tissue from one uninfected Dungeness crab and one uninfected red rock crab were also subjected to the spore purification and spore lysis protocols. Agarose plugs prepared from these samples were used as negative controls.

Pulsed field gel electrophoresis conditions

Five different PFGE conditions were used to resolve the chromosome-sized DNA bands from samples NC1and NC2 (Table 1). Condition 1 was used to obtain a general profile of *N. canceri's* karyotype, Condition 2 was used to resolve DNA bands in the 565-680 kilobase (Kb) range, Condition 3 was initially used to resolve DNA bands in the 945-1,125 Kb range, Condition 4 was used to determine whether *N. canceri* had DNA bands greater than 2,200 Kb, and Condition 5 was used to determine whether *N. canceri* had DNA bands smaller than 225 Kb. The DNA bands were resolved on 1% agarose gels (1 g agarose in 100 ml 0.5X TBE) placed onto a contour clamped homogenous electric field apparatus (CHEF DR II) (Bio-Rad, Hercules, USA). Each PFGE condition was run at least twice with similar results obtained. Gels were stained with 0.5 mg/ml ethidium bromide for 30 min. The gels were rinsed twice in deionized water and results were recorded using a gel documentation device (UVP, Upland, USA). To estimate the size of the chromosome-sized DNA bands, standard curves were created based on distance traveled by the *Saccharomyces cerevisiae* DNA markers (Bio-Rad, Hercules, USA) run simultaneously on each gel.

RESULTS

Figure 1 shows the results from running Conditions 1, 2, and 3. Figure 1A shows the results from running Condition 1. In Fig. 1A, bands I and II were well resolved near the bottom of the gel, bands III to VII were grouped closely together, and bands VIII, IX, and X were well resolved near the top of the gel. Lack of resolution among bands V to VII indicated another set of PFGE conditions was needed to separate DNA bands in the 565-680 Kb range. Figure 1B shows the results from running Condition 2. Condition 2 was used to resolve DNA bands in the 565-680 Kb range (Table 1, Fig. 1B). For sample NC1, bands V and VI were still close together and running the gel for an additional 4 h did not improve resolution. The adjacent *S. cerevisiae* DNA marker showed good separation between bands that were 610 Kb and 680 Kb in size (Fig. 1B). The separation of DNA size markers in the 610-680 Kb range indicates Condition 2 was optimal for resolution of bands V to VII. Condition 2 not only resolved bands V to VII (Table 1, Condition 2), but also compressed bands VIII, IX, and X (Fig. 1B). The *S. cerevisiae* DNA

Table 1. PFGE conditions used to estimate karyotype and genome size of several *Nadelspora canceri* spore isolates.

	Condition 1	Condition 2	Condition 3	Condition 4	Condition 5
Switch Time (Ramp)	45-100 s	60 s	85-100 s	250-900 s	4.3-21.4 s
Voltage	200 V (6 V/cm)	200 V (6 V/cm)	200 V (6 V/cm)	100 V (3 V/cm)	200 V (6 V/cm)
Temperature	14°C	14°C	14°C	14°C	14°C
Time	24 h	24 h	24 h	50 h	24 h

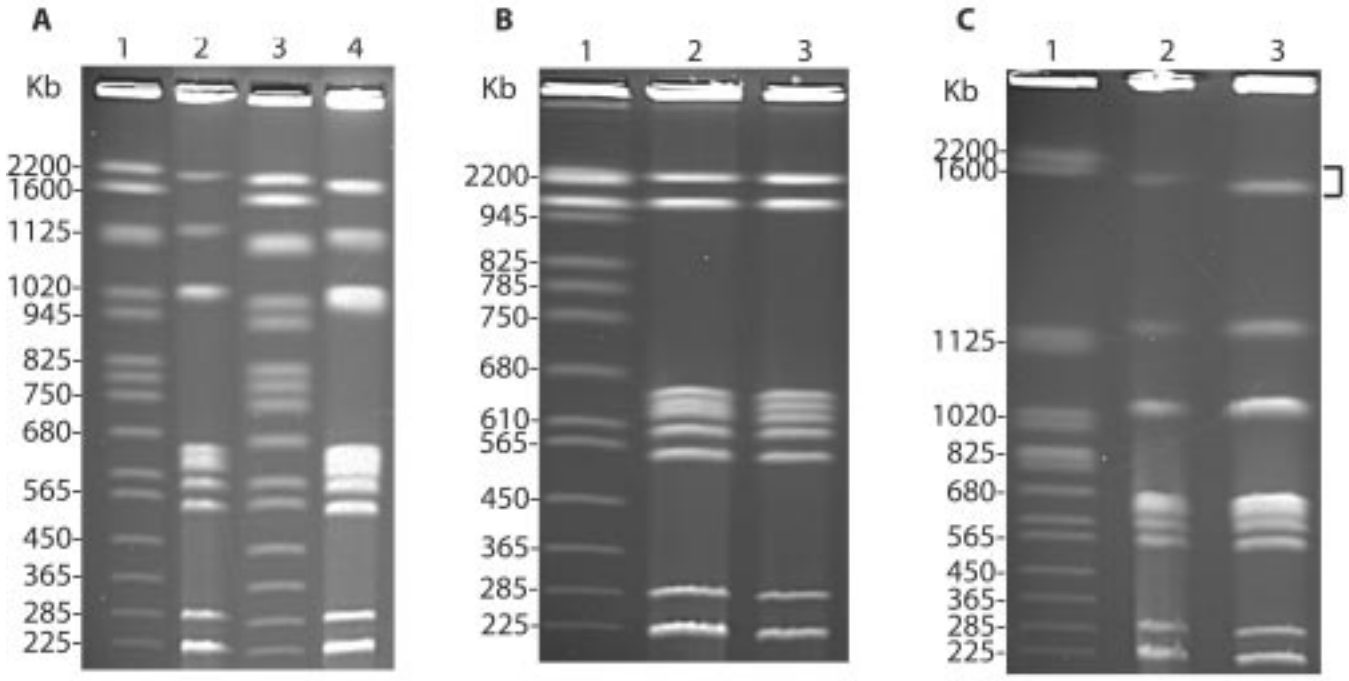

Figs 1A-C. Agarose gels showing resolution of chromosome-sized DNA from *Nadelspora canceri*. **A** - resolution of chromosome-sized DNA using Condition 1. Lanes identified from left to right as numbers 1-4: (1) *Saccharomyces cerevisiae* DNA marker, (2) NC1; *N. canceri* spores obtained from Dungeness crab, (3) *S. cerevisiae* DNA marker, (4) NC2; *N. canceri* spores obtained from red rock crab. **B** - resolution of chromosome-sized DNA in the 565-680 Kb range using Condition 2. Minimal migration observed for DNA bands in the 945-2,200 Kb size range. Lanes identified from left to right as numbers 1-3:(1) *S. cerevisiae* DNA marker, (2) NC1, (3) NC2. **C** - agarose gel showing a difference in migration rate between band X of NC1 and band X of NC2 (indicated by a bracket). Result obtained using Condition 3. Lanes identified according to Fig. 1B.

marker in Fig. 1B indicated minimal migration and loss of resolution for bands in the 945-2,200 Kb size range (Fig. 1B).

In various pulsed field results (data not shown), band VIII appeared brighter and wider than the other bands and called into question whether the band was a singlet or a doublet. Various switch times to improve resolution in the 945-1,125 Kb range did not further resolve band VIII into more bands. However, using Condition 3 (Table 1), a difference in size between band X of NC1 and band X of NC2 was detected (Fig. 1C). The bands differed in size by approximately 81 Kb, suggesting variation in chromosome size between the two spore samples (Table 2).

A total of 10 chromosome-sized DNA bands were identified by PFGE. Use of conditions appropriate for resolution of *Hansenula wingeii* chromosomes (Table 1, Condition 4) showed no additional chromosomes greater than 2,200 Kb for either NC1 or NC2 (data not shown). Pulsed field conditions designed to

Table 2. Estimates of number and size (in Kb) of chromosome-sized DNA bands obtained from *Nadelspora canceri* using PFGE. (NC1: spores isolated from Dungeness crab, NC2: spores isolated from red rock crab). Average Band Size in Kb

Band Number	NC1	NC2
X	1879	1798
IX	1223	1172
VIII	978	943
VII	598	592
VI	575	575
V	555	552
IV	533	533
III	496	499
II	327	330
I	280	290
Total	7444 Kb	7284 Kb

further separate the smallest DNA band (Table 1, Condition 5) also failed to reveal any bands smaller than 225 Kb (data not shown). Observed band patterns for both NC1 and NC2 were repeatable under all PFGE conditions used. Also, agarose plugs generated from uninfected Dungeness and red rock crab muscle tissue yielded no DNA bands on a pulsed field gel (data not shown). The absence of crab DNA indicates the DNA bands observed in Fig. 1 are from the *N. canceri* samples.

DISCUSSION

The estimated genome size of characterized microsporidians ranges from 2.9-19.5 Mb. Insect-infecting microsporidians vary widely in their karyotype, chromosome size range, and genome size (Table 3). In contrast, the mammal-infecting microsporidians have a karyotype of 10-12 chromosome-sized DNA bands, and a genome size range of 2-3 Mb (Table 3). *N. canceri's* genome size of 7.3-7.4 Mb is well within the genome size range of known microsporidians. The estimated genome and chromosome size range of *N. canceri* is most similar to the microsporidian *Nosema costelytrae* (Table 3). Unlike *N. canceri* which is a crustacean-infecting microsporidian, *N. costelytrae* is an insect-infecting microsporidian parasitic to the grass grub *Costelytra zealandica* (Malone and McIvor 1993).

Based on pulsed field conditions listed in Table 1, *N. canceri's* karyotype was estimated to be 10 chromosome-sized DNA bands. Although PFGE was carried out using conditions that should have resolved DNA bands in the 220-2,200 Kb size range, some DNA bands may yet be unresolved due to co-migration. In particular, band VIII may consist of several DNA bands. The use of densitometry or telomere probes could help determine whether band VIII is a singlet or a doublet (Blunt *et al.* 1997, Amigo *et al.* 2002, Zhong *et al.* 2002).

Table 3. Estimates of chromosome number and genome size of microsporidians, with *Nadelspora canceri* shown in bold.

Species	Host	Karyotype	Chromosome size range (Kb)	Genome size (Mb)	References
Vairimorpha sp.	Insects	8	720 to 1,790	9.2	Malone and McIvor 1993
Nosema costelytrae	Insects	8	290 to 1,810	7.4	Malone and McIvor 1993
Nadelspora canceri	Crustacea	10	280 to 1,879	7.4	Present work
Nadelspora canceri	Crustacea	10	290 to 1,798	7.3	Present work
Encephalitozoon cuniculi	Mammals	11	217 to 315	2.9	Biderre *et al*. 1995
Encephalitozoon intestinalis	Mammals	10	190 to 280	2.3	Peyretaillade *et al.* 1998
Encephalitozoon hellem	Mammals	12	175 to 315		Peyretaillade et al., 1998
Spragea lophii	Fish	12	230 to 980	6.2	Biderre *et al*. 1994
Nosema furnacalis	Insects	13	440 to 1,360	10.2	Munderloh *et al*. 1990
Nosema pyrausta	Insects	13	440 to 1,390	10.6	Munderloh *et al*. 1990
Vavraia oncoperae	Insects	14	130 to 1,930	8	Malone and McIvor 1993
Spragea lophii	Fish	15	266 to 1,076	7.3	Amigó *et al*. 2002
Spragea lophii	Fish	15	271 to 1,120	7.3	Amigó *et al*. 2002
Glugea stephani	Fish	15	340 to 2,654	16.8	Amigó *et al*. 2002
Vavraia oncoperae	Insects	16	140 to 1,830	10.2	Malone and McIvor 1993
Glugea atherinae	Fish	16	420 to 2,700	19.5	Biderre *et al*. 1994
Nosema locustae	Insects	18	139 to 651	5.4	Street 1994
Nosema bombycis	Insects	18	380 to 1,500	15.3	Kawakami *et al*. 1994

By using Condition 3, a difference in band size was detected for samples NC1 and NC2. Band X from sample NC1 appeared to be approximately 81 Kb larger than the corresponding band in sample NC2 (Table 2, Fig. 1C). Condition 3 was run twice on the spore samples and in both runs band X showed a difference in band migration. Bands V and VI in Fig. 1B also show a slight difference in migration pattern between samples NC1 and NC2. The differences in migration pattern were reflected in the mean DNA band sizes for NC1 and NC2 (Table 2).

Genome plasticity and intraspecies variation in karyotype has been documented in microsporidians. Genome analysis of three different strains of *E. cuniculi* gave six different electrophoretic band patterns (Biderre *et al.* 1998). *Vavria oncoperae*, isolated from two different host species (the porina caterpillar *Wiseana* spp. and the grass grub *Costelytra zealandica*), gave karyotype values of 14 and 16 respectively (Table 3). *Spragea lophii* isolates gave karyotypes of 12 and 15 and a genome size of 6.2 Mb and 7.3 Mb respectively (Table 3). Intraspecies variation in electrophoretic band patterns has also been detected among fungi, and protists other than microsporidians (Monaco 1995, Venegas *et al.* 1997). For example, the protist *Leishmania* displays variation in band patterns due to chromosomal rearrangement; the protist *Trypanosoma cruzi* gives different band patterns among isolates obtained from separate geographic areas; and the yeast *Candida albicans* exhibits variation in chromosome number and size which may vary among individual hosts (Malone and McIvor 1993, Monaco 1995, Venegas *et al.* 1997).

The mechanism for inducing variations in chromosome number or size among microsporidians is not well understood. Malone and McIvor (1993) suggested that variations in DNA band patterns might be common among microorganisms with high reproductive rates. The possibility of unequal crossing over during mitosis may account for the variability in chromosome size. Since sexual reproduction can occur in microsporidians and other protists, then there is also the possibility of unequal crossing over in meiosis. Subtelomeric deletions or insertions of repeat sequences may also account for the variability in chromosome size (Monaco 1995, Biderre *et al.* 1998).

The temporal stability of *N. canceri's* karyotype and chromosome size is also an intriguing question. If *N. canceri* exhibits significant plasticity in its genome, then the band pattern should change over time. In a study by Biderre *et al.* (1998) clonal cultures of *T. cruzi* exhibited variations in electrophoretic band pattern over a 5-year period. In contrast, cultures of *E. cuniculi* failed to show any significant variation within the same 5-year period (Biderre *et al.* 1998).

The estimation of *N. canceri's* genome size and karyotype serves as a platform to further understand the molecular biology of the parasite. Our study has shown *N. canceri* spore isolates (obtained from two separate crab species) to have a karyotype of 10 chromosome-sized DNA bands. The size range of *N. canceri's* DNA bands ranges from 280-1,879 Kb for NC1, and 290-1,798 Kb for NC2 (Table 3). The total genome size for *N. canceri* is estimated to be 7.3-7.4 Mb. *N. canceri* is the first crustacean-infecting microsporidian to have its genome characterized, and it will be interesting to see whether other crustacean-infecting microsporidians have a similar karyotype, chromosome size range, and genome size.

Acknowledgements. This work was supported by a Mamie Markham Fund at the Hatfield Marine Science Center, and by funding from the Oregon Agricultural Experiment Station headquartered in Oregon State University's College of Agricultural Sciences. We thank Dr. Robert Olson for his assistance in obtaining an infected Dungeness crab for this study.

REFERENCES

Amigó J. M., Gracia M. P., Salvadó H., Vivarès C. P. (2002) Pulsed field gel electrophoresis of three microsporidian parasites of fish. *Acta Protozool.* **41:** 11-16

Amogan H. P. (2004) Molecular Characterization of Crustacean Parasite *Nadelspora canceri*. Thesis. Oregon State University, Corvallis, OR

Baker M. D., Vossbrinck C. R., Didier E. S., Maddox J. V., Shadduck J. A. (1995) Small subunit ribosomal DNA phylogeny of various microsporidia with emphasis on AIDS related forms. *J. Eukaryot. Microbiol.* **42:** 564-570

Biderre C., Pages M., Méténier G., David D., Bata J., Prensier G., Vivarès C. P. (1994) On small genomes in eukaryotic organisms:molecular karyotypes of two microsporidian species (Protozoa) parasites of vertebrates. *C. R. Acad. Sci. III.* **317:** 399-404

Biderre C., Pages M., Méténier G., Canning E. U., Vivarès C. P. (1995) Evidence for the smallest nuclear genome (2.9 Mb) in the microsporidian *Encephalitozoon cuniculi*. *Mol. Biochem. Parasitol.* **74:** 229-231

Biderre C., Mathis A., Deplazes P., Weber R., Méténier G., Vivarès C. P. (1998) Molecular karyotype diversity in the microsporidian *Encephalitozoon cuniculi*. *Parasitology* **118:** 439-445

Blunt D. S., Khramtsov N. V., Upton S. J., Montelone B. A. (1997) Molecular karyotype analysis of *Cryptosporidium parvum*: evidence for eight chromosomes and a low-molecular-size molecule. *Clin. Diag. Lab. Immunol.* **4:** 11-13

Childers R. K., Reno P. W., Olson R. E. (1996) Prevalence and geographic range of *Nadelspora canceri* (Microspora) in Dungeness crab *Cancer magister*. *Dis. Aquat. Org.* **24:** 135-142

Kawakami Y., Inoue T., Ito K., Kitamizu K., Hanawa C., Ando T., Iwano H., Ishihara R. (1994) Identification of a chromosome

harboring the small subunit ribosomal RNA gene of *Nosema bombycis*. *J. Invert. Pathol.* **64:** 147-148
Malone L. A., McIvor C. A. (1993) Pulsed field gel electrophoresis of DNA from four microsporidian isolates. *J. Invert. Pathol.* **61:** 203-205
Monaco A. P. (1995) Pulsed Field Gel Electrophoresis: A Practical Approach. Oxford University Press, Inc., NY
Munderloh U. G., Kurtti T. J., Ross S. E. (1990) Electrophoretic characterization of chromosomal DNA from two microsporidia. *J. Invert. Pathol*. **56:** 243-248
Peyretaillade E., Biderre C., Peyret P., Duffiex F., Méténier G., Gouy M., Michot B., Vivarès C. P. (1998) Microsporidian *Encephalitozoon cuniculi*, a unicellular eukaryote with an unusual chromosomal dispersion of ribosomal genes and a LSU rRNA reduced to the universal core. *Nucleic Acids Res.* **26:** 3513-3520
Olson R. E., Tiekotter K. L., Reno P. W. (1994) *Nadelspora canceri* N. G., N. Sp., an unusual microsporidian parasite of the Dungeness crab, *Cancer magister*. *J. Eukaryot. Microbiol.* **41:** 349-359
Street D. A. (1994) Analysis of *Nosema locustae* (Microsporidia: Nosematidae) chromosomal DNA with pulsed-field gel electrophoresis. *J. Invert. Pathol.* **63:** 301-303
Venegas J., Ortiz S., Munoz S., Solari A. (1997) Molecular karyotype and schizodeme analysis of *Trypanosoma cruzi* stocks from Chilean triatomines. *Parasitology* **118:** 439-445
Wittner M., Weiss L. M. (1999) The Microsporidia and Microsporidiosis. ASM Press, Washington, D.C.
Zhong S., Steffenson B. J., Martinez J. P., Ciuffetti L. M. (2002) A molecular genetic map and electrophoretic karyotype of the plant pathogenic fungus *Cochliobolus sativus*. *Mol. Plant-Microbe Interact.* **15:** 481-492

Received on 9th December, 2005; revised version on 28th February, 2006; accepted on 15th March, 2006

Acta Protozool. (2006) 45: 255 - 263

ACTA
PROTOZOOLOGICA

Intraspecific Variation of Diagnostic rDNA Genes in *Paramecium dodecaurelia*, *P. tredecaurelia* and *P. quadecaurelia* (Ciliophora: Oligohymenophorea)*

Sebastian TARCZ[1], Ewa PRZYBOŚ[1], Małgorzata PRAJER[1] and Magdalena GRECZEK-STACHURA[2]

[1]Institute of Systematics and Evolution of Animals, Polish Academy of Sciences; [2]Institute of Biology, Educational Academy, Kraków, Poland

Summary. Fragments of the 3' end of SSU rRNA - ITS1 (210bp) and the 5' end of LSU rRNA (350bp) were analysed in a study of intraspecific polymorphism in species of the *Paramecium aurelia* complex. These species have shown various levels of intraspecific polymorphism in previous RAPD, RFLP and ARDRA analyses, i.e. *Paramecium dodecaurelia* (high intraspecific polymorphism), *P. quadecaurelia* and *P. tredecaurelia* (no intraspecific polymorphism). Studies were performed on six strains of *P. dodecaurelia* and in two strains each (only available) of *P. tredecaurelia* and *P. quadecaurelia*, originating from geographically remote collecting sites. Alignment of both rDNA gene fragments containing 3'SSU rRNA-ITS1 and 5' LSU rRNA revealed a distinct polymorphism within *P. dodecaurelia*, i.e six polymorphic sites were found in a fragment of rDNA at the 3' end of SSU rRNA-ITS1, only one site differentiating strains of *P. tredecaurelia*, and no changes in *P. quadecaurelia.* Similarly, at 5' LSU several polymorphisms characteristic for the particular strains of *P. dodecaurelia* were observed, three polymorphic sites when two strains of *P. tredecaurelia* were compared, and one polymorphic site in the case of two strains of *P. quadecaurelia*. Neighbor- joining and maximum parsimony phylogenies showed that *P. dodecaurelia* strains are scattered, particular strains differ as much as different species of the *P. aurelia* complex. Our present study confirmed previous results (RAPD, RFLP, and ARDRA analyses) which revealed such exceptional intraspecific differentiation in *P. dodecaurelia.* This is the first analysis of the 5'end fragment of LSU rRNA at the intraspecific level in the *P. aurelia* complex, showing that the fragment seems very useful at this level.

Key words: intraspecific polymorphism, ITS1 region, LSU rRNA gene sequences, *Paramecium aurelia* species complex, *P. dodecaurelia*, *P. quadecaurelia*, *P. tredecaurelia*, ribosomal DNA, sequence analyses, SSU rRNA gene sequences.

Abbreviations used: bp - base pairs, ITS1 - internal transcribed spacer, LSU - large subunit ribosomal RNA, SSU - small subunit ribosomal RNA.

INTRODUCTION

The *Paramecium aurelia* complex is composed of 15 species, 14 of which have been named by Sonneborn (1975) and the 15th - *P. sonneborni* by Aufderheide *et al.* (1983). The relationships of species of the complex as well as possible intra-specific polymorphism of particular species have been studied (Przyboś *et al.* 2006b). Genetic studies were carried out by classical strain crosses and molecular analyses such as RAPD fingerprinting, RFLP analysis, and ARDRA riboprinting. RAPD fingerprinting revealed intraspecific polymorphism (different band patterns characteristic for the studied strains) within several species. RFLP analysis and ARDRA riboprinting showed the existence of different groups of species within the complex, characterized by different band patterns as well as intraspecific polymorphism,

Address for correspondence: Sebastian Tarcz, Institute of Systematics and Evolution of Animals, Polish Academy of Sciences, Sławkowska 17, 31-016 Kraków, Poland; Fax: 00 4812 422 42 94; E-mail: starcz@isez.pan.krakow.pl

* Supported by the Ministry of Science and Information Society Technologies, Warsaw, Poland, grant No. 2P04C 011 26

depending on the enzyme used and the investigated species. High intraspecific polymorphism was revealed in *P. dodecaurelia* and high similarity of band patterns in *P. tredecaurelia* and *P. quadecaurelia*. However, high survival of inter-strain hybrids in both generations was observed in *P. dodecaurelia* and *P. quadecaurelia* but not in *P. tredecaurelia*. A fragment of rDNA of *P. dodecaurelia* strains (revealing high intra-specific polymorphism), *P. tredecaurelia,* and *P. quadecaurelia* (showing no intra-specific polymorphism) was sequenced with the aim to find explanation of such great differences between species as intra-specific polymorphism is concerned.

DNA sequencing of the small subunit of ribosomal RNA (SSU rRNA) has recently been applied in systematics for comparisons at the specific and subspecific levels as well as for phylogenetic reconstruction (cf Hammerschmidt *et al.* 1996, Schlegel 2003). Sequence analyses of SSU rRNA gene have been frequently applied in ciliate taxonomy, e.g. in Heterotrichea (Fu *et al.* 2004), Spirotrichea (Bernhard *et al.* 2001, Chen and Song 2001, Petroni *et al.* 2002, Modeo *et al.* 2003), and recently 18 S rRNA gene phylogenies were compared with those based on morphological and ontogenetical data in the stichotrichines (Foissner *et al.* 2004) and in Oligotrichea (Agatha *et al.* 2005). In Oligohymenophorea within subclass Peniculia, the SSU rRNA genes were sequenced also in *Paramecium* (Strüder-Kypke *et al.* 2000b). The authors concluded that "the *Paramecium* species form at least four clades with the *Paramecium aurelia* subgroup being the most derived". The same authors also studied phylogenetic relationships of the genus *Paramecium* based on sequences from the small subunit rRNA gene (Strüder-Kypke *et al.* 2000a) in the species: *P. bursaria, P. calkinsi, P. duboscqui, P. jenningsi, P. nephridiatum, P. primaurelia, P. polycaryum.* The genus seems to be a monophyletic group. Within the *P. aurelia* species complex, *P. primaurelia* and *P. tetraurelia* differed by five nucleotides from each other and from *P. jenningsi* by six or seven nucleotides, respectively.The SSU rRNA sequence analysis placed the new species *P. schewiakoffi* into the monophyletic "aurelia" subgroup as the sister species of *P. jenningsi* (Fokin *et al.* 2004).

Ribosomal DNA (rDNA) composed of conserved and variable regions is useful for taxonomic analyses. Particularly useful are ITS (ITS - internal transcribed spacer) regions containing DNA sequences between genes of particular ribosomal subunits "as they are non-coding regions that evolve at a high rate" (Li and Graur 1991). Studies have been carried out in different organisms for testing the validity of species, e.g. for the dragonfly species *Cordulegaster bilineata* the entire ITS-1 region of rDNA was applied (Pilgrim *et al.* 2002). In another paper, ITS-1, 5.8 S and ITS-2 r DNA sequences were used as diagnostic tools for assessing the variability within amoeboflagellate species of the genus *Naegleria* (De Jonckheere 2004), and a new species *Naegleria angularis* was identified based on differences in ITS1 and ITS2 sequences when compared with *N. pussardi* (De Jonckheere and Brown 2005). In ciliates intraspecific variation in *Cryptocaryon irritans* (cl. Oligohymenophorea, subcl. Hymenostomatia) was examined using sequences of ITS-1 rDNA combined with developmental and morphological characters (Diggles and Adlard 1997), characterizing four strains. At present, the *Paramecium tetraurelia* genome has also been sequenced (e.g. Sperling *et al.* 2004). Coleman (2005) has recently sequenced the ITS region, of the nuclear ribosomal cistron of 13 species of the *P. aurelia* complex for analysis of their genetic relatedness based on one or two strains for species.

Here we examine two rRNA gene fragments in six unique strains of *P. dodecaurelia* and two strains each of *P. tredecaurelia* and *P. quadecaurelia*, all originating from remote collecting sites with hope to find the proper marker (DNA fragment) presenting intraspecific differentiation. The studied strains of *P. dodecaurelia* are very different as shown by our previous studies (RAPD, RFLP and ARDRA analyses) (Przyboś *et al.* 2006b) so worth of examination.

MATERIALS AND METHODS

The strains of *Paramecium dodecaurelia*, *P. tredecaurelia*, and *P. quadecaurelia* examined here (listed in Table 1) have been kept in the collection of the Institute of Systematics and Evolution of Animals, Polish Academy of Sciences, Kraków.

DNA isolation, amplification, and electrophoresis

Paramecia were cultivated on lettuce medium inoculated with *Enterobacter aerogenes* according to Sonneborn (1970). Genomic DNA was isolated from vegetative cells, representing 12 strains listed in Table 1, at the end of the exponential phase using the QIamp DNA Kit (Qiagen™, Germany) as described by Przyboś *et al.* (2003c); 200µl of cell culture was used for the DNA extraction. The primers amplified two regions of rDNA: the 3' end of SSU rRNA - the ITS1 fragment and the fragment which contains 5' end of LSU rRNA. The primers used for the PCR reaction are listed in Table 2. One of the

primers - LSU_R has the same sequence as in Jerome and Lynn (1996). The others primers were constructed using Oligoanalyzer 3.0 (http://scitools.idtdna.com/analyzer/). Primer construction was based on data from Genbank (Accesion numbers: X03772 - for ITS1_F primer, and AY833401 - for ITS1_R). Primer LSU_F was constructed basing on unpublished sequences of ITS2 fragment of *Paramecium dodecaurelia*.

PCR amplification was carried out in a final volume of 30 µl containing: 2 µl of template, 1.5 U Taq-Polymerase (Qiagen™, Germany); 0.6 µl 10mM of each primer; 10× PCR buffer; 0.6 µl of 10mM dNTPs in a Tpersonal thermocycler (Biometra GmbH, Germany). The amplification protocol consisted of initial denaturation at 94°C, followed by 34 cycles of denaturation at 94°C for 45 s, annealing at 50°C for 60 s, and extension at 72°C for 60 s, with final extension at 72° for 5 min. After amplification the PCR products were electrophoresed in 1% agarose gel for 45 min at 85V with a DNA molecular weight marker (XIV ™ Roche, France) (Fig. 1).

Sequencing

30 µl of each PCR product was separated on a 1.8 % agarose gel (100V/60min). Then, the band representing the examined fragment was cut out and transferred into an 1.5ml Eppendorf tube. Purification was performed by Qiaquick Gel Extraction Kit™ protocol (Qiagen). Sequencing cycle was done in both directions using the BigDye Terminator v3.1™ chemistry (Applied Biosystems, USA). Sequencing products were precipitated using sodium acetate/ethanol and separated on an ABI PRISM 377 DNA Sequencer™ (Applied Biosystems, USA).

Data analysis

Sequences were examined using Chromas Lite (Technelysium ™, Australia). Alignment and consensus of the study sequences was performed by ClustalW (Thomphson *et al.* 1994) in BioEdit program (Hall 1999). Phylogenetic trees were constructed for both studied fragments in Mega version 3.1 (Kumar *et al*. 2004), using NJ (Neighbor-joining method) (Saitou and Nei 1987) and MP (Maximum Parsimony). The NJ analysis was performed using a Kimura 2-parameter correction model (Kimura 1980) by bootstrapping with 1000 replicates (Felsenstein 1985). The MP analysis was evaluated with Min-mini heuristic (level = 2) and bootstrapping with 1000 replicates.

RESULTS

Two rDNA fragments were analyzed: one fragment is 210 bp long and contains the 3' end of SSU rRNA and ITS1 and the second fragment is 350 bp long and contains the 5' end of LSU rRNA (Fig. 2). Both sequences were compared with sequences available in Genbank (AF149979, AY833401, AY833394, AY833386). Alignment of the fragment containing 3'SSU rRNA-ITS1 revealed 23 polymorphisms in ITS1 in three studied *Paramecium* species (*P. cadatum*, *P. multimicronucleatum* and the *P. aurelia* complex), however, in the *P. aurelia* spp. only six polymorphic sites were observed (Table 3a). In turn, 50 polymorphisms were found in all studied *Paramecium* spp. In the fragment of 5' end of LSU rRNA, among which 26 polymorphisms in *P. aurelia* spp. were found. A 130bp stretch of DNA at the 5' end did not harbour polymorphism (Table 3b) in the LSU fragment. We found 88.5 % identity in the 3' SSU rRNA-ITS1 fragment of all studied strains belonging to the investigated species of the *P. aurelia* complex and 97.1 % between *P. dodecaurelia* strains. In the 5' LSU 85.7 % of nucleotides were identical among all studied species (Tables 3a,b) and in *P. dodecaurelia* 94.3% were identical. Strains of *Paramecium caudatum* and *P. multimicronucleatum* were used as outgroups. Polymophism is highly recognizable within the *P. dodecaurelia* strains, as well as in 3'SSU rRNA - ITS1 fragment and especially in 5' LSU rRNA fragment. All sequences were deposited in Genbank (accession numbers in Table 1).

SSU rRNA - ITS1 fragment

6 polymorphic sites were found in the fragment of rDNA at the 3' end of SSU rRNA – ITS1 in the studied strains of *P. dodecaurelia*. They appear at positions #90, #152, #165, #180, #181, #188. Site #180 seems interesting as three different bases can be found there (C in 246 and HHS strain, A in JU strain, and T in the other strains). At site #188, an A appears in strains G and IE. No differences were found within *P. tredecaurelia* *P. quadecaurelia* (Table 3a).

5' LSU fragment of rRNA

Particular strains of *P. dodecaurelia* can be characterized by the type of polymorphism. Several polymorphisms characteristic for the European strains G and IE were found at sites #192, #193, #201, #213, #265, #301 at 5' LSU rRNA as well as polymorphisms differentiating European strains from the others at #158, #227, #284. Strain HHS from Hawaii, most distant from the other strains, is also characterized by the most numerous changes characteristic for this strain only, at #136, #139, #147, #149, #155, #214, #216.

Three polymorphic sites (#287, #311, #316) are characteristic only for two *P. tredecaurelia* strains and they differentiate them from the other species of the complex, polymorphic site at #205 is characteristic for two strains of *P. quadecaurelia* (Table 3a). There are also three variable sites (#147, #167, #195) within *P. quadecaurelia* strains.

Table 1. Strains of the *Paramecium aurelia* complex, *P. caudatum* and *P. multimicronucleatum* used in analyses.

Species	Locality	Reference	GenBank Accession No.	
			3'SSU rRNA - ITS1	5'LSU rRNA
P. dodecaurelia, strain G	Germany, Münster.	Przyboś and Fokin 2003b	DQ 207378	DQ 207370
P. dodecaurelia, strain IE	Italy, Elbe Island, Azurro	Przyboś and Fokin 2003b	DQ 207380	DQ 207372
P. dodecaurelia, strain JU	Japan, Honsiu Island, Ube city	Przyboś *et al*. 2003a	DQ 207381	DQ 207373
P. dodecaurelia, strain 246	USA, southern state	Sonneborn 1974	DQ 207377	DQ 207369
P. dodecaurelia, strain HHS	Hawai, Honolulu	Przyboś and Fokin 2003a	DQ 207379	DQ 207371
P. dodecaurelia, strain TR	Italy, Trento	Przyboś *et al*. 2005	DQ 207382	DQ 207374
P. tredecaurelia, strain 209	France, Paris	Rafalko and Sonneborn 1959	DQ 207383	DQ 138112
P. tredecaurelia, strain IKM	Israel, Kinet Motzkin	Przyboś *et al*. 2002	DQ 207384	DQ 138113
P. quadecaurelia, strain 328	Austraila, Emily Gap	Sonneborn 1975	DQ 207385	DQ 138114
P. quadecaurelia, strain AN	Africa, Namibia	Przyboś *et al*. 2003b	DQ 207386	DQ 138115
P. caudatum, strain PC	Cyprus, Akamas	Przyboś (unpublished)	DQ 207387	DQ 207375
P. multimicronucleatum, strain PM	USA, Louisiana	Przyboś (unpublished)	DQ 207388	DQ 207376

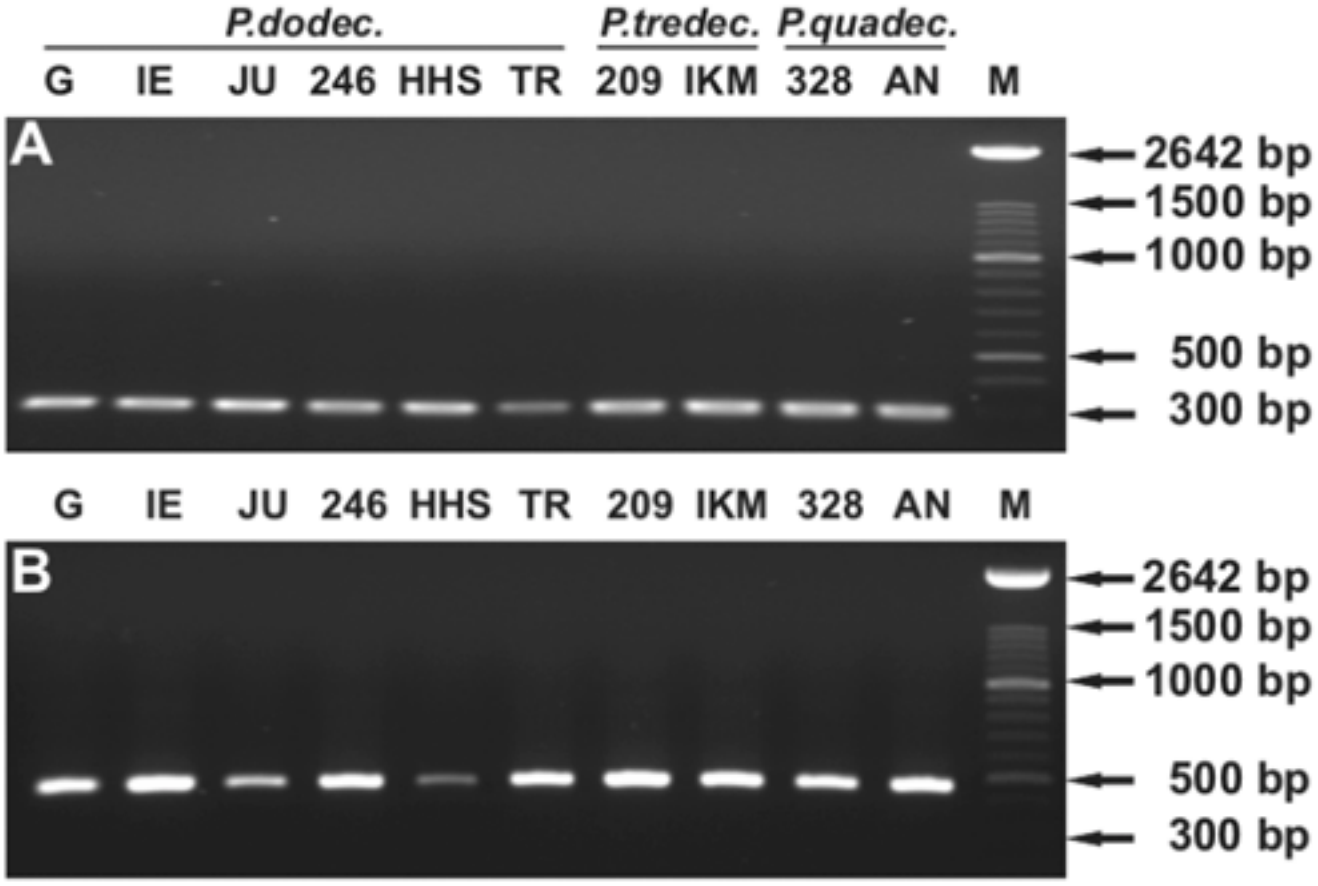

Fig. 1. Gel presenting the examined fragments: A- 3' end of small subunit rRNA-internal transcribed spacer 1 fragment (310bp); B- 5'end of large subunit rRNA LSU rRNA fragment (450bp). Designation of strains: G - Germany, Münster, IE- Italy, Elbe Island, JU- Japan, Honsiu Island, 246- USA, southern state, HHS - Hawaii, Honolulu, TR- Italy, Trento, 209- France, Paris, IKM- Israel, Kinet Motzkin, 328- Australia, Emily Gap, AN- Africa, Namibia, M- weight marker (XIV, Roche ™).

Table 2. Sequences of applied primers

Amplified region	Primer designation	Primer sequence	References
3' SSU rRNA - ITS1	ITS1_F	5'-TAAACCTTATCACTTAGAGGA-3'	This study
	ITS1_R	5'-CGAAAATCTAATGTCTCGCA-3'	This study
5' LSU rRNA	LSU_F	5'-CCCGTATTTGGTTAGGACT-3'	This study
	LSU_R	5'-TTGGTCCGTGTTTCAAGACG-3'	Jerome and Lynn 1996

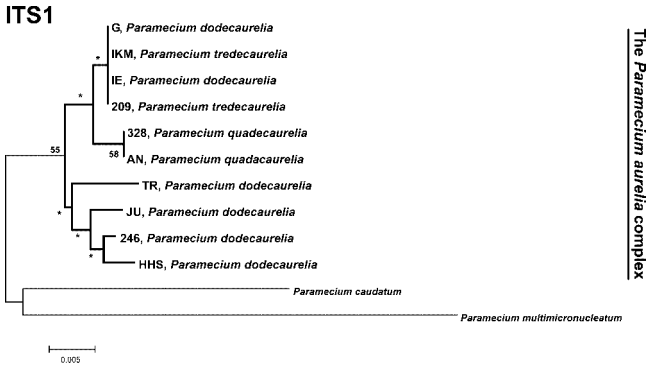

Fig. 2. Phylogenetic tree constructed for 12 strains of the *P. aurelia* complex with a single strain of *P. caudatum* and *P. multimicronucleatum* as outgroups, based on a comparison of sequences the 3' end of small subunit rRNA-internal transcribed spacer 1 fragment using the NJ (neighbor joining) method with the application of the Kimura two-parameter correction model. Bootstrap values are presented as percentages for 1000 comparisons. In the case of bootstrap values less than 50, the asterisks appear.

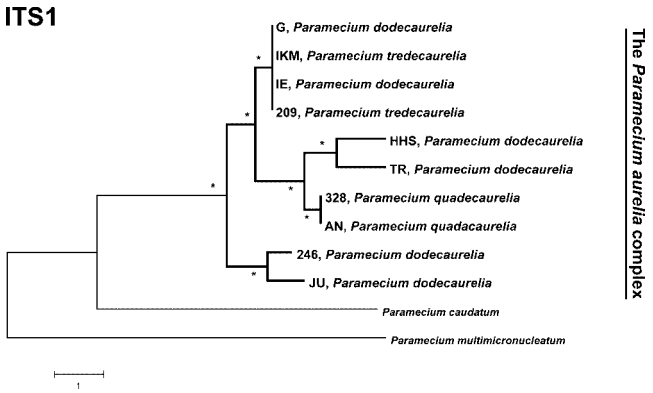

Fig. 3. Phylogenetic tree constructed for 12 strains of the *P. aurelia* complex with a single strain of *P. caudatum* and *P. multimicronucleatum* as outgroups based on a comparison of sequences the 3' end of small subunit rRNA-internal transcribed spacer 1 fragment using MP (maximum parsimony). Bootstrap values are presented as percentages for 1000 comparisons. In the case of bootstrap values less than 50, the asterisks appear.

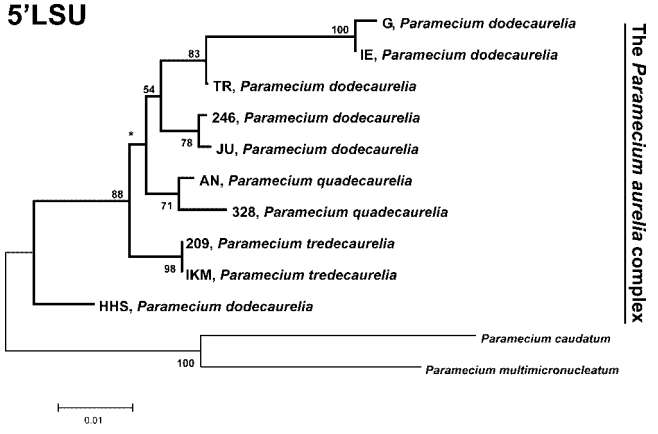

Fig. 4. Phylogenetic tree constructed for 12 strains of the *P. aurelia* complex with a single strain of *P. caudatum* and *P. multimicronucleatum* as outgroups based on a comparison of sequences the 5' end of large subunit rRNA fragment using the NJ (neighbor joining) method with the application of the Kimura two-parameter correction model. Bootstrap values are presented as percentages for 1000 comparisons. In the case of bootstrap values less than 50, the asterisks appear.

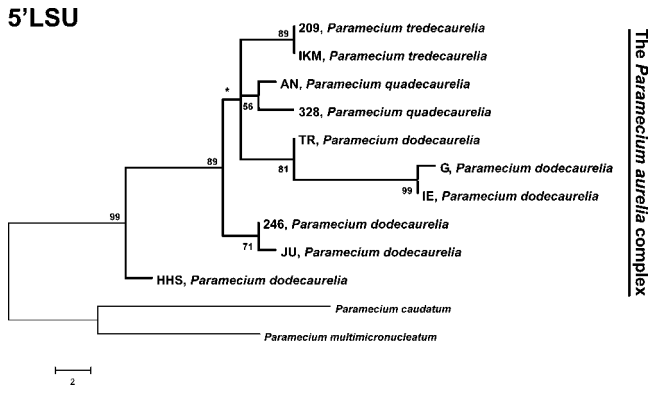

Fig. 5. Phylogenetic tree constructed for 12 strains of the *P. aurelia* complex with a single strain of *P. caudatum* and *P. multimicronucleatum* as outgroups based on comparison of sequences 5' end of large subunit rRNA fragment using MP (maximum parsimony). Bootstrap values are presented as percentages for 1000 comparisons. In the case of bootstrap values less than 50, the asterisks appear.

Table 3a. Polymorphisms in 3' SSU rRNA-ITS1 studied fragment.

	# 73	# 86	# 90	# 92	# 105	# 106	# 108	# 137	# 152	# 156	# 157	# 158	# 160	# 164	# 165	# 175	# 178	# 180	# 181	# 184	# 186	# 188	# 189
246, *P. dodecaurelia*	T	G	A	C	T	T	A	A	C	T	C	-	C	T	T	C	G	C	T	A	T	T	A
G, *P. dodecaurelia*	.	.	.	.	.	.	.	.	.	.	.	.	.	.	.	.	.	T	.	.	.	A	.
HHS, *P. dodecaurelia*	.	.	.	.	.	.	.	.	.	.	.	.	.	.	C	.	.	.	A	.	.	.	.
IE, *P. dodecaurelia*	.	.	.	.	.	.	.	.	.	.	.	.	.	.	.	.	.	T	.	.	.	A	.
JU, *P. dodecaurelia*	.	.	-	.	.	.	.	.	.	.	.	.	.	.	.	.	.	A	.	.	.	.	.
TR, *P. dodecaurelia*	.	.	.	.	.	.	.	.	T	.	.	.	.	.	C	.	.	T	.	.	.	.	.
209, *P .tredecaurelia*	.	.	.	.	.	.	.	.	.	.	.	.	.	.	.	.	.	T	.	.	.	A	.
IKM, *P. tredecaurelia*	.	.	.	.	.	.	.	.	.	.	.	.	.	.	.	.	.	T	.	.	.	A	.
328, *P. quadecaurelia*	.	.	.	.	.	.	.	.	.	.	.	.	.	.	C	.	.	T	-	.	.	A	.
AN, *P. quadecaurelia*	.	.	.	.	.	.	.	.	.	.	.	.	.	.	C	.	.	T	-	.	.	A	.
P. caudatum	.	T	.	A	A	-	C	G	T	.	T	A	.	.	.	.	.	.	A	.	.	.	.
P. multimicronucleatum	C	T	.	.	.	.	G	.	.	C	T	A	A	A	.	T	A	T	.	-	A	A	C

We suppose that there are some sites in rDNA fragments (e.g. #108 in 3'SSU rRNA-ITS1 fragment and #150 in 5'LSU fragment) which could be recognized as characteristic markers for variability in genus *Paramecium*, as they appeared in the studied *P. aurelia* species as well as *P. caudatum* and *P. mulitmicronucleatum* (Tables 3a, b).

Trees

A gene phylogeny constructed on the basis of the 3'SSU-ITS1 fragment of rRNA, using the NJ method (Fig. 2), reveals a very close relationship of *P. quadecaurelia* strains (328 and AN), strains of *P. tredecaurelia* also appear together (IKM and 209), while *P. dodecaurelia* strains are scattered: European strains G and IE cluster with *P. tredecaurelia*, the other European strain TR is in a different group with the strain JU (Japan), 246 (USA), HHS (Hawaii). They are paraphyletic.

A phylogeny reconstructed on the basis of the 5' LSU fragment of rRNA using the NJ method similarly discriminates between *P. caudatum*, *P. multimicronucleatum* and the species of the *P. aurelia* complex. Strains of *P. dodecaurelia* are scattered, European strains appear together: G, IE and TR, and together strains 246 (USA) and JU (Japan). The strain HHS (Hawaii) is distant. Strains of *P. tredecaurelia* and *P. quadecaurelia* appear in two species specific clusters (Fig. 4).

Analysis was also performed using MP (Maximum Parsimony) (Figs 3, 5). Figure 3 presents relationship of species based on analysis of the 3'SSU rRNA - ITS1 fragments of rRNA. *P. caudatum* and *P. multimicronucleatum* are distant, *P. quadecaurelia* strains cluster together. Again strains of *P. dodecaurelia* are scattered, European strains G and IE are close, as well as strains from Japan (JU) and USA (246), but strain TR and HHS are less related. Strains of *P. tredecaurelia* (209 and IKM) form one cluster with strains G and IE of *P. dodecaurelia.* Analysis of LSU rRNA (Fig. 5) shows that strains of *P. tredecaurelia* and *P. quadecaurelia* form their own clusters. Strains of *P. dodecaurelia* appear in different clusters.

DISCUSSION

Coleman (2005) recently studied relationships between species of the *P. aurelia* complex based on the ITS region of the nuclear ribosomal cistron in 13 species. According to this author, polymorphic sites should not be numerous in the ITS region (non coding fragment of rDNA) of the species of the *P. aurelia* complex. This was confirmed by our analysis of a 120 bp long ITS1 fragment in which only 6 polymorphic sites were found, mainly within *P. dodecaurelia*.

The sequences we obtained for *P. dodecaurelia*, *P. tredecaurelia*, and *P. quadecaurelia* were compared

Table 3b. Polymorphisms in 5' LSU rRNA studied fragment.

	# 104	# 133	# 136	# 139	# 147	# 149	# 150	# 151	# 155	# 158	# 165	# 166	# 167	# 171	# 192	# 193	# 195	# 196	# 197	# 201	# 203	# 205	# 207	# 212	# 213
246, *P. dodecaurelia*	G	A	T	A	A	T	T	A	A	T	T	G	C	G	G	C	G	T	A	C	G	G	C	T	G
G, *P. dodecaurelia*	.	.	.	.	.	.	.	T	.	C	.	.	.	.	A	T	.	.	.	T	A	.	.	.	C
HHS, *P. dodecaurelia*	.	.	C	G	G	C	.	T	T	.	.	.	.	A	.	.	.	.	.	.	.	.	.	.	.
IE, *P. dodecaurelia*	.	.	.	.	.	.	.	T	.	C	.	.	.	.	A	T	.	.	.	T	.	.	.	.	C
JU, *P. dodecaurelia*	.	.	.	.	.	.	.	.	.	.	.	.	.	.	.	.	.	.	.	.	.	.	.	.	.
TR, *P. dodecaurelia*	.	.	.	.	.	.	.	T	.	C	.	.	.	A	.	.	.		.	.	.	.	.	.	.
209, *P. tredecaurelia*	.	.	.	.	.	.	.	T	.	.	.	.	.	A	.	.	.	.	.	.	.	.	.	.	.
IKM, *P. tredecaurelia*	.	.	.	.	.	.	.	T	.	.	.	.	.	A	.	.	.	.	.	.	.	.	.	.	.
328, *P. quadecaurelia*	.	.	.	.	.	.	.	T	.	.	.	.	T	A	.	.	A	.	.	.	.	A	.	.	.
AN, *P. quadecaurelia*	.	.	.	.	G	.	.	T	.	.	.	.	.	A	.	.	.	.	.	.	.	A	.	.	.
P. caudatum	.	G	C	.	G	C	A	T	T	C	A	T	T	.	.	.	.	G	T	.	.	.	T	A	.
P. multimicronucleatum	A	G	.	.	G	C	G	T	T	C	.	.	.	A	.	.	.	.	.	.	.	.	T	A	.

	# 214	# 216	# 225	# 227	# 228	# 246	# 248	# 250	# 253	# 265	# 267	# 272	# 273	# 281	# 284	# 287	# 288	# 289	# 290	# 291	# 301	# 311	# 314	# 316	# 318
246, *P. dodecaurelia*	C	G	G	G	T	C	C	C	G	C	A	G	G	C	T	C	G	C	T	G	G	C	G	C	G
G, *P. dodecaurelia*	.	.	.	A	.	.	.	.	.	T	.	A	.	.	C	.	.	.	.	.	A	.	.	.	.
HHS, *P. dodecaurelia*	T	A	.	.	.	.	.	.	.	.	.	.	.	.	.	.	.	.	.	.	.	.	.	.	.
IE, *P. dodecaurelia*	.	.	.	A	.	.	.	.	.	T	.	A	.	.	C	.	.	.	.	.	A	.	.	.	.
JU, *P. dodecaurelia*	.	.	.	.	.	.	.	.	.	.	.	A	.	.	.	.	.	.	.	.	.	.	.	.	.
TR, *P. dodecaurelia*	.	.	.	A	.	.	.	.	.	.	.	A	.	.	C	.	.	.	.	.	.	.	.	.	.
209, *P. tredecaurelia*	.	.	.	A	.	.	.	.	.	.	.	.	.	.	.	A	.	.	.	.	.	T	.	T	.
IKM, *P. tredecaurelia*	.	.	.	A	.	.	.	.	.	.	.	.	.	.	.	A	.	.	.	.	.	T	.	T	.
328, *P. quadecaurelia*	.	.	.	A	.	.	.	.	.	.	.	.	.	.	.	.	.	.	.	.	.	.	.	.	.
AN, *P. quadecaurelia*	.	.	.	A	.	.	.	.	.	.	.	.	.	.	.	.	.	.	.	.	.	.	.	.	.
P. caudatum	T	A	.	.	C	.	.	T	.	.	G	A	.	T	C	T	A	T	C	.	.	T	A	T	.
P. multimicronucleatum	T	A	A	.	C	T	T	T	A	.	G	.	C	.	.	T	.	.	.	A	.	T	A	T	A

with a similar fragment studied by Coleman (2005) in 18 strains representing different species of the *P. aurelia* complex. The six polymorphic sites which appeared in our strains of *P. dodecaurelia* were also found in all species of the *P. aurelia* complex studied by Coleman. They appears in single stranded nucleotides positions (except #152).

Coleman (2005) used only one or two strains representing the particular species, we were able to use up to six strains in the case of the very polymorphic *P. dodecaurelia*. It is worth emphasizing that our strains of *P. dodecaurelia* originate from distant and geographically isolated collecting sites making intra-specific differentiation possible.

Nanney *et al.* (1998) compared sequence differences in a variable D2 domain of 23 rRNA (190 bp long) among several species of the *P. aurelia* complex. They found that genetic species in the *P. aurelia* complex are separated from each other by one or more site changes "but constitute a dense evolutionary cluster".

The 5' LSU rRNA fragment seems very useful in studies concerning relationships within species of the *P. aurelia* complex as well as within the genus. Similar studies using 5'LSU rRNA have also been carried out within *P. novaurelia* (Tarcz unpublished), however, only a few polymorphic sites were found and differences between strains were not so striking as those found within *P. dodecaurelia*. This may be caused by different characteristics of the species and different distances between places of strain origin in the *P. novaurelia* and *P. dodecaurelia* comparison. The first species is known mainly from Europe, so the divergence between strains

is not as great as between strains of *P. dodecaurelia* (from Europe, Hawaii, Japan, USA).

Here we have shown that much polymorphism exists within *P. dodecaurelia*. Our studies confirmed previous results showing exceptional intra-specific differentiation in this species when compared to other species of the *P. aurelia* complex. A high level of intra-specific polymorphism has also been shown by the application of RAPD, RFLP, and ARDRA methods (Przyboś *et al.* 2006b). It seems that intra-specific differentiation within *P. dodecaurelia* is as great as that between different species of the *P. aurelia* complex. Studies in which hsp70 (Hori *et al.* 2006) and H4 histone (Przyboś *et al.* 2006a) genes were sequenced also showed the isolated (distant) position of the species within the phylogenetic tree constructed for species of the *P. aurelia* complex. There are no strong correlation between the geographical origin and molecular differentiation of *P. dodecaurelia* strains, however, some kind of correlation exists, e.g. strain HHS from Hawaii is very distant from the other strains of the species, and the European strains (G, IE, TR) are in one cluster (5'LSU rRNA fragment).

A gene phylogeny constructed on both studied fragments rDNA reveals a very close relationship of *P. quadecaurelia* (328 and AN) and of *P. tredecaurelia* strains (IKM and 209) in the present paper. Similarly, studies of cytosol-type *hsp70* (Przyboś *et al.* 2003b) also revealed a close cluster of *P. quadecaurelia* and *P. tredecaurelia*. It is worth to mention that two strains of *P. quadecaurelia* show 99% similarity in cytosol-type *hsp70* and in studied presently 5' LSU rRNA fragment.

The 5'LSU rRNA fragment is a variable region at the species level and even within species as in the case of *P. dodecaurelia*. At present however, it is impossible to check if it is a good marker for phylogenetic studies (as the ITS1 fragment is) because no comparative data are available in the other *Paramecium* species. It seems worth testing its usefulness also at higher taxonomic levels in Ciliophora. Analysis of the 5' fragment of the LSU rRNA is the first at the intraspecific level in the species of the *P. aurelia* complex. Previous studies (cf Strüder-Kypke 2000a, b; Coleman 2005) concerned relations between the particular genera within Oligohymenophorea, between species within genus *Paramecium*, and between the particular species of the *P. aurelia* complex in which the fragments SSU rRNA, ITS1-5.8S, and ITS1 were analysed. However, there is no resolution in the ITS1 trees, concerning *P. dodacaurelia*. In future studies we are going to use the ITS2 fragment as well for comparison of intraspecific differentiation of *P. dodacaurelia* strains. Probably, strains of that species are some kind of subspecies?

REFERENCES

Agatha S., Strüder-Kypke M.C., Beran A., Lynn D.H. (2005) *Pelagostrobilidium neptuni* (Montagnes and Taylor, 1994) and *Strombidium biarmatum* nov. spec. (Ciliophora, Oligotrichea): phylogenetic position inferred from morphology, ontogenesis, and gene sequence data. *Eur. J. Prot.* **41:** 65-83

Aufderheide K. J., Daggett P.-M., Nerad T. A. (1983) *Paramecium sonneborni* n. sp., a new member of the *Paramecium aurelia* species-complex. *J. Protozool*. **30:** 128-131

Bernhard D., Stechmann A., Foissner W., Ammermann D, Hehn M., Schlegel M. (2001) Phylogenetic relationships within the class Spirotrichea (Ciliophora) inferred from small subunit rRNA gene sequences. *Mol. Phylogen. Evol.* **21:** 86-92

Chen Z., Song W. (2001) Phylogenetic positions of *Uronychia transfuga* and *Diophrys appendiculata* (Euplotida, Hypotrichia, Ciliophora) within hypotrichous ciliates inferred from the small subunit ribosomal RNA gene sequences. *Eur. J. Protis.* **37:** 291-301

Coleman A. W. (2005) *Paramecium aurelia* revisited. *J. Euk. Microbiol.* **52:** 68-77

De Jonckheere J. F. (2004) Molecular definition and the ubiquity of species in the genus. *Naegleria. Protist* **155:** 89-103

De Jonckheere J. F., Brown S. (2005) Description of a new species with a remarkable cyst structure in the genus *Naegleria*: *Naegleria angularis* sp. n. *Acta Protozool.* **44:** 61-65

Diggles B. K., Adlard R. D. (1997) Intraspecific variation in *Cryptocaryon irritans*. *J. Euk. Microbiol.* **44:** 25-32

Felsenstein J. (1985) Confidence limits on phylogenies: an approach using the bootstrap. *Evolution* **39:** 783-791

Foissner W., Moon-van der Staay S. Y., van der Staay G. W. M., Hackstein J. H. P., Krautgartner W.-D., Berger H. (2004) Reconciling classical and molecular phylogenies in the stichotrichines (Ciliophora, Spirotrichea), including new sequences from some rare species. *Eur. J. Protist.* **40:** 265-281

Fokin S. I., Przyboś E., Chivilev S. M., Beier C. L., Horn M. , Skotarczak B., Wodecka B., Fujishima M. (2004) Morphological and molecular investigations of *Paramecium schewiakoffi* sp. nov. (Ciliophora, Oligohymenophorea) and current status of distribution and taxonomy of *Paramecium* spp. *Eur. J. Protist*. **40:** 225-243

Fu Cheng-Jie, Miao W., Lobban C., Shen Yun-Fen (2004) 18S-ITS1 rDNA sequence and phylogenetic analysis of *Maristentor dinoferus* (Ciliophora). *Acta Zootaxon. Sin.* **29:** 615-621

Hall T. A. (1999) BioEdit: a user-friendly biological sequence alignment editor and analysis program for Windows 95/98/NT. *Nucl. Acids, Symp. Ser.* **41:** 95-98

Hammerschmidt B., Schlegel M., Lynn D. H., Leipe D. D., Sogin M. L., Raikov I. B. (1996) Insight into the evolution of nuclear dualism in the ciliates revealed by phylogenetic analysis of rRNA sequences. *J. Euk. Microbiol.* **43:** 225-230

Hori M., Tomikawa I., Przyboś E., Fujishima M. (2006) Comparison of the evolutionary distances among syngens and sibling species of Paramecium. *Mol. Phylogenet. Evol.* **38:** 697-704

Jerome C. A., Lynn D. H. (1996) Indentifying and distinguishing sibling species in the *Tetrahymena pyriformis* complex (Ciliophora, Oligohymenophorea) using PCR/RFLP analysis of nuclear ribosomal data. *J. Euk. Microbiol.* **43:** 492-497

Kimura M. (1980) A simple method for estimating evolutionary rates of base substitutions through comparative studies of nucleotide sequences. *J. Mol. Evol*. **16:** 111-120

Kumar S., Tamura K., Nei M. (2004) MEGA3: Integrated software for molecular evolutionary genetic analysis and sequence alignment. *Brief. Bioinfor.* **5:** 150-163

Li W., Graur D. (1991) Fundamentals of Molecular Evolution. Sinauer Associates, Sunderland, MA

Modeo L., Petroni G., Rosati G., Montagnes D. J. S. (2003) A multidisciplinary approach to describe Protist: redescriptions of *Novistombidium testaceum* Anigstein 1914 and *Strombidium inclinatum* Mongagnes, Taylor, and Lynn 1990 (Ciliophora, Pligotrichia). *J. Euk. Microbiol*. **50:** 175-189

Nanney D. L., Park C., Preparata R., Simon E. M. (1998) Comparison of sequence differences in a variable 23S rRNA domain among sets of cryptic species of ciliated protozoa. *J. Euk. Microbiol.* **45:** 91-100

Petroni G., Dini P., Verni F., Rosati G. (2002) A molecular approach to the tangled intrageneric relationships underlying phylogeny in *Euplotes* (Ciliophora, Spirotrichea). *Mol. Phylogenet. Evol.* **22l:** 118-130

Pilgrim E. M., Roush S. A., Krane D. E. (2002) Combining DNA sequences and morphology in systematics: testing the validity of the dragonfly species *Cordulegaster bilineata*. *Heredity* **89:** 184-190

Przyboś E., Fokin S. I. (2003a) *Paramecium dodecaurelia* strains from Hawaii. *Folia biol. (Kraków)* **51:** 179-180

Przyboś E., Fokin S. I. (2003b) Habitats of *Paramecium dodecaurelia* in Europe. *Protistology* **3:**136-137

Przyboś E., Nevo E., Pavlicek T. (2002) *Paramecium tredecaurelia* of the *Paramecium aurelia* complex in Israel. *Folia biol. (Kraków)* **50:** 221-222

Przyboś E., Fujishima M., Nakaoka Y. (2003a) *Paramecium decaurelia* and *Paramecium dodecaurelia* from the *P. aurelia* spp. complex in Japan. *Folia biol. (Kraków)* **51:** 223-224

Przyboś E., Hori M., Fokin S. I. (2003b) Strains of *Paramecium quadecaurelia* from Namibia, Africa. Genetic and molecular studies. *Acta Protozool.* **42:** 357-360

Przyboś E., Skotarczak B., Wodecka B. (2003c) Phylogenetic relationships of *Paramecium jenningsi* strains (classical analysis and RAPD studies). *Folia biol. (Kraków)* **51:** 85-95

Przyboś E., Prajer M., Greczek-Stachura M., Fokin S.I., Rautian M., Potekhin A. (2005) New European stands of *P. pentaurelia*, *P. septaurelia*, and *P. dodecaurelia*, genetic and molecular studies. *Folia biol. (Kraków)* **53:** 123-128

Przyboś E., Maciejewska A., Skotarczak B. (2006a) Relationships of species of the *Paramecium aurelia* complex (Protozoa, Ph. Ciliophora, Cl. Oligohymenophorea) based on sequencing of histone H4 gene fragment. *Folia biol. (Kraków)* **54:** (in press)

Przyboś E., Prajer M., Greczek-Stachura M., Skotarczak B., Maciejewska A., Tarcz S. (2006b) Genetic and molecular studies of the *Paramecium aurelia* species complex. *Syst. Biodiv.* (in press)

Rafalko M., Sonneborn T. M. (1959) A new syngen (13) of *Paramecium aurelia* consisting of stocks from Mexico, France and Madagascar. *J. Protozool.* **6(Suppl.):** 30

Saitou N., Nei M. (1987) The neighbor-joining method: a new method for reconstructing phylogenetic trees. *Mol. Biol. Evol*. **4:** 406-425

Schlegel M. (2003) Phylogeny of Eukaryotes recovered with molecular data: highlights and pitfalls. *Eur. J. Protistol*. **39:** 113-122

Sonneborn T. M. (1970) Methods in *Paramecium* research. In: Methods in Cell Physiology, (Ed. D. M. Prescott).Academic Press, New York, London, **4:** 242-339

Sonneborn T. M. (1974) *Paramecium aurelia.* In: Handbook of Genetics, (Ed. R. C. King) Plenum Press, New York, **2:** 469-594

Sonneborn T. M. (1975) The *Paramecium aurelia* complex of fourteen sibling species. *Trans. Amer. Micros. Soc.* **94:** 155-178

Sperling L., Blanc I., Cohen J., Gogendeau D., Dessen P., Durre L. (2004) Global organization of the *Paramecium tetraurelia* macronuclear genome. Second Meeting of the GDRE "*Paramecium* Genomics", 7-10 October, 2004. Blaubeuren, Germany. P. 10

Strüder-Kypke M. C., Wrigth A.-D. G., Fokin S. I., Lynn D. H. (2000a) Phylogenetic relationships of the genus *Paramecium* inferred from small subunit rRNA gene sequences. *Mol. Phylogenet. Evol.* **14:** 122-130

Strüder-Kypke M. C., Wrigth A.-D. G., Fokin S. I., Lynn D. H. (2000b) Phylogenetic relationships of the subclass Peniculia (Oligohymenophorea, Ciliophora) inferred from small subunit rRNA gene sequences. *J. Euk. Microbiol.* **47:** 419-429

Thompson J. D., Higgins D. G., Gibson T. J. (1994) CLUSTAL W: improving the sensitivity of progressive multiple sequence alignment through sequence weighting, position-specific penalties and weight matrix choice. *Nucleic Acids Res.* **22:** 4673-80

Received on 13th April, 2006; revised version on May 15th, 2006; accepted on 29th May, 2006

Acta Protozool. (2006) 45: 265 - 270

ACTA
PROTOZOOLOGICA

Phylogenetic Positions of Two Crytophorid Ciliates, *Dysteria procera* and *Hartmannula derouxi* (Ciliophora: Phyllopharyngea: Dysteriida) Inferred from the Complete Small Subunit Ribosomal RNA Gene Sequences

Lifang LI and Weibo SONG

Laboratory of Protozoology, KLM, Ocean University of China, Qingdao, P. R. China

Summary. The complete small subunit rRNA (SSrRNA) gene was sequenced for two poorly known marine crytophorid ciliates, *Dysteria procera* Kahl, 1931 and *Hartmannula derouxi* Gong *et* Song, 2004. The phylogenetic positions within the class Phyllopharyngea were deduced using Bayesian, distance matrix and maximum parsimony methods. *Dysteria procera* and *Hartmannula derouxi*, together with other available ciliates of the class Phyllopharyngea, form a monophyletic clade with strong bootstrap support in all the tree construction methods (values of 100% Bay, 100% LS, 100% NJ, 100% MP). The SSrRNA genealogy showed that the class Phyllopharyngea contained two monophyletic subclasses Chonotrichia and Suctoria, while the subclass Phyllopharyngia was paraphyletic. Our results revealed that some taxa of the subclass Chonotrichia (e.g. *Isochona* species) had a close relationship with the subclass Phyllopharyngia, suggesting that heteromeric nuclear apparatus and the dorsal-reduced ciliature are likely phylogenetically informative. Additionally, consisting with traditional morphological descriptions, dysteriids may be a specialized group within the class in our phylogenetic trees.

Key words: *Dysteria procera*, *Hartmannula derouxi*, marine ciliate, Phyllopharyngea, phylogenetic position, SSrRNA.

INTRODUCTION

The Phyllopharyngea, an understudied class in the phylum Ciliophora, is named for the radially arranged mocrotubular structures (phyllae) around the cytopharynx (de Puytorac *et al.* 1974; de Puytorac 1994; Lynn and Corliss 1991; Lynn 1996; Lynn and Small 1997, 2002). Taxonomic and systematic studies on this class are traditionally based morphological characters revealed with silver impregnation methods (Song and Wilbert 2002).

Address for correspondence: Weibo Song, Laboratory of Protozoology, College of Fisheries, Ocean University of China, Qingdao 266003, P. R. China; Fax: +86 532 8203 2283; E-mail: wsong@ouc.edu.cn

Molecular analyses have been used recently to refine our knowledge of phylogenetic relationships within the ciliated protozoa (phylum Ciliophora). The application of the polymerase chain reaction (PCR) to phylogenetic studies of ciliates finally provides us with the opportunity to acquire molecular sequence information. The genes used to reconstruct phylogenetic trees have mainly included small subunit rRNA (SSrRNA), large subunit rRNA (LSrRNA), tubulin, histone, Hsp70, and DNA polymerase á sequences (Hoffman and Prescott 1997, Baroin-Touranchean *et al.* 1998, Bernhard and Schlegel 1998, Budin and Philippe 1998, Lynn *et al.* 2000). However, sequence data for phyllopharyngean ciliates remain comparatively rare and incomplete. To date, SSrRNA gene sequences have been determined for only about 23 species within this species-rich class (Leipe *et*

al. 1994, Riley and Katz 2001, Snoeyenbos-West *et al.* 2004).

As a part of a comprehensive analysis of ciliate phylogeny carried out recently in the authors' group, we have sequenced the SSrRNA gene for these two poorly-known marine crytophorid ciliates, *Dysteria procera* Kahl, 1931 and *Hartmannula derouxi* Gong *et* Song, 2004. Results were presented to provide more molecular information on these rare-known organisms.

MATERIALS AND METHODS

Ciliate collection and identification. *Dysteria procera* and *Hartmannula derouxi* were collected from the littoral area off Qingdao (Tsingtao, 36°08'N; 120°43'E), China. Isolated specimens of both species were maintained in the laboratory for about 1 week as raw cultures in Petri dishes for observation and further studies.

Their morphology was described recently by Gong and Song (2003, 2004) (Fig. 1). Systematic and terminology at the order and above level are mainly referred from Lynn and Small (2002).

DNA extraction, PCR, and cloning. Cells were starved overnight, rinsed with sterile artificial marine water and then centrifuged at low speed. Lysis buffer (Shang *et al.* 2003) was added and the mixture incubated at 56°C for 1~2 h to extract DNA, then 94°C for 15 min to denature the proteinase K. An equal mixture of the regular DNA polymerase (Promega, USA) and the *Pfu* Taq DNA polymerase (High Fidelity, Sangon, Canada) was utilized for PCR reaction (Chen and Song 2002). Oligonucleotide primer sequences used in this work are available from the authors.

The amplified products were purified (UNIQ-5 DNA Cleaning Kit), inserted into a pUCm-T vector (Sangon, Canada), and sequenced on an ABI Prism 377 Automated DNA Sequencer. Subsequent sequencing was performed using primer walking.

The GenBank/EMBL accession numbers are DQ057347 (*Dysteria procera*) and AY378113 (*Hartmannula derouxi*).

Sequence availability. The nucleotide sequences used for analysis are available from the GenBank/EMBL databases under the following accession numbers: *Isochona* sp. OOSW-1 AY242116, *Isochona* sp. OOSW-2 AY242117, *Isochona* sp. OOSW-3 AY242118, *Isochona* sp. OOSW-4 AY242119, *Chilodonella uncinata* AF300281, *Trithigmostoma steini* X71134, *Chlamydodon excocellatus* AY331790, *Chlamydodon triquetrus* AY331794, *Dysteria derouxi* AY378112, *Dysteria* sp. 1 AY331797, *Dysteria* sp. 2 AY331798, *Tokophrya quadripartita* AY102174, *Discophrya collini* L26446, *Heliophrya erhardi* AY007445, *Prodiscophrya* sp. OOS-2003 AY331802, *Ephelota* sp. RJL2001 AF326357, *Ephelota* sp. OOS-2003 AY331804, *Pseudocohnilembus marinus* Z22880, *Mesanophrys carcini* AY103189, *Pseudocohnilembus hargisi* AY212806, *Aspidisca steini* AF305625, *Diophrys appendiculata* AY004773, *Uronychia transfuga* AF260120, and a karyorelictid ciliate, *Loxodes magnus* L31519 was used as the outgroup species.

Phylogenetic analyses. SSrRNA gene sequences were aligned using the Clustal W, ver. 1.80 (Thompson *et al.* 1994). The computer program, MrBayes v3.0b4 (Huelsenbeck and Ronquist 2001) was used for the Markov Chain Monte Carlo (MCMC) algorithm to construct Bayesian tree. PHYLIP package, version 3.57c (Felsenstein 1985) was used to calculate the sequence similarity and evolutionary distances between pairs of nucleotide sequences using the Kimura (1980) two-parameter model. Distance-matrix trees were constructed using the least-squares [LS] method (Fitch and Margoliash 1967) and the neighbor-joining [NJ] method (Saitou and Nei 1987). Maximum parsimony (MP) tree was constructed by a heuristic search in the program PAUP* v4.0b10 (Swofford 2002). For maximum parsimony analysis, nucleotide sequences were reduced to phylogenetically informative sites. Data were bootstrap resampled 1,000 times.

RESULTS

Sequences and comparisons

The complete SSrRNA gene sequences were determined consisting of 1728 nucleotides (for *Dysteria procera*) and 1708 nucleotides (for *Hartmannula derouxi*) in length. The GC content (44.44% in *D. procera* and 44.91% in *H. derouxi* respectively) is in the same range as in other ciliates (Elwood *et al.* 1985, Sogin and Elwood 1986, Schlegel *et al.* 1991).

The sequence of *Dysteria procera* differs in 131 nucleotides from the sequence of *Dysteria derouxi* (structural similarity 92.40%). 284 sites are different from that in *Hartmannula derouxi* (structural similarity 83.34%), while 233 sites differ from that of *Isochona* sp. OOSW-1 (structural similarity 86.27%), 242 sites are different from that in *Chlamydodon excocellatus* clone 1 (structural similarity 85.96%).

Bayesian and distance matrix analysis

Both Bayesian and distance-matrix based analyses provided strong bootstrap support for the monophyly of the class Phyllopharyngea, Oligohymenophorea and Spirotrichea *sensu* Lynn and Small 2002 (see Fig. 2).

The SSrRNA genealogy showed that the class Phyllopharyngea contains two monophyletic subclasses Chonotrichia and Suctoria, while the subclass Phyllopharyngia is paraphyletic. The family Hartmannulidae (e.g. *Hartmannula derouxi*), together with Chilodonellidae, Chlamydodontidae and Dysteriidae, was clustered within the subclass Phyllopharyngia, but closely related to Isochonidae. The members of the subclass Suctoria, represented by Endogenida, Evaginogenida and Exogenida, were grouped as a sister group to the traditional crytophorids though the suctorian ciliates exhibit extraordinary differences both in general morphology and other biological feathers, e. g. life style, morphogenetic pattern, reproduction behaviors etc.

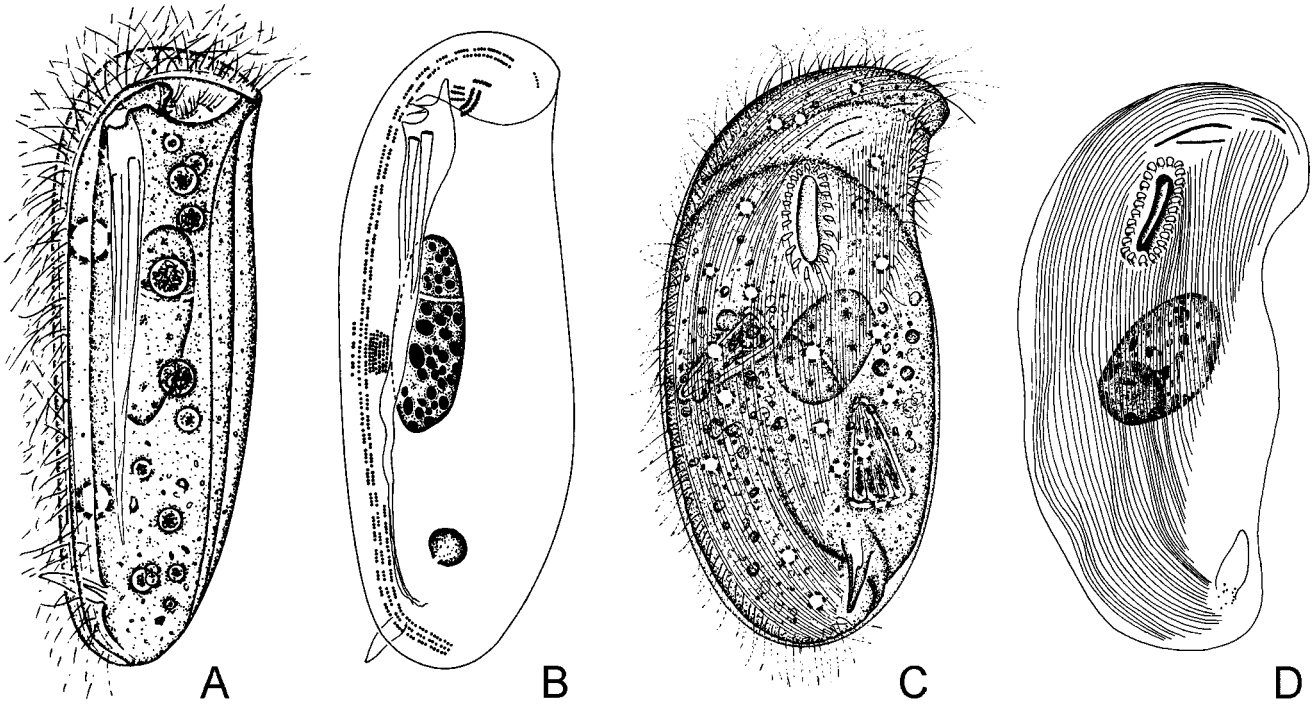

Fig. 1. Morphology and infraciliature of *Dysteria procera* (A, B) and *Hartmannula derouxi* (C, D), from life (A, C) and after protargol impregnated specimens (B, D). Reproduced with permission from Gong and Song (2003, 2004).

Maximum parsimony analysis

The major aspects of the topology of the maximum parsimony tree (Fig. 3) were similar to those of the Bayesian and distance-matrix trees (Fig. 2). *Dysteria procera* and *Hartmannula derouxi* were placed within the subclass Phyllopharyngia. The family Dysteriidae and Hartmannulidae are in variably close with the Chlamydodontidae, where the "well-known" Chilodonellidae forms a clearly outlined group. A remarkable degree of correlation was the relative positions of *Isochona*, *Hartmannula* and *Dysteria*, which means that the subclass Chonotrichia (e.g. *Isochona* species) showed a very close relationship with the subclass Phyllopharyngia (Fig. 3).

DISCUSSION

As demonstrated in the present work, the class Phyllopharyngea was strongly confirmed as a monophyletic clade containing three major subclasses so far represented by SSrRNA gene sequences (100% Bay, 100% LS, 100%NJ, 100% MP, Figs 2, 3). It is consistent with the traditional taxonomy based on the shared morphological characters.

Within the class Phyllopharyngea, the subclass Suctoria branched basally with a strong bootstrap support (100% Bay, 100% LS, 100% NJ, 100% MP), whereas the clades for the Phyllopharyngia and Chonotrichia branched later with moderate support (see Figs 2, 3).

As shown in Figs 2, 3, Chilodonellidae was separated from other Phyllopharyngia groups, while the families Chlamydodontidae, Dysteriidae (represent by *Dysteria*) and Hartmannulidae branched above it and formed a monophyletic clade severally with high bootstrap support in all trees.

Both Dysteriidae and Hartmannulidae were characterized by laterally compressed body; ventral cilia not thigmotactic, juxtaposed heteromerous macronucleus, etc, but differed in the pattern of the left ventral somatic kineties. According to the molecular characters inferred from SSrRNA gene sequences, two families were closely related, which was consistent with the morphological

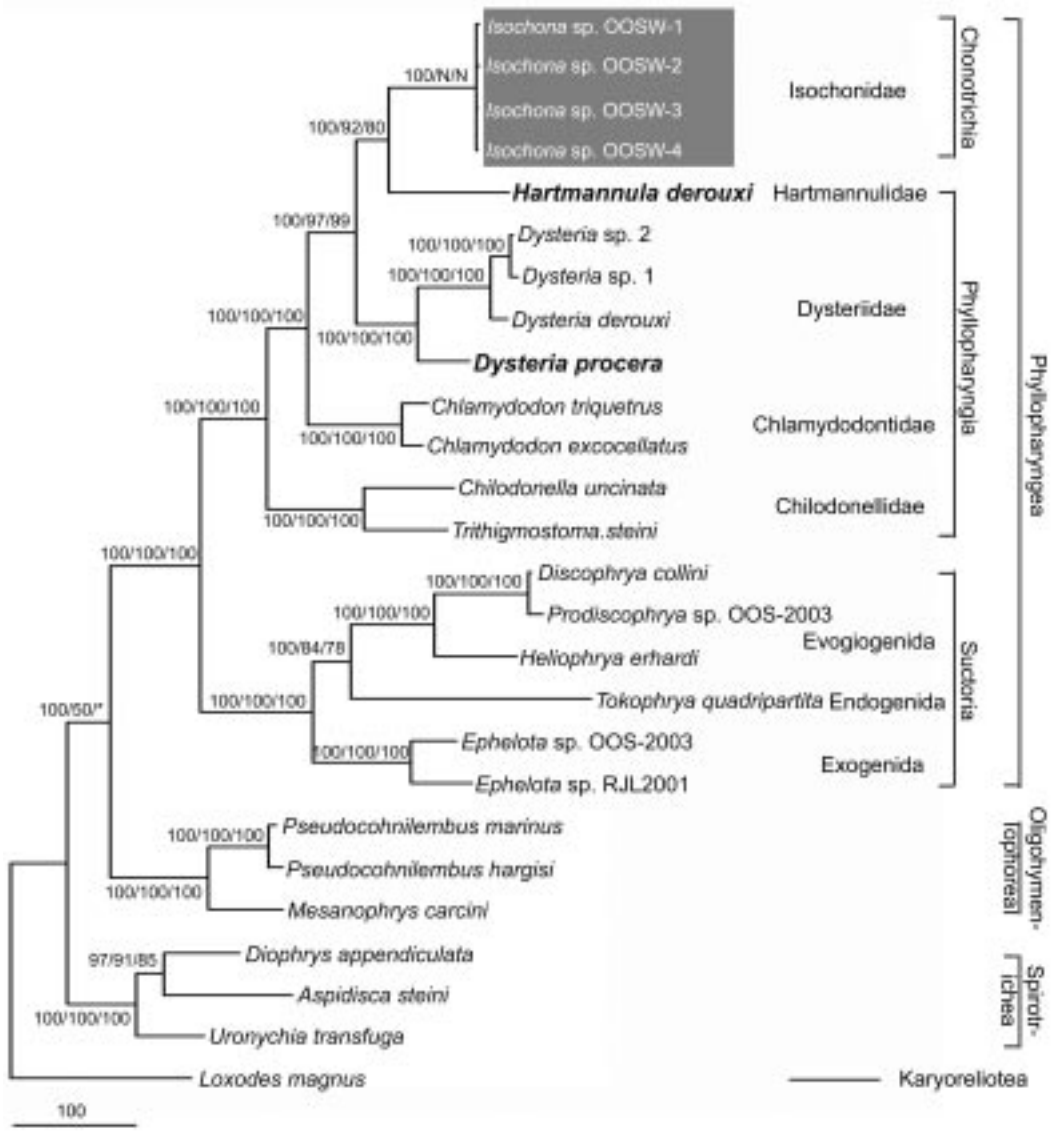

Fig. 2. Bayesian tree inferred from the nucleotide sequences of complete small subunit rRNA (SSrRNA) of phyllopharyngean ciliated protozoa. Numbers on branches indicate support indices from 1000 bootstrap estimations using each of the algorithms in the following order: Bayesian credibility value using the MrBayes, distance-matrix based least-squares (LS) and neighbor joining (NJ) bootstrap percentage using the Phylip package. Asterisks indicate bootstrap values less than 50%. "N" reflects disagreement between a method and the reference Bayesian tree at a given node. Evolutionary distance is represented by the branch length to separate the species in the figure. The scale bar corresponds to five substitutions per 100 nucleotide positions. Numbers at nodes represent bootstrap values (%) out of 1,000 replicates. The new sequences are represented in boldface.

comparison (Lynn and Small 2002, Gong and Song 2003).

The SSrRNA genealogy showed that the class Phyllopharyngea contained two monophyletic subclasses Chonotrichia and Suctoria, while the subclass Phyllopharyngia was paraphyletic. Our results revealed that some taxa of subclass the Chonotrichia (e.g. *Isochona* species) had a close relationship with the subclass Phyllopharyngia, suggesting that heteromeric nuclear apparatus and the dorsal-reduced ciliature are phylogenetically informative (Corliss 1979, Grell and Meister 1982, Puytorac *et al.* 1994, Foissner 1996, Snoeyenbos-West *et al.* 2004). Migratory "larval" form of Chonotrichs resembles adult Phyllopharyngia (Kent

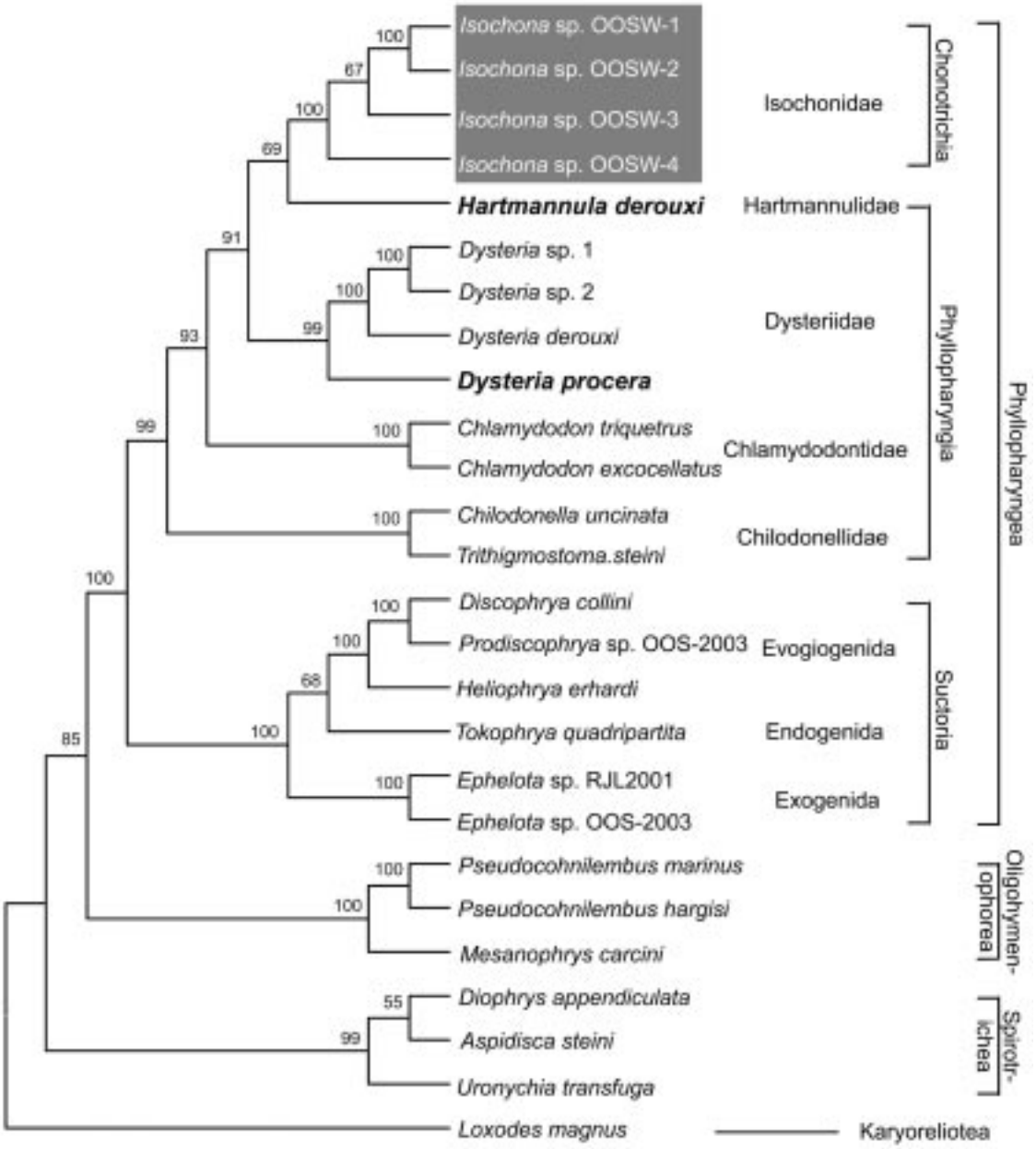

Fig. 3. Maximum Parsimony (MP) tree of the phyllopharyngean ciliates. The numbers at the forks exhibit the percentage of times the group occurred out of the 1,000 trees. No significance is placed on branch lengths connecting the species. The new sequence is highlighted in boldface.

1880-1882, Dobrzańska-Kaczanowska 1963), which implies that morphological differences between adult chonotrichs and Phyllopharyngia may be misleading taxonomically (Snoeyenbos-West *et al.* 2004).

In addition, our results clearly indicated that dysteriids were outlined from other related taxa and may be a specialized group within Phyllopharyngea, which corresponds well with the traditional morphological descriptions (Gong and Song 2003, Li and Song 2006).

Nevertheless, the present study did not provide an unambiguous branching order for all orders within the class Phyllopharyngea, since until now, only 23 species

with this species-rich group have been sequenced and represented on SSrRNA phylogenetic trees. To determine details of their relationships in these highly specialized organisms, more data are definitely needed.

Acknowledgements. This work was supported by the "Nature Science Foundation of China" (Project number 30430090, 40376045). We are grateful to Dr. Jun Gong, ex-graduate student of our laboratory, for his kindly help in identifying the material.

REFERENCES

Baroin-Tourancheau A., Villalobo E., Tsao N., Torres A., Pearlman R. E. (1998) Protein-coding gene trees in ciliates: comparison with rRNA-based phylogenies. *Mol. Phylogen.. Evol.* **10:** 299-309

Bernhard D., Schlegel M. (1998) Evolution of histone H4 and H3 genes in different ciliate lineages. *J. Mol. Evol.* **46:** 344-354

Budin K., Philippe H. (1998) New insights into the phylogeny of eukaryotes based on ciliate Hsp70 sequences. *Mol. Biol. Evol.* **15:** 943-956

Chen Z., Song W. (2002) Phylogenetic positions of *Aspidisca steini* and *Euplotes vannus* within the order Euplotida (Hypotrichia: Ciliophora) inferred from complete small subunit ribosomal RNA gene sequences. *Acta Protozool.* **41:** 1-9

Corliss J. O. (1979) The Ciliated Protozoa: Characterization, Classification and Guide to the Literature. 2nd ed. Pergamon Press, New York

Dobrzańska-Kaczanowska J. (1963) Comparaison de la morphogenèse des ciliés: *Chilodonella uncinata* (Ehrbg.), *Allosphaerium paraconvexa* sp. n. *et Heliochona scheuteni* (Stein). *Acta Protozool.* **1:** 353-394

Elwood H. J., Olsen G. J., Sogin M. L. (1985) The small-subunit ribosomal RNA gene sequences from the hypotrichous ciliates *Oxytricha nova* and *Stylonychia pustulata*. *Mol. Biol. Evol.* **2:** 399-410

Felsenstein J. (1985) Confidence limits on phylogenies: An approach using the bootstrap. *Evolution* **39:** 783-791

Fitch W. M., Margoliash E. (1967) Construction of phylogenetic trees. *Science* **155:** 279-284

Foissner W. (1996) Ontogenesis in ciliated protozoa, with emphasis on stomatogenesis. In: Ciliates: Cells as Organisms (Eds. K. Hausmann, P. C. Bradbury). Gustav Fisher Verlag, Stuttgart 95-177

Gong J., Song W. (2003) Morphology and infraciliature of two marine benthic ciliates, *Dysteria procera* Kahl, 1931 and *Dysteria magna* nov. spec. (Protozoa, Ciliophora, Cyrtophorida), from China. *Europ. J. Protistol.* **39:** 301-309

Gong J., Song W. (2004) Morphology and infraciliature of two marine species of *Harmannula* (Protozoa, Ciliophora, Cyrtophorida), from scallop-farming waters off Qingdao (Tsingtao), China. *J. Nat. Hist.* **38:** 1327-1337

Grell K. G., Meister A. (1982) On the taxonomic position of Hypocomidae (Ciliata). *Z. Naturfosch.* **37:** 1050-1052

Hoffman D. C., Prescott D. M. (1997) Phylogenetic relationships among Hypotrichous ciliates determined with the macronuclear gene encoding the large, catalytic subunit of DNA polymerase á. *J. Mol. Evol.* **45:** 301-310

Huelsenbeck J. P., Ronquist F. (2001) MRBAYES: Bayesian inference of phylogeny. *Bioinformatics* **17:** 754-755

Kent W. S. (1880-1882) A Manual of the Infusoria. David Bogue, Lodon

Kimura M. (1980) A simple method of estimating evolutionary rates of base substitutions through comparative studies of nucleotide sequences. *J. Mol. Evol*. **16:** 111-120

Leipe D. D., Bernhard D., Schlegel M., Sogin M. L. (1994) Evolution of 16S-like ribosomal RNA genes in the ciliophoran taxa Litostomatea and Phyllopharyngea. *Europ. J. Protistol*. **30:** 354-361

Li L., Song W. (2006) Phylogenetic position of *Dysteria derouxi* (Ciliophora: Phyllopharyngea: Dysteriida) inferred from the small subunit ribosomal RNA gene sequences. *Acta Oceanol. Sinica* **25:** 119-126

Lynn D. H. (1996) Systematics of ciliates. In: Ciliates: Cells as Organisms (Eds. K. Hausmann, P. C. Bradbury). Gustave Fischer Verlag, Stuttgart 51-72

Lynn D. H., Corliss J. O. (1991) Ciliophora. In: Microscopic Anatomy of Invertebrates. (Ed. F. W. Harrison). John Wiley and Sons, Inc., New York 333-467

Lynn D. H., Small E. B. (1997) A revised classification of the phylum Ciliophora Doflein, 1901. *Rev. Soc. Mex. Hist. Nat.* **47:** 65-78

Lynn D. H., Small E. B. (2002) Phylum Ciliophora Doflein, 1901. In: An Illustrated Guide to the Protozoa, 2nd ed. (Eds. J. J. Lee, G. F. Leedale, P. C. Bradbury). Society of Protozoologists, Lawrence, Kansas 371-656

Lynn D. H., Gransden S. G., Wright A.-D. G., Josephson G. (2000) Characterization of a new species of the ciliate *Tetrahymena* (Ciliophora: Oligohymenophorea) isolated from the urine of a dog: first report of *Tetrahymena* from a mammal. *Acta Protozool.* **39:** 289-294

Puytorac P. de (1994) Phylum Ciliophora Doflein, 1901. In: Traité de Zoologie, Tome II, Infusoires Ciliés, Fasc. 2, Systématoque (Ed. P. de Puytorac). Masson, Paris 1-15

Puytorac P. de, Batisse A., Bohatier J., Corliss J. O., Deroux G., Didier P., Dragesco J., Fryd-Vesavel G., Grain J., Groliére C.-A., Iftode F., Laval M., Roque M., Savoie A., Tuffrau M. (1974) Proposition d'une classification du phylum Ciliophora Doflein, 1901. *C. R. Acad. Sci. Paris* **278:** 2799-2802

Puytorac P. de, Grain J., Legendre P. (1994) An attempt at reconstructing a phylogenetic tree of the Ciliophora using parsimony methods. *Eur. J. Protist.* **30:** 1-17

Riley J. L., Katz L. A. (2001) Widespread distribution of extensive genome fragmentation in ciliates. *Mol. Biol. Evol.* **18:** 1372-1377

Saitou N., Nei M. (1987) The neighbor-joining method: a new method for reconstructing phylogenetic trees. *Mol. Biol. Evol.* **4:** 406-425

Schlegel M., Elwood H. J., Sogin M. L. (1991) Molecular evolution in hypotrichous ciliates: sequence of the small subunit RNA genes from *Onychodromus quadricornutus* and *Oxytricha granulifera* (Oxytrichidae, Hypotrichida, Ciliophora). *J. Mol. Evol.* **32:** 64-69

Shang H., Song W., Warren A. (2003) Phylogenetic positions of two ciliates, *Paranophrys magna* and *Mesanophrys carcini* (Ciliophora: Oligohymenophorea), within the subclass Scuticociliatia inferred from complete small subunit rRNA gene sequence. *Acta Protozool*. **42:** 171-181

Snoeyenbos-West O. L. O., Cole J., Campbell A., Coats D. W., Katz L. A. (2004) Molecular phylogeny of Phyllopharyngean ciliates and their group I introns. *J. Euk. Microbiol.* **51:** 441-450

Sogin M. L., Elwood H. J. (1986) Primary structure of the *Paramecium tetraurelia* small-subunit rRNA coding region: phylogenetic relationships within the Ciliophora. *J. Mol. Evol.* **23:** 53-60

Song W., Wilbert N. (2002) Faunistic studies on marine ciliates from the Antarctic benthic area, including descriptions of one epizoic form, 6 new species and 2 new genera (Protozoa: Ciliophora). *Acta Protozool.* **41:** 23-61

Swofford D. L. (2002) PAUP*: Phylogenetic Analysis Using Parsimony (*and Other Methods). Version 4. Sinauer Associates, Sunderland, Massachusetts

Thompson J. D., Higgins D. G., Gibson T. J. (1994) CLUSTAL W: improving the sensitivity of progressive multiple sequence alignment through sequence weighting, positions-specific gap penalties and weight matrix choice. *Nucl. Acis. Res.* **22:** 4673-4680

Received on 11th October, 2005; revised version on 24th March, 2006; accepted on 4th May, 2006

Acta Protozool. (2006) 45: 271 - 287

ACTA
PROTOZOOLOGICA

Comparison and Redefinition of Four Marine, Coloured *Pseudokeronopsis* spp. (Ciliophora: Hypotrichida), with Emphasis on Their Living Morphology

Weibo SONG[1], Alan WARREN[2], Dave ROBERTS[2], Norbert WILBERT[3], Lifang LI[1], Ping SUN[1], Xiaozhong HU[1] and Honggang MA[1]

[1]Laboratory of Protozoology, KLM, Ocean University of China, Qingdao, P. R. China; [2]Department of Zoology, the Natural History of Museum, London, UK; [3]Institut für Molekulare Physiologie und Entwicklungsbiologie, Universität Bonn, Bonn, Germany

Summary. Species separation among some brightly coloured marine *Pseudokeronopsis* spp. is difficult because of the accumulation of inaccurate descriptions or misinterpretations in previous studies. Based on isolates collected from Chinese coastal waters, four "well-known" yellow, brown or reddish species, i.e. *P. carnea*, *P. flava*, *P. flavicans*, and *P. rubra*, are re-examined, particularly with respect to their cortical granules, cell colour, infraciliature and other morphological features *in vivo*. Improved diagnoses for these organisms are given, synonyms are listed and a key to their identification is supplied. A recently reported marine form, *Pseudokeronopsis pararubra* Hu, Warren *et* Suzuki, 2004, is believed to be a junior synonym of *P. carnea* and is synonymized with the latter.

Key words: coloured *Pseudokeronopsis*, marine ciliates, species separation.

INTRODUCTION

Species separation among the brightly coloured *Pseudokeronopsis* spp. is difficult (Cohn 1866; Entz 1884; Kahl 1932; Jerka-Dziadosz and Janus 1972; Borror and Wicklow 1983; Song *et al*. 2004a, b). This is mainly because many morphogenetic and morphological characters, including the ciliary pattern, either overlap or are very similar while others, such as the colour and arrangement of the pigment granules, are usually superficially and/or incorrectly described or overlooked (Borror 1972; Ruthmann 1972; Foissner 1984; Wirnsberger *et al.* 1987; Hu and Song 2000, 2001; Hu *et al.* 2004; Song *et al.* 2004a, b; Sun and Song 2005). Marine *Pseudokeronopsis* spp. with brown, red, orange or yellow colour are commonly reported yet there is much confusion concerning their identification and circumscription (Hu and Song 2000, 2001; Song *et al.* 2002, 2004a, b). Numerous ambiguities have therefore accumulated in the literature pertaining to these organisms.

Wirnsberger *et al.* (1987) reviewed in detail the morphometric and infraciliature data for three species, i.e. *P. carnea*, *P. flava* and *P. rubra*. That study, however, was based primarily on silver-impregnated specimens so the living features remained inadequately documented. At least five more nominal morphotypes

Address for correspondence: Weibo Song, Laboratory of Protozoology, KLM, Ocean University of China, Qingdao 266003, P. R. China; E-mail: wsong@ouc.edu.cn

from marine biotopes have since been described thus adding to the confusion for species identification and circumscription (Hu and Song 2000, 2001; Song *et al.* 2002, 2004b; Shi and Xu 2003; Hu *et al.* 2004; Wanick and Silva-Neto 2004).

In recent years four brightly coloured marine *Pseudokeronopsis* spp., i.e. *P. carnea, P. flava, P. flavicans* and *P. rubra*, have been isolated from coastal waters of China, mostly from the north China sea near Qingdao, but also from the south China sea near Zhanjiang. This provided the opportunity to make a detailed examination of these "well-known" organisms. Previous studies have demonstrated that these forms are morphologically and morphometrically similar and that their infraciliature is generally less useful than expected for species identification (Song *et al.* 2002). Consequently greater attention is here given to the living morphology. Random amplified polymorphic DNA fingerprinting (RAPD) was also carried out since this technique is known to have potential for separating morphologically similar taxa (Chen *et al.* 2000).

The aims of the present study were: to evaluate the characters for species identification and separation; to redefine the four species and provide an improved diagnosis for each; to supply a key to their identification.

MATERIALS AND METHODS

Population origins, cultivation and morphological observations. Populations of four species were examined during the present study (Table 1). Among these, one population of *Pseudokeronopsis flava* (Cohn, 1866) was collected in July 2001 from the littoral water near Zhanjiang, Guangdong Province, south China. The water salinity was ~33‰, water temperature was about 28°C. All other populations and species were isolated during the period 1997-2003 from coastal waters of Jiaozhou Bay near Qingdao, north China. The water salinity was ~30‰, water temperature was 10-24°C.

After isolation pure (uniprotistan) cultures were established with rice grains as food source for bacteria. Investigations were carried out both on newly sampled and on cultivated specimens in order to observe variations in cell morphology including pigment colour. For observing cell and pigment colour, bright field microscopy only was used. Protargol staining (Wilbert 1975) was performed to reveal the infraciliature. Measurements were made at a magnification of 1250×. Drawings were made with the help of a camera lucida. Terminology is mainly according to Foissner (1984) and Borror and Wicklow (1983).

DNA extraction and RAPD reaction. The following species were analyzed by RAPD: *Pseudokeronopsis rubra, P. carnea* and *P. flava* (two populations). Each species was isolated from two separate cultures. Briefly, the nucleotide extraction protocols were: cells were rinsed three times with sterile artificial marine water after being starved overnight and were then pelleted by centrifugation. Genomic DNA extraction, amplification by PCR with primers S2001, S2006, S2007 and S2010 (defined in Chen *et al.* 2000) and RAPD reactions were carried out according to Chen *et al.* (2000).

RESULTS

Comparative description of four similar *Pseudokeronopsis* spp.

In view of the fact that previous reports might contain inaccurate or inconsistently interpreted data, the descriptions provided here are based only on the populations isolated from the China seas by the research group in the Laboratory of Protozoology, OUC. The improved diagnoses, however, also take into account previously reported data.

Body shape, size, flexibility or rigidity

Although the body shape *in vivo* of all four species is basically similar (i.e. slender or belt-like) there are consistent, albeit comparatively small, differences between them (Fig. 9). Clearly the cell size is variable even within the same population, especially after a long-term culture. All morphotypes are flexible but seldom or never contractile. Locomotion is generally similar in all four species and so is not regarded as a useful character for species separation.

Pseudokeronopsis carnea. This species is the most plump of the four; ratio of length to width of about 3-4:1; body often flattened and folded but seldom twisted (Figs 2C, F, H). Cells in culture mostly about 200-250 µm long *in vivo* although some individuals might be 300 µm or more in length. Anterior end bluntly rounded, which is unlike the other three species, while the posterior end is inconspicuously narrowed (Figs 1A, D, E; 2C). The buccal field is wide and conspicuous, its ratio to body length is about 1:3 which is the highest of the four congeners.

Pseudokeronopsis flava. Specimens in freshly collected samples mostly about 200-250 µm long with ratio of length to width about 4:1 (Figs 1H, L). In culture the body size and shape are extremely variable, i.e. from 120 to >400 µm long, and usually conspicuously more slender than freshly collected forms with a ratio of length to width up to 6-9:1 though with some "abnormal" forms that are worm- or band-like (Figs 1I; 4A, F). The ratio of buccal field to body length is also the most variable of the four species ranging from 1:4 up to 1:6 in the worm-like forms (Fig. 4A).

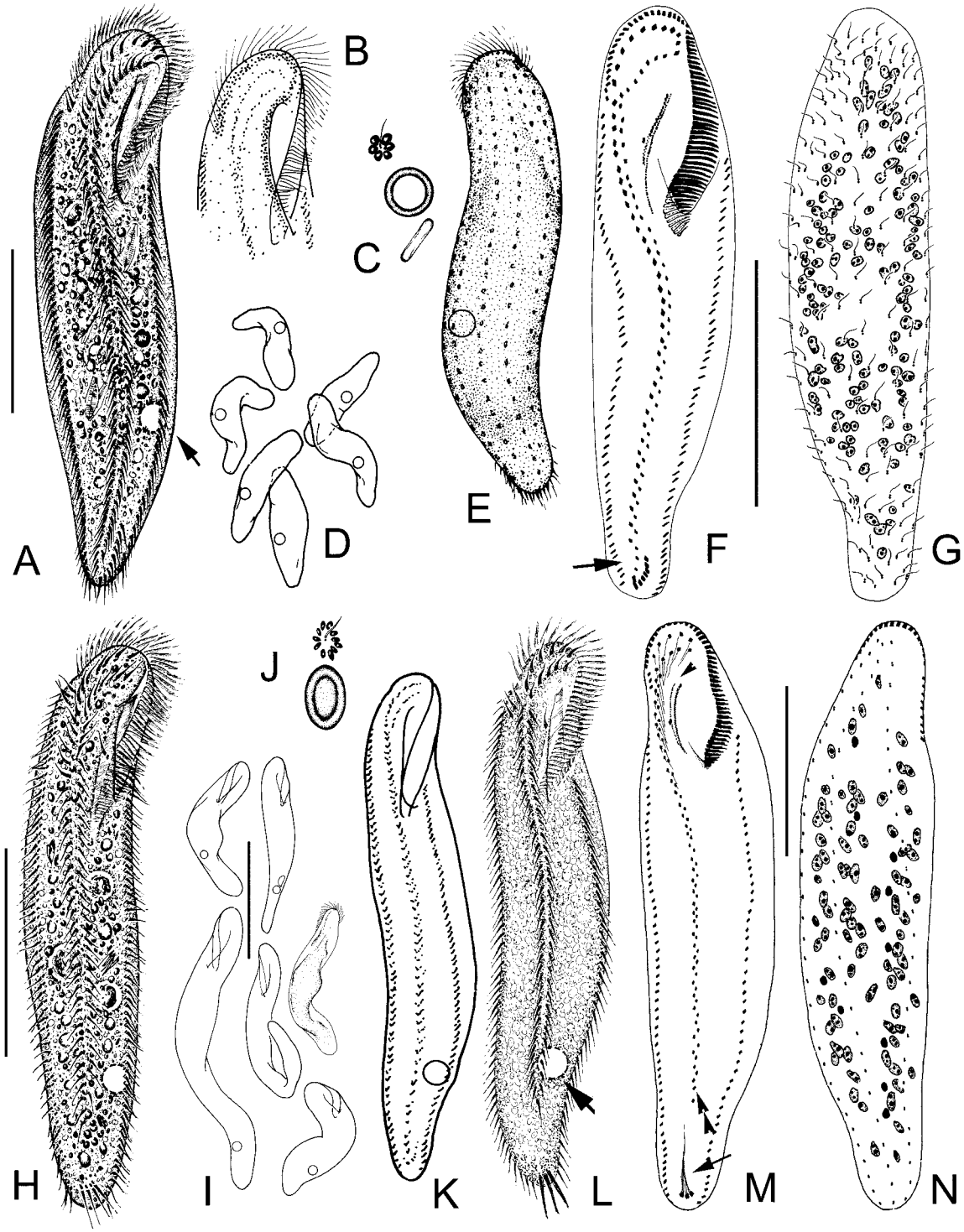

Fig. 1. *Pseudokeronopsis carnea* (A-G) and *Pseudokeronopsis flava* (H-N) from life (A-E, H-L) and after protargol impregnation (F, G, M, N) (I, L-N, from Song *et al.* 2004a, the rest are original). **A** - ventral view of a typical individual, arrow marks the contractile vacuole; **B** - anterior portion, to show the distribution of the pigment granules; **C, J** - to show the "blood-cell-shaped" granules (BCS-granules) and the pigment granules which are dark red in bright field microscopy; **D** - various body shapes; **E** - dorsal view at lower magnification, note the pattern of distribution of the pigment granules (marked as rows of dots); **F, G, -** ventral (F) and dorsal (G) views of the same specimen, arrow in F marks the last cirri of the midventral rows; **H** - ventral view of a typical individual; **I** - to show the various body shapes; **J, K, L** - ventral view, to demonstrate the distribution of pigment granules and the location of the contractile vacuole (arrow); **M, N** - ventral (M) and dorsal (N) views of the same specimen; arrowhead shows the undulating membranes; double arrowheads in M mark the last cirri of the midventral rows; arrow indicates the fibers of the transverse cirri. Scale bars: 60 µm (A, F, H); 50 µm (M); 100 µm (I).

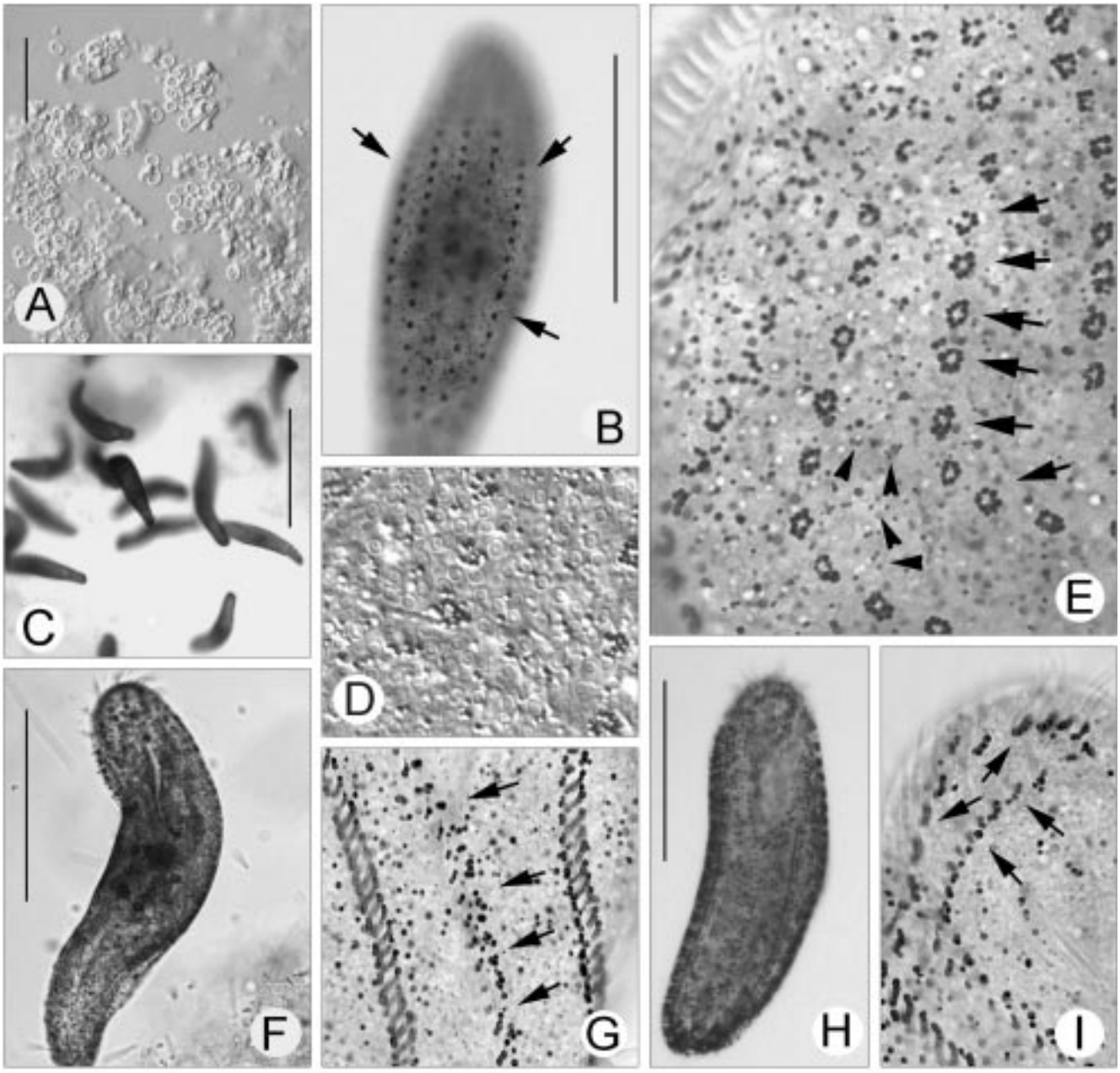

Figs 2A-I. Photomicrographs of *Pseudokeronopsis carnea in vivo* (G, I, from Hu *et al.* 2004, called *P. pararubra*; the rest are original). **A** - to show the blood-cell-shaped granules (BCS-granules); **B** - dorsal view, to show the grouped pigment granules along the dorsal kineties (arrows); **C** - cells in natural state (without cover glass) at low magnification; **D** - dorsal view, to demonstrate both the grouped pigment granules and the BCS-granules; **E** - detailed portion of the dorsal side; arrowheads mark the sparsely distributed pigment granules; arrows indicate the grouped pigment granules which are arranged along the dorsal kineties; **F, H** - two individuals, to show the dark colour when observed at low to medium magnifications (100-200×); **G, I** - ventral view, to show the arrangement of the pigment granules; arrows mark the pigment granules along the midventral rows (G) and the frontal cirri (I). Scale bars: 10 μm (A); 80 μm (B, F, H); 200 μm (C).

Pseudokeronopsis flavicans. This form is less flexible than the other three species, often somewhat snake-like, distorted or ridged in middle portion, slightly uneven and irregularly bulged on the dorsal side (Fig. 6B). The body is slender with the posterior portion distinctly narrowed and tail-like (Fig. 6A). Body length *in vivo*

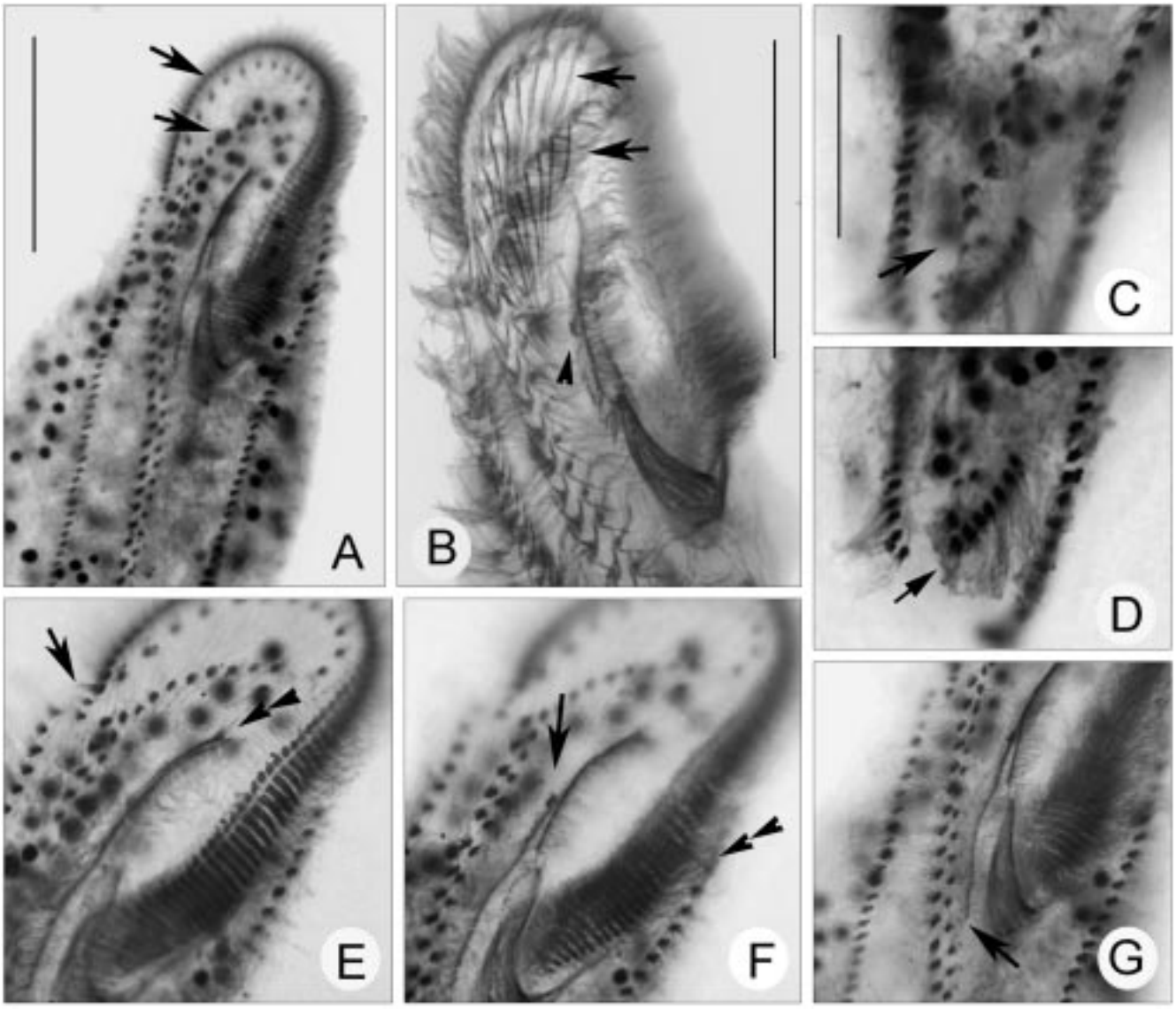

Figs 3A-G. Photomicrographs of *Pseudokeronopsis carnea* after protargol impregnation. **A, B** - ventral view, to show the general ciliature of the anterior portion; arrows mark the bicorona; **C, D** - ventral view of the posterior portion of the body; arrows mark the posterior end of the midventral rows (C) and the transverse cirri (D); **E** - ventral view; arrow marks the frontoterminal cirri; double-arrowheads mark the anterior ends of the undulating membranes; **F** - the same specimen as E; arrow indicates the buccal cirrus, double-arrowheads mark the left marginal row; **G** - ventral view of the buccal area, arrow marks the posterior end of the paroral membrane. Scale bars: 40 µm.

about 200-300 µm, cell length to width ratio about 5:1 (Figs 6A, B). The ratio of buccal field to body length is *ca* 1:4.

Pseudokeronopsis rubra. Body folded and flexible, shape relatively constant but often becomes plumper in culture (Figs 6G, 7A). Body length *in vivo* about 160-200 µm, less variable than the other three congeners. Both ends are conspicuously narrowed, especially the anterior end in freshly collected specimens. The ratio of buccal field to body length is about 1:4.

Cortical granules, pigments and cell colour

All four species possess two types of cortical granules: one is the typical pigment granule that renders the cell brightly coloured while the other is colourless. The pigment granules are about 1 µm in size and are invari-

ably arranged in a '*rubra*-pattern' (Song *et al.* 2004a), i.e. on the ventral side they are always densely arranged in short rows near the ciliary organelles and hence form belts along the cirral rows (Figs 1K, 2G, 6K), while on the dorsal side they are grouped in rosette-patterns around the dorsal cilia (Figs 1C, J; 2B, E, arrows; 4E; 6I). In addition to these grouped pigment granules there are also some that are sparsely distributed throughout the body giving the cell a weak colour when observed under higher magnifications (Fig. 2E, arrowheads). These granules disappear after fixation and/or impregnation but are detectable using epifluorescence microscopy (Fig. 7E).

The second type of cortical granule is colourless, larger than the pigment granules (about 1.5 μm in size), oval or circular in shape and flattened like that of a red blood cell, i.e. the margin is thicker than the central area (Figs 1C, J; 2A; 4C; 5A; 6I; 7B, C). These blood-cell-shaped granules (BCS-granules) are positioned beneath the pigment granules and are densely arranged on both ventral and dorsal sides without forming any discernible pattern.

The cell colour is rendered mainly by the pigment granules hence it can fade when the pigments lose the strength of their colour, which can happen during long-term (several months) culture. The food contents might be another cause of variability in cell colour since this usually makes the cell appear darker. In addition, it is recommended that cell colour is recorded at both lower (<100×) and higher (>200×) magnifications since there can be significant differences between these in the same specimen.

Pseudokeronopsis carnea. Pigment granules are more conspicuous than in the other three congeners, about 1 mm in size, always dark red or brown-reddish, arranged in typical *rubra*-pattern (Figs 2E, G, I), which can be clearly detected even at low magnification, e.g. 40× (Fig. 2B). The BCS-granules are larger (about 2 μm across) in this species than in the other three, completely circular in shape and densely packed (Figs 1C, 2A).

The cell colour is usually uneven, always dark-reddish or brown-reddish at lower magnification but less brightly coloured at higher magnifications, i.e. more or less brown-greyish except for the grouped pigment granules (Fig. 2B). No change in colour was observed during long-term (several months) culture.

Pseudokeronopsis flava. Pigment granules are smaller than those of *P. carnea*, about 0.5 μm across, bright yellow to yellow-brownish, and arranged in a typical *rubra*-pattern (Fig. 4E). No conspicuous change in the strength or brightness of the colour was observed during long-term culture, even after three years. BCS-granules about 1.5 μm long, always ellipsoidal in shape (Figs 4C, D; 5A).

The cell colour is generally constant (especially compared with that of *P. rubra*, for example), always yellow to yellow-brownish at lower magnification (Figs 4A, F, H) while less yellowish at higher magnifications (Figs 4C, E). It is clear that the colour is conspicuously stronger than that in *P. flavicans* (see below).

Pseudokeronopsis flavicans. Pigment granules yellow-brownish, ellipsoidal in shape and about 1 mm long, i.e. relatively larger than that in *P. flava* (*vs. ca* 0.5 μm). Since the colour of these pigment granules is weak, they are difficult to detect at lower magnifications. BCS-granules about 1.5 μm long, oval to ellipsoidal in shape, densely packed.

The general cell colour of this species appears much less bright than that of *P. flava*. It is yellowish to yellow-brownish at lower magnifications and yellow-greyish at higher magnifications.

Pseudokeronopsis rubra. As a unique character, the colour both of the pigment granules and of the whole cell may change and/or fade during long-term culture. The pigment granules are small (<0.5 μm in diameter) and generally dark brick-reddish in colour in freshly collected specimens (Figs 7D, F), but this may change while in long-term culture to orange-brownish or even brown-yellowish, similar to *P. flava* and *P. flavicans*. One isolate became completely yellow-brownish after six years in culture. The BCS-granules are about the same size as those in other congeners, oval in shape, densely packed (Figs 7B, C).

Cell colour in freshly collected samples is dark brick-reddish (Fig. 7A) at low magnification but light brick-reddish at higher magnifications.

Contractile vacuole

In some cases, the contractile vacuole is difficult to detect or even undetectable, especially in freshly collected specimens or cells kept in high salinity (>30‰) media. The rate of pulsation is slow, i.e. at several-minute intervals in our populations. The position of the contractile vacuole is constant as in most other hypotrichs (*s.l.*) and is here considered to be one of the most reliable characters for species identification. The appearance and position of the contractile vacuole within the cell are as follows:

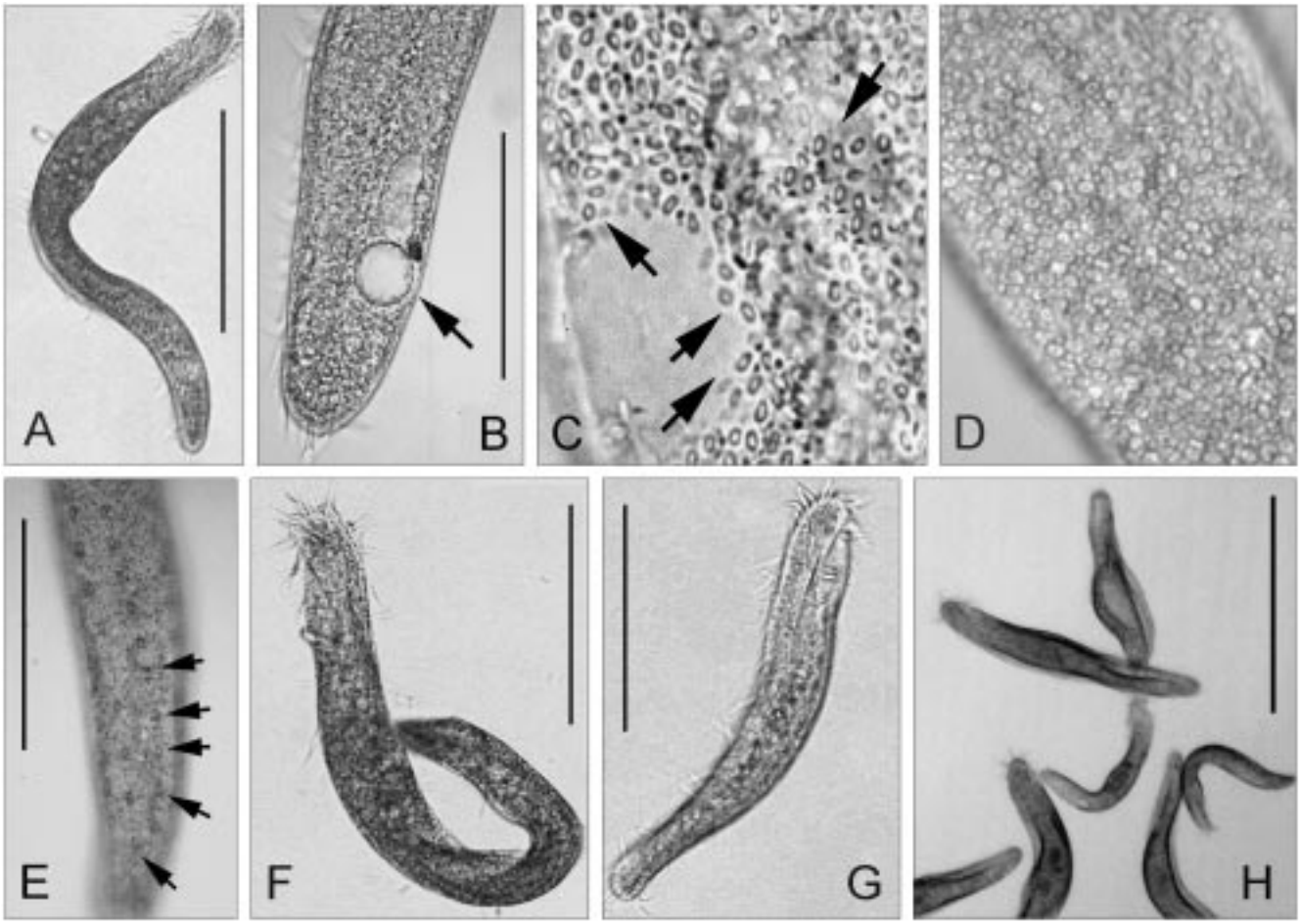

Figs 4A-E. Photomicrographs of *Pseudokeronopsis flava in vivo* (A-C, E-G, from Song *et al.* 2004a, the rest are original). **A, F-H** - to show different body shapes and sizes; **B** - caudal portion, arrow indicates the contractile vacuole; **C, D** - detail of cell to demonstrate the BCS-granules (arrows in C); **E** - to show the grouped pigment granules arranged along the dorsal kineties (arrows). Scale bars: 100 µm (A, B, F-H); 50 µm (E).

Pseudokeronopsis carnea. Contractile vacuole in posterior half of cell, usually in posterior 2/5-1/3, easily recognizable (Figs 1A, D, E).

Pseudokeronopsis flava. Contractile vacuole in posterior half of cell, usually in posterior 1/4-1/6, large and detectable in most cases (Figs 1H, K, L; 4B).

Pseudokeronopsis flavicans. Contractile vacuole in anterior half of cell, usually in anterior 1/3 (Fig. 6A); sometimes undetectable.

***Pseudokeronopsis rubra*.** Contractile vacuole in posterior half of cell, usually in posterior 1/3 (Figs 6G, J, K), often undetectable.

Infraciliature

The infraciliature of three forms, i.e. *P. carnea*, *P. rubra* and *P. flava*, originating from a variety of locations in South Africa, the Indopacific region and several European countries, were described in detail by Wirnsberger *et al*. (1987). These data demonstrated a great deal of inter- and intraspecific diversity (Wirnsberger *et al*. 1987). Consequently consideration of the ciliary features of these taxa, plus those of *P. flavicans*, are here based exclusively on the Chinese populations in order to maintain the consistency of the data.

As Table 1 shows, most aspects of the infraciliature show a high degree of variability between populations of the same species and there is a significant degree of overlap among the four species. Even characters that are very reliable in most other hypotrichs (*s.l.*), e.g. the number of dorsal kineties, tend to be rather variable in these species. Therefore, most aspects of the infraciliature are of limited value for species separation and identifica-

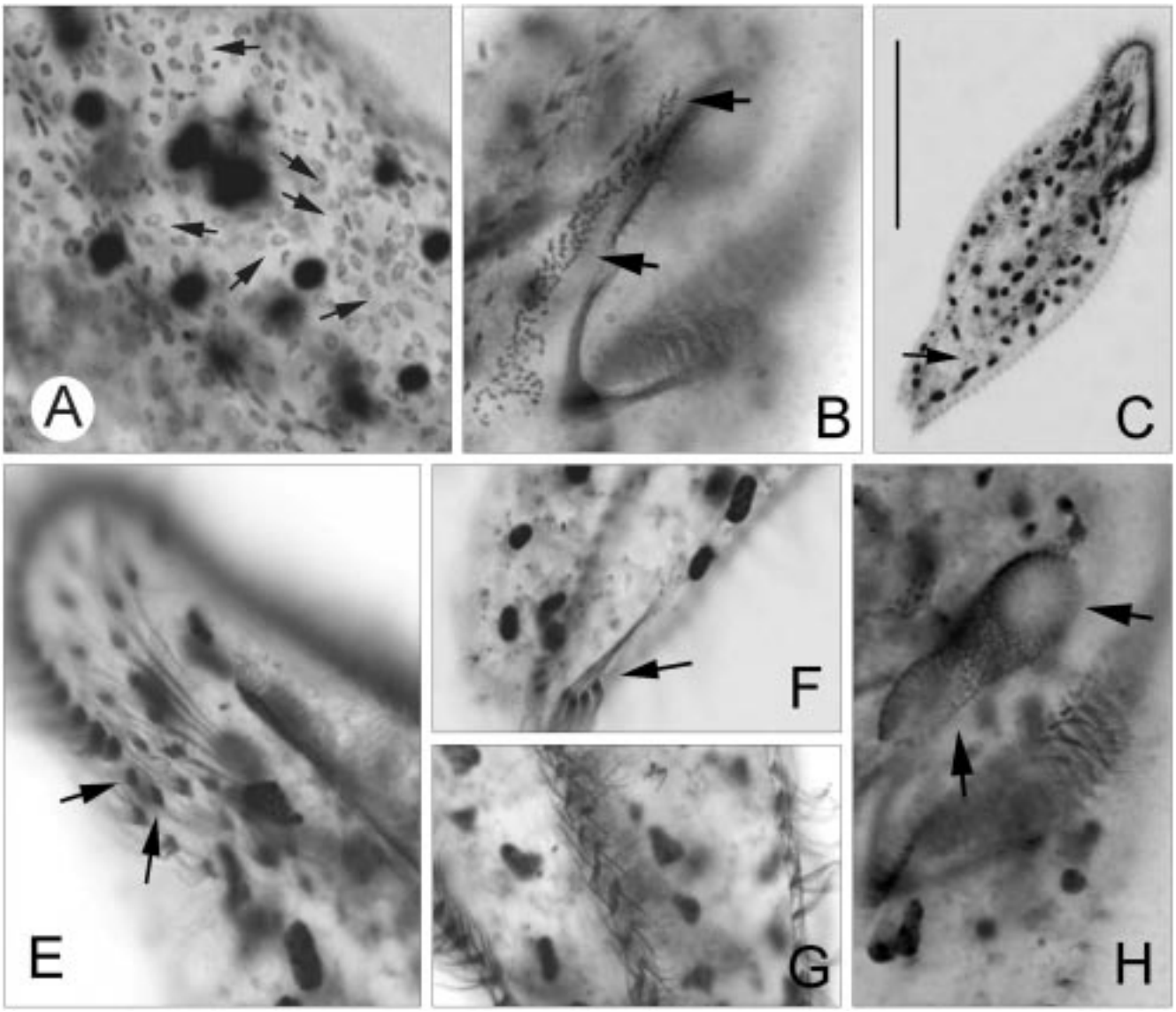

Figs 5A-H. Photomicrographs of *Pseudokeronopsis flava* after protargol impregnation (E-G, from Song *et al.* 2004a, the rest are original). **A** - detailed portion, to show the BCS-granules (arrows); **B** - ventral view, to show the cirral anlagen in the proter (arrows); **C** - ventral view; arrow marks the posterior end of the midventral rows; **E** - ventral view of anterior portion of cell, arrows mark the frontoterminal cirri; **F** - to show the short transverse row (arrow); **G** - ventral view, to show the closely arranged midventral rows; **H** - buccal area in proter, arrows indicate the oral primordium which is located beneath the buccal cavity. Scale bar: 80 µm.

Figs 6A-M. *Pseudokeronopsis flavicans* (A-F) and *Pseudokeronopsis rubra* (G-M) from life (A, B, G-K) and after protargol impregnation (C-F, L, M); (A, C, D, from Song *et al.* 2002; H, from Hu and Song, 2001, the rest are original). **A, B** - ventral view of two typical individuals; note the position of the contractile vacuole; **C, D** - ventral (C) and dorsal (D) views of the same specimen, to show the general infraciliature, arrow in **C** marks the last cirral pair of the midventral rows; **E, F** - ventral (E) and dorsal (F) views of the same specimen; arrows in E mark the posterior portion of the midventral rows; **G, H** - ventral view of two individuals, to demonstrate the different body shapes; **I** - to show the pigment granules, which are grouped around the dorsal cilia, and the BCS-granules; **J** - dorsal view, to show the distribution pattern of the pigment granules and the location of the contractile vacuole (arrow); **K** - ventral view, to demonstrate the distribution of pigment granules; **L, M** - ventral and dorsal views of an atypical specimen with strongly shortened midventral rows; arrow in L indicates the last cirral pair of the midventral rows. Scale bars: 80 µm (A, B, G, H); 50 µm (C-F, L, M).

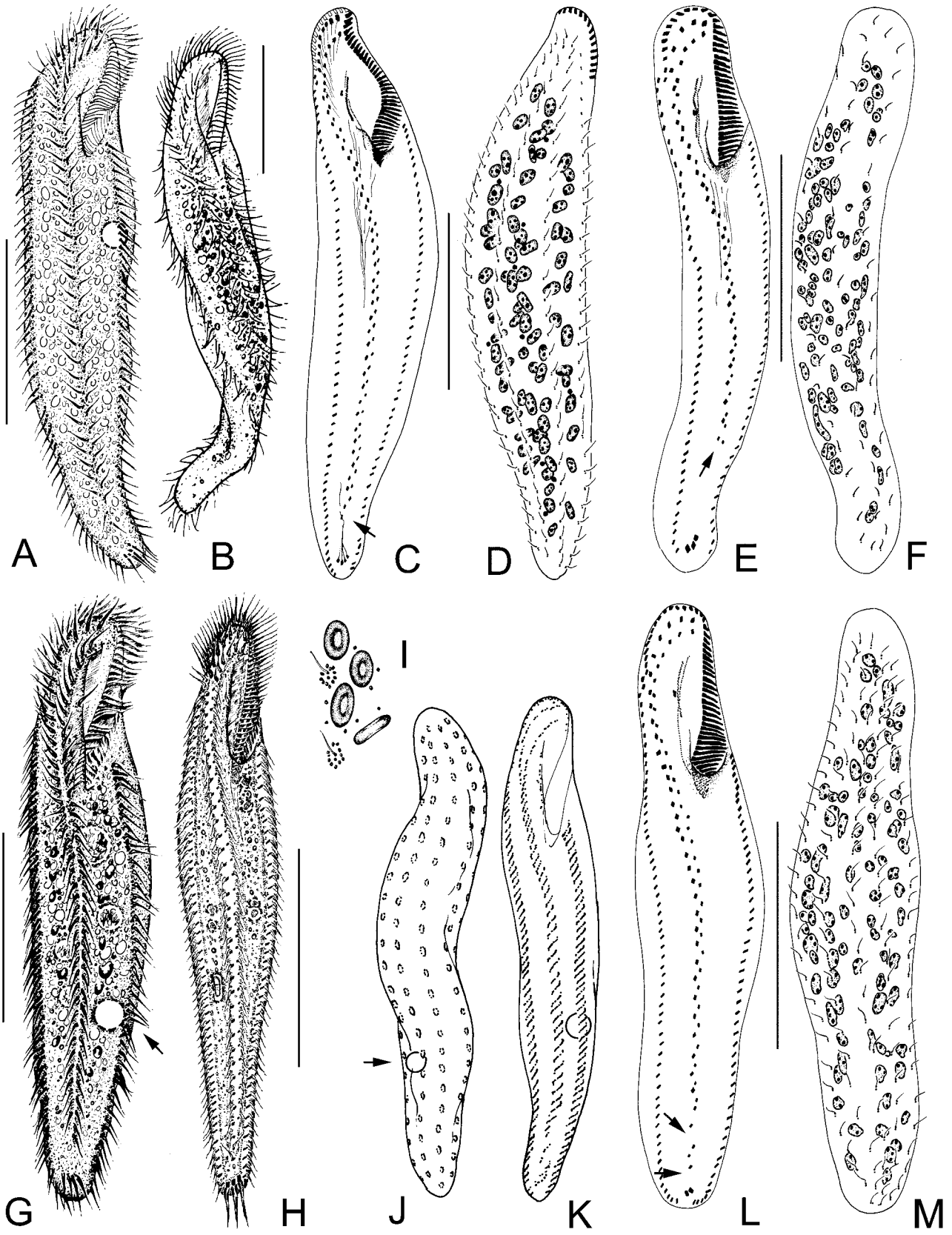
A
B
C
D
E
F
G
H
I
J
K
L
M

Table 1. Morphometrical characterization of *Pseudokeronopsis carnea* (1st line), *P. flava* (2nd line), *P. rubra* (1999-population 3rd line; 2000-population 4th line), and *P. flavicans* (5th line). All data based on protargol impregnated specimens of China-populations. CV - coefficient of variation in %, Max - maximum, Min - minimum, n - number of cells measured, SD - standard deviation, SE - standard error of mean.

Character	Min	Max	Mean	SD	SE	CV	n
Body length in µm	208	288	249.6	24.8	6.2	9.9	16
	144	246	175.5	27.1	6.8	15.5	16
	124	264	180.7	37.5	8.2	20.8	21
	152	248	180.3	23.7	5.4	13.1	19
	183	238	209.1	21.2	8.0	8.1	14
Body width in µm	56	96	76.3	10.3	2.6	13.4	16
	48	72	51.75	8.7	2.2	16.8	16
	32	64	50.8	8.2	1.9	16.0	19
	32	56	39.3	6.9	1.6	17.6	19
	40	65	60.1	4.7	1.8	6.2	14
Number of membranelles	69	79	73.1	3.0	0.8	4.1	16
	43	51	45.4	2.6	0.6	5.6	16
	46	60	51.6	3.7	0.8	7.2	20
	40	53	46.9	3.7	0.9	7.9	19
	50	66	56.1	5.5	2.1	9.8	7
Number of cirri in left marginal row	58	79	66.4	5.7	1.4	8.6	16
	41	57	47.8	5.0	1.3	10.4	16
	45	62	52.7	5.2	1.3	9.9	17
	40	64	48.1	6.6	1.5	13.7	19
	40	57	52.4	3.1	1.4	5.8	8
Number of cirri in right marginal row	63	72	67.5	2.8	0.7	4.2	16
	43	60	52.63	5.6	1.4	10.7	16
	48	67	57.9	4.6	1.1	8.0	17
	40	60	49.7	5.6	1.3	11.3	18
	44	65	60.2	3.2	1.3	5.3	8
Number of transverse cirri	8	9	8.6	0.5	0.2	6.0	12
	3	4	3.7	0.5	0.1	12.6	14
	2	4	3.1	0.6	0.2	19.8	16
	3	4	3.7	0.5	0.1	12.6	18
	3	6	3.6	0.9	0.3	26.8	9
Number of frontoterminal cirri	2	2	2	0	0	0	16
	2	3	2.3	0.5	0.1	20.1	12
	2	2	2	0	0	0	20
	2	2	2	0	0	0	18
	2	2	2	0	0	0	11
Number of buccal cirri	1	1	1	0	0	0	14
	1	1	1	0	0	0	7
	1	1	1	0	0	0	21
	1	1	1	0	0	0	18
	1	2	1.1	0.3	0.1	30.9	9
Number of dorsal kineties	7	8	7.5	1.8	0.5	24.1	15
	3	3	3	0	0	0	16
	4	7*	5.1	0.7	0.2	14.0	16
	3	6*	3.8	0.4	0.1	10.6	16
	4	5	4.1	0.4	0.1	8.8	14
Number of cirral pairs in midventral rows	38	43	40.3	1.7	0.4	4.2	16
	24	36	29.6	3.7	0.9	12.3	16
	25	38	30.8	4.2	1.1	13.1	16
	23	35	27.1	3.7	1.0	13.8	13
	25	40	33.4	4.4	1.5	13.1	9
Number of cirral pairs in bicorona**	9	11	10.1	0.8	0.2	7.6	16
	4	6	5.6	0.7	0.2	13.2	13
	5	7	6.3	1.1	0.2	8.4	19
	5	6	5.1	0.4	0.1	6.9	15
	5	9	7.4	1.0	0.3	13.1	10

Table 1. (contd)

Length of buccal field in µm	80	94	87.6	3.3	0.8	3.8	16
	46	65	55.8	5.3	1.3	9.6	16
	51	76	62.2	7.2	1.6	11.6	20
	52	73	59.8	5.7	1.3	9.5	19
	55	72	65.1	7.4	2.8	9.0	14

* This data include the highly shortened, fragment-like kineties (usually one, seldom two); ** Bicorona: anteriormost frontal cirri, which are positioned in two widely spaced rows.

Table 2. Comparison of living morphology of four *Pseudokeronopsis* spp. All data based on the China-populations.

Character	*P. flavicans*	*P. carnea*	*P. flava*	*P. rubra*
Cell length *in vivo* in µm	200-300	180-350	140-350*	140-250
Main features of body shape	slender and often twisted, both cell ends narrowed	plump, frontal area wide, seldom twisted	band-like, cell size extremely variable	slender, both cell ends narrowed
General cell colour at low magnification (<100×)**	yellowish	dark brown- or brick-reddish	yellowish	brick-reddish to orange, yellowish***
Cell colour at mid- to high magnifications****	yellowish	reddish	yellowish	yellow-brownish to reddish***
Pigments on dorsal side at low magnification	undetected	grouped in rows	undetected	undetected
Size of pigments in µm	*ca* 1	*ca* 1	*ca* 0.5	*ca* 0.5
Colour of pigments	yellow-brown	dark, red-brown	yellow-brown	yellow-brown, orange to brick reddish
Shape of blood-cell-shaped granules	ellipsoid*****	completely circular	ellipsoid	ellipsoid*****
Size or length of blood-cell-shaped granules in µm	*ca* 1.2	*ca* 1.5	*ca* 1.2	*ca* 1.2
Ratio of buccal field to the body length	*ca* 1:4	*ca* 1:3	*ca* 1:4-5******	*ca* 1:4
Position of contractile vacuole	anterior 1/3	posterior 2/5-1/3	posterior 1/4-1/6	posterior 1/3
Data sources	Song *et al.* (2002)	present work; Hu *et al.* (2004)	Song *et al.* (2004a)	Hu and Song (2001)

* Some "abnormal", long band-shaped forms occasionally <400 µm long (see Fig. 4A); ** Observed under the stereo-microscope; *** Colour both of pigment granules and of the whole cell clearly fading during long-term culture, i.e. conspicuously variable from dark reddish when freshly collected to yellowish or orange after several weeks/months in culture; **** Cell colour here concerns the general appearance of the cytoplasm instead of the pigment granules (with bright field microscopy at 200× to 600× magnification); ***** Incorrectly depicted/described as round in shape according to Hu and Song (2001) and Song *et al.* (2002); ****** Not including the "abnormal" forms which have extreme length: width ratios (see text).

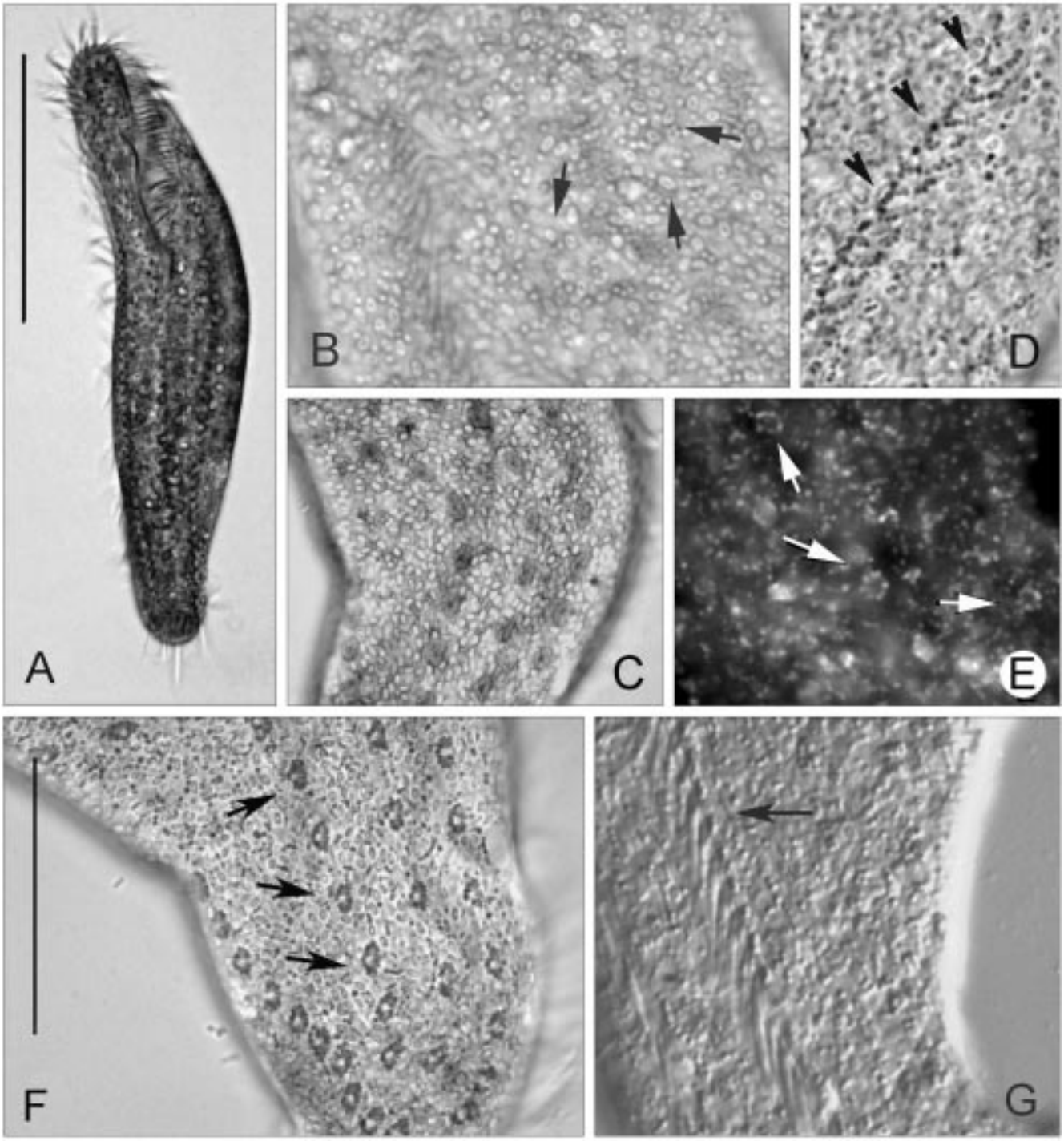

Figs 7A-F. Photomicrographs of *Pseudokeronopsis rubra* from life. **A -** to show a typical individual; **B, C** - to show the BCS-granules (arrows); **D, G** - ventral view, arrowheads (in D) and arrow (in G) indicate the pigment granules along the marginal row; **E** - with epifluorescence microscopy, arrows mark the grouped pigment granules; **F** - dorsal view, to show the pigment granules (arrows). Scale bars: 100 µm (A); 50 µm (F).

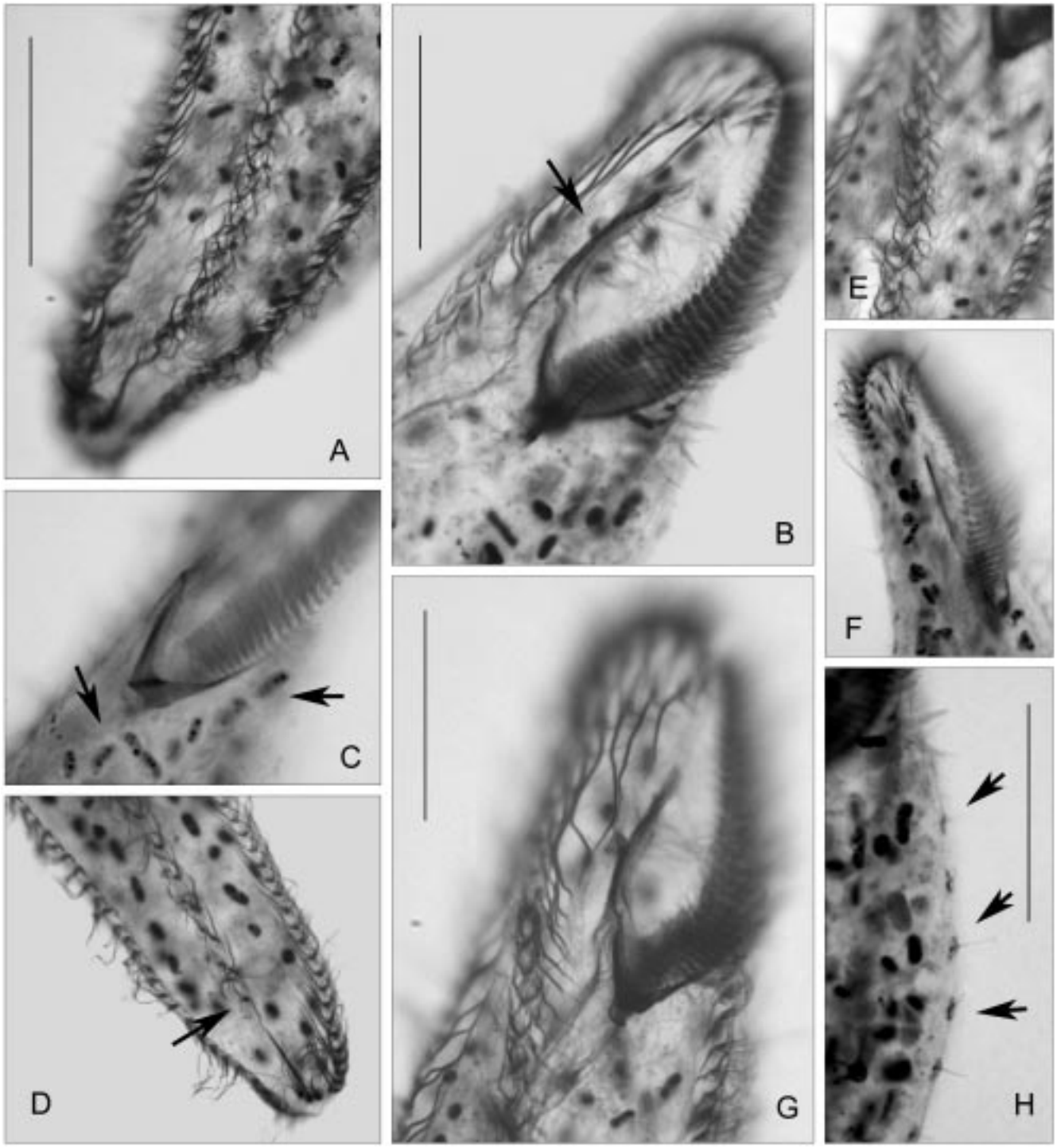

Figs 8A-H. Photomicrographs of *Pseudokeronopsis rubra* after protargol impregnation. **A, B, E-G** - ventral view of different portions of the cell, to show the general infraciliature, arrow in B marks the buccal cirrus; **C** - ventral view, to show the macronuclear segments (arrows); **D** - ventral view of posterior portion, arrow marks the posterior ends of the midventral rows; **H** - to show the dorsal cilia (arrows). Scale bars: 50 µm.

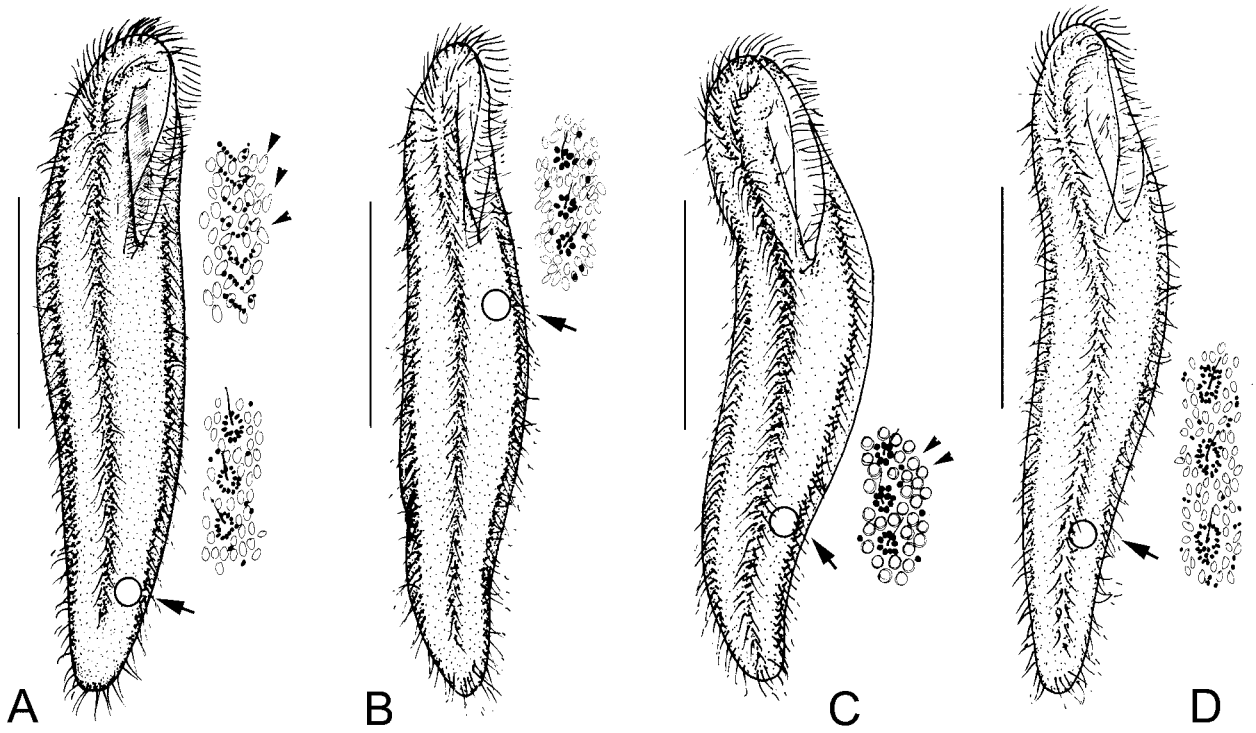

Fig. 9. Schema of four *Pseudokeronopsis* spp., (**A**) *P. flava*, (**B**) *P. flavicans*, (**C**) *P. carnea*, and (**D**) *P. rubra*, to show the general appearance of the living cells and arrangement of the pigment- and BCS-granules (arrowheads in insets). Arrows mark the contractile vacuole. Scale bars: 100 µm.

Table 3. Morphometric comparison of four *Pseudokeronopsis* spp, which are most informative in species separation at infraciliature level. All data are based on China-populations only. Distances are in µm.

Characters	*P. flavicans*	*P. carnea*	*P. flava*	*P. rubra*
Number of dorsal kineties	4-5	7-8 (5-8)	constantly 3	mostly 5 (3-7)
Number of cirral pairs in bicorona	~7 (5-9)	9-11 (8-12)	~ 5 (4-6)	~6 (5-7)
Number of transverse cirri	3-6	8-9 (7-11)	3-4	2-4
Number of membranelles	~55	~70 (70-120)	~45	~50
Distance (gap) from the posterior end of midventral rows to the transverse cirri	~15	no gap	~30	0*~15
Source of data	Song *et al.* (2002)	present work; Hu *et al.* (2004)	present work; Song *et al.* (2004a)	present work; Hu and Song (2001)

* This gap is usually so small as to be essentially absent in most specimens.

tion. Since the details of the infraciliature of each of the four species were reported comparatively recently (Hu and Song 2000, 2001; Song *et al.* 2002, 2004a; Shi and Xu 2003; Hu *et al.* 2004), only those of diagnostic value are highlighted here:

Pseudokeronopsis carnea. This species can be separated from the other three species by having: more cirral pairs in both the bicorona (9-11 *vs.* <7) and the midventral rows (*ca* 40 *vs. ca* 30); more transverse cirri (8-9 *vs.* <6); more dorsal kineties (7-8 *vs.* <7). The number of

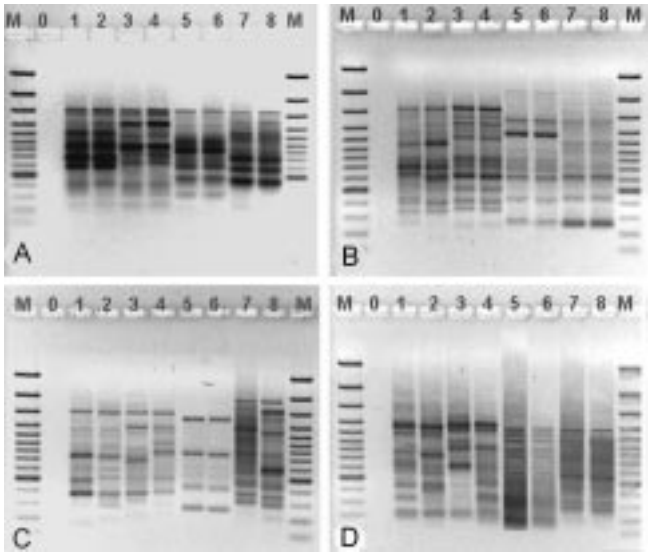

Figs 10 A-D. RAPD banding patterns of three *Pseudokeronopsis* spp. (six strains) using the following oligonucleotide random primers: (**A**) S2001, (**B**) S2006, (**C**) S2007, and (**D**) S2010. M - 100 bp molecular markers; 0 - control without DNA; 1, 2 - *Pseudokeronopsis flava* pop I; 3, 4 - *P. flava* pop II; 5, 6 - *P. rubra*; 7, 8 - *P. carnea.*

adoral membranelles in this organism is also conspicuously higher than in the other three (*ca* 70 *vs.* <60) (Table 3). In addition, the AZM is relatively long compared to the body length (ratio 1:3), and there is almost no gap between the midventral rows and the transverse cirri (Fig. 1F, arrow).

Pseudokeronopsis flava. The most characteristic features in this species are: the large gap between the midventral rows and the transverse cirri, this being the largest in relation to the body length of the four congeners (Figs 1L, M); the comparatively low number of pairs of cirri in the bicorona (4-6); it constantly has three dorsal kineties. In addition, the AZM is relatively less dominant, the bases of the membranelles being comparatively shorter than those of other three species (Figs 1M, N; 5C).

Pseudokeronopsis flavicans. The general pattern of the infraciliature of this species is very similar to that of *P. flava* although the gap between the midventral rows and the transverse cirri is relatively smaller and there are often more cirral pairs in the bicorona (Fig. 6C). Unlike *P. flava*, *P. flavicans* has four (occasionally 5) dorsal kineties.

Pseudokeronopsis rubra. The infraciliature of this species is similar to *P. flava* and *P. flavicans* (Figs 6E, F). Its most distinctive feature is the number of dorsal kineties which varies from 3 (rarely) to 7 (also very rare, including some shortened fragments of kineties), but is normally in the range 4-6 (Table 1). Also noteworthy is the gap between the midventral rows and the transverse cirri which is so small as to be almost absent in most cases (Figs 6E; 8A, D) whereas it can be conspicuously larger in some specimens (Fig. 6L, arrow).

DNA fingerprinting patterns

RAPD band patterns for three species, *P. flava*, *P. rubra* and *P. carnea* (we failed to extract the genomic DNA for *P. flavicans*), are shown in figure 10. The two strains of the same morphospecies are clearly aligned and distinct from the other strains (1 and 2; 3 and 4; 5 and 6; and 7 and 8). Although some bands differ in brightness, analysis of bands showed that the two populations of *P. flava* have >80% bands in common whereas they have only approximately 30% common bands with the strains of *P. rubra* and *P. carnea*.

Synonyms and improved diagnoses

The diagnoses of all four species have been presented in separate publications in recent years (Wirnsberger *et al.* 1987; Hu and Song 2000, 2001; Song *et al.* 2002, 2004a; Hu *et al.* 2004). Wirnsberger *et al.* (1987) listed the synonyms and re-diagnosed three of the four species discussed here, i.e. *Pseudokeronopsis rubra, P. flava* and *P. carnea*, and we completely agree with their findings. Nevertheless, we consider it necessary to provide updated diagnoses based upon a standard set of criteria. Additional information and revised lists of synonyms are also supplied.

Pseudokeronopsis carnea (Cohn, 1866) Wirnsberger, Larsen *et* Uhlig, 1987

Oxytricha flava var. *carnea* Cohn, 1866

Pseudokeronopsis pulchra Borror *et* Wicklow, 1983

Pseudokeronopsis pararubra Hu, Warren *et* Suzuki, 2004

Pseudokeronopsis rubra sensu Shi *et* Xu, 2003

Improved diagnosis. Marine, dark reddish *Pseudokeronopsis*, usually 150-350 µm long *in vivo* with buccal field about 1/3 of body length; pigment granules dark brown-reddish or brick-reddish, arranged in typical *rubra*-pattern; BCS-granules completely circular in shape bicorona comprises 8-12 pairs of frontal cirri. 6-11 transverse cirri and 5-8 dorsal kineties; contractile vacuole positioned in posterior 2/5 to 1/3 of body; almost no gap between midventral rows and transverse cirri.

***Pseudokeronopsis flava* (Cohn, 1866) Wirnsberger, Larsen *et* Uhlig, 1987**

Oxytricha flava Cohn, 1866
Holosticha flavorubra var. *flava* Entz, 1884
Keronopsis flava (Cohn, 1866) Kahl, 1932

Improved diagnosis. Marine yellowish *Pseudokeronopsis*, usually 140-350 µm long *in vivo*; pigment granules dark brown-yellow, arranged in typical *rubra*-pattern; BCS-granules oval in shape; bicorona comprises 5 pairs of frontal cirri. 2-4 transverse cirri; midventral rows terminate conspicuously above the transverse cirri; 3 dorsal kineties; contractile vacuole positioned in posterior 1/4 to 1/6 of body; conspicuous gap between midventral rows and transverse cirri.

***Pseudokeronopsis flavicans* (Kahl, 1932) Borror *et* Wicklow, 1983**

Keronopsis flavicans Kahl, 1932

Improved diagnosis. Yellowish-coloured marine *Pseudokeronopsis*, about 200-300 µm long *in vivo*; pigment granules dark yellow-brown, arranged in typical *rubra*-pattern; BCS-granules oval in shape; bicorona comprising 5-9 pairs of frontal cirri; 3-6 transverse cirri; midventral rows terminate conspicuously above the transverse cirri; 4-5 dorsal kineties; contractile vacuole in anterior 1/3 of body; gap between midventral rows and transverse cirri inconspicuous.

***Pseudokeronopsis rubra* (Ehrenberg, 1838) Borror *et* Wicklow, 1983**

Oxytricha rubra Ehrenberg, 1835
Holosticha rubra Wallengren, 1900
Keronopsis rubra Kahl, 1932

Improved diagnosis. Brown-reddish to orange-yellowish marine *Pseudokeronopsis*, 140-250 µm in length *in vivo*; pigment granules brick-reddish to dark yellow-brown; BCS-granules oval in shape; bicorona with 5-7 pairs of frontal cirri; 2-4 transverse cirri; midventral rows usually terminate conspicuously above the transverse cirri; normally 4-6 dorsal kineties; contractile vacuole in posterior 1/3 of body; gap between midventral rows and transverse cirri variable, very small to conspicuous.

Deposition of the neotypes and voucher material

Neotype specimens of three forms, i.e. *P. flava*, *P. rubra* and *P. carnea*, have been deposited by Wirnsberger *et al.* (1987) in the Upper Austrian Museum in Linz, Austria, while the neotype slide of *P. flavicans* is deposited in the Laboratory of Protozoology, OUC, China (see Song *et al.* 2002). Voucher slides with protargol-impregnated specimens of China-isolates of all four species are deposited in the Natural History Museum, London, UK with the following registration numbers: *Pseudokeronopsis carnea* - one slide was deposited as the holotype of *Pseudokeronopsis pararubra* (misidentification - see Hu *et al.* 2004) - 2004:6:2:1, and a second as a voucher slide - 2005:3:24:10. *Pseudokeronopsis flava* - 2005:3:24:9. *Pseudokeronopsis flavicans* - 2001:12:28:3. *Pseudokeronopsis rubra* - 2005:3:24:11.

Key to the four morphologically similar *Pseudokeronopsis* spp.

1 Contractile vacuole positioned in anterior part of the cell.....*Pseudokeronopsis flavicans*
1' Contractile vacuole positioned in posterior part of the cell.....2
2 Blood-cell-shaped cortical granules completely round in shape; 8-9 transverse cirri; 8-12 pairs of cirri in bicorona.....*Pseudokeronopsis carnea*
2' Blood-cell-shaped cortical granules oval in shape; 5 transverse cirri; <8 pairs of cirri in bicorona.....3
3 Cell brown- to brick-reddish; 4-6 dorsal kineties; midventral rows not conspicuously shortened posteriad.. .....*Pseudokeronopsis rubra*
3' Cell yellowish; constantly 3 dorsal kineties; midventral rows conspicuously shortened posteriad..... .....*Pseudokeronopsis flava*

Conclusions

With reference to the data relating to the infraciliature, the four marine, coloured, *Pseudokeronopsis* spp. discussed here are difficult to identify. Consequently, a revised list of reliable and informative characters for species circumscription and separation is supplied, which are mostly obtained from live observations. These are: (1) position of the contractile vacuole; (2) shape of BCS-granules; (3) colour of cell and pigments; (4) number of dorsal kineties; (5) number of transverse cirri; (6) the number of pairs of frontal cirri in the bicorona, and (7) the gap between the midventral rows and the transverse cirri.

It is noteworthy that in their excellent work, Wirnsberger *et al.* (1987) reached similar conclusions and could distinguish three species, i.e. *Pseudokeronopsis rubra*, *P. flava* and *P. carnea*, by chromatography of the pigments. Likewise, as shown

here, the RAPD banding patterns demonstrate that the species separated by morphology are also clearly distinct genomically. By contrast, as revealed by both previous and the present studies, the infraciliature in all these four morphotypes is generally stable within populations but may show significant differences between populations, especially among those that are geographically well separated. Therefore care should be taken when using such characters for species identification.

Acknowledgements. This work was supported by 'The Natural Science Foundation of China' (Project No. 30430090), the Darwin Initiative Programme through funding from the Department for Environment, Food and Rural Affairs (DEFRA), UK (Project No. 14-015), and the DFG (Germany).

REFERENCES

Borror A. C. (1972) Revision of the order Hypotrichida (Ciliophora, Protozoa). *J. Protozool.* **19:** 1-23

Borror A. C., Wicklow B. J. (1983) The suborder Urostylina, Jankowski (Ciliophora, Hypotrichida): morphology, systematics and identification of species. *Acta Protozool.* **22:** 97-126

Chen Z., Song W., Warren A. (2000) Studies on six *Euplotes* spp. (Ciliophora: Hypotrichida) using RAPD fingerprinting, including a comparison with morphological analysis. *Acta Protozool.* **39:** 209-216

Cohn F. (1866) Neue Infusorien im Seeaquarium. *Z. Wiss. Zool.* **16:** 253-302

Entz G. (1884) Über Infusorien des Golfes von Neapel. *Mitteil. Zool. Stat., Neapel Berlin* **5:** 289-444

Foissner W. (1984) Infraciliatur, Silberliniensystem und Biometrie einiger neuer und wenig bekannter terrestrischer, limnischer und mariner Ciliaten (Protozoa: Ciliophora) aus den Klassen Kinetofragminophora, Colpoda und Polyhymenophora. *Stapfia* **12:** 1-165

Hu X., Song W. (2000) Infraciliature of *Pseudokeronopsis qingdaoensis* sp. nov. from marine biotope (Ciliophora: Hypotrichida). *Acta Zootax. Sin.* **25:** 361-364 (in Chinese with English summary)

Hu X., Song W. (2001) Morphological redescription and morphogenesis of the marine ciliate, *Pseudokeronopsis rubra* (Ciliophora: Hypotrichida). *Acta Protozool.* **40:** 107-115

Hu X., Warren A., Suzuki T. (2004) Morphology and morphogenesis of two marine ciliates, *Pseudokeronopsis pararubra* n. sp. and *Amphisiella annulata* from China and Japan (Protozoa, Ciliophora). *Acta Protozool.* **43:** 351-368

Jerka-Dziadosz M., Janus I. (1972) Localization of primordia during cortical development in *Keronopsis rubra* (Ehrbg., 1838) (Hypotrichida). *Acta Protozool.* **10:** 249-262

Kahl A. (1932) Urtiere oder Protozoa I: Wimpertiere oder Ciliata (Infusoria). *Tierwelt Dtl.* **25:** 399-650

Ruthmann A. (1972) Division and formation of the macronuclei of *Keronopsis rubra*. *J. Protozool.* **19:** 661-666

Shi X., Xu R. (2003) Morphology and infraciliature of *Pseudokeronopsis rubra* in Jieshi waters of south China sea. *J. Trop. Ocean.* **22:** 23-30 (in Chinese with English summary)

Song W., Wilbert N., Warren A. (2002) New contribution to the morphology and taxonomy of four marine hypotrichous ciliates from Qingdao, China (Protozoa: Ciliophora). *Acta Protozool.* **41:** 145-162

Song W., Sun P., Ji D. (2004a) Redefinition of the yellow hypotrichous ciliate, *Pseudokeronopsis flava* (Cohn, 1866) Wirnsberger, Larsen & Uhlig, 1987 (Hypotrichida, Ciliophora). *J. Mar. Biol. Ass. U. K.* **84:** 1137-1142

Song W., Wilbert N., Hu X. (2004b) New contributions to the marine hypotrichous ciliate, *Pseudokeronopsis qingdaoensis* Hu & Song, 2000 (Protozoa, Ciliophora, Stichotrichida). *Cah. Biol. Mar.* **45:** 335-342

Sun P., Song W. (2005) Morphogenesis of the marine ciliate *Pseudokeronopsis flava* (Cohn, 1866) Wirnsberger E., Larsen H. F. *et*. Uhlig G., 1987 (Protozoa: Ciliophora: Hypotrichia). *Acta Zool. Sin.* **51:** 81-88 (in Chinese with English summary)

Wanick R. C., Silva-Neto I. D. (2004) Benthic ciliates from Sepetiba Bay (Rio de Janeiro, Brazil) with description of *Pseudokeronopsis sepetibensis* n. sp. (Spirotrichea: Urostylida). *Zootaxa* **587:** 1-11

Wilbert N. (1975) Eine verbesserte Technik der Protargolimprägnation für Ciliaten. *Mikrokosmos* **64:** 171-179

Wirnsberger E., Larsen H. F., Uhlig G. (1987) Rediagnoses of closely related pigmented marine species of the genus *Pseudokeronopsis* (Ciliophora, Hypotrichida). *Europ. J. Protistol.* **23:** 76-88

Received on 17th January, 2006; revised version on 28th February, 2006; accepted on 6th May, 2006

Acta Protozool. (2006) 45: 289 - 294

ACTA
PROTOZOOLOGICA

Trichodina haldari n. sp. and *Paratrichodina bassonae* n. sp. (Ciliophora: Peritrichida) from Indian Fresh Water Fishes

Amlan Kumar MITRA[1] and Probir K. BANDYOPADHYAY[2]

Parasitology Laboratory, Department of Zoology, University of Kalyani, Kalyani West Bengal, India

Summary. One new species of the genus *Trichodina* Ehrenberg, 1838 was obtained from the Churni River system of Nadia district and one new species of the genus *Paratrichodina* Lom, 1963 was obtained from the Ichamati river system of North 24 Parganas. These are *T. haldari* n. sp. from *Glossogobius giuris* (Hamilton-Buchanan) and *P. bassonae* n. sp. from *Mystus cavasius* (Hamilton-Buchanan). *T. haldari* n. sp. is characterized by large and dark central area, broad blade, robust central part, well developed and straight rays without any ray apophysis. *P. bassonae* n. sp. is unique in its class in having granular central area, crooked blades and delicate rays. This paper deals with taxonomic descriptions of the two new species based on Klein's dry silver nitrate technique along with prevalence and morphometric comparisons with closely related species.

Key words: Ciliophora, fish parasite, India, *Paratrichodina bassonae* n. sp., *Trichodina haldari* n. sp., Trichodinidae.

INTRODUCTION

Trichodinid ciliophorans parasitize or are symbionts of aquatic invertebrate and vertebrate hosts (Van As and Basson 1989). Work on this particular group in India gained momentum since 1980 although Annandale (1912) was the first who reported the occurrence of *Trichodina pediculus* Ehrenberg, 1838 from the lymnocnidid medusa, *Lymnocnida indica* in Bombay Presidency of British India. In India, the main focus has always been on describing new species, and as a result twelve new species belonging to the genus *Trichodina* Ehrenberg, 1838 and *Paratrichodina* Lom, 1963 have been described so far (Asmat and Haldar 1998; Asmat 2000, 2001a, b, c; 2002a, b; Mitra and Haldar 2004, 2005). As part of an attempt to explore the biodiversity of trichodinid ciliophorans in West Bengal, an icthyoparasitological survey was conducted in the river Churni and Ichamati and two new species of trichodinid ciliophorans belonging to the genus *Trichodina* and *Paratrichodina* were obtained. These are *T. haldari* n. sp. obtained from the gills of *Glossogobius giuris* (Hamilton-Buchanan) and *P. bassonae* n. sp. found to be associated with the gills of *Mystus cavasius* (Hamilton-Buchanan). The present paper deals with descriptions of these two new species based on Klein's dry silver nitrate

Address for correspondence: Probir K. Bandyopadhyay, Parasitology Laboratory, Department of Zoology, University of Kalyani, Kalyani 741235, West Bengal, India; E-mail: [1]amlan_mitra@hotmail.com, [2]prabir0432@hotmail.com

impregnation technique along with taxonomy, prevalence and comparisons with closely related species.

MATERIALS AND METHODS

Churni is one of the many tributaries of the river Ganges and flows through the district of Nadia in West Bengal (23°E, 88.5°W). It is a small and docile river and provides a complete fresh water environment. River Ichamati flows through the district of North 24 Parganas (22.1°N, 89.5°E) and also provides a freshwater habitat to the host fishes. Samplings were carried out to collect host fishes from both the rivers and adjacent water bodies. Live fishes were brought to the laboratory and gill and skin smears were made on grease free slides. Slides containing trichodinid ciliophorans were impregnated using Klein's dry silver impregnation technique (Klein 1958). Examinations of preparations were made under an Olympus phase contrast microscope at × 100 magnifications with an oil immersion lens and photographs were taken with an Olympus camera. All measurements are in micrometers (µm) and follow the uniform specific characteristics as proposed by Lom (1958), Wellborn (1967) and Arthur and Lom (1984). In each case minimum and maximum values are given, followed in parentheses by the arithmetic mean and standard deviation. In the case of denticles and radial pins, the mode is given instead of the arithmetic mean. The span of the denticle is measured from the tip of the blade to the tip of the ray. Body diameter is measured as the adhesive disc plus border membrane. The description of denticle elements follows the guidelines of Van As and Basson (1989). The sequence and method of the description of denticle elements follows the recommendations of Van As and Basson (1992).

RESULTS AND DISCUSSION

Trichodina haldari n. sp. (Figs 1-4, 9; Table 1)

Medium sized trichodinid. Denticle consisting of broad blade. Distal surface of blade rounded. Tangent point flat, like small line rather than point and situated lower than distal surface. Anterior surface sloping down backward to form distinct apex, never reaches or extends beyond y+1 axis. Blade apophysis not visible. Anterior and posterior surfaces of blade almost parallel. Deepest point of curve formed by posterior margin of blade remains at same level as apex. Blade connection thick. Central part robust, elongated, tapering to a rounded end, fitting tightly into preceding denticle and extends almost halfway to y-1 axis. Sections of central part above and below x axis similar. Indentation in lower half of central part not visible. Ray well developed. Ray apophysis absent. Width of ray almost same along entire length, that tapers to rounded end. Rays directed towards geometric centre of adhesive disc. Macronucleus horse-shoe shaped but micronucleus could not be detected. Adoral ciliary spiral makes a turn of 390-400°.

Taxonomic summary

Type host: *Glossogobius giuris* (Hamilton-Buchanan)

Fish family: Gobiidae

Type locality: Ranaghat, W. Bengal, India

Location: Gills

Prevalence: 05/17 (29.4 %)

Etymology: The specific epithet "*haldari*" is given after the name of Prof. Durga P. Haldar, Retired Professor of Department of Zoology, University of Kalyani, Kalyani 741235, West Bengal, India for his outstanding contribution in the taxonomy and systematics of trichodinid ciliophorans.

Reference material: Holotype, slide GG-1/2004, and paratype slides GG-2/2004, GG-4/2004, GG- 5/2004 are deposited in the Museum of the Department of Zoology, University of Kalyani, Kalyani 741235, West Bengal, India

Remarks

The present trichodinid species resembles a freshwater *Trichodina, T. porocephalusi* Asmat, 2001. Asmat (2001c) reported *T. porocephalusi* from an Indian flathead sleeper, *Ophiocara porocephalus* (Valenciennes) (Eleotrididae). The new species mainly differs from the *T. porocephalusi* in not having a clear central area. The shape of the denticle is also different in the two species. In *T. porocephalusi* a notch is present just below the apical cone in the anterior margin. Any type of notch is absent in the anterior margin of the blade of *T. haldari*. The central part of the denticle of *T. porocehalusi* is sharply triangular, which is almost conical in case of the new species. A ray apophysis is present in *T. porocephalusi,* which is completely absent in the new species. The ray of *T. porocephalusi* is stumpy, and slightly bent backward, while the ray of the new species is straight and the width is the same along the entire length. The rays of *T. porocephalusi* is directed slightly posteriorly, but the rays are directed towards the geometric centre of the adhesive disc in *T. haldari*.

Paratrichodina bassonae n. sp. (Figs 5-8, 10; Table 2)

Small sized trichodinid. Central area granular, consisting of several small whitish spots, slightly elevated off from rest of central area. The denticulate ring consists

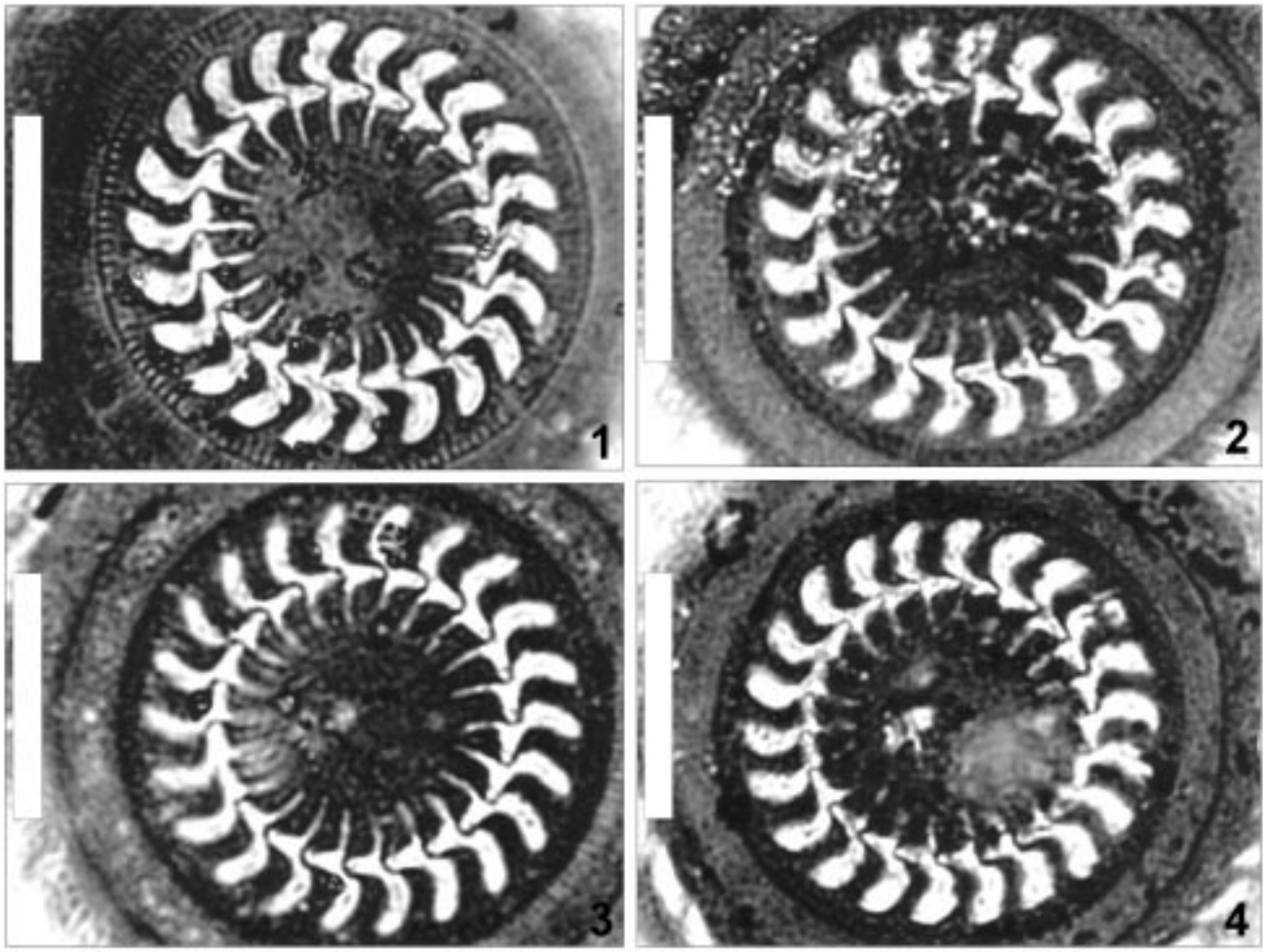

Figs 1-4. Photomicrographs of silver nitrate impregnated adhesive discs of *Trichodina haldari* n. sp. obtained from the gills of *Glossogobius giuris* (Hamilton-Buchanan). Scale bars: 20 µm.

of loosely arranged denticles. Blade broad, crooked. Distal margin of blade rounded, remains in close proximity and almost parallel to border membrane. Tangent point like a point, situated almost at same level or slightly lower than distal point of distal surface. Anterior margin slopes down gradually to form conspicuous apex, which in most cases extends beyond y+1 axis. Deepest point of curve formed by posterior margin of blade is lower than the apex. Blade connection thick. Central part delicate, triangular, tip of which bluntly rounded, fits loosely into preceding denticle. Sections above and below x axis similar in shape. Ray apophysis absent. Ray connection broad. Rays short after tapering rapidly to bluntly rounded end. Rays directed slightly towards y-1 axis. Macronucleus horseshoe-shaped. Micronucleus could not be detected. Adoral ciliary spiral makes a turn of about 230°.

Taxonomic summary

Type host: *Mystus cavasius* (Hamilton-Buchanan)

Fish family: Bagridae

Type locality: North 24 Parganas (22.1°N, 89.5°E), W. Bengal,India

Location: Gills

Prevalence: 14/26 (53.8 %)

Etymology: The specific epithet "*bassonae*" is given after the name of Prof. Linda Basson, Department of Zoology and Entomology, University of Free State, South

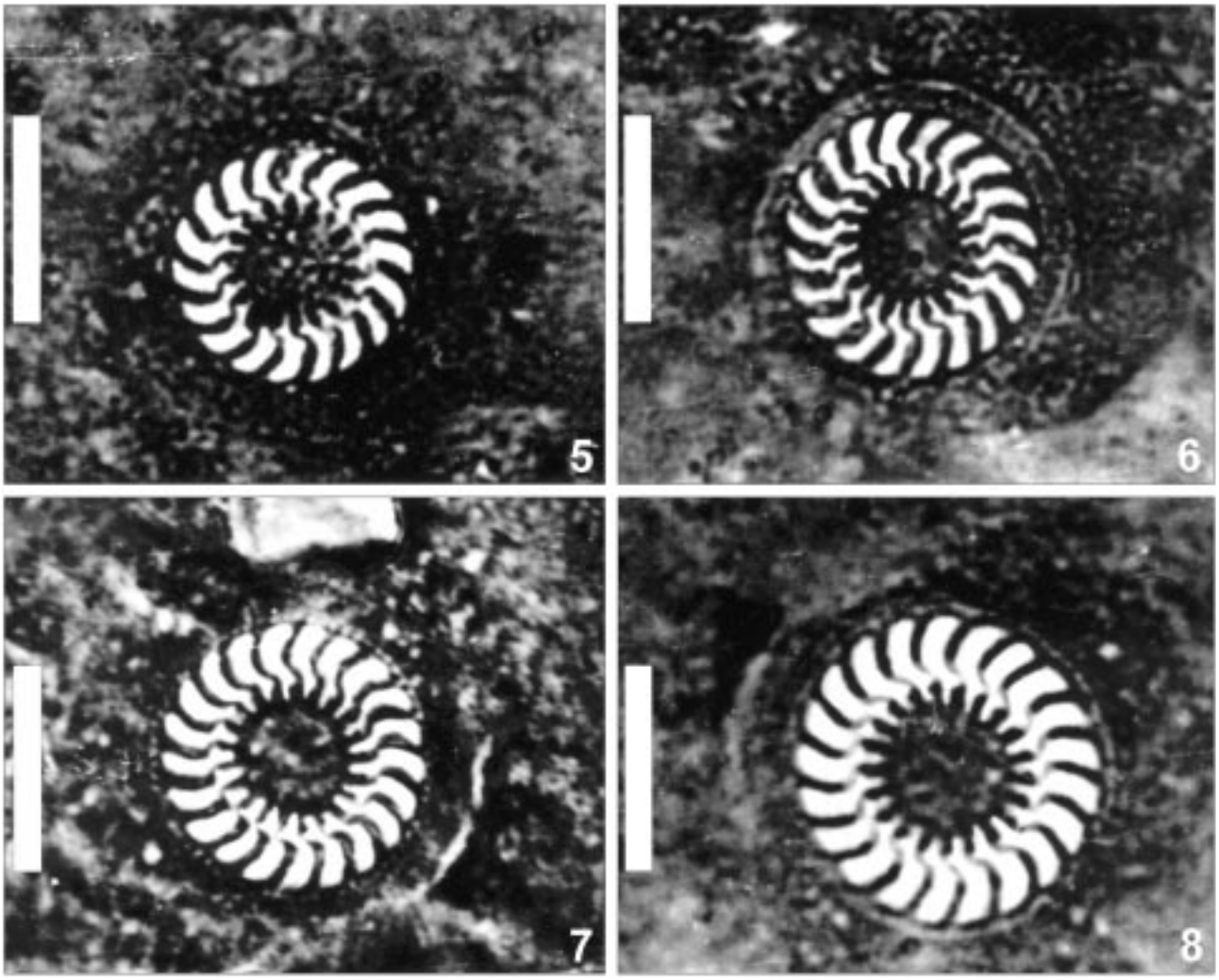

Figs 5-8. Photomicrographs of silver nitrate impregnated adhesive discs of *Paratrichodina bassonae* n. sp. obtained from the gills of *Mystus cavasius* (Hamilton-Buchanan). Scale bars: 10 µm.

Africa in recognition for her outstanding contribution in the field of taxonomy and systematics of trichodinid ciliophorans.

Reference material: Holotype, slide MC-6/2003, and paratype slide MC-2/2003, MC-5/2003, MC-8/2003 are deposited in the Museum of the Department of Zoology, University of Kalyani, Kalyani 741235, West Bengal, India.

Remarks

The *Paratrichodina* species, obtained in the present study from the gills of *Mystus cavasius* (Hamilton-Buchanan) in the river Ichamati only resembles a fresh-water species, *P. corlissi* Lom *et* Haldar, 1977 when denticle morphology is taken into consideration. The new species under discussion resembles *P. corlissi* (Lom and Haldar 1977) in not having a distinct blade apophysis, otherwise the shape of the denticles and morphometric data are different. The central area of the adhesive disc of *P. corlissi* does not have any granules, but the central area of the new *Paratrichodina* species consists of several small, whitish granules scattered throughout the area. In *P. corlissi* the blade becomes slightly wider towards the distal margin. But in the new species, the width is almost the same along the entire length and somewhat crooked. In *P. corlissi* the tangent point is like

Table 1. Morphometric comparison of *Trichodina haldari* n. sp. with *T. porocephalusi* Asmat, 2001. Measurements in µm.

Species	*T. haldari* n. sp. (n = 17)	*T. porocephalusi* (n = 20)
Host fish	*Glossogobius giuris*	*Ophiocara porocephalus*
Locality	India	India
Location	gills	gills
Reference	present study	Asmat (2001c)
Diameter of		
body	40.0-55.0 (51.2 ± 5.3)	32.5-50.5 (42.3 ± 5.2)
adhesive disc	34.5-45.0 (40.1 ± 1.9)	27.0-42.3 (35.2 ± 35.2-4.8)
Dimension of body		
denticulate ring	18.0-24.3 (20.2 ± 1.7)	16.3-26.0 (20.9 ± 2.8)
central area	6.9-18.9 (15.4 ± 1.3)	7.1-17.4 (12.4 ± 2.6)
clear area	-	6.1-15.3 (10.4 ± 2.5)
Width of border membrane	2.6-3.5 (2.8 ± 0.5)	2.0-4.8 (3.5 ± 0.7)
Number of		
denticles	20-22 (21)	20-27 (24.3 ± 1.5)
radial pins/denticle	5-7 (6)	6-9 (7.4 ± 1.0)
Dimension of denticle		
span	8.8-11.0 (8.9 ± 0.7)	8.2-10.7 (9.7 ± 0.7)
length	5.1-6.2 (5.6 ± 0.7)	2.5-5.6 (4.7 ± 0.8)
Dimension of denticle components		
length of ray	2.8-3.2 (2.9 ± 0.6)	2.5-4.1 (3.0 ± 0.5)
length of blade	3.5-4.5 (4.1 ± 0.4)	3.1-5.1 (4.2 ± 0.6)
width of central part	1.5-2.2 (1.9 ± 0.3)	1.5-3.1 (2.5 ± 0.6)
Adoral ciliary spiral	390-400°	380-390°

n = number of specimens measured

Table 2. Morphometric comparison of *Paratrichodina bassonae* n. sp. with *P. corlissi* Lom *et* Haldar, 1977. Measurements in µm.

Species	*P. bassonae* n. sp. (n = 30)	*P. corlissi*
Host fish	*Mystus cavasius*	*Gobio kessleri*
Locality	India	Bulgaria
Location	gills	gills
Reference	present study	Lom and Haldar (1977)
Diameter of		
body	14.8-19.3 (17.1 ± 1.2)	33 (27-39)
adhesive disc	11.2-14.8 (13.4 ± 3.2)	22 (19-25)
Dimension of body		
denticulate ring	12.2–24.5 (19.0 ± 4.6)	12 (10-15)
central area	3.6-7.5 (5.4 ± 1.3)	-
Width of border membrane	1.8-2.5 (2.2 ± 0.6)	1.8-2.2
Number of		
denticles	18-21 (20)	21 (18-24)
radial pins/denticle	3-5 (4.0 ± 0.5)	6 (5)
Dimension of denticle		
span	3.3-6.6 (5.4 ± 0.8)	-
length	1.9-2.3 (2.0 ± 0.1)	-
Dimension of denticle components		
length of ray	1.1-1.9 (1.8 ± 0.3)	2.2-3.3
length of blade	1.7-3.5 (2.7 ± 1.1)	3.3-3.8
width of central part	0.5-1.2 (0.9 ± 1.7)	1-2
Adoral ciliary spiral	170-230°	180-240°

n = number of specimens measured

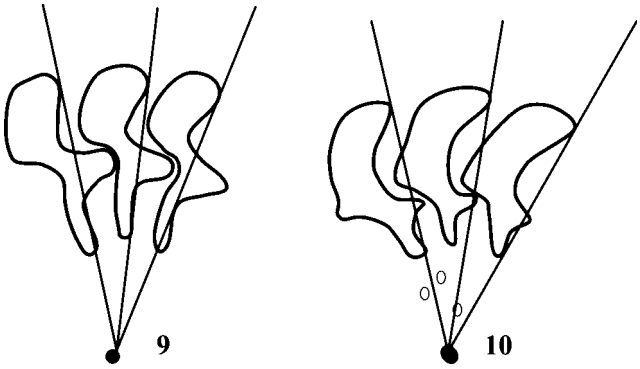

Figs 9, 10. Diagrammatic drawings of the denticles of trichodinid ciliophorans. **9** - *Trichodina haldari* n. sp. obtained from the gills of *Glossogobius giuris* (Hamilton-Buchanan); **10** - *Paratrichodina bassonae* n. sp. obtained from the gills of *Mystus cavasius* (Hamilton-Buchanan).

a small straight line, which is almost a point rather than a line in case of the new species. The rays are also different in both the species. In *P. corlissi* the width of the rays are almost the same along the entire length. But in case of the new species described from *Mystus cavasius* (Hamilton-Buchanan) the rays rapidly taper to rounded ends. Morphometic data of the new species also varies when it is compared with that of *P. corlissi*. *P. bassonae* is comparatively a small sized ciliophoran (Table 2).

REFERENCES

Annandale N. (1912) Preliminary description of a freshwater medusa from the Bombay Presidency. *Rec. Ind. Mus.* **7:** 235-256

Arthur J. R., Lom J. (1984) Trichodinid Protozoa (Ciliophora: Peritrichida) from freshwater fishes of Rybinsk Reservoir, USSR. *J. Protozool.* **31:** 82-91

Asmat G. S. M. (2000) *Trichodina cuchiae* sp. n. (Ciliophora: Trichodinidae) from Gangetic mudeel, *Monopterus cuchia* (Hamilton-Buchanan, 1822) (Synbranchiformes: Synbranchidae) in India. *The Chittagong Univ. J. Sc.* **24:** 55-61

Asmat G. S. M. (2001a) *Trichodina cancilae* sp. n. (Mobilina: Trichodinidae) from the Gills of a Freshwater Gar, *Xenentodon cancila* (Hamilton) (Belonidae). *Acta Protozool.* **40:** 141-146

Asmat G. S. M. (2001b) *Trichodina canningensis* sp. n. (Ciliophora: Trichodinidae) from an Indian estuarine fish, *Mystus gulio* (Hamilton) (Bagridae). *Acta Protozool.* **40:** 147-151

Asmat G. S. M. (2001c) *Trichodina porocephalusi* sp. n. (Ciliophora: Trichodinidae) from an Indian flathead sleeper, *Ophiocara porocephalus* (Valenciennes) (Eleotrididae). *Acta Protozool.* **40:** 297-301

Asmat G. S. M (2002a) Trichodinid ciliates (Ciliophora: Trichodinidae) from Indian fishes with description of two new species. *Bangladesh J. Zool.* **30:** 87-100

Asmat G. S. M. (2002b) Two new species of trichodinid ciliates (Ciliophora: Trichodinidae) from Indian fishes. *Univ. J. Zool. Rajshahi Univ.* **21:** 31-34

Asmat G. S. M., Haldar D. P. (1998) *Trichodina mystusi*- a new species of trichodinid ciliophoran from Indian estuarine fish, *Mystus gulio* (Hamilton). *Acta Protozool.* **37:** 173-177

Klein B. M. (1958) The dry silver method and its proper use. *J. Protozool.* **5:** 99-103

Lom J. (1958) A contribution to the systematics and morphology of endoparasitic trichodinids from amphibians with proposal of uniform specific characteristics. *J. Protozool.* **5:** 251-263

Lom J., Haldar D.P. (1977) Ciliates of the genera *Trichodinella*, *Tripartiella* and *Paratrichodina* (Peritricha, Mobilina) invading fish gills. *Folia Parasitol.* **24:** 193-210

Mitra A. K., Haldar D. P. (2004) First Record of *Trichodinella epizootica* (Raabe, 1950) Šramek-Hušek, 1953, with Description of *Trichodina notopteridae* sp. n. (Ciliophora: Peritrichida) from freshwater fishes of India. *Acta Protozool.* **43:** 269-274

Mitra A. K., Haldar D. P. (2005) Descriptions of two new species of the genus *Trichodina* Ehrenberg, 1838 (Protozoa: Ciliophora: Peritrichida) from Indian fresh water fishes. *Acta Protozool.* **44:** 159-165

Van As J. G., Basson L. (1989) A further contribution to the taxonomy of Trichodinidae (Ciliophora: Peritrichida) and a review of the taxonomic status of some ectoparasitic trichodinids. *Syst. Parasitol.* **14:** 157-179

Van As J. G., Basson L. (1992) Trichodinid ectoparasites (Ciliophora: Peritrichida) of freshwater fishes of the Zambesi River System, with a reappraisal of host specificity. *Syst. Parasitol.* **22:** 81-109

Wellborn T. L. Jr. (1967) *Trichodina* (Ciliata: Urceolariidae) of freshwater fishes of the southeastern United States. *J. Protozool.* **14:** 399-412

Received on 20th September, 2005; revised version on 29th March, 2006; accepted on 4th May, 2006

Acta Protozool. (2006) 45: 295 - 299

ACTA
PROTOZOOLOGICA

Cryptodifflugia leachi n. sp., a Minute New Testate Rhizopod Species (Rhizopoda: Phryganellina)

Kenneth H. NICHOLLS

S-15 Concession 1, RR # 1 Sunderland, Ontario, Canada

Summary. A previously undescribed, very small species of *Cryptodifflugia* has been discovered in a calcareous wetland on the Niagara Escarpment, a significant geologic feature in southern Ontario, Canada. *Cryptodifflugia leachi* n. sp. is characterized by its very small size, elliptical outline in optical cross-section (contrasting it with the similarly-sized *C. minuta* Playfair, which is strongly narrowed in the anterior pseudostomal region) and the presence of crystalline inclusions in the anterior region of the cell. The abundance of specimens in the collection afforded study of both living and encysted specimens.

Key words: *Cryptodifflugia*, *Difflugiella*, testate amoebae.

INTRODUCTION

The genus *Cryptodifflugia* [sensu Page (1966) and Hedley *et al*. (1977)] includes some 20 species of amoeboid protists housed in mostly small (< 30 µm long), smooth-walled tests. Until now, the smallest known species of *Cryptodifflugia* have included three species described by Playfair (1918) from Australia having test lengths in the range of 10-14 µm, a size that is similar to that found for *C. leachi*, the new species described here. The cylindrical, flask-shaped or angular shapes of the tests of those three Australian species are, however, in marked contrast to the smooth elliptical-ovoid shape described here for *C. leachi*. Although test size and shape are the most important criteria for distinguishing species of this genus [see also Beyens and Chardez (1982) and Bobrov (2001) for accounts of more recently described species of *Cryptodifflugia*], other details of the live cell of *C. leachi*, notably pseudopod structure and behaviour, encystment structures and crystalline inclusion bodies have also been documented for this new species.

MATERIALS AND METHODS

Samples were collected from an extensive wetland complex at the base of limestone cliffs forming part of the Niagara Escarpment in an area known locally as “The Glen”, located 10 km NNW of the City of

Address for correspondence: Kenneth H. Nicholls, S-15 Concession 1, RR # 1 Sunderland, Ontario, Canada L0C 1H0; E-mail: khnicholls@interhop.net

Owen Sound, Ontario, Canada (44°35'50''W; 80°55'50''N). Three samples of bottom sediments were collected by submerging wide-mouthed 500 ml polycarbonate bottles in the shallow water (<0.5 m depth) along the eastern edge of The Glen. These samples were combined into a single sample consisting of about 20-50 ml of loose organic sediment and about 400 ml of water. Samples were returned to the laboratory and examined periodically over the ensuing several days and weeks.

Subsamples of the collections, consisting of several drops of the sediment suspension placed on a 23 × 50 mm No. 1 cover glass, were examined with an inverted microscope. Measurements of tests were made with a ×100 oil immersion objective and a ×10 WF relay lense in the camera port, utilizing a pre-calibrated transparent ruler applied to the LCD monitor of the digital camera. Application of the 4 × digital zoom feature of the camera afforded a view of the image in the camera LCD with a magnification of about 3100×, from which the measurements were attained. For permanent slide preparations, including a specimen selected as the type of the new species described here as *Cryptodifflugia leachi* n. sp., isolations were made with a single hair brush and a micropipette drawn out in a flame to a working apex of about 100 µm ID. Specimens were air dried on No. 1 cover glasses and cemented to glass microscope slides with Canada Balsam.

RESULTS

Cryptodifflugia leachi n. sp., Figs 1-14

Phylum: Rhizopoda, Class: Lobosea, Suborder: Phryganellina, Family: Cryptodifflugiidae.

Diagnosis: Cell with a centrally located nucleus about 4 µm in diameter and a single nucleolus 1.5 µm in diameter; a single contractile vacuole, 2-3 µm diameter, is located in the posterior region of the cell, surrounded by many small refractive granules and particles. Many cells also contain one or two large (up to 4 µm) crystalline inclusions in an anterio-central position. Pseudopodia (1-3) long, straight and narrow, emanating from a thick-walled, transparent test. Tests with a smooth surface and an oval-elliptical shape in optical cross-section; 10-16 µm long by 8-12 µm wide, with a pseudostomal aperture 1.5-2.5 µm in diameter.

Etymology: The specific epithet (*leachi*) is in honour of Dr. J. H. Leach, who introduced me to the genus *Difflugia* in Lake Erie in 1970 - an exposure to testate rhizopods that only recently has developed into an important research interest.

Type specimen: The type specimen mounted in Canada Balsam on a # 1 cover glass and standard microscope slide, was deposited with the Invertebrate Zoology Division, Canadian Museum of Nature (Ottawa, Ontario, Canada), Catalogue No. CMNI-2006-0011.

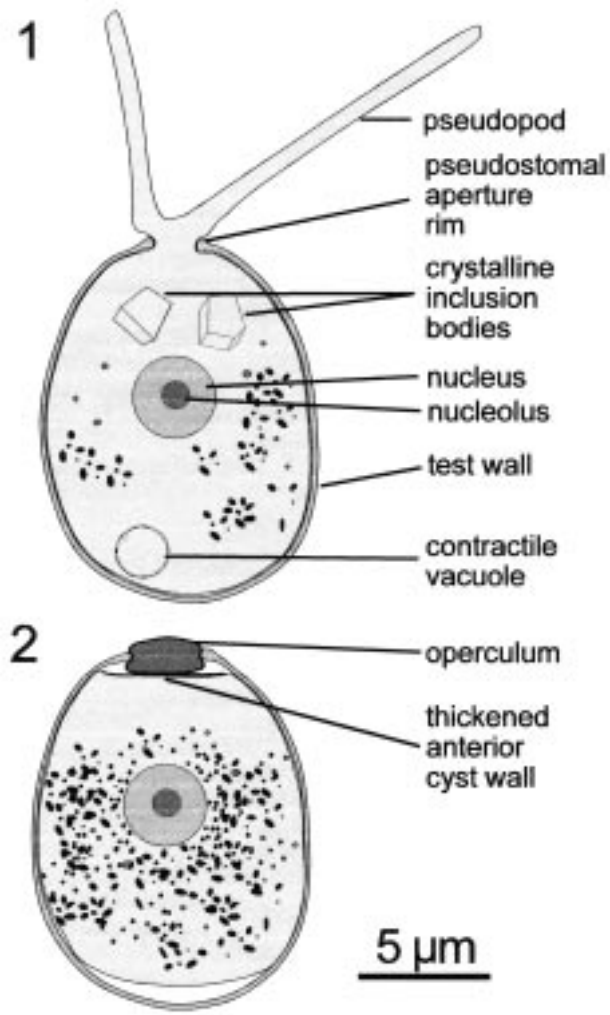

Figs 1, 2. Diagrammatic representations of *Cryptodifflugia leachi* n. sp. **1** - a free-living (non-encysted) cell housed in rigid thick-walled test with main cell components labelled. **2** - encysted cell showing the operculum and the thickened cyst wall.

Material from type locality: A preserved sample of aqueous sediment containing specimens of *C. leachi* collected May 25, 2002 was retained by the author as sample No. V-1919.

Type locality: An extensive wetland at the base of the Niagara Escarpment, an area known locally as "The Glen", 10 km NNW of the City of Owen Sound, Ontario, Canada (44°35'50"W; 80°55'50"N).

With median test length, width and pseudostomal diameter of only 13, 10 and 2 µm, respectively (Table 1), *C. leachi* ranks among the smallest of the testate amoebae. Other distinctive features of living specimens include the narrow, cylindrical pseudopodia, which were

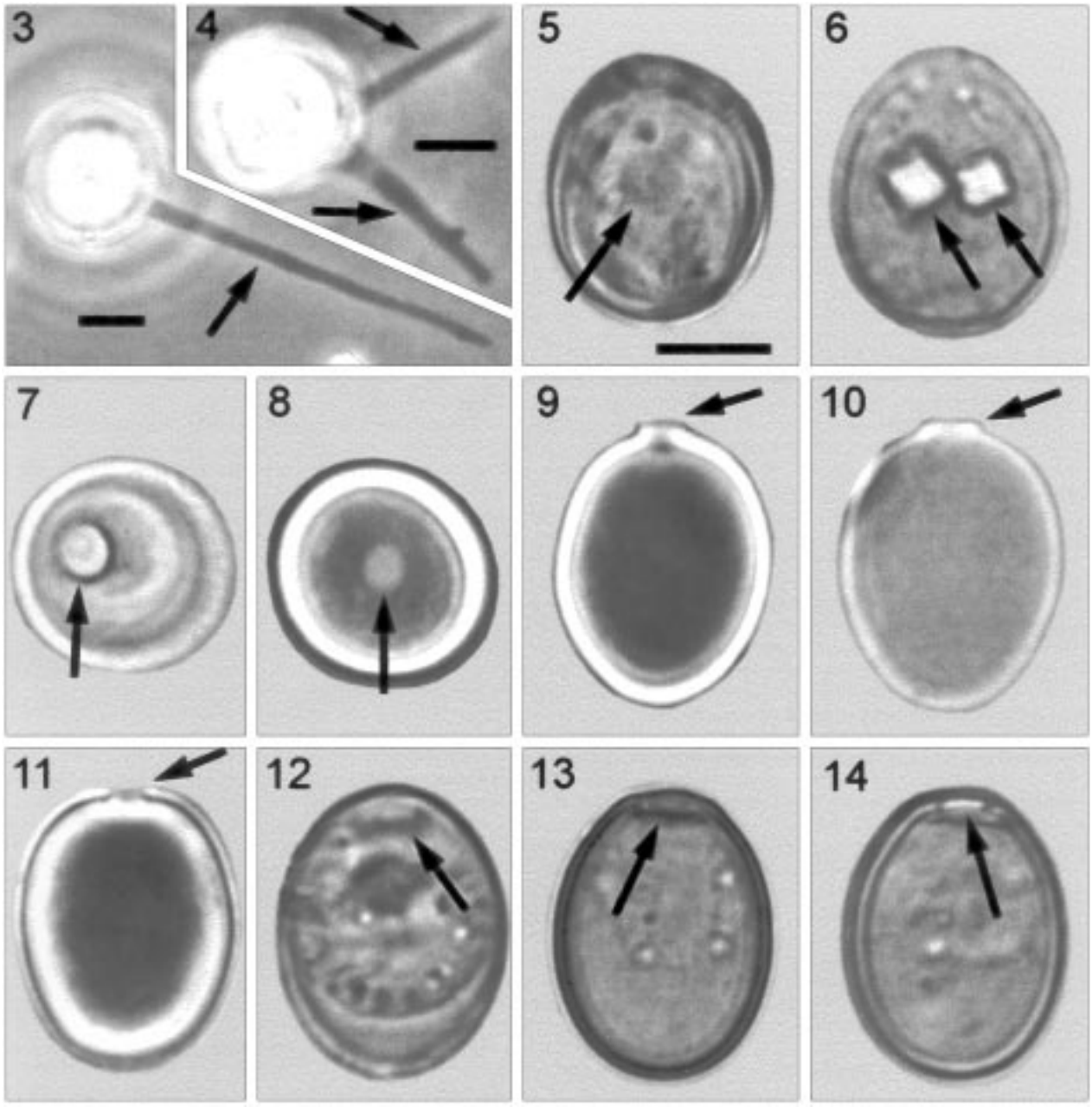

Figs 3-14. Digital images of *Cryptodifflugia leachi* n. sp. **3, 4** - living cells showing pseudopodia (arrows); **5** - cell within test showing anterio-central location of the nucleus (arrow). **6** - cell within test showing presence of two large crystalline inclusions (arrows). **7, 8** - polar views of tests showing the pseudostomal aperture (arrow). **9, 10** - two specimens with a slightly raised rim surrounding the oral aperture (arrow). **11** -laterval view of a test lacking apertural rim (arrow). **12** - early development of the anterior cyst wall (arrow). **13** - later development of anterior cyst wall (arrow) and operculum in pseudostomal aperture. **14** - operculum (arrow). Scale bars: 5 µm.

never observed with major branching, but sometimes with small "buds". Pseudopodia with rounded terminal apices extended up to 3-times the test length (Figs 1, 3, 4). Present also were one or two large refractive crystal-like bodies in the anterior region of many cells (Figs 1, 6). The thick-walled test was generally elliptical in optical cross-section (Figs 6, 10, 13) with a small pseudostomal aperture, 1-2.5 µm in diameter (Figs 7, 8,

Table 1. Test size in *Cryptodifflugia leachi* n. sp.

	median	minimum	maximum	mean	SD	CV (%)
Total test length	13	10	16	13.1	1.4	11.1
Test diameter at the widest part of the test	10	8	12	10	1.1	10.6
Internal diameter of the oral aperture	2	1	2.5	1.8	0.6	30.2

All measurements in µm, n = 28, SD - standard deviation, CV - coeficient variation.

11). In some specimens the aperture was bordered by a slightly raised rim (Figs 9, 10); in others this rim was lacking (Fig. 11). Encysted forms were easily identified by the simultaneous development of a thickened plug, or operculum, in the pseudostomal aperture and a thickening of the anterior cell membrane posterior to the operculum (Figs 2, 12-14).

DISCUSSION

The small size of *C. leachi* n. sp. sets this species apart from most other known species. A comparison with *C. oviformis* Penard in particular is useful because of its common and cosmopolitan occurrence. Hedley *et al*. (1977) reviewed the taxonomy and biology of the genus *Cryptodifflugia* and concluded that Page's (1966) *C. operculata* was a synonym of Penard's (1890, 1902) *C. oviformis* based on cultures of both taxa and the discovery that encysted forms of both may possess an operculum - an organic plug-like structure that occludes the oral aperture of the test. The presence of an operculum in *C. operculata* had been proposed by Page (1966) as the main feature distinguishing these two species. The presence of an operculum in *C. leachi* n. sp., suggests that this structure may be a unifying feature within the genus, but the life histories of other *Cryptodifflugia* species need to be studied before such a statement can be made with any degree of certainly.

The shape of the test of *C. leachi* n. sp. is elliptical in outline in contrast to the ovoid shape of *C. oviformis* where the posterior 1/3 is hemispherical and the anterior 1/3 is more conical in shape. Hedley *et al*.'s (1977) measurements of 100 specimens of *C. oviformis* revealed a range in test length of 14.5-22.2 µm, a width of 12.8-17.6 µm, and an apertural diameter of 3.2-6.4 µm. In an independent set of measurements of this species (but reported as *C. operculata*), Page (1966) found test lengths of 15.2-24.2 µm, widths of 13.8-20.7 and apertural diameters of 3.4-6.9 µm. His averages for test length and width were 17.6 and 15.7 µm, respectively. Thus, the mean test length (13.1 µm) and mean test width (10.0 µm) of *C. leachi* n. sp. are smaller than the smallest *C. oviformis* tests. Similarly, the maximum apertural diameter found for *C. leachi* n. sp. was smaller than the largest aperture measured in previous studies of *C. oviformis* and further emphasizes the overall consistent and significant size difference in the tests of these species.

Hedley *et al*. (1977) determined by EM X-ray analysis that the test wall of *C. oviformis* was comprised of a thin outer organic layer and a much thicker inner, non-crystalline calcareous layer, possibly dominated by amorphous calcium phosphate (previous authors had presumed the wall to be "chitinous"). They found large mainly spherical calcareous inclusions within some mitochondria that may have some homologous relationship to the large crystal-like bodies found in the cytoplasm of many *C. leachi* n. sp. specimens. If calcareous, these crystals may serve in young thinner tests as a reservoir of calcium for reinforcement (thickening) of the test wall.

Among other small species of *Cryptodifflugia*, three species from Australia described by Playfair (1918) are comparable in size to *C. leachi* n. sp. One, *C. pusilla* Playfair, 1918, has tests 10-12 µm long but with nearly parallel sides; another, *C. minuta* Playfair, 1918 has test lengths of 10-13 µm, but is flask-shaped (markedly narrowing toward the anterior end); the third, *C. angulata* Playfair, 1918, is 13-14 µm long but has an angular shape in longitudinal view. All of these distinctions based on test shape were judged to be valid criteria for separation of *Cryptodifflugia* species as manifested in Page's (1966) review of the taxonomy and key to species.

Although there can be no confusion of living specimens of *Cryptodifflugia leachi* n. sp. with small species of related testate rhizopod genera such as *Microgromia* and *Difflugiella* with their distinctive

anastomosing filose pseudopodia, empty tests of these species might pose identification problems. The shape of the test of *Microgromia levipes* Penard, 1904, for example, resembles more that of *C. leachi* n. sp. than *C. oviformis*, but the average size given by Penard (1904), L = 18 µm; W = 15 µm, is within the range reported for *C. oviformis* (significantly larger than tests of *C. leachi* n. sp.). The test dimensions of *Difflugiella collum* Chardez, 1971 have been reported in two different size categories (i) 16-18 × 13-14 µm, with a pseudostome diameter of 5-6 µm (Chardez 1971) or (ii) 10-12 × 7-8 µm with a pseudostome diameter of 2.5-3 µm (Chardez and Thomas 1980). The latter specimens may represent a different species as judged by the much smaller size and the fact that they were collected in a seawater habitat, as opposed to a freshwater habitat for the original (Chardez 1971) specimens. In both cases, however, the tests of *D. collum* have a pseudostome situated at the apex of a short neck or collar - a structure lacking in *C. leachi* n. sp.

REFERENCES

Beyens L., Chardez D. (1982) *Cryptodifflugia angustastoma* et *Nebela carinatella*, nouveaux thécamoebiens des toubières dans la Campine belge. *Arch. Protistenk.* **126:** 169-172

Bobrov A. A. (2001) *Cryptodifflugia bassini* is a new species of sphagnobiontic testate amoebas (Protozoa, Testacea). *Zool. Zh.* **80:** 1010-1013 (in Russian with English summary)

Chardez D. (1971) Étude sur les thécamoebiens des biotopes interstitiels, psammons littoraux et zones marginales souterraines des eaux douces. *Bull. Rech. Agr. Gembloux* **6:** 257-268

Chardez D., Thomas R. (1980) Thecamoebiens du mesopsammon des plages de Lacanau et Leporge-Ocean (Gironde, France) (Protoza, Rhizopoda, Testacea) *Acta Protozool*. **19:** 277-285

Hedley R. H., Ogden C. G., Mordan N. J. (1977) Biology and fine structure of *Cryptodifflugia oviformis* (Rhizopodea: Protozoa). *Bull. Br. Mus. nat. Hist. (Zool.)* **30:** 313-328

Page F. C. (1966) *Cryptodifflugia operculata* n. sp. (Rhizopodea: Arcellinida, Cryptodifflugiidae) and the status of the genus *Cryptodifflugia*. *Trans. Amer. Microsc. Soc.* **85:** 506-515

Penard E. (1890). Étude sur les rhizopodes d'eau douce. *Mem. Soc. Phys. Hist. Nat. Genève* **31:** 1-230

Penard E. (1902). Faune Rhizopodique du Bassin du Léman. H. Hündig, Genève

Penard. E. (1904). Quelques nouveaux rhizopods d'eau douce. *Arch Protistenk.* **3:** 391-422

Playfair G. I. (1918). Rhizopods of Sydney and Lismore. *Proc. Linn. Soc. New South Wales* **42:** 633-675

Received on 27th December, 2005; revised version on 7th April, 2006; accepted on 28th April, 2006

Acta Protozool. (2006) 45: 301 - 312

ACTA
PROTOZOOLOGICA

New Data to the Shell Ultrastructure and the Biometry of the Marine Interstitial Testate Amoebae (Rhizopoda: Testaceafilosia)

Vassil GOLEMANSKY and Milcho TODOROV

Institute of Zoology, Bulgarian Academy of Sciences, Sofia, Bulgaria

Summary. The data about the shell ultrastructure of 6 interstitial testate amoebae: *Chardezia caudata*, *Psammonobiotus balticus*, *P. golemanskyi*, *Corythionella minima*, *C. pontica* and *Micramphora pontica* is presented for the first time. A biometric analysis of all of them, found in rich populations in the North-Eastern Black Sea littoral, is also accomplished. On the basis of the present investigations some morphometric descriptions and taxonomic diagnoses of the studied interstitial testate amoebae are supplemented and corrected. The summarized data on their geographical distribution so far in the World Ocean is given, too.

Key words: biometry, distribution, shell ultrastructure, taxonomy, testate amoebae.

INTRODUCTION

The marine interstitial testate amoebae form a specific taxocenose in the underground waters of the marine sand supralittoral. They became a subject of more detailed investigations only in the last four decades. The morphological descriptions and taxonomic diagnoses of most of the taxa reported so far have been performed mainly by light microscopy. Because of that, the information about some essential details of the shell morphology, the structure and the character of the idiosomes and xenosomes, forming the shells, is scanty and incomplete. As a result the taxonomic status of some of the established taxa and their phylogenetic relations with close genera and species are still unclear.

Eighty psammobiotic interstitial testate amoebae from the marine sand supralittoral have been established so far, but more detailed information about their structure and ultra-morphology has been given only for 26 of them (Golemansky and Ogden 1980; Golemansky and Coûteaux 1982; Ogden and Coûteaux 1986, 1989; Anderson *et al.* 1996; Golemansky and Todorov 1996, 2004). Further investigations on the ultra-morphology of other taxa of this group (especially of genera and species with problematic systematic status) are necessary, so that, the taxonomic problems with the marine interstitial testate amoebae and their relations with the freshwater testate amoebae can be solved and explained.

Address for correspondence: Vassil Golemansky, Institute of Zoology, Bulgarian Academy of Sciences, 1 Tsar Osvoboditel Blvd., 1000 Sofia; Fax: (3592) 9888-28-97; E-mail: golemansky@zoology.bas.bg; mtodorov@zoology.bas.bg

The purpose of this article is to present the results of our last investigations on the shell ultra-morphology of 6 interstitial testate amoebae that have not been studied so far by scanning electron microscopy (SEM). Because of the presence of rich populations of some of them in our samples, a biometric analysis of their morphological variability also has been accomplished. Some corrections and supplements to the taxonomic diagnoses and descriptions of the studied interstitial testate amoebae have been made on the basis of the obtained results.

MATERIALS AND METHODS

The materials were collected from several localities in sandy beaches of the Bulgarian Black Sea Coast during the period from April to October 2005. Samples were taken from the level of the underground water in holes with a depth of 0.20-1.00 m, which were excavated in the sand at different distances from the waterline. Samples were kept live until the moment of their study.

The biometric characterization of the studied species was made by the method of Schönborn *et al.* (1983). The following parameters were calculated: arithmetic mean ($\overline{X}$); median (M); standard deviation (SD); standard error of the mean (SE); coefficient of variation in % (CV); extreme values (Min and Max); number of examined individuals (n). Size measurements in micrometers (μm) of shells were made by light microscopy at 400× magnification.

For scanning electron microscopy (SEM) the shells were isolated, cleaned through several washes with distilled water, mounted directly on stubs and air-dried. The shells were coated evenly with gold in a vacuum coating unit. Microphotographs were obtained by using a Phillips SEM 515, operated at 25 kV.

RESULTS AND DISCUSSION

Chardezia caudata Golemansky, 1970 (Figs 1-4, Table 1)

Shell morphology. The shell is elongate-elliptical, plagiostomic, colourless and translucent by light microscopy. The aboral end of the shell is prolonged in a hallow spine, reaching to 1/3 of its total length. The cross section of the shell is circular. In lateral view the shell is slightly curved, narrowed at the anterior end, and forms a brief neck. The ventral wall is almost flat and the dorsal wall is blown up. After the neck the shell is enlarged in a funnel-like circular collar around the aperture (Figs 1, 2).

According to the original description of the shell by light microscopy it is proteinaceous, smooth, without idiosomes or xenosomes (Golemansky 1970a). Our SEM investigations of the shell structure show that it is formed of many ellipsoidal or oval idiosomes (2.5-3.0 μm length and 1.2-1.3 μm width) which are randomly arranged to overlap each other (Figs 3, 4). By its shell ultra-structure *C. caudata* is close to the genus *Corythionella*, but by its shell form, cross section and the presence of the caudal spine it is similar to the genus *Pseudocorythion.* The periphery of the collar rim is formed of smaller elliptic idiosomes, united together by organic cement like that of *Corytionella.* Undoubtedly, the genus *Chardezia* is a member of the family Psammonobiotidae, close to the genera *Pseudocorythion* and *Corythionella*.

Biometry. Coefficients of variation of the measured taxonomical characters (except the length of spine) are less or near to 10% and show that shell parameters are moderately variable. The length of spine is more variable (CV=22.78) and range between 5 and 14 μm. This variability of the spine length is the main reason for variability in measurements of the total shell length in *C. caudata* (between 40 and 51 μm). As a whole our values correspond well to the original description (Golemansky 1970a).

Analysis of the size frequency distribution indicates that *C. caudata* is a size-monomorphic species (Figs 5A, B). The presence of comparatively well-expressed main-size class of the shell length (46-48 μm), as well as of the shell diameter (13-14 μm), and the lack of subsidiary peaks (bell-shaped curves) indicate a normal distribution (Figs 5A, B). The average length and diameter of *C. caudata* shells amounted to 46.3 ± 3.3 ($\overline{X}$ ± SD; n=35) and 13.1 ± 0.7 ($\overline{X}$ ± SD; n=35), respectively. These arithmetical means agree well with the main size classes of both, shell length and shell diameter, and testify to the monomorphism of the species.

Geographical distribution. So far *Chardezia caudata* was sporadically known from the underground waters of a few sandy beaches of the Black Sea (Golemansky 1970a, 1974), Mediterranean and Aegean Seas (Golemansky 1976a, 1982), the Pacific (Golemansky and Todorov 1996) and the Atlantic (Golemansky 2000). Undoubtedly, *C. caudata* has a cosmopolitan distribution in the World Ocean, but it is often imperceptible by light microscopy because of the perfect transparency of its shell and the small dimensions.

Psammonobiotus balticus Golemansky, 1973 (Fig. 6, Table 1)

Shell morphology. In ventral view the shell is ovoid, colourless and translucent. It has two distinct parts: a

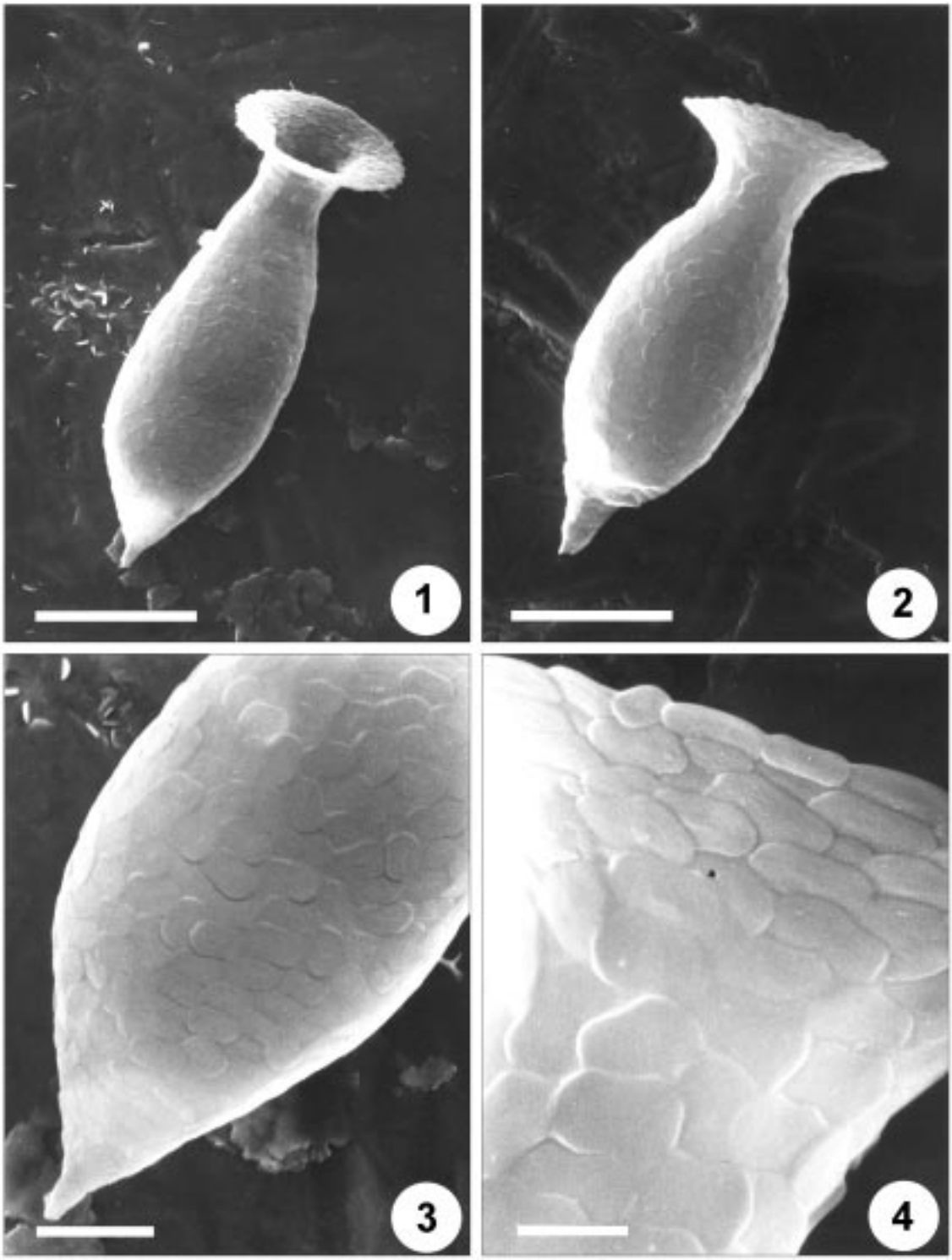

Figs 1-4. SEM photographs of *Chardezia caudata*. **1, 2** - lateral view of two specimens; **3** - posterior end of the shell; **4** - shell structure of the neck. Scale bars: 15 µm (1, 2); 5 µm (3), 2 µm (4).

Table 1. Biometric characterization of the investigated testacean species. $\bar{x}$ - arithmetic mean; M - median; SD - standard deviation; SE - standard error of the mean; CV - coefficient of variation in %; Min - minimum; Max - maximum; n - number of examined individuals (measurements in µm).

Character	$\bar{x}$	M	SD	SE	CV	Min	Max	N
Chardezia caudata								
Total length	46.28	47	3.32	0.56	7.17	40	51	35
Diameter of shell	13.11	13.5	0.69	0.12	5.22	11.5	14	35
Diameter of aperture	6.16	6	0.62	0.1	10.06	5	7	35
Diameter of collar	17.42	17.5	1.24	0.21	7.12	15	20	35
Length of spine	9.7	10	2.21	0.37	22.78	5	14	35
Psammonobiotus balticus								
Length	22.14	22	1.62	0.35	7.31	20	26	21
Width	17.04	17	0.86	0.2	5.04	15.5	19	21
Height	19.52	19.5	1.17	0.25	5.99	18	22	21
Diameter of aperture	8.5	8.5	0.89	0.2	10.47	7	10	21
Length / Width	1.29	1.29	0.05	0.01	3.87	1.22	1.39	21
Width / Height	0.87	0.87	0.02	0.01	2.29	0.83	0.92	21
Psammonobiotus golemanskyi								
Length	31.25	31.5	1.98	0.25	6.33	28	36	62
Width	19.93	20	1.28	0.17	6.42	17	22	62
Height	18.31	18	1.16	0.15	6.33	16	20	62
Diameter of aperture	8.17	8	0.61	0.08	7.46	6.5	9.5	62
Large axis of collar	22.00	22	1.29	0.16	5.86	20	25	62
Small axis of collar	18.00	18	1.40	0.17	7.77	15	21	62
Length / Width	1.57	1.56	0.09	0.01	5.73	1.4	1.79	62
Width / Height	1.08	1.1	0.07	0.01	6.48	0.9	1.25	62
Corythionella minima								
Length	50.1	50	3.24	0.48	6.46	44	60	47
Width	23.09	23	1.85	0.27	8.01	18	27	47
Height	14.72	15	0.64	0.1	4.34	13.5	16	47
Diameter of aperture	9.97	10	0.67	0.1	6.72	8	11	47
Large axis of collar	23.84	24	1.28	0.18	5.37	21	26	47
Small axis of collar	21.74	22	1.29	0.19	5.93	20	24	47
Length / Width	2.18	2.18	0.25	0.04	11.46	1.74	2.94	47
Corythionella pontica								
Length	96.11	98	6.79	1.04	7.06	80	105	43
Width	38.79	39	1.72	0.26	4.43	35	43	43
Height	26.53	27	0.63	0.10	2.37	25	28	43
Diameter of aperture	19.95	20	0.99	0.15	4.96	17	22	43
Large axis of collar	46.86	48	3.21	0.49	6.85	39	52	43
Small axis of collar	39.25	40	1.51	0.23	3.84	35	42	43
Length / Width	2.47	2.47	0.13	0.02	5.26	2.16	2.71	43
Micramphora pontica								
Total length	23.35	23	3.04	0.55	13.01	20	32	31
Diameter of shell	16.83	16	2.06	0.37	12.24	15	22	31
Diameter of aperture	8	8	0.84	0.15	10.5	7	10	31
Diameter of collar	18.79	19	1.94	0.35	10.32	16	24	31
Length of collar	9	8	2.77	0.5	30.77	7	17	31

rounded central part and a peak elongated in the form of a crescent overlaying the aperture. The aperture is round or oval, disposed in a slight invagination of the ventral wall. In lateral view the shell is like a helmet with a round basis and an elongated overlaying peak (Golemansky 1973).

The SEM investigations show that the central part of the shell is composed of a proteinaceous matrix, covered with irregular flat plates (Fig. 6). Some larger plates can be observed on the dorsal part of the shell. The elongated peak is composed mainly of organic cement and its periphery is thin and flexible (Fig. 6).

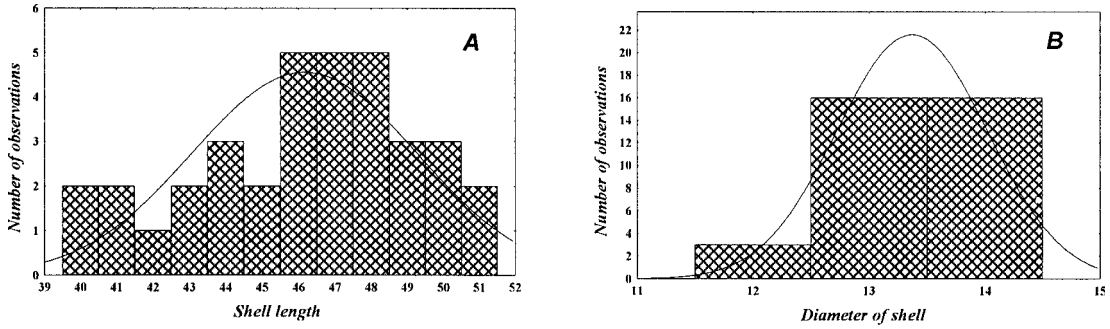

Fig. 5. Histograms showing the size frequency of the shell length (A) and the shell width (B) of *Chardezia caudata*.

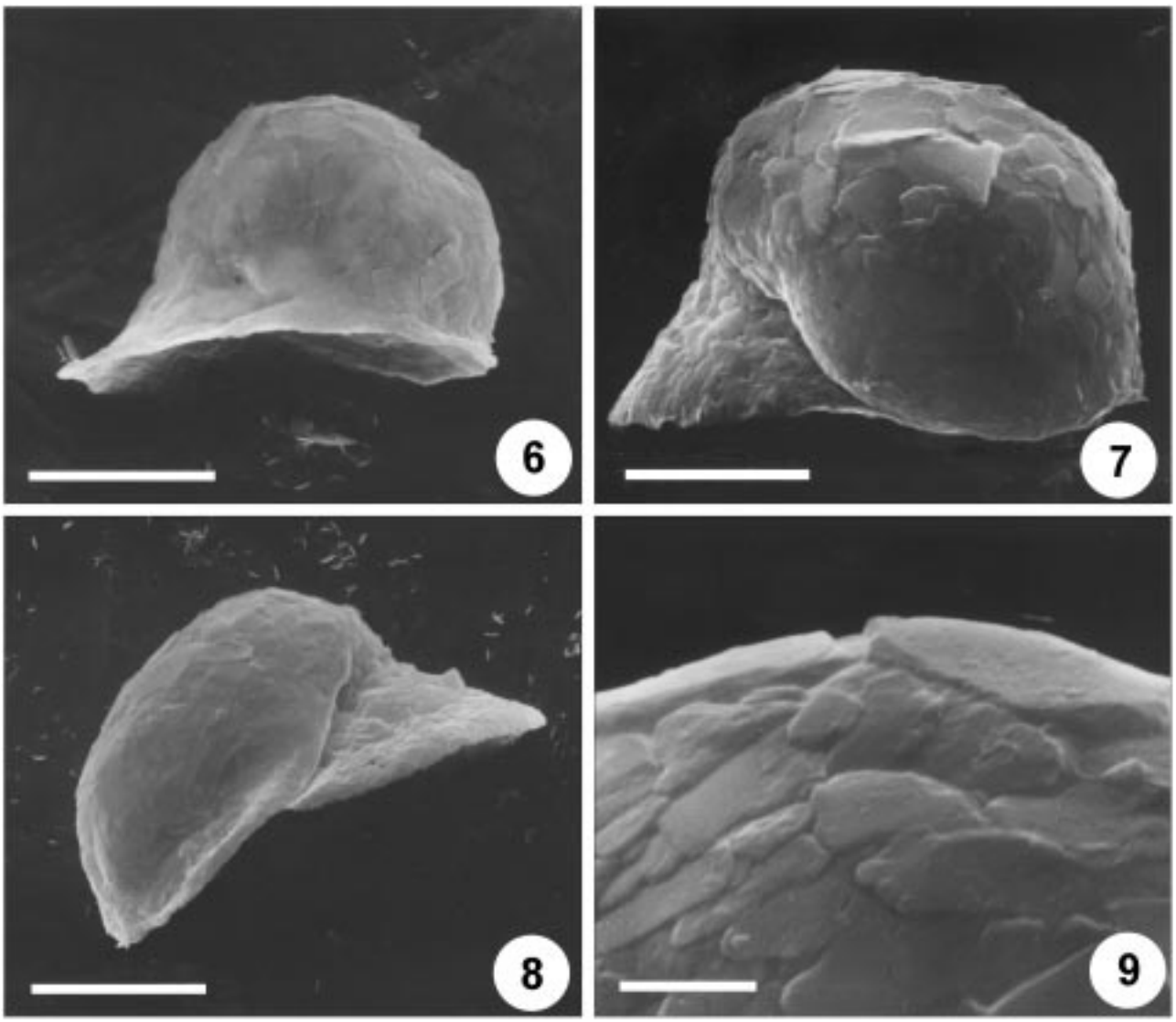

Fig. 6. *Psammonobiotus balticus* - lateral view. Scale bar: 10 µm.
Figs 7-9. SEM photographs of *Psammonobiotus golemanskyi*. **7, 8** - lateral view of two specimens, showing the invagination of the neck; **9** - detail of the dorsal structure of the shell, composed of flattened plates. Scale bars: 10 µm (6-8); 3 µm (9).

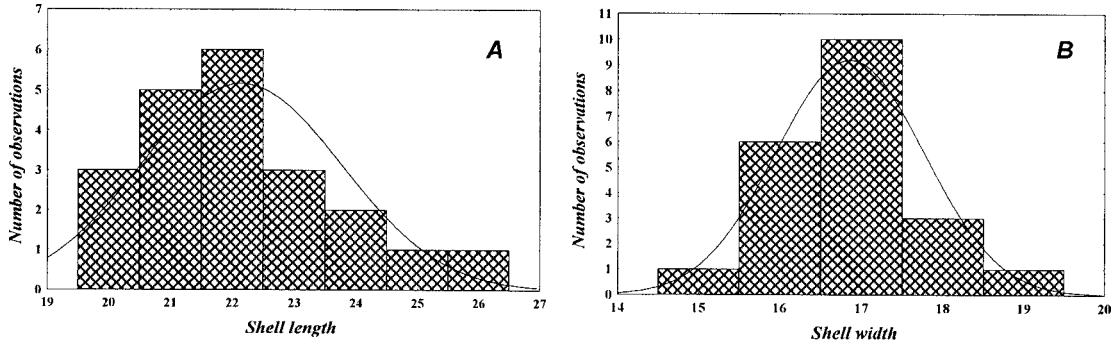

Fig. 10. Histograms showing the size frequency of the shell length (A) and the shell width (B) of *Psammonobiotus balticus.*

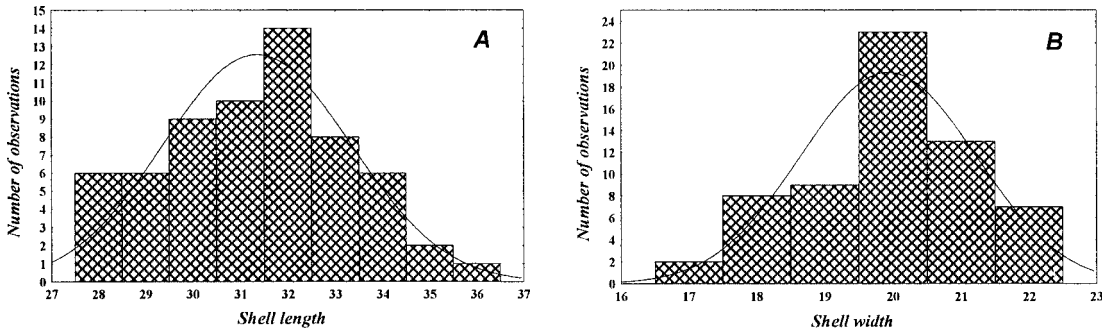

Fig. 11. Histograms showing the size frequency of the shell length (A) and the shell width (B) of *Psammonobiotus golemanskyi*.

Biometry. Most of the measured characters (shell length, width and height) are fairly constant and have low variability (CV between 5.04 and 7.31). Only the aperture diameter is more variable (CV=10.47). Obtained values correspond to the original description of species (Golemansky 1973).

The analysis of the size frequency distribution indicates that *P. balticus* is a size-monomorphic species, characterized by a main-size class and a small size range (Figs 10A, B). All measured specimens of our population have a shell length 20-26 µm and shell width 15.5-19 µm. The presence of comparatively well-expressed main-size class of the shell length (21-22 µm), as well as of the shell width (16-17 µm), and the lack of the subsidiary peaks (bell-shaped curves) indicate a normal distribution (Figs 10A, B). The average length and width of *P. balticus* shells were 22.1 ± 1.62 ($\overline{X}$ ± SD; n=21) and 17.0 ± 0.86 ($\overline{X}$ ± SD; n=21), respectively. These arithmetical means agree well with the main size classes of the shell length and width, and testify to the monomorphism of the species.

Geographical distribution. *P. balticus* is a widely spread psammobiotic testate amoeba with a cosmopolitan distribution. It has been observed in the following seas and oceans: the Baltic Sea (Golemansky 1973), the Black Sea (Golemansky 1974), the North and Mediterranean Seas (Chardez 1977, 1986; Golemansky 2000), the Aegean and Marmara Seas (Golemansky 1982,

1998a, c), the Pacific and Indian Oceans (Sudzuki 1976, 1979, 1986), the Atlantic (Chardez and Thomas 1980, Golemansky 1992).

Psammonobiotus golemanskyi Chardez, 1972 (Figs 7-9, Table 1)

Shell morphology. According to the light microscopic description of Chardez (1972) the shell of *P. golemanskyi* is plagiostomic, with a flat ventral wall and a rounded dorsal wall. In lateral view there is a clearly visible point at the posterior end of the shell (Figs 7, 8). The aperture is in the center of a well-invaginated neck and is surrounded by a large funnel-like collar. The collar is in the same plane with the ventral wall of the test (Figs 7, 8). The shell and the collar are laterally flattened.

Psammonobiotus golemanskyi and *P. balticus* are morphologically very close and it is difficult to distinguish them in ventral view. But in lateral view *P. golemanskyi* differs well from *P. balticus* by its invaginated neck, the characteristic posterior point and the laterally flattened shell and collar.

The shell of *P.golemanskyi* is composed of organic cement, covered with irregularly disposed flattened plates, like *P. balticus*. At the dorsal edge some bigger overlapping plates are visible (Fig. 9).

Biometry. All measured characters of the species are fairly constant and have low variability (CV between 5.73 and 7.77). Our values are somewhat larger than those of the original description of species (Chardez 1972).

The size frequency distributions yield bell-shaped curves (normal distribution) and indicate that *P. golemanskyi* is a size-monomorphic species, characterized by well-expressed main-size class (31-32 µm shell length and 20-21 µm shell width) and by a small size range. Figures 11A, B show that in all measured specimens the shell length and the shell width range in close limits of 28-36 µm and 17- 22 µm, respectively.

Geographical distribution. *Psammonobiotus golemanskyi* has a cosmopolitan distribution in the underground waters of different marine sandy beaches. After the first observation from the North Sea (Chardez 1972, 1977) it was reported from the Pacific (Sudzuki 1977a, b, 1980, 1981b, 1985, 1986; Golemansky 1979), the Indian Ocean (Sudzuki 1979), the Atlantic (Chardez and Thomas 1980, Sudzuki 1983, Golemansky 1992), the Mediterranean, Aegean, Black and Marmara Seas (Chardez 1989); Golemansky 1982, 1994, 1998a, b). During the present investigation, a rich population of *P. golemanskyi* was also observed in the Black Sea (Varna). The biometry of the species was made on the observed Black Sea population.

Corythionella minima Golemansky, 1970 (Figs 12-13, Table 1)

Shell morphology. According to the original description, made by light microscopy, the shell of *C. minima* is elongate-elliptical, plagiostomic, narrowed at the anterior end and lancet-arched at the posterior end. The shell is dorso-ventrally flattened, colourless and translucent. The aperture is round, oblique as regards the longitudinal axis. In the region of the aperture the shell is enlarged and forms a large funnel-like collar. In lateral view the collar is funnel-like, but in ventral view it is like a large round or oval disc around the aperture (Golemansky 1970b). Sometimes a little spine is observed at the posterior end of the shell.

The ultrastructural investigation shows that the shell is composed of numerous oval or elliptic idiosomes (2-2.5 × 1.5-2.0 µm), randomly arranged or overlapping each other (Figs 12, 13). The neck and the collar are composed of the same plates as those in the shell. The rim of the flexible collar is composed of organic cement and small elliptic plates.

Data about the ultra-structure of *C. minima* have been given by Ogden and Coûteaux (1989), but they related it to *C. pontica*. Those authors studied only two specimens with body length of 39 and 45 - typical dimensions for *C. minima*. However, it is important to remember that the shell dimensions of *C. pontica* are twice bigger (length: 61-105 µm) and they are never smaller than 60 µm. (See also the biometric data about two species in Table 1).

Biometry. The coefficients of variation of all characters are less than 10% and show that shell measurements of the Black Sea population of *C. minima* are moderately variable. The present values correspond well to those of the original description of species (Golemansky 1970a).

The analysis of the size frequency distribution indicates that *C. minima* is a size-polymorphic species, characterized by increasing size range (shell length 44-60 µm, shell width 18-27 µm) and by reduced main size-class in favour of subsidiary classes (Figs 16A, B). The average length and width of *C. minima* shells amounted to 50.1 ± 3.24 ($\overline{X}$ ± SD; n=47) and 23.1 ± 1.85 ($\overline{X}$ ± SD; n=47), respectively. These arithmetical means do not agree with the main size classes of both, shell length and width, and testify to the polymorphism of the species.

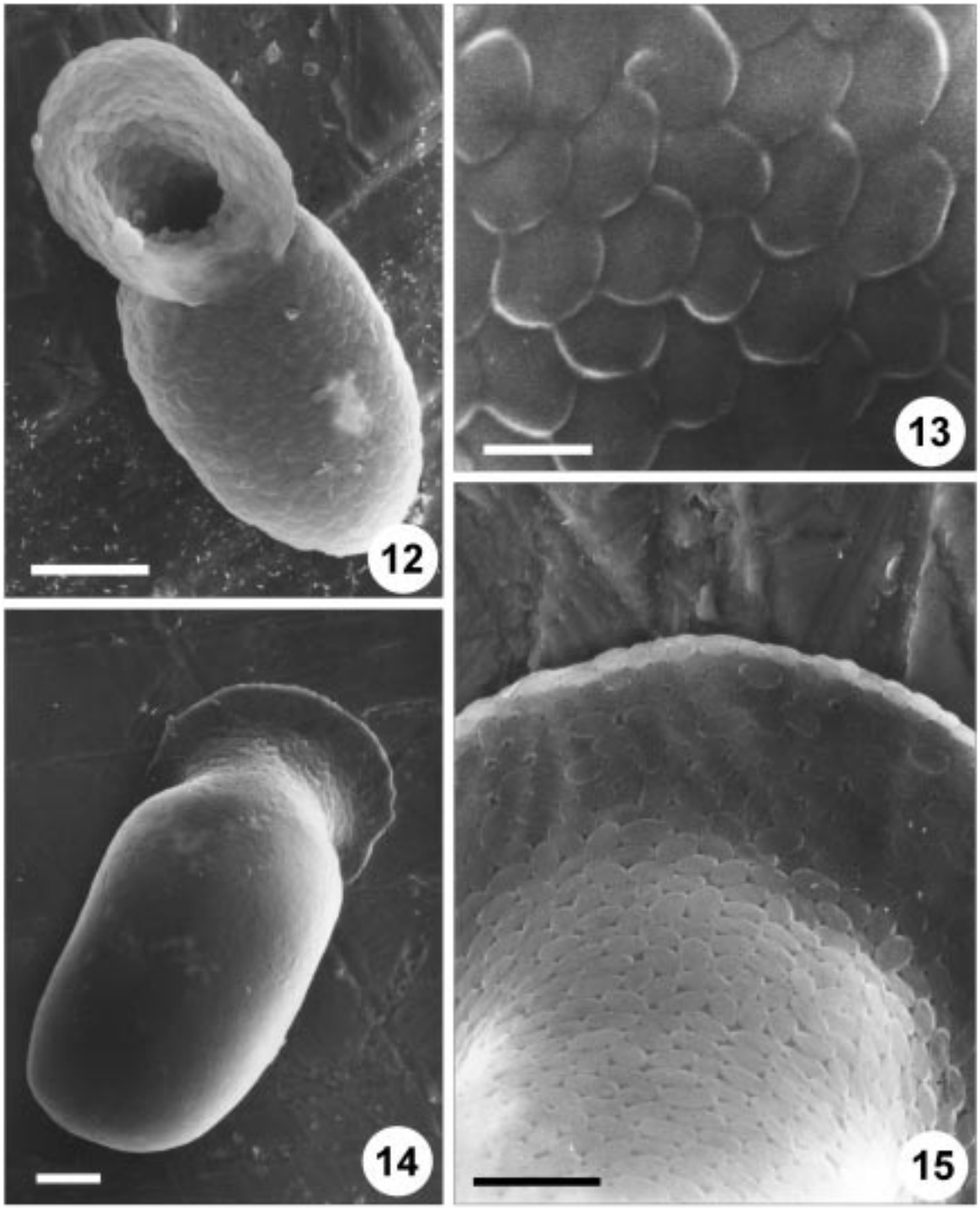

Figs 12, 13. SEM photographs of *Corythionella minima*. **12** - ventral view; **13** - shell structure, showing the overlaping silicious plates (idiosomes) on the ventral shell surface. Scale bars: 10 µm (12); 2.5 µm (13).
Figs 14, 15. SEM photographs of *Corythionella pontica*. **14** - dorsal view; **15** - shell structure, showing the irregularly arranged elliptic plates (idiosomes) on the dorsal shell surface and on the collar. Scale bars: 10 µm (14); 5 µm (15).

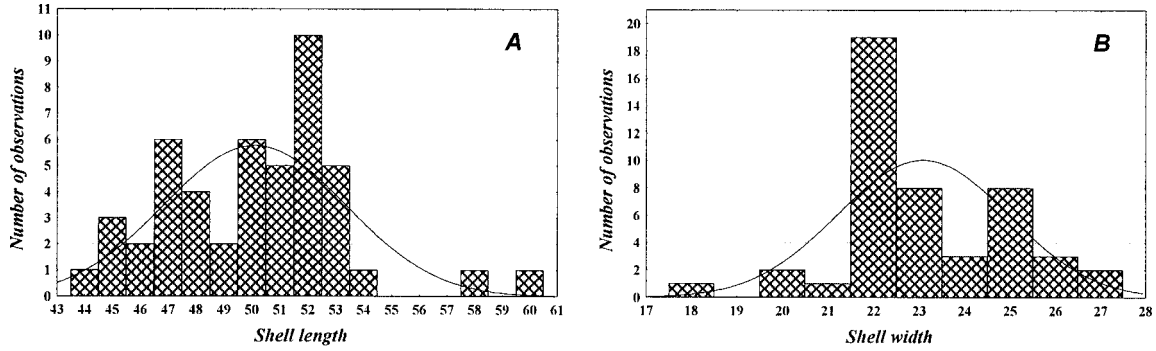

Fig. 16. Histograms showing the size frequency of the shell length (A) and the shell width (B) of *Corythionella minima.*

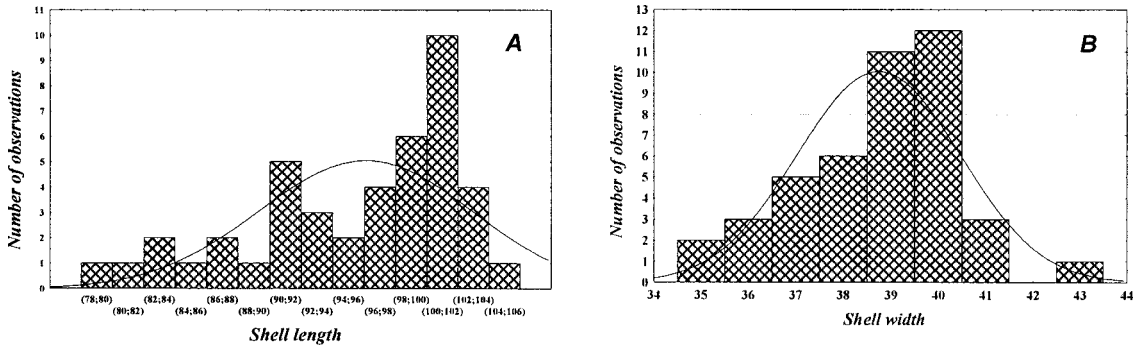

Fig. 17. Histograms showing the size frequency of the shell length (A) and the shell width (B) of *Corythionella pontica.*

Geographical distribution. Firstly described from the sand supralittoral of the Caribbean Sea by Golemansky (1970b), *C. minima* was later observed in more than 27 different localities in all studied seas and oceans. It has a cosmopolitan distribution and it is a frequent habitant of the marine interstitial habitats (Golemansky 1980).

Corythionella pontica Golemansky, 1970 (Figs 14-15, Table 1)

Shell morphology. In ventral and dorsal view the test is elliptic, slowly narrowed in the region of the aperture, colourless and translucent, dorso-ventrally flattened (Fig. 14). Aborally it is rounded, rarely narrow, without any spine or spike. In lateral view the shell is plagiostomic, with a large collar surrounding the aperture. Usually the collar is circular, rarely large-elliptic, with a diameter of the test.

The shell and the funnel-like collar are formed of elliptic or oval idiosomes. As distinct from *C. minima*, the body and collar plates are irregularly arranged and the organic cement matrix is visible between them (Fig. 15). The flexible periphery of the collar is also formed of smaller plates, embedded within organic cement and forming a thin organic rim (Fig. 15).

Biometry. The coefficients of variation of all characters are low (CV between 2.37 and 7.06) and show that the shell measurements of the Black Sea population of *C. pontica* are moderately variable. The species shows a great diversity only in shell length (CV=7.06). However, shell width, height, and diameter of aperture are

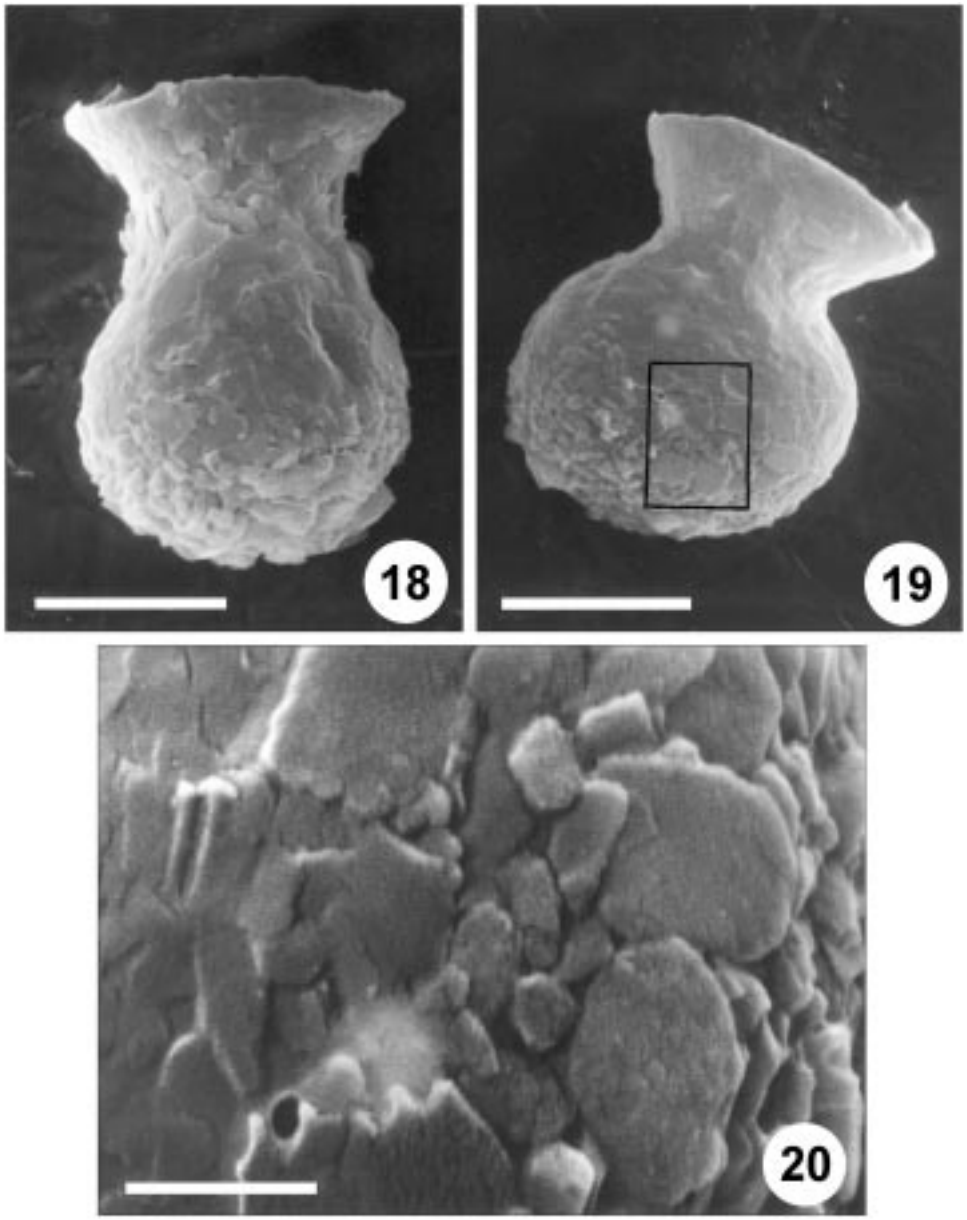

Figs 18-20. SEM photographs of *Micramphora pontica*. **18, 19** - lateral view of two specimens, showing the large funnel-like collar and the neck of the shell; **20** - detail of the shell structure of the specimen shown in fig. 19. Scale bars: 10 µm (18, 19); 2 µm (20).

fairly constant and have low variability (CV between 2.37 and 4.96). Our values correspond to those of the original description (Golemansky 1970c).

Analysis of the size frequency distribution indicates that *C. pontica* is a size-polymorphic species by the shell length and a size-monomorphic species by the shell width (Fig. 17). Figure 17A shows that the specimens of our population are characterized by big size range of the shell length (80-105 µm). The curve of the size classes shows one well-expressed main-size class (100-102 µm) and another not well-expressed subsidiary size class (90-92 µm). Figure 17B shows that the specimens of our population are constant by the shell width - all specimens measured are in limits of 35-43 µm and more than 75% of them have a shell width 37-40 µm. The average length and width of *C. pontica* shells amounted to 96.1 ± 7.06

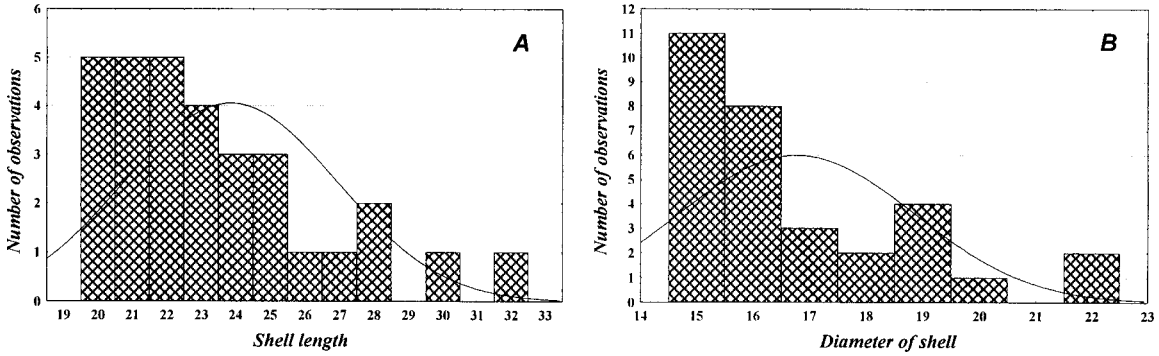

Fig. 21. Histograms showing the size frequency of the shell length (A) and the shell diameter (B) of *Micramphora pontica.*

($\overline{X}$ ± SD; n=43) and 38.8 ± 4.43 ($\overline{X}$ ± SD; n=43), respectively. These arithmetical means confirm the polymorphism of *C. pontica* by the shell length, and the monomorphism of the species by the shell width.

Geographical distribution. *C. pontica* is one of the biggest marine interstitial testate amoebae and it is easy to be observed by light microscopy. It seems that the species has a cosmopolitan distribution, but till now it has been observed only in 10 localities in the Black Sea (Golemansky 1970c, 1980), the Mediterranean Sea (Laminger 1973, the Atlantic (Golemansky 1976b), the Pacific (Sudzuki 1976, 1977b, 1981b), the Marmara Sea (Golemansky 1998c) and the North Sea (Golemansky 2002).

Micramphora pontica Valkanov, 1970 (Figs 18-20, Table 1)

Shell morphology. The shell is oval, with circular cross section, colourless and translucent. At the anterior end the shell is enlarged and forms a large funnel-like collar with a round aperture at the bottom. The diameter of the collar is equal to or bigger than the shell diameter. The aboral end of the shell is rounded.

According to Valkanov (1970) the shell is chitinoid and "the only visible by immersion structural elements are some rows of irregularly disposed pimples between the neck and the funnel-like collar". Our investigations show that the shell of *M. pontica* is covered with polygonal organic plates, closely arranged on the organic matrix and overlapping (Figs 18-20). Bigger organic plates, as well as some mineral xenosomes can be observed on the bases of the shell and in the region of the neck. The rim of the collar is formed of organic cement with smaller plates and it is flexible (Figs 18,19).

Biometry. Coefficients of variation of all measured characters are more to 10% and show that shell measurements of *M. pontica* are rather variable. The species shows a great diversity in length of col and in total length, which have high variability (CV=30.77 and 13.01, respectively). As a whole our values correspond well to the original description (Valkanov 1970).

Micramphora pontica show nearly a normal distribution of size classes, but there are some subsidiary peaks (Figs 21A, B). Also, this species is characterized by increasing size range (20-32 mm shell length and 15-22 µm diameter of shell). These features indicate that *M. pontica* is not well-defined monomorphic species. The average length and diameter of *M. pontica* shells amounted to 23.3 ± 3.04 ($\overline{X}$ ± SD; n=31) and 16.8 ± 2.06 ($\overline{X}$ ± SD; n=31), respectively. These arithmetical means do not agree well with the main size classes of both, shell length and shell diameter, and put a doubt about the monomorphism of the species.

Geographical distribution. *M. pontica* has a cosmopolitan distribution. So far it has been found in more than 39 localities of all studied seas and oceans (Golemansky 1980). It is an eurybiotic species, living at the salinity from 1.5 ‰ to 37.0 ‰.

Acknowledgements. We thank to Dr. L. Petrov and Mr. B. Andreev for their competent photographical help and to Ms. A. Zhecheva for her technical help in the preparation of the present work. This study was supported by the Bulgarian National Science Fund, Grant B-1310/2003.

REFERENCES

Anderson O. R., Rogerson A., Hannah F. (1996) A description of the testate amoeba *Ovulina parva* gen. n. sp. n. from coastal marine sediments. *J. biol. Ass. U. K.* **76:** 851-865

Chardez D. (1972) Étude sur les thécamoebiens des biotopes interstitiels, psammons littoraux et zones marginales souterraines des eaux douces. *Bull. Rech. Agron. de Gembloux*, N.S. **6:** 257-268

Chardez D. (1977) Thécamoebiens du Mésopsammon des plages de la Mer du Nord. *Rev. Verviétoise d'Hist. Nat.* **416:** 18-34

Chardez D. (1986) Thécamoebiens des plages de la Mer du Nord. *Acta Protozool.* **25:** 375-378

Chardez D. (1989) Sur quelques thécamoebiens psammobiontes des plages Italiennes de la Mer Adriatique. *Trav. Lab. Zool. Gen. Faun. Fac. Sc. Agr. Gembloux*, N.S. **7:** 1-3

Chardez D., Thomas R. (1980) Thécamoebiens du Mésopsammon des plages de Lacanau et Leporge - Ocean (Geronde - France). *Acta Protozool.* **19:** 277-285

Golemansky V. (1970a) *Chardezia caudata* gen. n. sp. n. et *Rhumbleriella filosa* gen. n. sp. n. - deux thécamoebiens nouveaux du psammon littoral de la Mer Noire (Rhizopoda, Testacea). *Bull. Inst. Zool. Mus. Sofia* **32:** 121-125

Golemansky V. (1970b) Thécamoebiens (Rhizopoda, Testacea) des eaux souterraines littorales de quelques plages de Cuba. *Bull. Inst. Zool. Mus. Sofia* **32:** 151-158

Golemansky V. (1970c) Rhizopodes nouveaux du psammon littoral de la Mer Noire (Note préliminaire). *Protistologica* **6:** 365-371

Golemansky V. (1973) Deuxième contribution à la connaissance des thécamoebiens (Rhizopoda, Testacea) du psammal littoral de la Mer Baltique. *Bull. Inst. Zool. Mus. Sofia* **38:** 49-60

Golemansky V. (1974) Sur la composition et la distribution horizontale de l'association thécamoebienne (Rhizopoda, Testacea) des eaux souterraines littorales de la Mer Noire en Bulgarie. *Bull. Inst. Zool. Mus. Sofia* **40:** 195-202

Golemansky V. (1976a) Contribution à l'étude des Rhizopodes et des Hélizoires du psammal supralittoral de la Méditeranée. *Acta Protozool.***15:** 35-45

Golemansky V. (1976b) Rhizopodes psammobiontes (Protozoa, Rhizopoda) du psammal supralittoral des côtes guinéennes de l'Atlantique. *Acta zool. bulg.* **4**: 23-29

Golemansky V. (1979) Thécamoebiens psammobionts du supralittoral coréen de la Mer Japonaise et description de deux nouvelles espèces - *Rhumbleriella coreana* n. sp. et *Amphorellopsis conica* n. sp. *Acta zool. bulg.* **12:** 5-11

Golemansky V. (1980) La faune técamoebienne interstitielle du psammal supralittoral des mers. Sofia, Dr Sc Thesis, (in Bulgarian)

Golemansky V. (1982) Thécamoebiens (Protozoa: Rhizopodea) interstitieles du supralittoral grec de la Mer Egée. *Biol. Gallohellenica* **9:** 271-276

Golemansky V. (1992) Thécamoebiens interstitiels (Rhizopoda: Arcellinida, Gromida et Monothalamida) du supralittoral français de l'Atlantique dans la région du Roscoff (Bai de Morlaix). *Acta zool. bulg.* **45:** 3-14

Golemansky V. (1994) Revue sur les thécamoebiens interstitiels (Protozoa: Testacea) du littoral grec de la Mer Egeé. *Biol. Gallohelenica* **22:** 269-278

Golemansky V. (1998a) Interstitial testate amoebae (Rhizopoda: Testacea) from the Italian coast of the Mediterranean Sea. *Acta Protozool.* **37:** 139-143

Golemansky V. (1998b) Interstitial testate amoebae (Rhizopoda: Arcellinida and Gromiida) from the Finish coast of the Baltic Sea and summary checklist of the interstitial testate amoebae in the Baltic Sea. *Acta Protozool.* **37:** 133-137

Golemansky V. (1998c) Intersitial testate amoebae (Rhizopoda: Testacea) from the sand supralittoral of the Eastern Marmorean coast (Turkey). *Acta zool. bulg.* **50:** 3-7

Golemansky V. (2000) Marine interstitial rhizopods (Rhizopoda: Arcellinida, Gromida and Foraminiferida) from the South-West Atlantic (Region of Rio de Janeiro) and description of *Psammolagynis atlantica* gen. n., sp. n. - *Acta zool. bulg.* **52:** 3-12

Golemansky V. (2002) Interstitial and benthic marine rhizopods (Protozoa: Rhizopoda) from the strait of Kattegat (Swedish coast). - *Acta zool. bulg.* **54:** 7-14

Golemansky V., Coûteaux M.-M. (1982) Etude en microscopie éléctronique a balayage de huit espèces de thécamoebiens interstitiels du supralittoral marin. *Protistologica (Paris)* **18:** 473-480

Golemansky V., Ogden C. (1980) Shell structure of three littoral species of testate amoebae from the Black Sea (Rhizopodea: Protozoa). *Bull. Br. Mus. Nat. Hist. (Zool.)* **38:** 1-6

Golemansky V., Todorov M. (1996) Interstitial Rhizopods (Rhizopoda: Testacea & Foraminiferida) from the Antarctic Region of Chile and Valparaiso in the Pacific. In: Bulgarian Antarctic Research. Life Sciences. Eds.V. Golemansky & N. Chipev. Sofia. *Pensoft Publ:* 62-69

Golemansky V., Todorov M. (2004) Shell Morphology, Biometry and Distribution of Some Marine Interstitial Testate Amoebae (Sarcodina: Rhizopoda). *Acta Protozool.* **43:** 147-162

Laminger H. (1973) Notes on some Testacea (Protozoa, Rhizopoda) of the Yugoslavian Coast of the Adria near Rab. *Hydrobiologia* **42:** 153-154

Ogden C. G., Coûteaux M.-M. (1986) The nature of the shell of *Alepiella tricornuta*, a marine testate amoeba (Sarcodina: Rhizopoda). *Protistologica* **22:** 213-220

Ogden C. G., Coûteaux M.-M. (1989) Interstitial marine rhizopods (Protozoa) from littoral sands of the east coast of England. *Europ. J. Protistol.* **24:** 281-290

Schönborn W., Foissner W., Meisterfeld R. (1983) Licht- und rasterelektronenmikroskopische Untersuchungen zur Schalenmorphologie und Rassenbildung bodenbewohnender Testaceen (Protozoa: Rhizopoda) sowie Vorschläge zur biometrischen Charakterisierung von Testaceen-Schalen. *Protistologica* **19:** 553-566

Sudzuki M. (1976) Recent portraits of Wild Biota in Japan. II. The Inland Sea of Japan around Kasado Island, Yamaguchi Prefecture. *Õbun Ronsõ* **7**: 11-32

Sudzuki M. (1977a) Protozoans in the Marine Beach Interstices. II. Taxonomy and Ecology of Testacea from a Sandy Island Recently Constructed. *Jap. J. Protozool.* **8**: 23

Sudzuki M. (1977b) Recent Portraits of Wild Biota of Japan. III. A man-made sandy beach constructed in the bay of Tokyo. *Õbun Ronsõ* **8**: 221-239

Sudzuki M. (1979b) Marine Interstitial Testacea from Plau Pinang, Malaysia. *Annot. Zool. Jap.* **52:** 50-53

Sudzuki M. (1980) Protozoans in the marine beach interstices. V. Psammobiont Protozoans from Victoria, South East Australia. *Jap. J. Protozool.* **13:** 11

Sudzuki M. (1981a) Protozoans in the Marine Beach Interstices. VI. Psammobiont Testacea from Niigata-Sado Area (37.9~38.1º N, 138.3~139.1º E). *Jap. J. Protozool.* **14:** 8

Sudzuki M. (1981b) Protozoans in the Marine Beach Interstices. VII. Psammobiont Testacea from River Mouth of Monogawa, Fukushima (37.8º N, 140.9º E). *Jap. J. Protozool.* **14:** 9

Sudzuki M. (1983) Protozoans in the Marine Beach Interstices. IX. Psammobiont Testacea from Abidjan, Côte d'Ivoire, West-Africa. *Jap. J. Protozool.* **16:** 8

Sudzuki M. (1985) Protozoans in the marine beach interstices. XI. Psammophilous testacea from Tasmania. *Jap. J. Protozool.* **18:** 15

Sudzuki M. (1986) Protozoans in the marine beach interstices. XII. Psammophilous Testacea from Taiwan (Formosa). *Jap. J. Protozool.* **19:** 33

Valkanov A. (1970) Beitrag zur Kenntnis der Protozoen des Schwarzen Meeres. *Zool. Anz.* **184:** 241-290

Received on 22nd December, 2005; revised version on 8th March, 2006; accepted on 28th April, 2006

Acta Protozool. (2006) 45: 313 - 316

ACTA
PROTOZOOLOGICA

Short Communication

Codon Usage in *Amoeba proteus* Significantly Differs from *Entamoeba histolytica* and *Acanthamoeba castellanii*

Elżbieta KOCIK*, Magdalena SOBCZAK* and Maria Jolanta RĘDOWICZ

Department of Muscle Biochemistry, Nencki Institute of Experimental Biology, Warsaw, Poland

Summary. Codon usage analysis performed on 5718 expressing codons (including stop codons) of nine *Amoeba proteus* proteins deposited in GenBank revealed that there was no bias in *A. proteus* codon usage and nucleotide frequencies in the three codon positions. This contrasts with codon usage in other amoebozoans, such as *Acanthamoeba castellanii* and *Entamoeba histolytica,* which are biased towards GC and AT, respectively. Interestingly, codon usage in *A. proteus* resembled that of human and *Escherichia coli.* The presence of tRNAs for all possible codons indicates that all heterologous genes may be expressed in these giant cells. However, based on this analysis it is impossible to deduce whether the observed differences and/or similarities are due to conservation or convergence.

Key words: *Acanthamoeba castellanii*, *Amoeba proteus*, codon usage, *Entamoeba histolytica.*

INTRODUCTION

Amoeba proteus has been widely used as a model to study cell motility (Jeon 1995). However, molecular mechanisms governing locomotion and intracellular trafficking remain poorly understood. Parallel to that, the studies on the genome of these giant cells have been also neglected. As the result of that, to date only several actin-binding proteins have been detected including caldesmon (Gągola *et al*. 2003), spectrin (Choi and Jeon 1992), α-actinin and vinculin (Brix *et al*. 1990), Rho and Rac (Kłopocka and Rędowicz 2003) as well as two myosin heavy chains (Oh and Jeon 1998, Dominik *et al*. 2005). Moreover, only nine *A. proteus* proteins have been cloned and sequenced, among them are: actin (Fahrni *et al*. 2003), myosin II heavy chain (Oh and Jeon 1998), and recently a novel actin-binding protein interacting with anti-filamin antibody (ApABP-FI; GenBank accession no: DQ374440).

Therefore, there is very little information on codon usage in *A. proteus*. Moreover, data available at the www.kazusa.orjp/codon web site are based only on the cDNA sequence of four *A. proteus* proteins. This

Address for correspondence: Maria Jolanta Rędowicz, Nencki Institute of Experimental Biology, Department of Muscle Biochemistry, ul. Pasteura, 02-093 Warszawa, Poland; Fax +48-22-8225342; E-mail: j.redowicz@nencki.gov.pl

* these authors have equally contributed to this manuscript

makes very difficult to perform studies on cloning *A. proteus* proteins based on the amino acid sequence obtained, for example, from mass spectrometry analysis.

In order to get more knowledge on the codon usage we performed codon usage analysis based on 5718 codons of nine *A. proteus* proteins (including the stop codons) deposited in the GenBank database. The analysis revealed that, unlike for other amoebozoans, there was no bias in codon usage in *Amoeba proteus*.

MATERIALS AND METHODS

The analysis of codon usage in *Amoeba proteus* was performed using Codon Usage tool, available at the web site http://bioinformatics.org/sms2/. 5718 codons (including the stop ones) of nine *A. proteus* protein sequences deposited in the GenBank database were subjected to the analysis: polyubiquitin (AF034789), S-adenosylmethionine synthetase (U91602), S-adenosylmethionine synthetase 2 (AY324626), pepstatin-insensitive carboxyl proteinase 2 (AF142415), pepstatin-insensitive carboxyl

Table 1. Codon frequency in *Amoeba proteus**.

Amino acid	Codon	Frequency per 10,000 codons	Amino acid	Codon	Frequency per 10,000 codons
Gly	GGG	49	Thr	ACG	61
Gly	GGA	229	Thr	ACA	100
Gly	GGT	267	Thr	ACT	185
Gly	GUC	74	Thr	ACC	153
Glu	GAG	375	Trp	TGG	89
Glu	GAA	539	End	TGA	2
ASP	GAT	438	Cys	TGT	66
Asp	GAC	194	Cys	TGC	56
Val	GTG	124	End	TAG	2
Val	GTA	88	End	TAA	12
Val	GTT	217	Tyr	TAT	128
Val	GTC	124	Tyr	TAC	105
Ala	GCG	82	Leu	TTG	354
Ala	GCA	294	Leu	TTA	74
Ala	GCT	324	Phe	TTT	177
Ala	GCC	257	Phe	TTC	151
Arg	AGG	135	Ser	TCG	68
Arg	AGA	154	Ser	TCA	95
Ser	AGT	67	Ser	TCT	221
Ser	AGC	33	Ser	TCC	140
Lys	AAG	436	Arg	CGG	25
Lys	AAA	190	Arg	CGA	91
Asn	AAT	196	Arg	CGT	154
Asn	AAC	180	Arg	CGC	39
Met	ATG	138	Gln	CAG	184
Ile	ATA	61	Gln	CAA	270
Ile	ATT	210	His	CAT	100
Ile	ATC	250	His	CAC	102

* Determined with the Codon Usage tool available at http://bioinformatics.org/sms2/

Table 2. Nucleotide frequencies (as percentage) in the three codon positions in *Amoeba proteus* (Ap), *Entamoeba histolytica* (Eh), *Acanthamoeba castellanii* (Ac), *Homo sapiens* (Hs) and *Escherichia coli* (Ec).

	First position					Third position				
	Ap	Eh	Ac	Ec	Hs	**Ap**	Eh	Ac	Ec	Hs
G	**37**	33	37	36	34	**23**	8	39	28	29
A	**27**	34	21	25	29	**25**	41	<0.01	18	19
T	**17**	21	12	15	24	**31**	43	4	26	22
C	**19**	12	26	24	13	**21**	8	57	28	30

proteinase 1 (AF142414), myosin II heavy chain (AF136711), peroxiredoxin (AY869722), actin (AY294160), and a novel 110-kDa actin binding proteins interacting with anti-filamin antibody (ApABP-FI; DQ374440).

RESULTS AND DISCUSSION

We have recently cloned and sequenced cDNA of a novel 110-kDa actin-binding protein interacting with anti-filamin antibody and we deposited its sequence in GenBank (accession number: DQ374440). This protein, termed as ApABP-FI, is encoded by 2634 nucleotides that give 878 codons, including a stop codon T(U)AG. Before that only eight mRNA sequences encoding eight *A. proteus* proteins, including two cytoskeletal proteins: myosin II heavy chain (Oh and Jeon 1998) and actin (Fahrni *et al*. 2003) were deposited in the GenBank database. These nine proteins are encoded by the total number of 5718 codons (including stop ones) that, based on a report on codon usage in pathogenic *Entamoeba histolytica* (Tannich and Horstmann 1992), is sufficient to perform the codon usage analysis.

The obtained results (see Table 1) showed that the A+T(U) content in *A. proteus* was 53.8%. This is in contrast with the codon usage in other amoebae, which was found to be biased towards G+C in *Acanthamoeba castellanii* (Hammer *et al*. 1987, Nakamura *et al*. 1996; www.kazusa.orjp/codon) and towards A+T(U) in *D. discoideum* and *E. histolytica* (Tannich and Horstmann 1992, Nakamura *et al*. 1996; www.kazusa.or.jp/codon). The codon usage similar to *A. proteus* was found in organisms evolutionary distant such as *Homo sapiens* and *Escherichia coli*, that had balanced (A+U):(G+C) ratio in the coding sequences of 52:48 and 48:52, respectively (www.kazusa.or.jp/codon, Wada *et al*. 1991).

Accordingly to the balanced nucleotide content in *A. proteus*, codon usage (Table 1) and the nucleotide frequencies in the three codon positions (Table 2) were also not found to be biased: C and G were found to be in the first position in 19% and 37% of codons, and in third position in 21% and 23% of codons, respectively. A and T were present in first position in 27% and 17% of codons, and in third position in 25% and 31% of codons, respectively. These nucleotide frequencies (see Table 2) are not similar to *E. histolytica* or *A. castellanii* but are similar to those found in *E. coli* and *H. sapiens* (www.kazusa.or.jp/codon).

As it can be seen in Table 1, all the possible codons are used in *A. proteus*, and no preference in codon usage for any amino acid has been found. For example, histidine is coded by CAT and CAC with nearly identical frequencies (49.6 and 50.4%, respectively) and all six codons for arginine and leucine are used with the frequency varying from ~ 4% to 25% or 35%, respectively. On the other hand, a stop codon T(U)AA was found in seven out of nine *A. proteus* protein sequences characterized so far. This finding may indicate the preference for this particular stop codon in these giant cells. The presence of tRNAs for all the possible codons suggests that all heterologous genes may be expressed in *A. proteus*.

The interpretation of these observations with regard to the evolutionary divergence between amoebozoan organisms, and evolution *per se*, remains open as it is impossible to deduce whether these differences and/or similarities are due to conservation or convergence.

Acknowledgments. This work was supported by a grant to the Nencki Institute from the State Committee for Scientific Research.

REFERENCES

Brix K., Reinecke A. Stockem W. (1990) Dynamics of the cytoskeleton in *Amoeba proteus*. Influence of microinjected antibodies on the organization and function of the microfilament system. *Eur. J. Cell Biol.* **51:** 279-284

Choi E. Y., Jeon K. W. (1992) Role of spectrin in *Amoeba proteus*, as studied by microinjection of anti-spectrin monoclonal antibodies. *Exp. Cell Res.* **199:** 174-178

Dominik M., Kłopocka W., Pomorski P., Kocik E., Rędowicz M. J. (2005) Characterization of *Amoeba proteus* myosin VI-immunoanalog. *Cell Motil. Cytoskeleton* **61:** 172-188

Fahrni J. F., Bolivar I., Berney C., Nassonova E., Smirnov A., Pawlowski J. (2003) Phylogeny of lobose amoebae based on actin and small-subunit ribosomal RNA genes. *Mol. Biol. Evol.* **20:** 1881-1886

Gągola M., Kłopocka W., Grębecki A., Makuch, R. (2003) Immunodetection and intracellular localization of caldesmon-like proteins in *Amoeba proteus*. *Protoplasma* **222:** 75-83

Hammer J. A. 3-rd, Bowers B., Paterson B. M., Korn E. D. (1987) Complete nucleotide sequence and deduced polypeptide sequence of a nonmuscle myosin heavy chain gene from *Acanthamoeba*: evidence of a hinge in the rodlike tail. *J. Cell Biol.* **105:** 913-25

Jeon K. W. (1995) The large, free-living amoebae: wonderful cells for biological studies. *J. Euk. Microbiol.* **42:** 1-7

Kłopocka W., Rędowicz M. J. (2003) Effect of Rho family GTP-binding proteins on *Amoeba proteus*. *Protoplasma* **220:** 163-172

Nakamura Y., Wada K., Wada Y., Doi H., Kanaya S., Gojobori T., Ikemura T. (1996) Codon usage tabulated from the international DNA sequence databases. *Nucleic Acids Res.* **24:** 214-215

Oh S. W., Jeon K. W. (1998) Characterization of myosin heavy chain and its gene in *Amoeba proteus. J. Euk. Microbiol*. **45:** 600-605

Tannich E., Hortsmann R. D. (1992) Codon usage in pathogenic *Entamoeba histolytica. J. Mol. Evol.* **34:** 272-273

Wada K., Wada Y., Doi H., Ishibashi F., Gojobori T., Ikemura T. (1991) Codon usage tabulated from the GenBank genetic sequence data. *Nucleic Acids Res*. **19 (Suppl):** 1981-1986

Received on 24th March, 2006; revised version on 25th April, 2006; accepted on 19th May, 2006

Acta Protozool. (2006) 45: 317

ACTA
PROTOZOOLOGICA

BOOK RECEIVED

„Festschrift 25 Jahre Deutsche Gesellschaft für Protozoologie" by Klaus Hausmann and Renate Radek; © 2006 by E. Schweizerbart'sche Verlagsbuchhandlung (Nägele u. Obermiller) Stuttgart, Germany; ISBN 3-510-65217-7; hardcover; 278 pages.

The authors of „Festschrift 25 Jahre Deutsche Gesellschaft für Protozoologie" Prof. Dr. Klaus Hausmann and Dr. Renate Radek should be congratulated on their efforts in collecting and elaborating on an important part of the Members of the German Protozoologists Society's undisputable achievements in protistology. Their activities are clearly and impressively presented. The authors have not only gone through the sequence of Society Members' activities of those years, but have also emerged as individuals, with their extensive contributions and recollections of prominent scientists who have passed away.

The twelve parts of the book consist, among other things, of: the history, formation-establishment and progress of the German area; consecutive appointments to the German Protozoologists Society's authority and presidency; membership; members awarded; obituary and memories; Annual Meetings; IX Congress on Protozoology; prominent scientists awards and medals; Eduard Reichenow's medal; Ilse and Wilhelm Foissner's research grant; books, journals and movies; new arrangements of the Society.

The book is addressed mainly to their German colleagues and written in German, however a number of documents concerning meetings or obituaries are in English.

The authors are to be congratulated on producing an extremely useful book, which gives an insight into our German colleagues' lifetime involvement in exploring the unicellular eukaryotes' world over the course of 25 years, 1981-2006. It should be underlined that the activities of the German Protozoologists Society inspired colleagues all over the world but mostly from neighbouring countries, to take part in their meetings and set a strong example to others to take up fruitful collaboration in research.

Special mention should be given to the excellent photography of a number of prominent German Protozoologists Society Members. Their unconventional way of illustrating consecutive chapters by means of spectacular pictures of protists is an excellent addition to the text.

Jerzy Sikora and Leszek Kuźnicki
Nencki Institute of Experimental Biology
Polish Academy of Sciences
Warszawa, Poland

INSTRUCTIONS FOR AUTHORS

Acta Protozoologica is a quarterly journal that publishes current and comprehensive, experimental, and theoretical contributions across the breadth of protistology, and cell biology of lower Eukaryote including: behaviour, biochemistry and molecular biology, development, ecology, genetics, parasitology, physiology, photobiology, systematics and phylogeny, and ultrastructure. It publishes original research reports, critical reviews of current research written by invited experts in the field, short communications, book reviews, and letters to the Editor. Faunistic notices of local character, minor descriptions, or descriptions of taxa not based on new, (original) data, and purely clinical reports, fall outside the remit of *Acta Protozoologica.*

Contributions should be written in grammatically correct English. Either British or American spelling is permitted, but one must be used consistently within a manuscript. Authors are advised to follow styles outlined in The CBE Manual for Authors, Editors, and Publishers (6th Ed., Cambridge University Press). Poorly written manuscripts will be returned to authors without further consideration.

Research, performed by "authors whose papers have been accepted to be published in *Acta Protozoologica* using mammals, shall have been conducted in accordance with accepted ethical practice, and shall have been approved by the pertinent institutional and/or governmental oversight group(s)"; this is Journal policy, authors must certify in writing that their research conforms to this policy.

Nomenclature of genera and species names must agree with the International Code of Zoological Nomenclature (ICZN), International Trust for Zoological Nomenclature, London, 1999; or the International Code of Botanical Nomenclature, adopted by XIV International Botanical Congress, Berlin, 1987. Biochemical nomenclature should agree with "Biochemical Nomenclature and Related Documents" (A Compendium, 2nd edition, 1992), International Union of Biochemistry and Molecular Biology, published by Portland Press, London and Chapel Hill, UK.

Except for cases where tradition dictates, SI units are to be used. New nucleic acid or amino acid sequences will be published only if they are also deposited with an appropriate data bank (e.g. EMBL, GeneBank, DDBJ).

All manuscripts that conform to the Instructions for Authors will be fully peer-reviewed by members of Editorial Board and expert reviewers. The Author will be requested to return a revised version of the reviewed manuscript within four (4) months of receiving the reviews. If a revised manuscript is received later, it will be considered to be a new submission. There are no page charges, but Authors must cover the reproduction cost of colour illustrations.

The Author(s) of a manuscript, accepted for publication, must transfer copyrights to the publisher. Copyrights include mechanical, electronic, and visual reproduction and distribution. Use of previously published figures, tables, or brief quotations requires the appropriate copyright holder's permission, at the time of manuscript submission; acknowledgement of the contribution must also be included in the manuscript. Submission of a manuscript to *Acta Protozoologica* implies that the contents are original, have not been published previously, and are not under consideration or accepted for publication elsewhere.

SUBMISSION

Authors should submit manuscript to: Dr Jerzy Sikora, Nencki Institute of Experimental Biology, ul. Pasteura 3, 02-093 Warszawa, Poland, Fax: (4822) 8225342; E-mail: jurek@nencki.gov.pl or j.sikora@nencki.gov.pl.

At the time of submission, authors are encouraged to provide names, E-mails, and postal addresses of four persons who might act as reviewers. Extensive information on *Acta Protozoologica* is available at the website: **http://www.nencki.gov.pl/ap.htm**; however, please do not hesitate to contact the Editor.

Hard copy submission: Please submit three (3) high quality sets of text and illustrations (figures, line drawing, and photograph). When photographs are submitted, arranged these in the form of plate. A copy of the text on a disk or CD should also be enclosed, in PC formats, preferably Word for Windows version 6.0 or higher (IBM, IBM compatible, or MacIntosh). If they do not adhere to the standards of the journal the manuscript will be returned to the corresponding author without further consideration.

E-mail submission: Electronic submission of manuscripts by e-mail is acceptable in PDF format only. Illustrations must be prepared according to journal requirement and saved in PDF format. The accepted manuscript should be submitted as a hard copy with illustrations (two copies, one with lettering + one copy without lettering) in accordance with the standards of the journal.

ORGANIZATION OF MANUSCRIPTS

Text: Manuscripts must be typewritten, double-spaced, with numbered pages (12 pt, Times Roman). The manuscript should be organized into the following sections: Title, Summary, Key words, Abbreviations, Introduction, Materials and Methods, Results, Discussion, Acknowledgements, References, Tables, and Figure legends. Figure legends must contain explanations of all symbols and abbreviations used. The Title Page should include the title of the manuscript, first name(s) in full and surname(s) of author(s), the institutional address(es) where the work was carried out, and page heading of up to 40 characters (including spaces). The postal address for correspondence, Fax and E-mail should also be given. Footnotes should be avoided.

Citations in the text should be ordered by name and date but not by number, e.g. (Foissner and Korganova 2000). In the case of more than two authors, the name of the first author and *et al.* should be used, e.g. (Botes *et al.* 2001). Different articles by the same author(s) published in the same year must be marked by the letters a, b, c, etc. (Kpatcha *et al.* 1996a, b). Multiple citations presented in the text must be arranged by date, e.g. (Small 1967, Didier and Detcheva 1974, Jones 1974). If one author is cited more than once, semicolons should separate the other citations, e.g. (Lousier and Parkinson 1984; Foissner 1987, 1991, 1994; Darbyshire *et al.* 1989).

Please observe the following instructions when preparing the electronic copy: (1) label the disk with your name; (2) ensure that the written text is identical to the electronic copy; (3) arrange the text as a single file; do not split it into smaller files; (4) arrange illustrations as separate files; do not use Word files; *.TIF, *.PSD, or *.CDR graphic formats are accepted; (5) when necessary, use only italic, bold, subscript, and superscript formats; do not use other electronic formatting facilities such as multiple font styles, ruler changes, or graphics inserted into the text; (6) do not right-justify the text or use of the hyphen function at the end of lines; (7) avoid the use of footnotes; (8) distinguish the numbers 0 and 1 from the letters O and l; (9) avoid repetition of illustrations and data in the text and tables.

References: References must be listed alphabetically. Examples for bibliographic arrangement:

Journals: Flint J. A., Dobson P. J., Robinson B. S. (2003) Genetic analysis of forty isolates of *Acanthamoeba* group III by multilocus isoenzyme electrophoresis. *Acta Protozool.* **42:** 317-324

Books: Swofford D. L. (1998) PAUP* Phylogenetic Analysis Using Parsimony (*and Other Methods). Ver. 4.0b3. Sinauer Associates, Sunderland, MA

Articles from books: Neto E. D., Steindel M., Passos L. K. F. (1993) The use of RAPD's for the study of the genetic diversity of *Schistosoma mansoni* and *Trypanosoma cruzi*. In: DNA Fingerprinting: State of Science, (Eds. S. D. J. Pena, R. Chakraborty, J. T. Epplen, A. J. Jeffreys). Birkhäuser-Verlag, Basel, 339-345

Illustrations and tables: After acceptance of the paper, drawings and photographs (two copies one with lettering + one copy without) must be submitted. Each table and figure must be on a separate page. Figure legends must be placed, in order, at the end of the manuscript, before the figures. Figure legends must contain explanations of all symbols and abbreviations used. All line drawings and photographs must be labelled, with the first Author's name written on the back. The figures should be numbered in the text using Arabic numerals (e.g. Fig. 1).

Illustrations must fit within either a single column width (86 mm) or the full-page width (177 mm); the maximum length of figures is 231 mm, including the legend. Figures grouped as plates must be mounted on a firm board, trimmed at right angles, accurately mounted, and have edges touching. The engraver will then cut a fine line of separation between figures.

Line drawings should be suitable for reproduction, with well-defined lines and a white background. Avoid fine stippling or shading. Prints are accepted only in *.TIF, *.PSD, and *.CDR graphic formats (Grayscale and Colour - 600 dpi, Art line - 1200 dpi) on CD. Do not use Microsoft Word for figure formatting.

Photographs should be sharp, glossy finish, bromide prints. Magnification should be indicated by a scale bar where appropriate. Pictures of gels should have a lane width of no more than 5 mm, and should preferably fit into a single column.

PROOF SHEETS

After a manuscript has been accepted, Authors will receive proofs for correction and will be asked to return these to the Editor within 48-hours. Authors will be expected to check the proofs and are fully responsible for any undetected errors. Only spelling errors and small mistakes will be corrected.

Indexed in: Current Contents, Biosis, Elsevier Biobase, Chemical Abstracts Service, Protozoological Abstracts, Science Citation Index, Librex-Agen, Polish Scientific Journals Contents - Agric. & Biol. Sci. Data Base at: **http://psjc.icm.edu.pl**, Microbes.info "Spotlight" at **http://www.microbes.info**, and electronic version at Nencki Institute of Experimental Biology website in *.PDF format at http://www.nencki.gov.pl/ap.htm now free of charge.

ACTA
PROTOZOOLOGICA

2006 AUGUST
VOLUME 45 NUMBER 3